ZooKeys 917: 1–13 (2020)
doi: 10.3897/zookeys.917.33020
http://zookeys.pensoft.net

RESEARCH ARTICLE

A peer-reviewed open-access journal
ZooKeys
Launched to accelerate biodiversity research

New species of *Furculanurida* (Collembola, Neanuridae, Pseudachorutinae) from the Luquillo Mountains, Puerto Rico

Claudia M. Ospina-Sánchez[1], José G. Palacios-Vargas[2], Grizelle González[1]

1 *USDA-FS, International Institute of Tropical Forestry, Río Piedras, PR 00926-1119, México* **2** *Laboratorio de Ecología y Sistemática de Microartrópodos, Departamento de Ecología y Recursos Naturales, Facultad de Ciencias, Universidad Nacional Autónoma de México, 04510 México, D.F., México*

Corresponding author: Claudia M. Ospina Sánchez (cmarcela.ospinas@gmail.com)

Academic editor: L. Deharveng | Received 11 January 2019 | Accepted 11 February 2020 | Published 9 March 2020

http://zoobank.org/4D2DBC43-950B-40E4-B333-993C5A76D1EC

Citation: Ospina-Sánchez CM, Palacios-Vargas JG, González G (2020) New species of *Furculanurida* (Collembola, Neanuridae, Pseudachorutinae) from the Luquillo Mountains, Puerto Rico. ZooKeys 917: 1–13. https://doi.org/10.3897/zookeys.917.33020

Abstract

A new species of *Furculanurida* is described and illustrated. *Furculanurida bistribus* **sp. nov.** differs from other species of the genus by the presence of three eyes, three setae on the dens, and the white and purple coloration pattern. A key for identification of the world species of the genus is included.

Keywords

Island, Luquillo Experimental Forest, subtropical forest, taxonomy

Introduction

In Puerto Rico, most studies of arthropod community dynamics have been done in the Luquillo Mountains. Designated as a US Experimental Forest in 1956, it became part of the International Network of Biosphere Reserves in 1976 (González and Barberena 2018; Quiñones et al. 2018; Richardson 1999). Four easily distinguishable forest types are dominated by an assortment of distinctive tree species. The Tabonuco forest

(*Dacryodes excelsa* Vahl) occupies areas below 600 m, in the mid-elevation zone. Palo Colorado forest (*Cyrilla racemiflora* L.) occurs in areas above the cloud condensation level from 600 to 900 m a.s.l. The Elfin forest (dominant tree *Tabebuia rigida* Urban), with stunted vegetation and waterlogged anoxic soils, is located only on the highest peaks above 900 m. Palm forests (*Prestoea montana* (R. Grah.) Nichols) occur at all elevations, predominantly on windward slopes, in wet gullies, and in stream valleys (Gould et al. 2006). These forests represent subtropical wet and subtropical rain forest life zones in Puerto Rico (Ewel and Whitmore 1973).

In most studies of litter and soil fauna in the Luquillo Experimental Forests (hereafter LEF), Collembola are an important group because of their numerical dominance, combined with their key responses to changes in disturbance, altitude, and vegetation type (Schowalter and Ganio 1999; Schowalter et al. 2003; Richardson et al. 2005; Richardson et al. 2010; Schowalter et al. 2014). In Puerto Rico, Collembola are well known in comparison to other groups of soil arthropods. However, not all Collembola species from LEF have been identified.

In a recent survey between 2014 and 2015, we identified 16 families (sensu Deharveng 2004; Soto-Adames et al. 2008; Bellinger et al. 1996–2019), 37 genera, and probably 60 species, of which 15 are new. As a result of this survey, the inventory of Collembola in the LEF increased to 44 genera and 70 species. The purpose of this paper is to describe a new species of *Furculanurida* Massoud, 1967, a genus not previously reported from Puerto Rico.

The genus *Furculanurida* was created to relocate *Micranurida africana* Massoud, 1963 because of the development of its furcula (Massoud 1967). The main characters of this genus have been discussed previously (Palacios-Vargas and Gao 2009; Queiroz and Fernandes 2011; Zon et al. 2014, Neves et al., 2019), and some species are dubiously placed within *Furculanurida* (Table 1). To date, the genus has 16 nominal species distributed in the Neotropical, Ethiopian, and Nearctic regions, with seven, six, and one described species, respectively. Reported in the Neotropical Region are *F. arawakensis* Thibaud & Massoud, 1983 from the Lesser Antilles; *F. guatemalensis* Palacios-Vargas & Gao, 2009 and *F. septemoculata* Palacios-Vargas & Gao, 2009 from Guatemala; *F. nessimiani* Fernandes & Mendonça 2002, *F. belemensis* Arlé & Rufino, 1976, *F. goeldiana* Arlé & Rufino, 1976, and *F. tropicalia* Queiroz & Fernandes, 2011 from Brazil; and *F. longisensillata* Najt, Thibaud & Weiner, 1990 from French Guiana.

Initially, the genus *Furculanurida* was established using the combination of the following characters: postantennal organ (PAO) present, eyes absent, maxilla styliform, and furcula present (Massoud 1967). According to Queiroz and Fernandes (2011) species of the genus have Ant IV with a trilobed apical bulb, dorsolateral microsensillum present or absent, 4–7 sensilla, and long ordinary setae; PAO circular or elliptical with 4–22 vesicles; eyes from zero to eight per side; mandible with 2–10 teeth; maxilla styliform with two fused lamellae; tenent hair on tibiotarsi acuminated; ventral tube with 3 or 4 setae on each side; tenaculum with 2 or 3 teeth on each ramus; furcula complete, with well-developed dens and mucro; dens with 5 or 6 setae on each side; mucro separated from dens and with two tapering lamellae, sensilla on body always

long. However, the more recently described *Furculanurida* species include specimens without the full development of the furcula (Zon et al. 2014). Zon et al. concluded that *Furculanurida* can only be separated from *Pseudachorutes* Tullberg, 1871 by a conditional combination of characters, i.e., "eyes less than 8+8, or, when 8+8, microchaeta ms absent on Ant. IV". Similarly, differences with *Stachorutes* Dallai, 1973 would be "mucrodens complete, or, if mucro absent, ms absent on Ant. IV" (Zon et al. 2014: 496). Therefore, these genera need an extensive revision to clarify the morphological differences between them.

Materials and methods

Abbreviations

a.s.l	above sea level	**S**	sensillum
Abd	abdominal segment	**Sgd**	dorsal guard sensillum of Ant. III
Ant	antennal segment	**Sgv**	ventral guard sensillum of Ant. III
Cx	coxa	**ss**	sensorial seta
Fe	femur	**Th**	thoracic segment
M	long macroseta	**Ti**	tibiotarsus
ms	microsensillum	**Tr**	trochanter
mi	microseta	**VT**	Ventral Tube
PAO	Postantennal organ		

The material used to describe the species was collected during the Collembola microhabitats project at the Luquillo Mountains, as part of a survey conducted in three forest types. Collembola were extracted using Berlese-Tullgren funnels into 95% ethanol. They were cleared using Nesbitt solution and fixed on slides using Mac André II solution (Mari Mutt 1979). The slides were then dried in a slide warmer at 45–50 °C for seven days. Finally, each specimen was labeled with its collecting data. Specimens were examined with a Leica DM500 phase-contrast microscope. The drawings were made with the aid of a drawing tube. All the type material is deposited at International Institute for Tropical Forestry laboratory.

Taxonomy

***Furculanurida bistribus* sp. nov.**
http://zoobank.org:act:FE803C73-165E-42D6-9588-1343C9984A61
Figures 1–13, Tables 1, 2

Type material. Holotype (female on slide) and 8 **paratypes** (2 males, 4 females, and 2 juveniles, each one on slides). Puerto Rico, Luquillo, Luquillo Mountains, Pico del

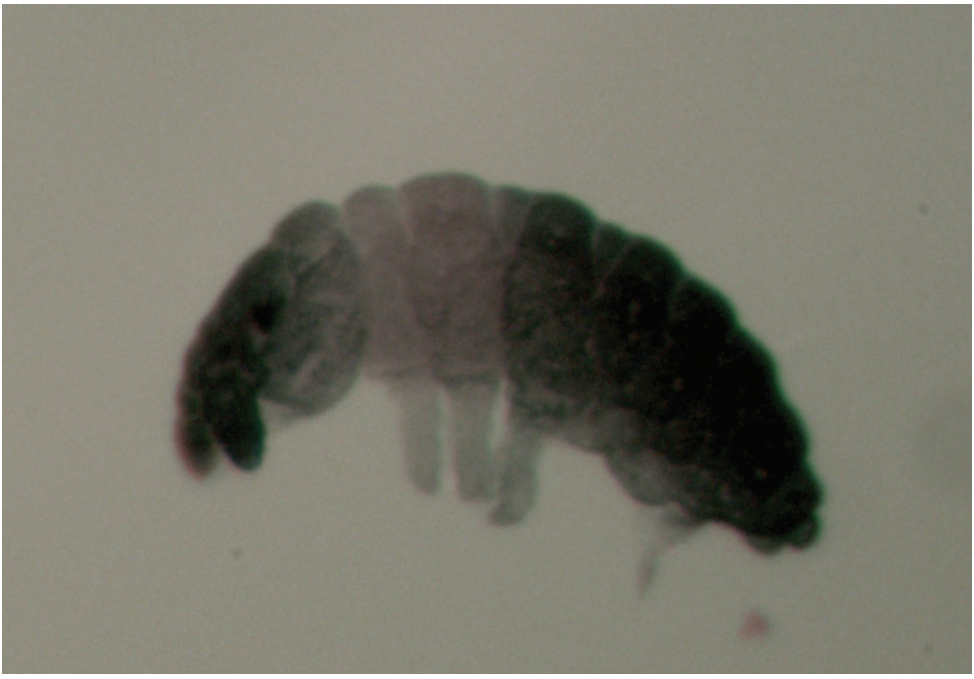

Figure 1. *Furculanurida bistribus* sp. nov. Specimen in ethanol 96%.

Este, 18° 16' 17"N; 65° 45' 40"W; 987.6 m a.s.l.; ex mosses, *Tabebuia rigida* forest type, from leaf litter and epiphytes, 04 Nov 2014, leg. CM Ospina.

Other material. 2 females on slides, Puerto Rico, Luquillo, Luquillo Mountains, Pico del Este, *Tabebuia rigida* forest type, epiphyte, 987.6 m a.s.l., 19 May 2015, leg. CM Ospina. 1 female on slide, Puerto Rico, Luquillo, Luquillo Mountains, Pico del Este, *Tabebuia rigida* forest type, epiphyte, 987.6 m a.s.l., 11 Feb 2015, leg. CM Ospina. 1 juvenile on slide Puerto Rico, Luquillo, Luquillo Mountains, Pico El Yunque, *Tabebuia rigida* forest type, leaf litter, 1044.8 m a.s.l., 4 Nov 2014, leg. CM Ospina. 1 female on slide Puerto Rico, Luquillo, Luquillo Mountains, Pico El Yunque, *Tabebuia rigida* forest type, leaf litter, 1044.8 m a.s.l., 19 May 2015, leg. CM Ospina.

Diagnosis. Eyes 3+3 eyes. Post antennal organ in rosette with 5 or 6 vesicles. Ant IV with six sensilla. Seta a0 on head absent. Mandible with four teeth. Dens with three setae. Unguis without internal tooth.

Description. Average body length: adults 1009 μm (n = 5); juveniles 847 μm (n = 2). Specimens in ethanol with antenna and abdomen evenly grey, ocular patch dark; head, legs III, and furcula light grey; thorax, legs I and II white to light purple (Fig. 1). Granulation coarse. Body setae comprising short, smooth and thin setae, and long and smooth sensorial setae.

Head: antenna shorter (0.6) than head diagonal. Ant III and IV fused dorsally, ventral separation clearly marked. Ant IV dorsally with trilobed apical vesicle, six subcylindrical thin sensilla and 14 long setae; subapical organite present; dorsoexternal

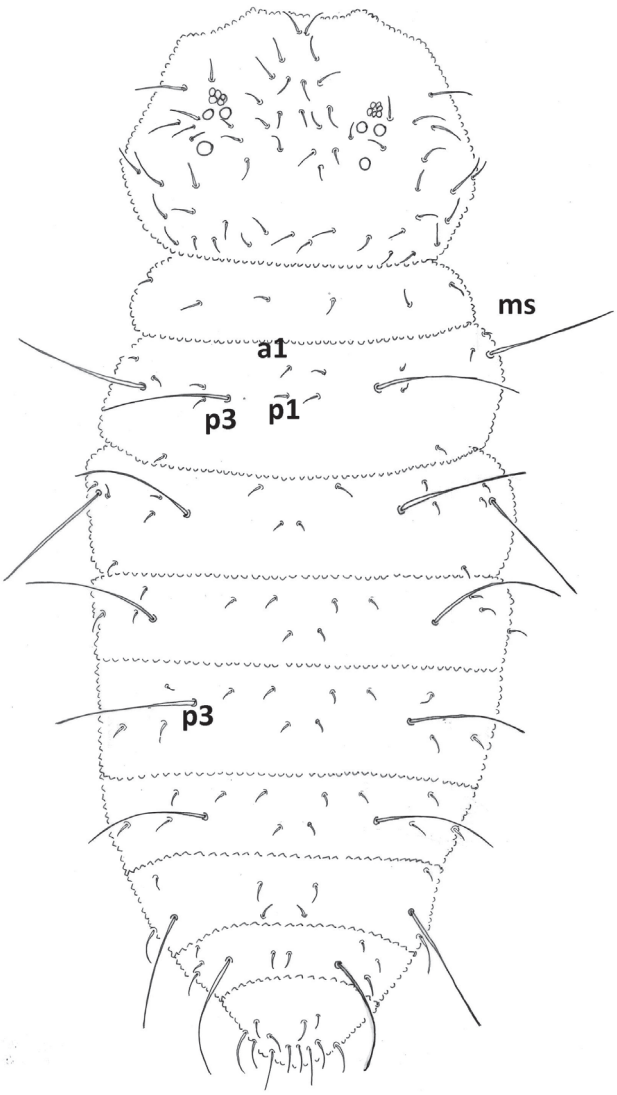

Figure 2. *Furculanurida bistribus* sp. nov. Dorsal chaetotaxy of body (female).

microsensillum absent (Fig. 3); no sensorial field ventrally on Ant IV (Fig. 4); Ant III sense organ with two small internal slightly bent sensilla, two subcylindrical guard sensilla, Sgv larger than Sgd, ventral microsensillum present (Figs 3, 5); Sgd apically displaced, towards Ant IV, aligned to S2 and S3; Ant II with 10 setae; Ant I with seven setae (Fig 3). Eyes 3+3 on a pigmented eyepatch; PAO with five or six vesicles disposed as a rosette (Fig. 2). Head dorsal chaetotaxy as in Figure 2; seta a0 absent; d row with 4 setae, sd row with three setae; setae Oc 1–3 present; c setae absent; p1–3 setae present. Buccal cone elongate, labium with complete chaetotaxy, A to G setae, C and D apically displaced (Fig. 6). Pre-labral/Labral chaetotaxy 4/2322 (Fig. 7). Mandible with four

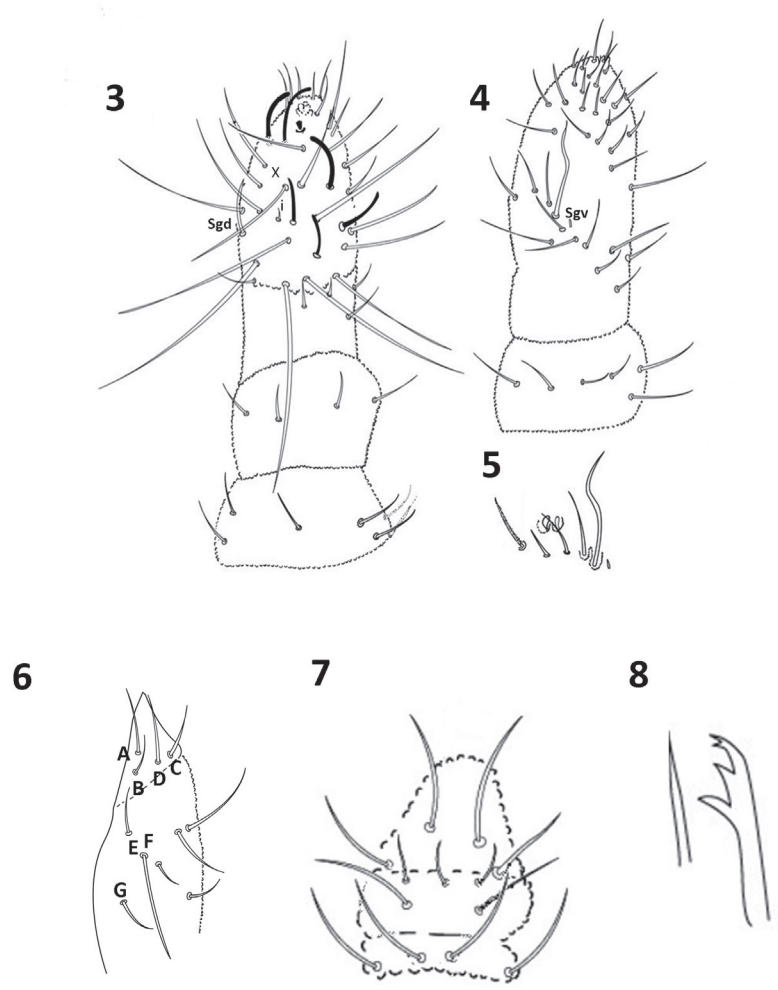

Figures 3–8. *Furculanurida bistribus* sp. nov. **3** Ant I–IV, dorsal view **4** Ant IV and III, ventral view **5** Sensorial Organ in Ant. III **6** Labium **7** Labrum **8** Maxilla and mandible.

teeth, two apical short and subequal, one medial and one basal large and subequal; maxilla styliform with one lamella (Fig. 8).

Dorsal chaetotaxy: ordinary setae smooth, distributed as in Figure 2. Th I with 2+2 setae; Th II and III with one dorsolateral seta posteriorly displaced. Sensory setae (s) clearly differentiated, in position p3 and p6 in Th II and III and in position p3 in Abd I–V; S-chaetotaxy formula = 022/11111.

Legs chaetotaxy: subcoxae 1, two; subcoxae 2, one; Cx, three; Tr, four; Fe, 10, and Ti 19 setae (Fig. 9). Seta M present between B4 and B5 without displacement. Tenent hair acuminate. Claws without teeth, unguis larger than Ti (ratio tibiotarsus: unguis = 1:1.2:); unguiculus absent.

Ventral chaetotaxy as in Figure 10. VT with 3+3 setae; tenaculum with 3+3 teeth and without setae; furcula well developed, manubrium with 14 setae, dens with three

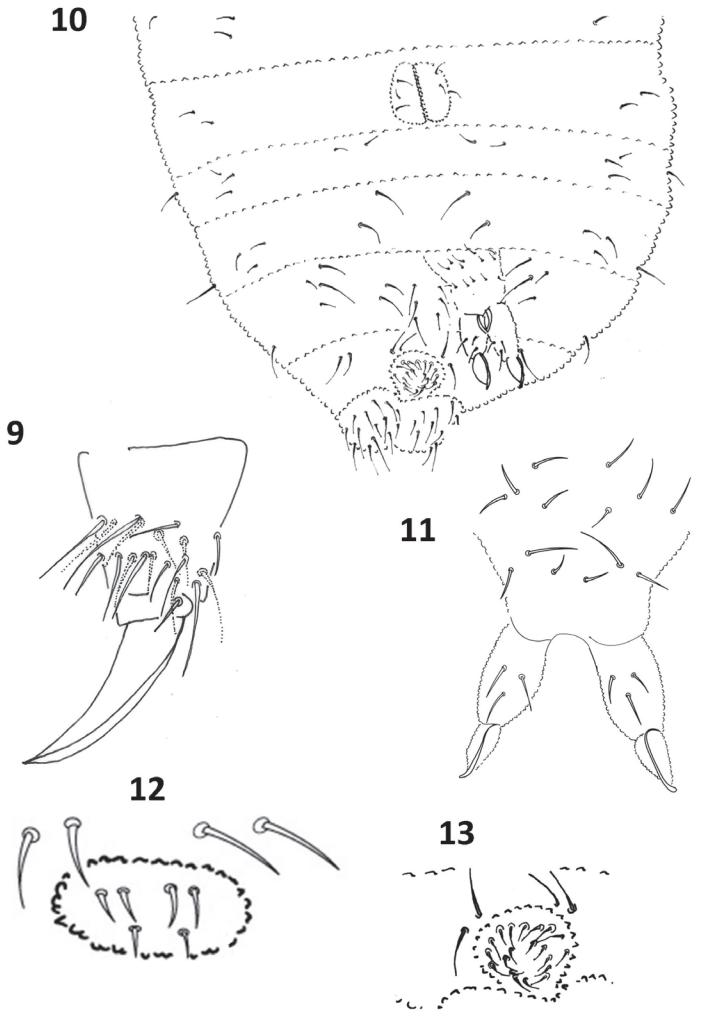

Figures 9–13. *Furculanurida bistribus* sp. nov. **9** Tibiotarsus II **10** Ventral quetotaxy **11** Manubrium and furcula **12** Female genital plate **13** Male genital plate.

setae, mucro straight with a broad hook-like apex (Fig. 11). Ratio mucro: dens = 1: 1.3. Female genital plate with 2+2 pregenital setae, four circumgenital setae, and 1+1 eugenital setae (Fig. 12). Male genital plate with 2+2 pregenital setae, ten circumgenital setae, and 4+4 eugenital setae (Fig. 13).

Etymology. *Bistribus*, Latin for two times three, in reference to the presence of 3+3 eyes and 3+3 setae on dens, diagnostic characters of the species.

Distribution. This species is only the *Furculanurida* known from the Luquillo Mountains in the *Tabebuia rigida* forest type, on Pico del Este 18° 16' 17"N; 65° 45' 40"W; 987.6 m a.s.l. and Pico El Yunque 18° 18' 37"N; 65° 47' 26"W; 1044.8 m a.s.l.

Ecology. *Furculanurida bistribus* sp. nov. was extracted from leaf litter and mosses in both dry and rainy seasons during November 2014, and May and August 2015.

Table 1. *Furculanurida* species with disputed generic placement and their taxonomic history.

Species	Original genus	Generic placement[+]	Character[++]
africana (Massoud, Z, 1963)	*Micranurida*	***Furculanurida*** (type species) Massoud 1967	Furcula developed
arlei Thibaud & Massoud, 1980	*Furculanurida*	***Stachorutes*** Weiner and Najt (1998)	Presence of a microsensillum on Ant IV, mandible with only 2 teeth and a reduced furcula with very small mucro
		Furculanurida Thibaud and Palacios–Vargas (2000)	Presence of Ant. IV with 8 thick sensilla on antennal segment IV and long sensorial setae on the body and a small tooth in the unguis
ashrafi (Yosii, 1966)	*Micranurida*	*Stachorutes* Deharveng and Lienhard (1983)	Furcula reduced
		Furculanurida Thibaud and Palacios–Vargas 2000	Presence of four teeth in the mandible
furculata (Salmon, 1956)	*Kenyura*	***Furculanurida*** Massoud (1967)	Furcula developed and post-antennal organ present
perplexa (Salmon, 1956)	*Hypanurida*	*Furculanurida* Massoud (1967)	Reduced furcula
		Hypanurida Thibaud and Palacios–Vargas (2000)	Reduced furcula and 3–4 setae in dens

[+] Generic placement according to cited authors (current genus in bold).
[++] Character to justify the placement in their current genus.

Table 2. Main characters of the all known species of *Furculanurida*, including species moved to other genera.

Species[+]	Locality	Eyes	PAO vesicles	Ant IV sensilla	Ant IV ms	Md. teeth	Inner unguis tooth	Dens setae	Mucro	VT setae	Tenaculum teeth
africana	Ivory Coast	0	8–10	6	-	9	absent	6	developed	-	-
arawakensis	Lesser Antilles	4(2–4)	5–9	6	absent	7	present	6	developed	3	–
arlei (*Stachorutes*)	Morocco	5		8	–	2	–	–	small	–	–
ashrafi (*Micranurida*)	Nepal	–	–	–	–	9	–	–	–	3	–
belemensis	Brazil	5	8–9	6	–	4–6	present	6	–	–	–
boiuna	Brazil	0	8–9	6	absent	7	present	5–6	developed	3	3
duodecimoculata	Morocco	–	11	–		4	–	–	–	3	–
emucronata	Ivory Coast	0	13–16	–	absent	–	present		absent	3	3
furculata	Rwanda	2	4	7		7	present	6	developed	–	
goeldiana	Brazil	7	7–10	7	–	4				–	
grandcolasorum	Tanzania	5	9–10		absent	3–6				3	
guatemalensis	Guatemala	5	15	6	present	4	present	6	developed	4	3
langdoni	USA	5	14–22	19	present	6	present	5	developed	4	3
longisensillata	French Guiana	6	6–7	6	absent	10–11	present	6	developed	3	–
nessimiani	Brazil			6	absent	4	–	–	–	3	–
perplexa (*Hypanurida*)	Rwanda	4	20–22		–	5	present	3–4	spiniform	–	–
septemoculata	Guatemala	7	15	6	present	2	present	6	developed	4	3
tropicalia	Brazil	8	8–10	6	absent	4	present	6	developed	3	3
bistribus sp. nov.	Puerto Rico	3	6	6	absent	4	absent	3	developed	3	3

[+] The current genus is in parenthesis.
– No information included in the original description.

Identification key to the species of *Furculanurida* Massoud, 1967

1	Eyes absent	**2**
–	Eyes present	**4**
2	Mucro developed, PAO with 8–10 vesicles	**3**
–	Mucro absent, PAO with 13–16 vesicles	***F. emucronata* Zon, Tano & Deharveng, 2014**
3	Internal tooth on unguis absent	***F. africana* Massoud, 1963**
–	Internal tooth on unguis present	***F. boiuna* Neves, Mendonça & Queiroz, 2019**
4	Eyes 8+8	***F. tropicalia* Queiroz & Fernandes, 2011**
–	Eyes 7+7 or less	**5**
5	Tenaculum with 2+2 teeth	**6**
–	Tenaculum with 3+3 teeth	7
6	PAO with 11 vesicles	***F. duodecimoculata* Thibaud & Massoud, 1980**
–	PAO with 6 vesicles	***F. nessimiani* Fernandes & Mendonça, 2002**
7	Setae on dens 3, internal tooth onunguis absent	***F. bistribus* sp. nov.**
–	Setae on dens 5 or 6, internal tooth on unguis present	**8**
8	Setae on dens 5	***F. langdoni* Bernard, 2007**
–	Setae on dens 6	**9**
9	Mandible with 10 teeth	***F. longisensillata* Najt, Thibaud & Weiner, 1990**
–	Mandible with 7 teeth or less	**10**
10	Ant IV with 7 sensilla, PAO with 4 vesicles, eyes 2+2	***F. furculata* Salmon, 1956**
–	Ant IV with 6 sensilla, PAO with more than 4 vesicles	**11**
11	Eyes 4+4 or less, mandible with 7 teeth	***F. arawakensis* Thibaud & Massoud, 1983**
–	Eyes 5+5 or 7+7, mandible with less than 7 teeth	**12**
12	Eyes 7+7	**13**
–	Eyes 5+5	**14**
13	PAO with 7-10 vesicles, mandible with 4 teeth	***F. goeldiana* Arlé & Rufino, 1976**
–	PAO with 15 vesicles, mandible with 2 teeth	***F. septemoculata* Palacios-Vargas & Gao, 2009**
14	PAO with 8 or 9 vesicles in a circular form	***F. belemensis* Arlé & Rufino, 1976**
–	PAO with 9 or more vesicles in an elliptical form	15
15	Setae on ventral tube 3+3, PAO with 9 or 10 vesicles	***F. grandcolasorum* Weiner & Najt, 1998**
–	Setae on ventral tube 4+4, PAO with 15 vesicles	***F. guatemalensis* Palacios-Vargas & Gao, 2009**

Discussion

Furculanurida bistribus sp. nov. is placed in *Furculanurida* because many of its characters are similar with those of the other species of that genus, and it matches the current genus diagnosis: apical bulb trilobed, long setae present on Ant IV, maxilla styliform, furcula fully developed, and ordinary setae on the body short but sensory setae long (Queiroz and Fernandes 2011). Although the presence of one tooth on the unguis is observed in most *Furculanurida*, there are two exceptions where the unguis is toothless: *F. africana* and the new species described here. In any case, the inner tooth on the claw is usually considered as a specific, not a generic character (Zon et al. 2014). The antennal chaetotaxy is also useful to characterize the genus; the new species has antennal characters of *Furculanurida*: apical vesicle trilobed, microsensillum absent, and presence of six S-sensilla and long setae on Ant IV (Queiroz and Fernandes 2011). The low number of dental setae is a character shared with *Hypanurida perplexa* Salmon, 1956, but the position of this species is controversial because of the reduction of the furcula (Queiroz and Fernandes 2011).

Although morphological characters, including furcal reduction, appear similar between some *Furculanurida* (including *F. bistribus* sp. nov.) and *Stachorutes* (Zon et al. 2014), the geographic separation of the two genera is remarkable. The genus *Furculanurida* was established for three sub-Saharan African neanurids: *Micranurida africana*, *Kenyura furculata* Salmon,1956, and *Hypanurida perplexa* (see Massoud 1967). Subsequently, other species were described or included in *Furculanurida* from the Lesser Antilles, Guatemala, Brazil, French Guiana, Tanzania, Morocco, Nepal, and Ivory Coast (Queiroz and Fernandes 2011; Zon et al. 2014). The genus, thus, conforms to a general Gondwanan distribution, with a few exceptions, like *Furculanurida langdoni* which is found in North America. In contrast, *Stachorutes* exhibits mostly an Holarctic distribution, with species known from China, France, Poland, Russia, Slovakia, Spain, and North America, except for a single species from Africa (Tanzania) (Simon-Benito et al. 2005; Fanciulli et al. 2017).

According to Queiroz and Zeppelini (2017), there are key diagnostic characters that define two groups of Pseudachorutinae in the Neotropics, which are chaetotaxy of antennae, head, thorax, and tibiotarsi. *Furculanurida bistribus* sp. nov. exhibits many similarities with *Arlesia* group of genera. In the antennal chaetotaxy, the only difference was the absence of S10 *sensu* Queiroz and Zeppelini (2017). Regarding head and thorax chaetotaxy, the main characters are similar, i.e. the absence of setae c2 and c3 and the presence of p1, p2 and p3 on head, the presence of only 2+2 setae on Th I, and one posterior setae displaced laterally on Th II and III. In consequence, this description reinforces the need for a revision of *Furculanurida*, as not only *F. bistribus* sp. nov. but possibly other species of *Furculanurida* might present characters that fit the pattern displayed by the *Arlesia*-group of genera *sensu* Queiroz and Zeppelini (2017).

Despite the differences of the new species with the most recent genus diagnosis of *Furculanurida* (Queiroz and Fernandes 2011), we place *F. bistribus* sp. nov. in this genus because of the fully developed furcula in this species (Fig. 11) and its distribution,

despite the number of setae on the dens. Inclusion of the new species in this genus thereby enlarges the generic diagnosis to include species with 3–6 setae on the dens. The characters that place the new species close to *Stachorutes* are of uncertain generic value and need more studies (Bernard 2007; Zon et al. 2014, Neves et al. 2019).

Furculanurida bistribus sp. nov. has this unique combination of characters: six sensilla on Ant IV, 3+3 eyes, three setae in the dens, and the absence of an internal tooth on the unguis, combined with its color pattern. Members of *Furculanurida* have between zero and eight eyes per side; *F. bistribus* sp. nov. has 3+3 eyes, though some specimens of *F. arawakensis* may have this number (usually 4+4 eyes). All the described species have a fully developed furcula, but more dental chaetae than the new species. Leaving aside the unique characters of *F. bistribus* sp. nov., it is more similar to *F. arawakensis* from which it differs by the presence of four teeth on mandibles (versus seven), less dental chaetae (3 versus 6), and the absence of tooth on unguis. The differences between all the species of the genus are summarized in Table 2.

Acknowledgements

This research was supported by Grant DEB 1239764 and 1546686 from the US National Science Foundation to the Institute for Tropical Ecosystem Studies, University of Puerto Rico, and to the International Institute of Tropical Forestry (IITF) USDA Forest Service, as part of the Luquillo Long-Term Ecological Research Program. The US Forest Service (Department of Agriculture) Research and Development Unit and the University of Puerto Rico provided additional support. We also thank to María M. Rivera (IITF) who helped with fieldwork and Edward Quigley assisted with the digitization of the figures.

References

Arlé R, Rufino E (1976) Contribuição ao conhecimento dos Pseudachorutinae da Amazônia (Collembola). Acta Amazonica 6: 99–107. https://doi.org/10.1590/1809-43921976061099

Bellinger P, Christiansen K, Janssens F (1996–2019) Checklist of the Collembola of the World. Last updated on 2019.11.30 by Frans Janssens. http://wwwcollembolaorg. Accessed on: 2019-01-06.

Bernard EC (2007) *Furculanurida langdoni* n. sp. (Collembola: Neanuridae), a Nearctic member of a Gondwanan genus. Proceedings of the Biological Society of Washington 120: 320–326. https://doi.org/10.2988/0006-324x(2007)120[320:flnscn]2.0.co;2

Dallai R (1973) Ricerche sui Collemboli. XVI. *Stachorutes dematteisi* n. gen., n. sp., *Micranurida intermedia* n. sp. e considerazioni sul genre *Micranurida*. Redia 54: 23–31. https://doi.org/10.21426/B63110007

Deharveng L (2004) Recent advances in Collembola systematics. Pedobiologia 48: 415–433. https://doi.org/10.1016/j.pedobi.2004.08.001

Deharveng L, Lienhard C (1983) Deux nouvelles espèces du genre *Stachorutes* Dallai, 1973 (Collembola). Revue Suisse de Zoologie 90: 929–934. https://doi.org/10.5962/bhl.part.82016

Ewel JJ, Whitmore JL (1973) Ecological Life Zones of Puerto Rico and US Virgin Islands. US Department of Agriculture, Forest Service, Institute of Tropical Forestry, Research Paper ITF-018.

Fanciulli PP, Dallai R, Frati F, Carapelli A (2017) *Stachorutes najtae* n. sp., a new psammophile species of Collembola from Italy (Neanuridae, Pseudachorutinae). Zoosystema 39 (1): 31-36. https://doi.org/10.5252/z2017n1a4

Fernandes LH, Mendonça MC (2002) Duas novas espécies de Pseudachorutinae (Collembola, Neanuridae) do Brasil. Boletim do Museu Nacional, Nova Série, Zoologia: 1–8.

González G, Barberena MF (2018) Ecology of soil arthropod fauna in tropical forests: a review of studies from Puerto Rico. The Journal of Agriculture of the University of Puerto Rico 101: 185–201.

Gould W, González G, Carrero Rivera G (2006) Structure and composition of vegetation along an elevational gradient in Puerto Rico. Journal of Vegetation Science 17: 653–664. https://doi.org/10.1111/j.1654-1103.2006.tb02489.x

Mari Mutt JA (1979) A revision of the genus *Dicranocentrus* Schött (Insecta: Collembola: Entomobryidae). The Journal of Agriculture of the University of Puerto Rico 63: 214–222.

Massoud Z (1963) Les collemboles pseudachorutiniens, brachystomelliens et neanuriens de la Côte d'Ivoire. Bulletin de l'Institut Français d'Afrique Noire: 25: 57–76.

Massoud Z (1967) Monographie des Neanuridae Collemboles Poduromorphes à pièces buccales modifies. Biologie de l'Amérique Australe: Volume III. Centre National de la Recherche Scientifique, Paris, 399 pp.

Najt J, Thibaud J, Weiner W (1990) Collemboles (Insecta) poduromorphes de Guyane française. Bulletin du Muséum National d'Histoire Naturelle 4: 95–121.

Neves ACR, Mendonça MC, Queiroz GC (2019) Two new species and new records of Neanuridae (Hexapoda: Collembola) from Brazilian central Amazonia. Zoologia (Curitiba) 36: 1–8. https://doi.org/10.3897/zoologia.36.e23269

Palacios-Vargas JG, Gao Y (2009) Two new species of *Furculanurida* (Collembola: Neanuridae) from Guatemala. Brenesia 71–72: 55–60.

Queiroz GC, Fernandes LH (2011) New Brazilian species of *Furculanurida* Massoud, 1967 (Collembola: Neanuridae). Zootaxa 2805: 57–64. https://doi.org/10.11646/zootaxa.2805.1.5

Queiroz G, Zeppelini D (2017) Neotropical Pseudachorutinae (Hexapoda: Collembola: Neanuridae): a comparative morphological study with emphasis on endemic taxa. Zoologischer Anzeiger 269: 127–154. https://doi.org/10.1016/j.jcz.2017.08.005

Quiñones M, Parés-Ramos IK, Gould WA, González G, McGinley K, Ríos P (2018) El Yunque National Forest Atlas. Department of Agriculture, Forest Service, International Institute of Tropical Forestry, San Juan, PR, 63 pp.

Richardson BA (1999) The bromeliad microcosm and the assessment of faunal diversity in a Neotropical forest. Biotropica 31: 321–336. https://doi/abs/10.1111/j.1744-7429.1999.tb00144.x

Richardson BA, Richardson MJ, González G, Shiels AB, Srivastava DS (2010) A canopy trimming experiment in Puerto Rico: the response of litter invertebrate communities to canopy loss and debris deposition in a tropical forest subject to hurricanes. Ecosystems 13: 286–301. https://doi.org/10.1007/s10021-010-9317-6

Richardson BA, Richardson MJ, Soto-Adames FN (2005) Separating the effects of forest type and elevation on the diversity of litter invertebrate communities in a humid tropical forest in Puerto Rico. Journal of Animal Ecology 74: 926–936. https://doi.org/10.1111/j.1365-2656.2005.00990.x

Salmon J (1956) Contribution à l'étude de la faune entomologique du Ruanda-Urundi (Mission P. Basilewsky 1953): LXXIX. Collembola. Sciences Zoologiques 8: 9–40.

Schowalter T, Ganio L (1999) Invertebrate communities in a tropical rain forest canopy in Puerto Rico following Hurricane Hugo. Ecological Entomology 24: 191–201. https://doi.org/10.1046/j.1365-2311.1999.00186.x

Schowalter TD, Ganio LM, Basset Y, Novotny V, Miller S, Kitching R (2003) Diel, seasonal and disturbance-induced variation in invertebrate assemblages. In: Basset Y, Kitching R, Miller S, Novotny V (Eds) Arthropods of Tropical Forests: Spatio-Temporal Dynamics and Resource Use in the Canopy. Cambridge University Press, Cambridge: 315–328.

Schowalter TD, Willig MR, Presley SJ (2014) Canopy arthropod responses to experimental canopy opening and debris deposition in a tropical rainforest subject to hurricanes. Forest Ecology and Management 332: 93–102. https://doi.org/10.1016/j.foreco.2013.12.008

Simón-Benito JC, Espantaleón D, Gracía-Barros E (2005) Stachorutes cabagnerensis n. sp., Collembola (Neanuridae) from Central Spain, and a preliminary approach to phylogeny of genus. Animal Biodiversity and Conservation 28: 149–157. https://www.raco.cat/index.php/ABC/article/view/56768/66538

Soto-Adames FN, Barra J, Christiansen K, Jordana R (2008) Suprageneric classification of Collembola Entomobryomorpha. Annals of the Entomological Society of America 101: 501–513. https://doi.org/10.1603/0013-8746(2008)101[501:SCOCE]2.0.CO;2

Thibaud J-M, Palacios–Vargas JG (2000) Remarks on *Stachorutes* (Collembola: Pseudachorutidae) with a new Mexican species. Folia Entomológica Mexicana 109: 107–112.

Thibaud J, Massoud Z (1983) Collemboles des Petites Antilles. III. Neanuridae (Pseudachorutinae). Revue d'Écologie et de Biologie du Sol: 20: 111–129.

Tullberg T (1871) Förteckning öfver Svenska Podurider. Öfversigt af Kongliga Vetenskaps-Akademiens Förhandlingar 28 :143–155.

Weiner WM, Najt J (1998) Collembola (Entognatha) from East Africa. European Journal of Entomology 95: 217–238.

Yosii R (1966) Collembola of Himalaya. Journal of the College of Arts and Sciences, Chiba University 4: 461–531.

Zon SD, Tano Y, Deharveng L (2014) A new species of *Furculanurida* (Collembola: Neanuridae) from Ivory Coast, with comments on related genera. Zootaxa 3878: 491–497. https://doi.org/10.11646/zootaxa.3878.5.8

ZooKeys 917: 15–50 (2020)
doi: 10.3897/zookeys.917.47444
http://zookeys.pensoft.net

RESEARCH ARTICLE

A peer-reviewed open-access journal
ZooKeys
Launched to accelerate biodiversity research

Fine-scale species delimitation: speciation in process and periodic patterns in nudibranch diversity

Tatiana Korshunova[1,2], Klas Malmberg[3], Jakov Prkić[4], Alen Petani[5], Karin Fletcher[6], Kennet Lundin[7,8], Alexander Martynov[2]

1 *Koltzov Institute of Developmental Biology RAS, 26 Vavilova Str., 119334 Moscow, Russia* **2** *Zoological Museum, Moscow State University, Bolshaya Nikitskaya Str. 6, 125009 Moscow, Russia* **3** *Aquatilis, Nostravägen 11, S-41743, Gothenburg, Sweden* **4** *Getaldiceva 11, C 21000 Split, Croatia* **5** *Put Kotlara 6, C 23000 Zadar, Croatia* **6** *Port Orchard, Washington, 98366, USA* **7** *Gothenburg Natural History Museum, Box 7283, SE-40235, Gothenburg, Sweden* **8** *Gothenburg Global Biodiversity Centre, Box 461, SE-40530, Gothenburg, Sweden*

Corresponding author: *Kennet Lundin* (kennet.lundin@vgregion.se); *Alexander Martynov* (martynov@zmmu.msu.ru)

Academic editor: *Nathalie Yonow* | Received 19 October 2019 | Accepted 2 January 2020 | Published 9 March 2020

http://zoobank.org/75B05B61-9395-44E9-95BC-AE945C2D3B83

Citation: Korshunova T, Malmberg K, Prkić J, Petani A, Fletcher K, Lundin K, Martynov A (2020) Fine-scale species delimitation: speciation in process and periodic patterns in nudibranch diversity. ZooKeys 917: 15–50. https://doi.org/10.3897/zookeys.917.47444

Abstract

Using the nudibranch genus *Amphorina* as a model, ongoing speciation is demonstrated, as well as how periodic-like patterns in colouration can be included in an integrated method of fine-scale species delimitation. By combining several methods, including BPP analysis and the study of molecular, morphological, and ecological data from a large number of specimens within a broad geographic range from northern Europe to the Mediterranean, five species are recognised within the genus *Amphorina*, reviewed here for the first time. Two new species from the southwestern coast of Sweden are described, *A. viriola* **sp. nov.** and *A. andra* **sp. nov.** Evidence is provided of a recent speciation process between the two closely related, yet separate, species which inhabit the same geographic localities but demonstrate strict water depth differentiation, with one species inhabiting the shallow brackish top layer above the halocline and the other species inhabiting the underlying saltier water. The results presented here are of relevance for currently debated issues such as conservation in relation to speciation, fine species delimitation, and integration of molecular, morphological and ecological information in biodiversity studies. The periodic approach to biological taxonomy has considerable practical potential for various organismal groups.

Keywords

biodiversity, biological periodicity, multilevel organism diversity, phylogeny, speciation, species problem

Introduction

Species delimitation, and hence the degree of separation between different groups of biological organisms, is a pivotal concept for modern biology, despite the fact that there is no universal agreement about the species concept itself (Stanton et al. 2019). The universal species concept proposed by de Queiroz (2007) – i.e., that species represent separately evolving evolutionary lines without any other defining characters – potentially implies the impossibility of taxonomically defining characters at a general scale. It also makes species delimitation a significant modern problem because of the considerable proportion of hidden diversity that is often seemingly impossible to detect by morphological examination alone. Thus, a majority of modern approaches imply that the addition of molecular methods to traditional morphology-based taxonomy is necessary for species identification (Nylander et al. 2004; Puillandre et al. 2012; Yang 2015; Sukumaran and Knowles 2017). In any outcome there are numerous discrepancies between species as a taxonomic unit and the underlying natural phenomenon (Callahan et al 2017; Zachos 2018a). For species as a systematic unit we only need to represent a firm taxonomic diagnosis (Winston 1999), whereas underlying natural phenomena may be represented by multilevel organism diversity fuelled by a dynamic evolutionary process (Korshunova et al. 2019a) in a species-population complex continuum (Coates et al. 2018). Therefore, it is quite common that when taxonomists come across morphologically difficult-to-distinguish species complexes at different levels of evolutionary differentiation they commonly simplify the underlying organism processes in order to taxonomically present an apparently "well-enough-delineated" species. Difficulties in assessing morphological distinctions, the apparent ease of species recognition through molecular analyses, and underestimation of the actual complex genetic and epigenetic processes within the ontogenetic framework of any organism often result in statements about the impossibility of finding reliable morphological diagnostic differences in many recently described species, thereby commonly denouncing them as cryptic (Singhal et al. 2018; Nygren et al. 2018; Bannikova et al. 2019; Struck et al. 2018). Therefore, developing approaches that will help reveal the multilevel nature of organism diversity is highly desirable, since that would place the issue within a more complex framework than traditional strictly hierarchical and diagnosis-based taxonomy.

Here we are using a complex case of nudibranch mollusc species of the genus *Amphorina* (family Eubranchidae), which are externally very difficult to distinguish as a suitable example to show the limits of currently prevailing species diagnostic methods. To delimit several closely related and similar-looking European species of this genus, we applied a suite of methods, including molecular phylogenetic analysis, BPP and ABGD, to show that several molecular clades contain all possible varieties of external morphological characters within the same species. This makes species identification and delimitation by external morphological characters apparently difficult and thus, at a first glance, calls for the existence of cryptic species. However, subsequent analysis of the colour variation within each species shows that the diversity is not fully ran-

dom but can be arranged in periodic-like rows for each species. Periodic patterns in the formation of morphological diversity were reliably estimated theoretically (Hess 2000; Hiscock and Megason 2015) and have most recently been confirmed, with robust developmental data, from different vertebrates such as fishes, birds, and mammals (Haupaix et al. 2019). However, a practical application of the periodic approach in biological taxonomy is extremely rare, although there are a few promising studies on the application of periodic patterns in proteins (Taylor 2002) and in the phylotypic ontogenetic stages of higher-level taxonomic categories (Martynov and Korshunova 2015). Therefore, we show that the combination of molecular methods with a periodic morphological approach plus ecological data facilitates species delimitation and allows the discovery of fine diagnostic characters even in externally difficult to distinguish and highly similar taxonomic complexes.

Materials and methods

Material for this study was obtained by scuba diving at widely separate locations in Europe: in the, Croatia, France, Norway, Sweden, Spain, and the United Kingdom. The specimens were deposited in the Gothenburg Natural History Museum (**GNM**) and in the Zoological Museum of Lomonosov Moscow State University (**ZMMU**). Integration of molecular and morphological data as well as phylogenetic and biogeographical patterns were used. The external and internal morphology of specimens was studied using digital cameras, under a stereomicroscope and with a scanning electron microscope.

Specimens of *Amphorina* were sequenced in Gothenburg and in Moscow for the mitochondrial genes cytochrome c oxidase subunit I (COI) and 16S rRNA, and the nuclear gene Histone 3 (H3). DNA extraction procedure, PCR amplification options, and sequence obtainment have been previously described in detail in Korshunova et al. (2017a; 2018). Protein-coding sequences were translated into amino acids to verify coding regions and avoid improper base-calling. All new sequences were deposited in GenBank (Suppl. material 1: Table S1, highlighted in bold). Additionally, publicly available sequences of representatives of the genus *Amphorina*, plus data for two *Eubranchus tricolor* (outgroup specimens) were included in the molecular analysis. Sequences were aligned with the MAFFT algorithm (Katoh et al. 2002). Separate analyses were conducted for COI (657 bp), 16S (447 bp), H3 (327 bp), and the concatenated dataset (1431 bp). Evolutionary models for each data set were selected using MrModelTest 2.3 (Nylander et al. 2004). The GTR + I + G model was chosen for the combined full dataset. Two different phylogenetic methods, Bayesian Inference (BI) and Maximum Likelihood (ML), were used to infer evolutionary relationships. Bayesian estimation of posterior probability was performed in MrBayes 3.2 (Ronquist et al. 2012). Four Markov chains were sampled at intervals of 500 generations. Analysis was started with random starting trees and 10^7 generations. Maximum Likelihood-based phylogeny inference was performed in RAxML 7.2.8 (Stamatakis et al. 2008) with bootstrap in 1000 pseudo-replications. Final phylogenetic tree images were rendered

in FigTree 1.4.2 (http://tree.bio.ed.ac.uk). To evaluate the genetic distribution of the different haplotypes a haplotype network was constructed using the Population Analysis with Reticulate Trees (PopART, http://popart.otago.ac.nz) with the TCS network method. The program MEGA7 (Kumar et al. 2016) was used to calculate the uncorrected p-distances. Alignment from the COI of *Amphorina* specimens was processed in Automatic Barcode Gap Discovery (ABGD, available at https://bioinfo.mnhn.fr/abi/public/abgd/abgdweb.html) with the following settings: a prior for the maximum value of intraspecific divergence between 0.001 and 0.1, 10 recursive steps within the primary partitions defined by the first estimated gap, and a gap width of 1.5. COI alignment was analysed separately using both Jukes-Cantor (JC69) and Kimura (K80) proposed models. The distance-based single-locus species delimitation was then used to generate primary species hypotheses, which were tested using the multi-species coalescent-based multi-locus species delimitation, BPP v.3.1. (Yang 2015). In this model, genes evolve inside a species phylogeny, the branches are species, and their properties restrict the gene trees. One of these restrictions is that the divergence times between species have to be more recent than the coalescent times for any genes shared between them, assuming no genetic transfer after speciation (Rannala and Yang 2003). This model can be used for statistical testing of species assignments (Fujita et al. 2012; Rannala 2015) and has been shown to outperform distance methods (Yu et al. 2017). COI, 16S, and H3 were used and the dataset was divided into eight primary species hypotheses to be tested based on the result of the phylogenetic and ABGD analyses, as well as brackish water or oceanic salinity environment, locality and depth of habitat (Suppl. material 1: Table S1). Two analyses (X and Y) with different population size (θs) and divergence time (τ0) priors were preformed, using the same settings and priors as in Martinsson and Erséus (2018) (X: θ 2,400, τ0 2,200; Y: θ 2,1000, τ0 2,200). All analyses were performed three times to confirm consistency between runs. We considered species delimited with a PP ≥ 0.90 in all analyses to be well supported. For clusters with a PP < 0.90, we accepted the best-supported more inclusive species. Bathymetric data were evaluated statistically using nonparametric Mann-Whitney rank sum tests.

The molecular phylogenetic and delimitation methods were combined with morphological data (Figs 1–7) to build periodic-like rows when similar colour varieties within each species were aligned using calibration by the degree of light to dark surface pigmentation and transparency of body tissue (Fig. 3), and where these similar forms establish several horizontal rows of similar looking specimens within each species.

Results

Molecular analysis

Phylogenetic analysis was performed using 46 specimens of the genus *Amphorina*, and two *Eubranchus tricolor*. Bayesian Inference (BI) and Maximum Likelihood (ML) analyses based on the combined dataset yielded similar results (Fig. 1).

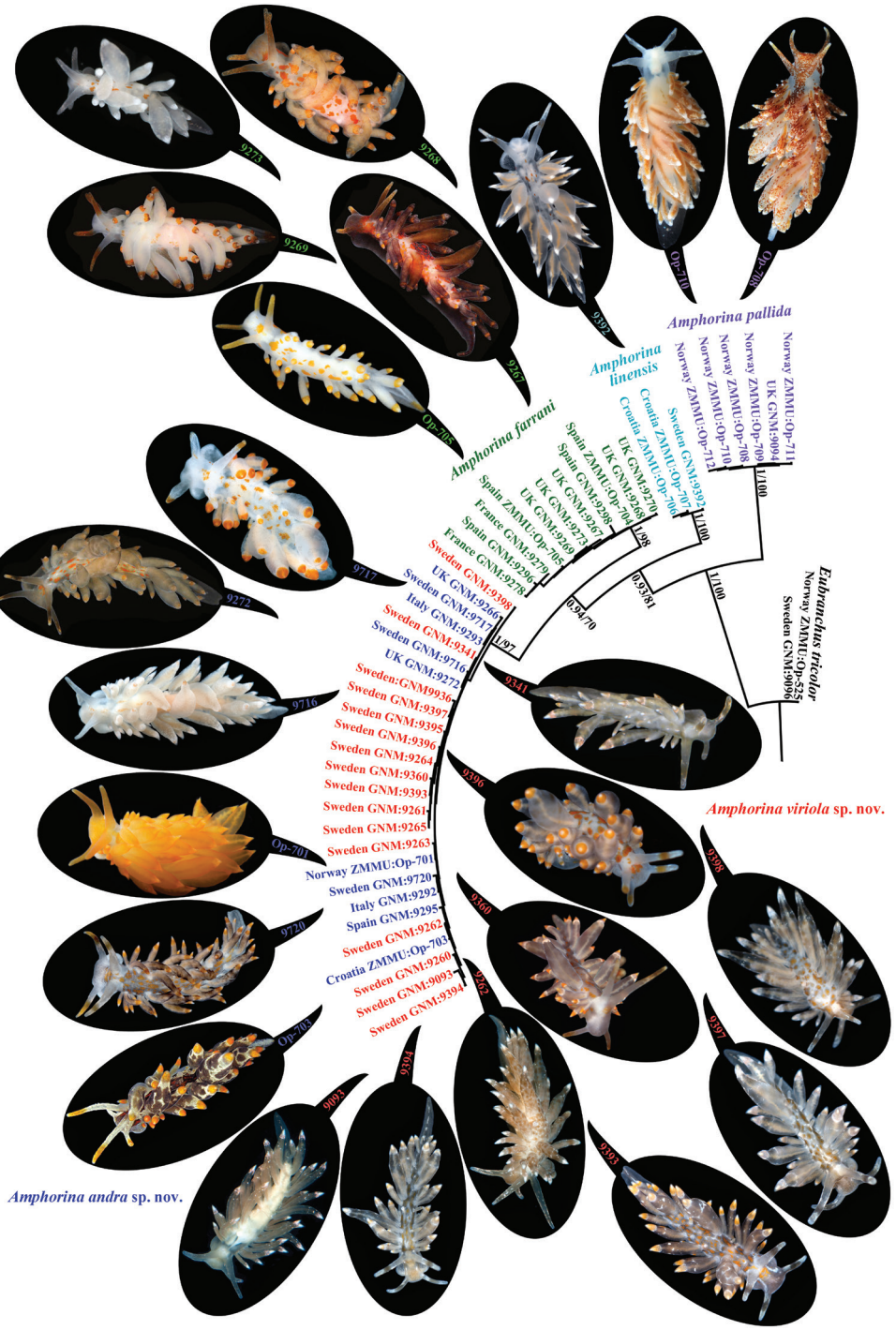

Figure 1. Phylogenetic relationships of *Amphorina* nudibranchs based on the COI+16S+H3 concatenated dataset inferred by Bayesian Inference (BI). The posterior probabilities from BI/ bootstrap values for Maximum Likelihood (ML) are shown.

Amphorina pallida and *A. linensis* species clustered in separate highly supported clades (PP = 1, BS = 100; Fig. 1). Eleven *A. farrani* specimens from the UK, France, and Spain clustered in a well-supported clade (PP = 1, BS = 98 %) and sister to another well-supported clade (PP = 1, BS = 97) containing the new species of the genus *Amphorina.*

Initially, Automatic Barcode Gap Discovery (ABGD) was used for species delimitation. ABGD analysis of the COI dataset run with two different models for species of the genus *Amphorina* and *Eubranchus tricolor* revealed five potential species: *A. pallida*, *A. linensis*, *A. farrani*, "*A.* sp. nov.", and *E. tricolor*. Nevertheless, the data of external and internal morphology of specimens in the clade "*Amphorina* sp. nov." and features of their ecology allowed us to make the assumption that the clade "*Amphorina* sp. nov." is composed of a complex of species. ABGD analysis underestimated species diversity among species with low divergence and is recommended as a first grouping hypothesis but it is not robust for definitive species delimitation proof (Puillandre et al., 2012; Suárez-Villota et al. 2018).

Analysis of multi-locus genomic sequence data under the multispecies coalescent model was conducted. The sequences were divided into an eight-species scenario (Suppl. material 1: Table S1). In analysis X, the six species model (O, P, L, F, CD, AB) is preferred with a mean PP of 0.93. In analysis Y, the same six species model is also preferred with a higher mean PP of 0.99. Based on the high support for separation, the conclusion is that these two groups represent an "*Amphorina* sp. nov." clade: *A. viriola* sp. nov. (AB), and *A. andra* sp. nov. (CD). It is important to note that all brackish water specimens from different localities were recognised as single group (AB). Specimens from the same locality (Smögen), but living deeper in oceanic saltwater below the halocline, were recognised as a separate group (CD). In the COI haplotype network (Fig. 2) haplotype groups are shown based on the results of the multilocus species delimitation analysis.

Integrating morphological and molecular data within a periodic-like framework

The molecularly and morphologically confirmed specimens of all species of the genus *Amphorina* were arranged as follows: by vertical rows indicating the topology of five recognised species according to the phylogenetic tree and by horizontal rows (periods) indicating a reduction of the transparency of the studied specimens of all species due to increasing colouration intensity (Fig. 3). Three main periods are recognised (with several subdivisions): transparent/faintly coloured; moderately transparent/coloured; and non-transparent/intensely coloured. Bottom row (period) – very little to no epidermal pigmentation, the colour is formed due to body colouration (which is almost transparent), and partly by the colouration of the digestive gland and other internal organs. With the succession of the periods upwards, there is an increasing appearance of epidermal pigmentation of several colours: opaque white, yellow, orange, red, and brown. Therefore, the higher the row, the more epidermal pigment coverage there is with a more homogeneously coloured and less transparent body. The penultimate row includes an intensely dark maroon colouration, that so far is known only for *Amphorina farrani*. Unknown, but potentially existing forms, are indicated by "unkn" for every species.

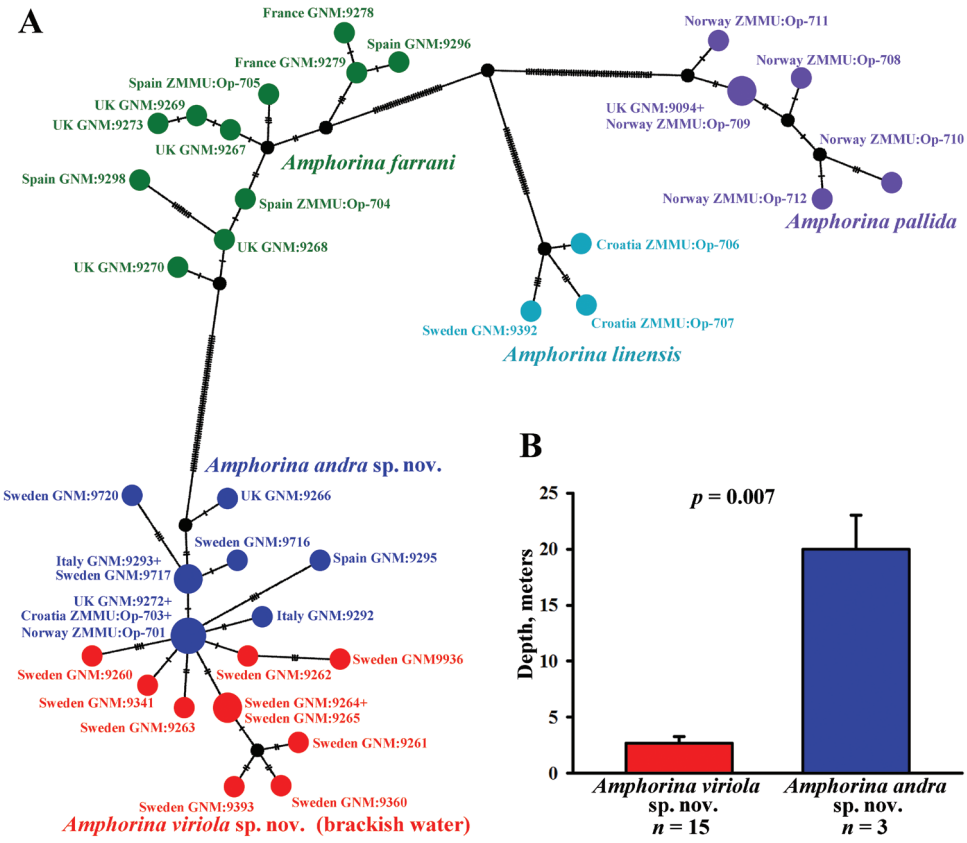

Figure 2. The haplotype network based on cytochrome c oxidase subunit I (COI) molecular data showing genetic mutations occurring within species of the genus *Amphorina* (**A**). Statistical test of the reliability of the bathymetric distribution patterns (and correlated with depths of brackish and marine environments) of *A. viriola* sp. nov. (red bar) and *A. andra* sp. nov. (blue bar) in Swedish waters (**B**). All specimens of *A. viriola* sp. nov. occur strictly in a very shallow brackish water layer above the halocline (salinity usually ca. 24–25‰), whereas in the same geographic region *A. andra* sp. nov. occur only below the halocline (at ca. 15 m depth) in waters with more stable oceanic salinity at 34–35‰.

Systematics

Phylum Mollusca
Order Nudibranchia Cuvier, 1817
Family Eubranchidae Odhner, 1934

Genus *Amphorina* Quatrefages, 1844

Amphorina Quatrefages 1844: 145–146; Martynov 1998: 774.
Non *Amphorina* sensu Trinchese 1877–1879 and auctt. (mixed with *Trinchesia* spp.)

Type species. *Amphorina alberti* Quatrefages, 1844.

Figure 3. Periodic-like presentation of colour variation patterns among all species of the genus *Amphorina*, represented as vertical rows. Three main periods (horizontal rows), each with several subperiods are presented with spotless body/colourless forms at the bottom to forms with a maximal number of spots/coloured body at the top. Note that different species fundamentally display similar colouration patterns, but not all species display all colourations, so some morphs in particular species (e.g., forms with extensive surface pigmentation and dark body in *A. farrani*, *A. linensis*, and *A. pallida*) can either be eventually discovered or do not exist, by some further constraints of the developmental system. Non-observed forms for each particular species are indicated as "unkn" = "unknown"). * = Image from Alder and Hancock 1845.

Diagnosis. Ceratal rows not branched. Up to six anterior ceratal rows (commonly no more than four). Cerata without tubercles, usually considerably swollen. Rhinophores smooth. Pharynx and jaws moderately broad. Central teeth with central cusp adpressed by adjacent lateral denticles. Prostate thick, readily distinct from vas deferens, moderate in length to very long. Distal receptaculum seminis oval to elongate on a moderately long stalk. Supplementary gland inserts into penis commonly via a narrowing stalk. Penis conical, always with a relatively short, slightly curved, hollow stylet.

Species composition. In this study, we confirm that genus *Amphorina* currently includes the following five species: *A. andra* sp. nov., *A. farrani* (Alder & Hancock, 1844), *A. linensis* (Garcia-Gomez, Cervera & Garcia, 1990), *A. pallida* (Alder & Hancock, 1842), and *A. viriola* sp. nov.

Amphorina farrani (Alder & Hancock, 1844)

Figures 1–3, 4a–c, 7A

Eolis farrani Alder & Hancock, 1844: 164–165; Alder & Hancock, 1845: fam 3, pl. 35.
Galvina farrani (Alder & Hancock, 1844): Bergh 1873: 622; Colgan 1914: 183–185.
Cavolina farrani (Alder & Hancock, 1844): Gray J.E. 1857: 226.
Eubranchus farrani (Alder & Hancock, 1844): O'Donoghue 1926: 128.
Eubranchus farrani: sensu Edmunds & Kress, 1969: forms A & B only: 890, fig. 2A, B.
Amphorina farrani (Alder & Hancock, 1844): Martynov 1998: 775.
Amphorina alberti Quatrefages, 1844: 146–151, pl. 3, fig. 5, pl. 4, fig. 3.
Aeolis adelaidae Thompson, 1860: 49.
Eolis robertianae M'Intosh, 1865: 393.
Eolis tricolor sensu Friele and Hansen 1876, non Forbes 1838.
Non *Amphorina alberti* sensu Trinchese 1877–1879 and auctt. (= *Trinchesia* spp.)
Non all forms of *Eubranchus farrani* sensu Edmunds and Kress 1969 (mixture of several species)
Non *Eubranchus farrani* sensu Schmekel and Portmann 1982: 241–243, taf. 14, figs 1–3, abb. 7.78 (= *Amphorina andra* sp. nov. + mixture of species).

Material examined. ***Neotype***. NE Atlantic, the United Kingdom, Cornwall, Newlyn Marina, (50°06'10.00"N, 05°32'45.00"W), 10–20 m depth, stones with hydroids, 12 Aug 2015, coll. David Fenwick (GNM Gastropoda – 9268, preserved length 4.5 mm).

Other specimens. NE Atlantic, the United Kingdom, Cornwall, Newlyn Marina (50°06'10.00"N, 05°32'45.00"W), 10–20 m depth, stones with hydroids, 12 Aug 2015, coll. David Fenwick (GNM Gastropoda – 9267, preserved length 3 mm, GNM Gastropoda – 9269, preserved length 2.5 mm, GNM Gastropoda – 9270, preserved length 4 mm, GNM Gastropoda – 9271, preserved length 3.5 mm), GNM Gastropoda – 9273, preserved length 5.5 mm). Mediterranean Sea, France, Banyuls (42°28'58.00"N, 03°08'13.00"E), 10–12 m depth, 07 Sept 2010, coll. Alexander Martynov and Tatiana Korshunova, one specimen (ZMMM Op-702, 9.5 mm in length, live, preserved length 4 mm). NE Atlantic, Spain, Vigo (42°24'06.00"N,

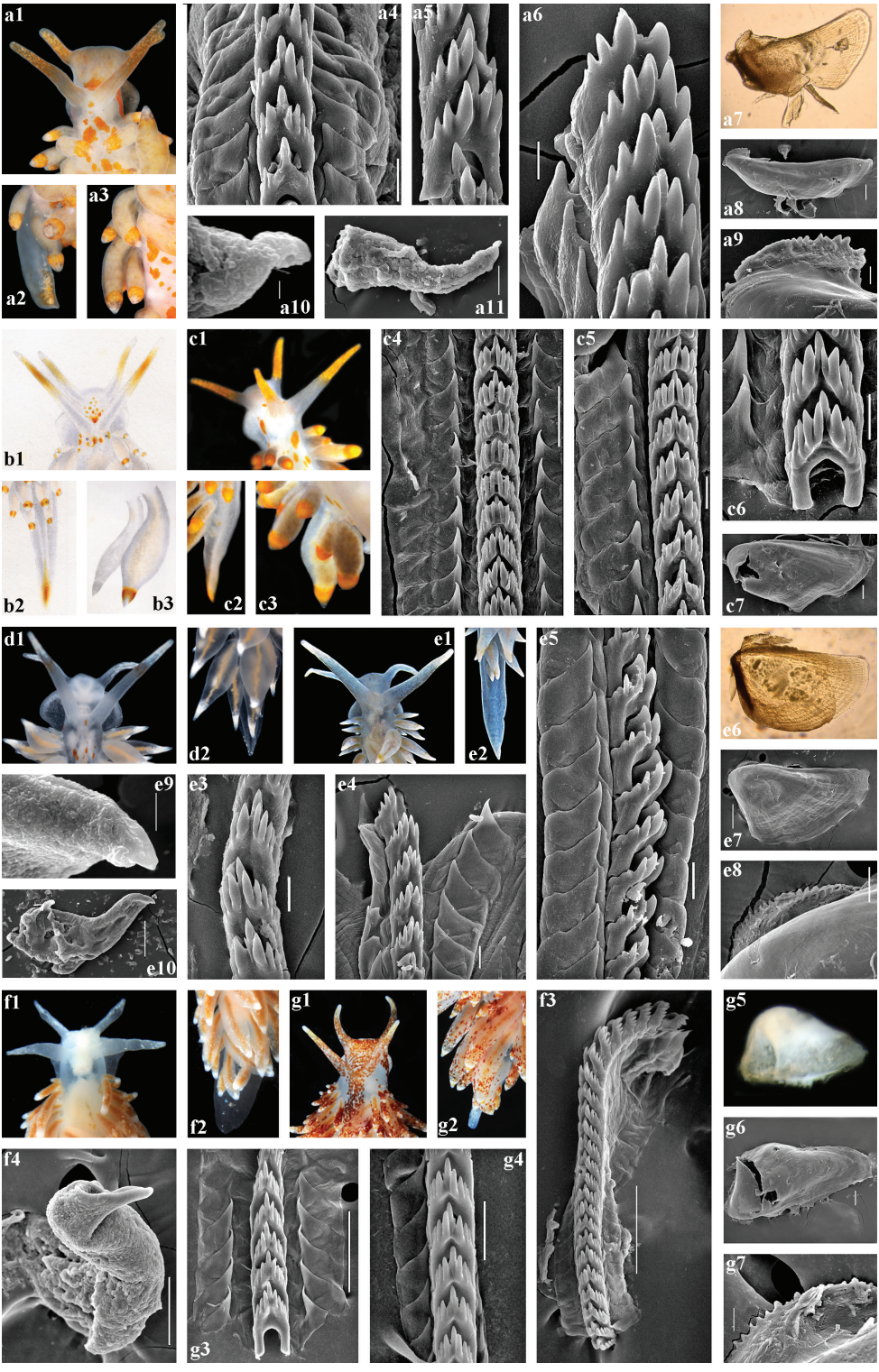
a1
a4
a5
a6
a7
a2
a3
a8
a10
a11
a9
b1
c1
c4
c5
c6
b2
b3
c2
c3
c7
d1
d2
e1
e2
e5
e6
e9
e3
e4
e7
e8
e10
f1
f2
g1
g2
f3
g5
f4
g3
g4
g6
g7

08°72'07.00"E), 5–10 m depth, 04 Sept 2010, coll. Tatiana Korshunova and Alexander Martynov, one specimen (ZMMU Op-704, 7.5 mm in length, live, preserved length ca. 4 mm). NE Atlantic, Spain, Vigo (42°24'06.00"N, 08°72'07.00"E), 5–10 m depth, 04 Sept 2010, coll. Tatiana Korshunova and Alexander Martynov, one specimen (ZMMU Op-705, 6.5 mm in length, live, preserved length 3 mm).

Diagnosis. Body up to 20 mm; large dorsal pigment spots, if present, yellow-orange, bright; in specimens with bright yellow-orange spots on dorsal side and cerata, a distinct yellow-orange spot or stripe on the tail is always present; completely pale specimens lacking tail spot or stripe; no light pinkish subapical ring on cerata; absence of punctuated white line on edge of foot; cerata commonly moderate in width without distinctly attenuated apices; digestive gland in cerata relatively broad without distinct short branches; up to four anterior rows of cerata; radular formula 35–38 × 1.1.1, copulative stylet short and slightly bent at the top, receptaculum seminis pear-shaped without short distinct stalk between reservoir and short wide base.

Description. ***External morphology.*** The live length of the neotype is ca. 10 mm (Fig. 1, GNM: 9268, Fig. 4a). The length of adult specimens may reach 20 mm and more. The body is narrow. The rhinophores are smooth and 1.5–2 times longer than the oral tentacles. The cerata are relatively long, swollen. Ceratal formula of the neotype: right (1, 3, 3; anus, 3, 3, 2, 1) left (1, 3, 4; anus, 4, 3, 2, 1). The foot is narrow, anteriorly without foot corners.

Colour. There are three main colour morphs with several subdivisions of colour variations (Fig. 3), from a completely pale body and cerata with reduced orange-yellow pigment spots, to specimens with distinct orange-yellow spots on the body and a broad subapical orange-yellow ring on each ceras, sometimes with a deep maroon body colour. No specimens with blotches of blackish surface pigmentation have been observed, nor any specimens with uniformly bright orange body. Specimens with distinct orange-yellow spots on the body always have an orange-yellow spot or stripe on

Figure 4. *Amphorina farrani* (Alder & Hancock, 1844) (**a–c**), *A. linensis* (Garcia-Gomez, Cervera & Garcia, 1990) (**d, e**) and *A. pallida* (Alder & Hancock, 1842) (**f, g**). **a** *A. farrani*, neotype GNM9268, UK, a1, head; a2, tail; a3, cerata; a4, posterior part of radula (SEM, scale bar 20 μm); a5, posterior part of radula (10 μm); a6, anterior part of radula (10 μm); a7, jaw (light microscopy); a8, jaw (SEM, 100 μm); a9, jaw details (20 μm); a10, details of stylet (3 μm); a11, penis with stylet (30 μm) **b** *A. farrani*, image from description of *Eolis farrani* in Alder and Hancock 1845 (not in copyright), b1, head; b2, tail with orange-yellow colouration; b3, cerata **c** *A. farrani*, France, Mediterranean, (external data – ZMMU Op-702), c1, head; c2, tail; c3, cerata; (internal data – GNM9278), c4, posterior part of radula (50 μm); c5, anterior part of radula (20 μm); c6, anterior part of radula (20 μm); c7, jaw (100 μm) **d** *A. linensis* GNM9392, Sweden, d1, head; d2, tail and cerata **e** *A. linensis* ZMMU Op-707, Mediterranean, Croatia, e1, head; e2, tail and cerata; e3, posterior part of radula (20 μm); e4, anterior part of radula (20 μm); e5, anterior part of radula (20 μm); e6, jaw (light microscopy); e7, jaw (SEM, 200 μm); e8, jaw details (50 μm); e9, stylet details (10 μm); e10, penis with stylet (100 μm) **f** *A. pallida* ZMMU Op-710, Norway, f1, head; f2, tail and cerata; f3, radula (100 μm); f4, penis with stylet (100 μm) **g** *A. pallida* ZMMU Op-712, Norway, g1, head; g2, tail and cerata; g3, posterior part of radula (100 μm); g4, anterior part of radula (30 μm); g5, jaw (light microscopy); g6, jaw (SEM, 100 μm); g7, jaw details (20 μm).

the tip of the tail. The upper part of the rhinophores is covered with orange pigment and scattered small white dots without a light pinkish pigment ring. The oral tentacles are similarly coloured.

Anatomy. Digestive system (Fig. 4, a4–a11, c4–c7). The jaws are triangularly ovoid. The masticatory processes of the jaws bear a single row of ca. 20–25 distinct denticles. The radular formula in three studied specimens is 35–38 × 1.1.1. The radular teeth are yellowish. The central tooth is narrow, with a low cusp and 3–7 lateral denticles, including smaller intercalated denticles that may occur in different parts of the tooth.

Reproductive system. (Fig. 7A). The ampulla is moderate in length and swollen (Fig. 7A, am). The prostate is distinct, moderately long and wide (Fig. 7A, pr). The prostate transits to a penial sheath, which contains a conical penis with a short, chitinous, very slightly curved stylet (Fig. 4, a10, a11). A supplementary ("penial") gland is relatively short and inserts into the base of the penis (Fig. 7A, pg). The receptaculum seminis is relatively small, irregularly oval, which transits directly to a large widened base without a distinct stalk (Fig. 7A, rs). The female gland mass includes mucous and capsular glands (Fig. 7A, fgm).

Distribution and habitats. Mediterranean Sea and all European Atlantic coasts to Norway, from very shallow water (0–0.5 m) to ca. 25 m. On the Swedish west coast, it lives below the halocline (15–25 m).

Remarks. Morphologically *A. farrani* differs from the closely related *A. andra* sp. nov. (which also inhabits waters with normal oceanic salinity) and the brackish *A. viriola* sp. nov. by the presence of orange-yellow colouration on the tail in spotted forms (see Discussion), the absence of forms with blackish surface pigmentation, and uniformly bright orange forms (Fig. 3). From the exclusively brackish-water species *A. viriola* sp. nov., *A. farrani* additionally differs by the absence of light pinkish subapical ceratal colouration. From *A. linensis*, *A. farrani* differs by the absence of a distinct dotted white line along the foot edge, orange-yellow and not reddish orange spots (in spotted forms), fewer ceratal rows and the shape of the cerata. From *A. pallida*, *A. farrani* differs by the larger size of dorsal spots (in spotted forms), the absence of small orange-brownish or brown spots on the cerata, and the smaller number of anterior ceratal rows. In *A. farrani*, the largest possible number of lateral denticles so far detected on the central teeth is up to seven, compared to up to five in *A. andra* sp. nov. and up to six in *A. viriola* sp. nov. The reproductive system of *A. farrani* differs from all *Amphorina* species (including *A. andra* sp. nov.) by the presence of an oval receptaculum seminis with a broad base but without a distinct stalk; from *A. viriola* sp. nov. and *A. linensis* by the shape of ampulla; from *A. pallida* by a considerably shorter prostate gland.

The species *Amphorina alberti* Quatrefages, 1844 was described the same year as *A. farrani* (Alder & Hancock, 1844) and morphologically they are essentially similar. Unfortunately, although the name *A. alberti* was referenced in some publications as a eubranchid (e.g., Bergh 1877; Iredale and O'Donoghue 1923) it was also incorrectly applied to several non-eubranchid *Trinchesia* species (Trinchese 1877–1879; Bergh 1882). *Eolis farrani* was treated as a eubranchid, although its synonymy was partially cleared up only after the mid-20th century (e.g., Edmunds and Kress 1969; Thompson

and Brown 1984; compared with the incorrect lumping synonymy of *A. farrani* in Iredale and O'Donoghue 1923). Therefore, in order to avoid confusion, the name *A. alberti* Quatrefages, 1844 was previously suppressed under plenary powers in favour of precedence of the name *Eolis farrani* Alder & Hancock, 1844 (ICZN 1966). At the same time, the genus name *Amphorina*, per se, in the original sense of Quatrefages (1844) was left as a potentially available genus name for the group of *"Eubranchus farrani"* (Heppel 1964), and that previous proposal corroborates well with the modern integrative data presented in this study.

Minimum uncorrected p-distances of the COI marker which separate *A. farrani* from *A. viriola* sp. nov., *A. andra* sp. nov., *A. linensis*, and *A. pallida* are 8.92%, 9.59%, 10.05%, and 14.31% respectively.

***Amphorina viriola* sp. nov.**
http://zoobank.org/D56F2608-384E-4C02-9BD0-8B66A679A4A9
Figures 1–3, 5, 7B

Material examined. ***Holotype.*** NE Atlantic, Skagerrak, Sweden, Region Västra Götaland, Bohuslän county, Ide fjord, close to Svarte Jan lighthouse (59°06'30"N, 11°19'30"E), 4–6 m depth, 21 Dec 2016, coll. Klas Malmberg (GNM Gastropoda – 9393, 6 mm in length, live, preserved length 3 mm). ***Paratypes.*** NE Atlantic, Skagerrak, Sweden, Region Västra Götaland, Bohuslän county, town of Lysekil, public marina, Dock D (58°16'00"N, 11°26'00"E), 0.1–0.5 m depth, a mix of algae on floating blocks, 09 May 2015, coll. Klas Malmberg, seven specimens (GNM Gastropoda – 9093, 6 mm in length, live, GNM Gastropoda – 9260, preserved length 5.5 mm, GNM Gastropoda –9261, 7 mm in length, live, preserved length 6.5 mm, GNM Gastropoda –9262, 8 mm in length, live, preserved length 6.5 mm, GNM Gastropoda –9263, 8 mm in length, live, preserved length 5 mm, GNM Gastropoda –9264, 6 mm in length, live, preserved length 5 mm, GNM Gastropoda –9265, 7 mm in length, live, preserved length 5.5 mm). NE Atlantic, Skagerrak, Sweden, Region Västra Götaland, Bohuslän county, town of Smögen, Kleven, Smögen Dyk och Upplevelse Dive centre (58°21'08.8"N, 11°13'40.6"E), 3 m depth, 25 Mar 2017, one specimen (GNM Gastropoda –9341, 7 mm in length, live). NE Atlantic, Skagerrak, Sweden, Region Västra Götaland, Bohuslän county, town of Smögen, Kleven, Smögen Dyk och Upplevelse Dive centre (58°21'30.8"N, 11°13'31.0"E), 4–4.5 m depth, 01 Apr 2017, coll. Sebastian Spora, one specimen (GNM Gastropoda –9360, 7 mm in length, live, preserved length 5 mm). NE Atlantic, Skagerrak, Sweden, Region Västra Götaland, Bohuslän county, Ide fjord, close to Svarte Jan lighthouse, five specimens (59°06'30"N, 11°19'30"E), 4–6 m depth, 21 Dec 2016, coll. Klas Malmberg (GNM Gastropoda – 9394, 8 mm in length, live, preserved length 4 mm, GNM Gastropoda – 9395, 7 mm in length, live, preserved length 3 mm, GNM Gastropoda – 9396, 6 mm in length, live, preserved length 3.2 mm, GNM Gastropoda – 9397, 8 mm in length, live, preserved length 2 mm, GNM Gastropoda – 9398, 8 mm in length, live, preserved length

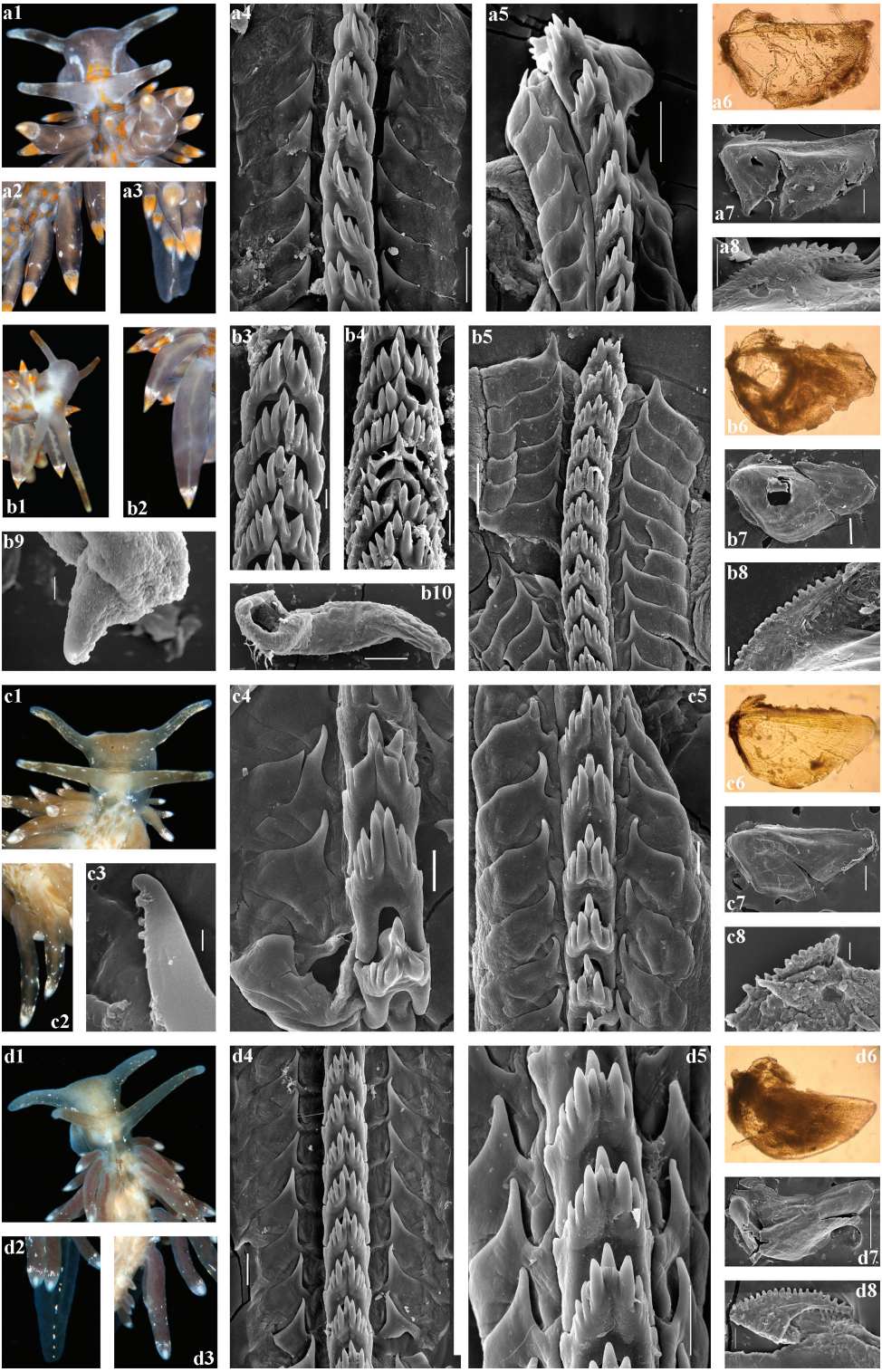
a1
a2
a3
a4
a5
a6
a7
a8
b1
b2
b3
b4
b5
b6
b7
b8
b9
b10
c1
c2
c3
c4
c5
c6
c7
c8
d1
d2
d3
d4
d5
d6
d7
d8

7 mm). NE Atlantic, Skagerrak, Sweden, Region Västra Götaland, Bohuslän county, Ide fjord, close to Svarte Jan lighthouse (59°06'30"N, 11°19'30"E), depth unknown, 2018–2019, coll. Mats Larsson, Michael Lundin (GNM Gastropoda – 9936).

Diagnosis. Body up to ca. 12 mm; large dorsal pigment spots, if present, yellow-orange, dull; in specimens with yellow-orange spots on body and cerata there is never any yellow-orange pigment spot or stripe on the tail, but there might be a median whitish line or broken line on the tail; completely pale specimens lack tail spot; light pinkish subapical ring on cerata present; absence of white punctuated line on external edge of foot; cerata commonly moderate in width without distinctly attenuated apices; digestive gland in cerata relatively broad without distinct short branches; up to four anterior rows of cerata; radular formula 31–47 × 1.1.1, copulative stylet relatively long and almost straight, at the top, receptaculum seminis pear-shaped with short distinct stalk between reservoir and long base.

Etymology. *viriola*, Lat. small bracelet, referring to the light pinkish subapical pigment ring on the cerata.

Description. ***External morphology.*** The live length of the holotype is 6 mm (Fig. 1, GNM: 9393; Fig. 5a). The length of adult specimens may reach 10–12 mm. The body is narrow. The rhinophores are smooth and 1.5–2 times longer than the oral tentacles. The cerata are relatively long, swollen. Ceratal formula of the neotype: right (2, 4, 4; anus, 3, 3, 2, 2, 1) left (2, 3, 3; anus, 3, 2, 2, 1, 1). The foot is narrow, anteriorly without foot corners.

Colour. There are three main colour morphs with several subdivisions of colour variations (Fig. 3), from a completely pale body and cerata without orange-yellow pigment spots on the body, to specimens with dull brownish orange-yellow spots. In the specimens with such spots there is never any orange-yellow colouration on the tail, but there can be a median whitish line or broken line on the tail. Specimens with greyish surface pigmentation are sometimes found, but not with blackish, non-transparent pigmentation (Fig. 3). No specimens with uniformly orange colour have been observed. The tips of the cerata may have orange-yellow pigmentation or lack pigment, leaving the cnidosacs visible. A light pinkish subapical ring on the cerata is usually present, or at least noticeable by some pinkish pigment dots. Absence of a punctuated white line on the edge of the foot. The upper part of the rhinophores are commonly covered with brownish to dark orange pigment and dispersed small white dots. The oral tentacles are similarly coloured.

Figure 5. *Amphorina viriola* sp. nov., Sweden. **a** *A. viriola* sp. nov., holotype GNM9393, a1, head; a2, cerata; a3, tail; a4, posterior part of radula (30 μm); a5, anterior part of radula (30 μm); a6, jaw (light microscopy); a7, jaw (SEM, 100 μm); a8, jaw details (30 μm) **b** *A. viriola* sp. nov., paratype GNM9360, b1, head; b2, cerata; b3, posterior part of radula (10 μm); b4, posterior part of radula (20 μm); b5, anterior part of radula (50 μm); b6, jaw (light microscopy); b7, jaw (200 μm); b8, jaw details (20 μm); b9, stylet details (10 μm); b10, penis with stylet (100 μm) **c** *A. viriola* sp. nov., paratype GNM9263, c1, head; c2, cerata; c3, apical part of lateral teeth with possible denticles (1 μm); c4, posterior part of radula (20 μm); c5, anterior part of radula (20 μm); c6, jaw (light microscopy); c7, jaw (SEM, 200 μm); c8, jaw details (20 μm) **d** *A. viriola* sp. nov., paratype GNM9260, d1, head; d2, tail; d3, cerata; d4, posterior part of radula (30 μm); d5, anterior part of radula (30 μm); d6, jaw (light microscopy); d7, jaw (300 μm); d8, jaw details (30 μm).

Anatomy. Digestive system (Fig. 5 a4–a8, b3–b8, c3–c8, d4–d8). The jaws are triangularly ovoid. The masticatory processes of the jaws bear a single row of ca. 15–21 distinct denticles. The radular formula in four studied specimens is 31–47 × 1.1.1. The radular teeth are yellowish. The central tooth is narrow, with a low cusp and 4–6 lateral denticles, including smaller intercalated denticles that may occur in different parts of the tooth.

Reproductive system. (Fig. 7B). The ampulla is moderate in length and swollen (Fig. 7B, am). The prostate is distinct, moderately long and wide (Fig. 7B, pr). The prostate transits to a penial sheath, which contains a conical penis with a short, chitinous, almost straight stylet (Fig. 5, b9, b10). A supplementary ("penial") gland is relatively short and inserts into the base of the penis (Fig. 7B, pg). The receptaculum seminis is moderate, pear-shaped (Fig. 7B, rs) with a distinct stalk, which transits to a long broad base. The female gland mass includes mucous and capsular glands (Fig. 7B, fgm).

Distribution and habitats. Swedish northwest Skagerrak coast, in the south from the town of Lysekil at the Gullmar fjord, onwards to Smögen and the Väderö Island archipelago, to the Ide fjord in the north by the border with Norway. It is always found very shallow and above the halocline (situated at 6–7 m depth within the fjords and 15 m outside the fjords), most often from 0.1 to 6 metres depth, commonly on wharf pontoons in the marina. Inhabits exclusively the brackish water layer, salinity-range: ordinarily ca. 24–25‰ but may vary from 12 to 30‰.

Remarks. Morphologically the brackish water-living *A. viriola* sp. nov. differs from the closely related *A. andra* sp. nov. by the presence of light pinkish subapical rings on the cerata, the absence of forms with non-transparent blackish pigmentation, or any forms with uniform orange colour (Fig. 3), a larger range of the number of lateral denticles on central radular teeth, a considerably smaller ampulla and an elongated and pear-shaped receptaculum seminis. From *A. farrani*, *A. viriola* sp. nov. differs by the absence of a yellow or orange median stripe on its tail, and the absence of forms with black surface pigmentation (Fig. 3). From *A. linensis*, *A. viriola* sp. nov. differs by the absence of a distinct white line (sometimes dotted) along the foot edge, orange-yellow and not reddish orange spots (in spotted forms), a smaller number of ceratal rows and the shape of the cerata, the shape and size of the ampulla and receptaculum seminis. From *A. pallida*, *A. viriola* sp. nov. differs by the larger size of dorsal spots (in spotted forms), fewer anterior ceratal rows, and the shape and size of the ampulla and receptaculum seminis.

Minimum uncorrected p-distances of the COI marker which separate *A. viriola* sp. nov. from *A. farrani*, *A. andra* sp. nov., *A. linensis*, and *A. pallida* are 8.92%, 0.15%, 9.15%, and 14.08% respectively.

Amphorina andra sp. nov.

http://zoobank.org/91211302-2EFC-4BC5-913E-1DE47D8DE2FA
Figures 1–3, 6, 7C

Eubranchus farrani: sensu Schmekel and Portmann 1982: 241–243, taf. 14, Figs 1–3, abb. 7.78 (= *Amphorina andra* sp. nov. + mixture of species).

Eubranchus farrani: sensu Trainito and Doneddu 2014: 117 (four lower figs), non Alder & Hancock, 1844.

Eubranchus farrani: sensu Prkić et al. 2018: 347, fig. 3a, b; p. 348, fig. 1a–e; p. 349, figs.1a–d; 350, fig. 1a–d; 351, fig. 1a–d, non Alder & Hancock, 1844.

Material examined. ***Holotype***. NE Atlantic, Skagerrak, Sweden, Region Västra Götaland, Bohuslän county, town of Smögen, outermost skerries (58°22'00"N, 11°11'00"E), 15–20 m depth, 29 Apr 2018, coll. Klas Malmberg (GNM Gastropoda – 9717, ca. 12 mm in length, live, preserved length ca. 5 mm).

Paratypes. NE Atlantic, the United Kingdom, Scotland, Loch Fyne (55°57'00"N, 05°23'00"W), 5–20 m depth, 24 May 2015, coll. Jim Anderson, one specimen (GNM Gastropoda –9266, preserved length 4 mm). NE Atlantic, the United Kingdom, Cornwall, Newlyn Marina (50°06'10"N, 05°32'45"W), 0–5 m depth, 12 Aug 2015, coll. David Fenwick, one specimen (GNM Gastropoda –9272, preserved length 3.5 mm). Mediterranean, Italy, Lecce (40°25'00"N, 18°16'00"E), 10–20 m depth, 20 Feb 2015, coll. Fabio Vitale, one specimen (GNM Gastropoda –9292, preserved length 2 mm). Mediterranean, Italy, Lecce (40°25'00"N, 18°16'00"E), 10–20 m depth, 05 Aug 2016, coll. Fabio Vitale, one specimen (GNM Gastropoda –9293, preserved length 2 mm). NE Atlantic, Skagerrak, Sweden, Region Västra Götaland, Bohuslän county, town of Smögen, outermost skerries (58°22'00"N, 11°11'00"E), 26 m depth, 29 Apr 2018, coll. Klas Malmberg (GNM Gastropoda – 9716, 12 mm in length, live, preserved length 10 mm). NE Atlantic, Skagerrak, Sweden, Region Västra Götaland, Bohuslän county, town of Smögen, Kleven, Smögen Dyk och Upplevelse Dive centre (58°16'00"N, 11°26'00"E), 15–20 m depth, 29 Apr 2018, coll. Klas Malmberg (GNM Gastropoda – 9720, 11 mm in length, live, preserved length 9 mm). Mediterranean Sea, Croatia, Split, Kašuni (43°50'55"N, 16°37'44"E), 20 m depth, 28 Jan 2018, coll. J. Prkić and Marko Lete, one specimen (ZMMU Op-703, ca. 11 mm in length, live, preserved length 6 mm).

Diagnosis. Body up to at least 20 mm; large dorsal pigment spots, if present, bright yellow-orange or reddish orange; in specimens with yellow-orange or reddish spots on dorsal side and cerata, there is never any yellow-orange spot or stripe on the tail, but there could be a whitish median line on the tail; completely pale specimens lack tail stripe or spot; light pinkish subapical ring on cerata absent; absence of a punctuated white line or row of dots on the edge of foot; cerata commonly moderate in width without distinctly attenuated apices; digestive gland in cerata relatively broad without distinct short branches; up to four anterior rows of cerata; radular formula 30–37 × 1.1.1, copulative stylet very short and conical, receptaculum seminis subcircular with long distinct stalk between reservoir and rapidly widening base.

Etymology. *andra* from Swedish meaning other referring to the separation from *A. viriola*.

Description. ***External morphology.*** The live length of holotype is ca. 12 mm (Fig. 1, GNM:9717). The length of adult specimens may reach 20 mm. The body is narrow. The rhinophores are smooth and 1.5–2 times longer than the oral tentacles. The cerata

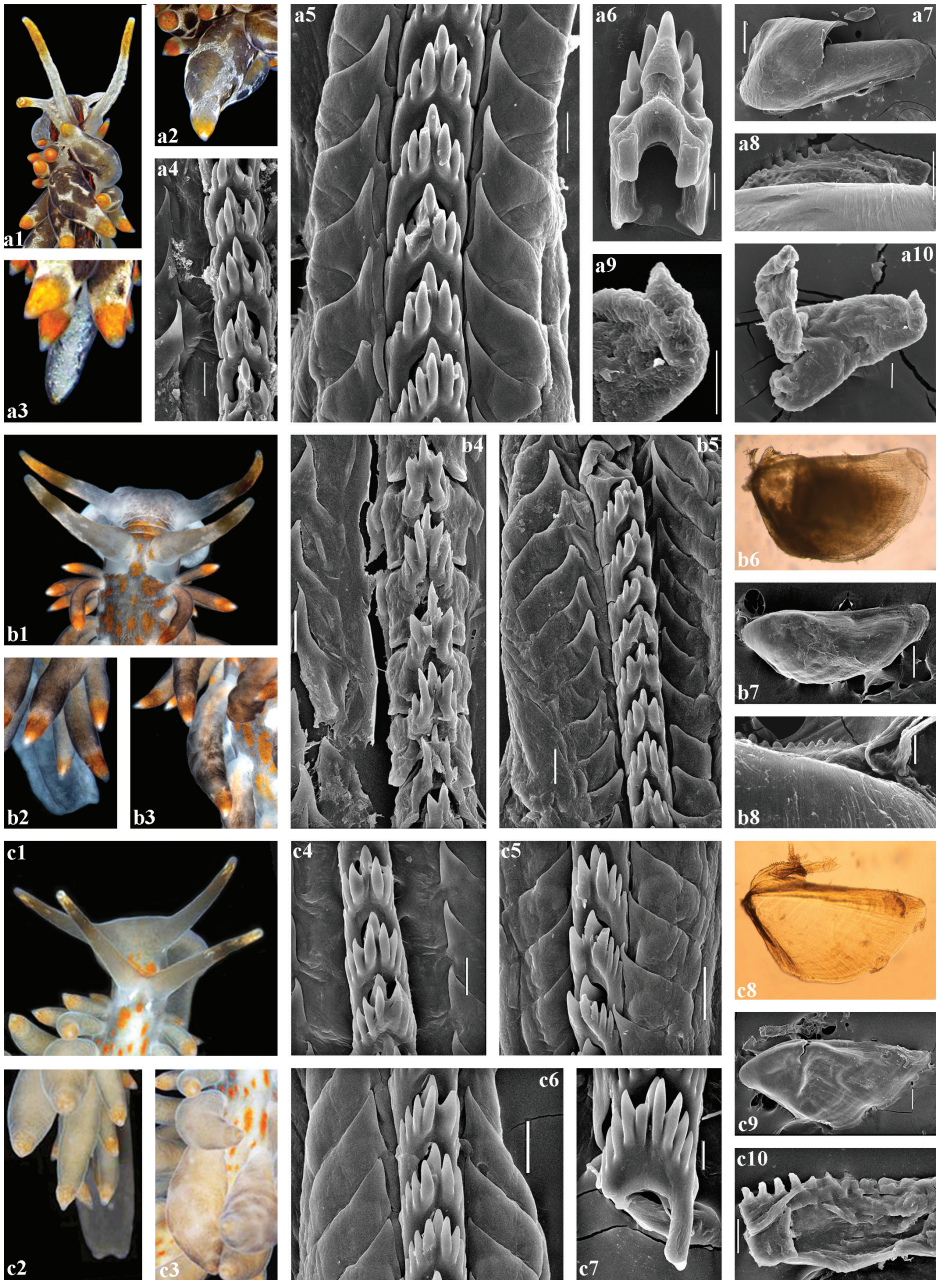

Figure 6. *Amphorina andra* sp. nov. **a** *A. andra* sp. nov., paratype ZMMU Op-703, Croatia, a1, head; a2, cerata; a3, tail; a4, posterior part of radula (20 μm); a5, anterior part of radula (20 μm); a6, posterior central tooth (10 μm); a7, jaw (200 μm); a8, jaw details (50 μm); a9, stylet details (30 μm); a10, stylet (30 μm) **b** *A. andra* sp. nov., paratype GNM9720, Sweden, b1, head; b2, tail; b3, cerata; b4, posterior part of radula (20 μm); b5, anterior part of radula (20 μm); b6, jaw (light microscopy); b7, jaw (200 μm); b8, jaw details (20 μm) **c** *A. andra* sp. nov., paratype GNM9272, UK, c1, head; c2, tail; c3, cerata; c4, posterior part of radula (20 μm); c5, posterior part of radula (10 μm); c6, anterior part of radula (20 μm); c7, anterior part of radula (20 μm); c8, jaw (light microscopy); c9, jaw (SEM, 100 μm); c10, jaw details (20 μm).

are relatively long and swollen. Ceratal formula of the holotype: right (2; 3; 3; anus, 2, 3, 2, 2) left (2, 3, 3; anus, 3, 2, 2, 1). The foot is narrow, anteriorly without foot corners.

Colour. There are three main and several subdivisions of colour variations (Fig. 3), from a completely pale body and cerata without orange-yellow pigment spots to specimens with dull orange-yellow spots on the body. In specimens with distinct dorsal spots, no distinct orange-yellow colouration on the tail has yet been observed, but there could be a whitish median line on the tail. The dorsal side of the body can be partially to almost completely covered with brown-greyish, dark brown or blackish pigment spots or blotches on some specimens and similar colours can also be present on the cerata. Yet other specimens can be without any blackish surface pigmentation but with a uniformly homogeneous bright orange to golden yellow body colour (Fig. 3). The tips of the cerata can be covered with orange-yellow pigment, or lack pigmentation, in which case the cnidosacs are visible. There is never any light pinkish subapical ring, nor any small subapical pinkish dots on the cerata. There is no distinct punctuated white line on the edge of the foot. The upper part of the rhinophores is commonly covered with orange to yellowish brownish pigment and dispersed small white spots, without the formation of a pinkish pigment ring, occasionally the entire surface of the rhinophores is covered with yellowish orange or brownish pigment. The oral tentacles are similarly coloured.

Anatomy. Digestive system (Fig. 6 a4–a8, b4–b8, c4–c10). The jaws are triangularly ovoid. The masticatory processes of the jaws bear a single row of ca. 19–28 distinct denticles. The radular formula in four studied specimens is 30–37 × 1.1.1. The radular teeth are yellowish. The central tooth is narrow, with a low cusp and 3–5 lateral denticles, including smaller intercalated denticles that may occur in different parts of the tooth.

Reproductive system. (Fig. 7C). The ampulla is large and conspicuously swollen (Fig. 7C, am). The prostate is distinct, relatively short and wide (Fig. 7C, pr). The prostate transits to a penial sheath, which contains a conical penis with a chitinous, very short, broadly conical stylet (Fig. 6, a9, a10). A supplementary ("penial") gland is relatively short and inserts into the base of the penis (Fig. 7C, pg). The receptaculum seminis is large, subcircular (Fig. 7C, rs) with a distinct long stalk which transits to a large, widened base. The female gland mass includes mucous and capsular glands (Fig. 7C, fgm).

Distribution and habitats. Mediterranean Sea and all European Atlantic coasts to Gulen at the mouth of Hardanger fjord, Norway, also possibly further north to the Trondheim fjord (Klas Malmberg, personal observation). Salinity-range: 33 to 35‰, ordinary oceanic salinity, or close to it. On the Swedish west coast, it lives below the halocline. In areas without a halocline and in more oceanic environments, it can be found closer to the surface or intertidally. In Croatia it is quite common from very shallow water (0–0.5 m) to ca. 20 m.

Remarks. Morphologically this inhabitant of waters with normal to nearly normal ocean salinity, *A. andra* sp. nov., differs from the closely related strict inhabitant of brackish waters, *A. viriola* sp. nov., by the absence of light pinkish subapical rings on the cerata, the presence of forms with blackish surface pigmentation or uniform orange colouration (Fig. 3), a lower range of the number of lateral denticles on the central radular teeth, and a considerably larger, strongly swollen ampulla and subcircular instead of pear-shaped receptaculum seminis. From *A. farrani*, *A. andra* sp. nov. differs

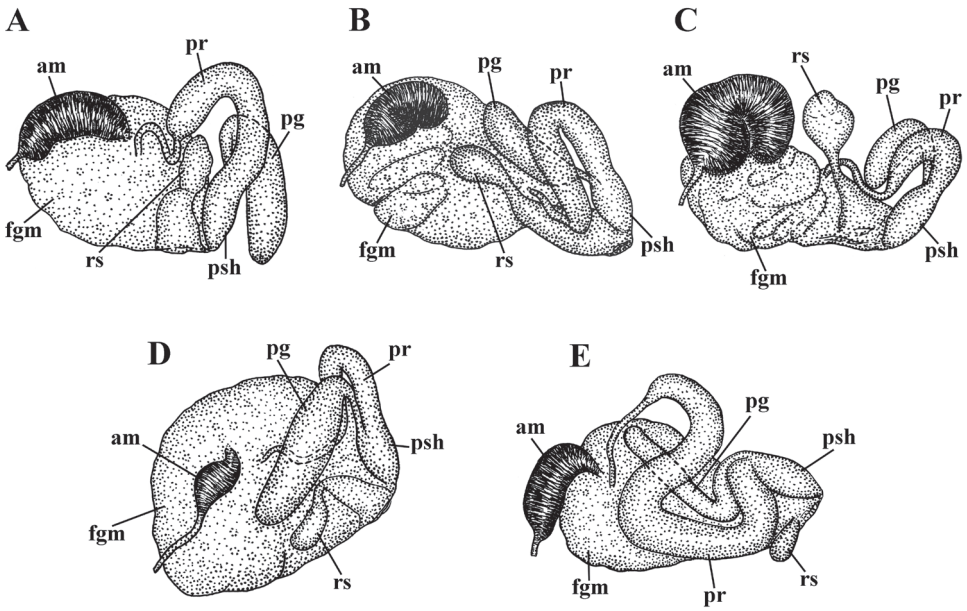

Figure 7. Reproductive systems, schemes. **A** *Amphorina farrani* **B** *Amphorina viriola* sp. nov. **C** *Amphorina andra* sp. nov. **D** *Amphorina linensis* **E** *Amphorina pallida.* Abbreviations: am–ampulla, fgm–female gland mass, pg–supplementary ("penial") gland, pr–prostate, psh–penial sheath, rs–receptaculum seminis.

by the absence of orange-yellow colouration in spotted forms (see Discussion), and the presence of forms with blackish surface pigmentation on the body and cerata (Fig. 3), *A. andra* sp. nov. differs from *A. linensis* by the absence of a distinct dotted white line along edge of the foot, fewer ceratal rows, the shape of the cerata, and the shape and size of the ampulla and receptaculum seminis. From *A. pallida*, *A. andra* sp. nov. differs by the larger size of the dorsal spots (in spotted forms), fewer anterior ceratal rows, and the shape and size of the ampulla and receptaculum seminis.

Minimum uncorrected p-distances of the COI marker which separate *A. andra* sp. nov. from *A. farrani*, *A. viriola* sp. nov., *A. linensis*, and *A. pallida* are 9.59%, 0.15%, 11.42%, and 14.92% respectively.

Amphorina linensis (Garcia-Gomez, Cervera & Garcia, 1990)

Figures 1–3, 4d–e, 7D

Eubranchus linensis Garcia-Gomez, Cervera & Garcia, 1990: 585–593.
Amphorina linensis (Garcia-Gomez, Cervera & Garcia, 1990): Martynov 1998: 775.
Eubranchus tricolor: sensu Trainito and Doneddu 2014: 118, non Forbes, 1838.
Eubranchus sp. 1: Prkić et al. 2018: 353–357.

Material examined. NE Atlantic, Skagerrak, Sweden, Västra Götalands län, Bohuslän, Väderöarna Islands (58°33'00"N, 11°02'30"E), 19 m depth, 09 Apr 2017, coll.

Klas Malmberg, one specimen (GNM Gastropoda – 9392, 10 mm in length, live, preserved length 4.2 mm). Mediterranean Sea, Croatia, Iž Island, Svežina (44°03'55"N, 15°07'15"E), 5 m depth, 13 Jan 2018, coll. A. Petani and Đani Iglić, two specimens (ZMMU Op-706, preserved length 6.5 mm, ZMMU Op-707, preserved length 6 mm).

Diagnosis. Body up to 30 mm; dorsal spots, if present, reddish orange; in specimens with dorsal and ceratal spots distinct colouration of tail absent; completely pale specimens lack tail stripe or spot; light pinkish subapical ring on cerata absent; presence of distinct line of white pigment, sometimes punctuated, on the edge of the foot; cerata commonly broad with distinctly attenuated apices; digestive gland in cerata relatively thin without distinct short branches; up to six anterior rows of cerata; radular formula 38–61 × 1.1.1, copulative stylet relatively long, slightly bent at the middle, receptaculum seminis elongate oval with moderate distinct stalk between reservoir and rapidly widening base.

Description. ***External morphology.*** The length of adult specimens may reach 30 mm. The body is narrow. The rhinophores are smooth and 1.5–2 times longer than the oral tentacles. The cerata are relatively long, very broad, with distinctly attenuated apices. Ceratal formula of the specimen from Sweden (GNM 9392): right (2, 3, 3, 4; anus, 3, 2, 2, 1) left (2, 3, 4; anus, 3, 2, 2, 1). The foot is narrow, anteriorly without foot corners.

Colour. There are three main and eight subdivisions of colour variations (Fig. 3), from a completely pale body and cerata without pigment spots to specimens with very distinct reddish orange pigment spots on the body. In specimens with distinct dorsal spots, there is never any pigmentation on the tail. A distinct white line is present on the external edge of the foot, although this could be broken or punctuated. No specimens found with blackish non-transparent pigmentation on the body, nor any homogeneously orange specimens. Absence of light pinkish subapical ring on cerata. Small white pigment dots of various density can be present on the cerata. The upper part of rhinophores commonly covered with white, relatively dense dots with small insertions of yellowish brownish pigment in some specimens, without the formation of ring-shaped colouration. The oral tentacles are similarly coloured.

Anatomy. Digestive system (Fig. 4, e3–e8). The jaws are triangularly ovoid. The masticatory processes of the jaws bear a single row of ca. 25 distinct denticles. The radular formula in the specimen studied from Croatia (Op-707) is 38 × 1.1.1. The radular teeth are yellowish. The central tooth is narrow, with a low cusp and four or five lateral denticles (three or less on the anteriormost eroded teeth), including smaller intercalated denticles that may occur in different parts of the tooth.

Reproductive system. (Fig. 7D). The ampulla is relatively small, not distinctly swollen (Fig. 7D, am). The prostate is distinct, relatively short and narrow (Fig. 7D, pr). The prostate transits to a penial sheath, which contains a conical penis with a chitinous, very short, broadly conical stylet (Fig. 4, e9, e10). A supplementary ("penial") gland is relatively long and inserts into the base of the penis (Fig. 7D, pg). The receptaculum seminis is an elongate oval (Fig. 7D, rs) with a moderate distinct stalk between the reservoir and the rapidly widening base. The female gland mass includes mucous and capsular glands (Fig. 7D, fgm).

Distribution and habitats. Mediterranean Sea and all European Atlantic coasts to Sweden and Southwest Norway. On the Swedish west coast, it lives below the halocline.

Remarks. Morphologically *A. linensis* differs from *A. farrani*, *A. viriola* sp. nov., *A. andra* sp. nov., and *A. pallida* by having reddish orange and not orange-yellow pigment spots (in spotted forms), the presence of a distinct, sometimes dotted white line along the foot edge, the shape of the cerata with attenuated apices, and a small ampulla. The present materials are well consistent with the original description of *A. linensis* (Garcia-Gomez et al. 1990) in such key characters as the shape of the cerata, the presence of a distinct white dotted line along the foot and reddish spots in some specimens, and the shape of the receptaculum seminis and prostate, but there are some differences in the number of rows of the radula, most likely due to specimen size differences. Adriatic specimens differ from the Atlantic ones in having a larger size and different colouration. There is often a light blue pigmentation that covers the cerata, rhinophores and oral tentacles, partially or completely, often the whole animal has a bluish appearance. No specimens with dorsal reddish spots have been found so far on the Adriatic coast. Mediterranean specimens of *A. linensis* have been frequently misidentified in the literature as *Eubranchus tricolor*.

Minimum uncorrected p-distances of the COI marker which separate *A. linensis* from *A. viriola* sp. nov., *A. andra* sp. nov., *A. farrani*, and *A. pallida* are 9.15%, 11.42%, 10.05%, and 13.70% respectively.

Amphorina pallida (Alder & Hancock, 1842)

Figures 1–3, 4f–g, 7E

Eolis pallida Alder & Hancock, 1842: 35–36.
Eolis minuta Alder & Hancock, 1842: 36.
Eolis picta Alder & Hancock, 1845: fam. 3, pl. 33.
Eolis flavescens Friele & Hansen, 1876: 78.
Eubranchus pallidus (Alder & Hancock, 1842): Edmunds and Kress 1969: 893–896, text figs 1, 3–6.
Amphorina pallida (Alder & Hancock, 1842): Martynov 1998: 775.

Material examined. NE Atlantic, Skagerrak, Sweden, Region Västra Götaland, Bohuslän county, town of Smögen, outermost skerries, Pesaskär (58°35'71"N, 11°18'81"E), 16–30 m depth, 14 Apr 2012, coll. Klas Malmberg (GNM Gastropoda – 8883, two specimens in same lot 10 and 7 mm in length, live, preserved length 7 and 5 mm, respectively). NE Atlantic, Skagerrak, Sweden, Region Västra Götaland, Bohuslän county, town of Smögen, outermost skerries, Pesaskär (58°07'00"N, 10°83'33"E), 10–30 m depth, 01 May 2012, coll. Klas Malmberg (GNM Gastropoda – 8928, four specimens in same lot, 13, 10, 10, and 8 mm in length, respectively, live, preserved length 9,7,7 and 6 mm, respectively). NE Atlantic, the United Kingdom, Scotland, Loch Fyne, Glas Eilean, (56°00'00"N, 05°22'00"W), 16 m depth, 25 Jan 2015, coll. Jim Anderson, one specimen (GNM Gastropoda –9094, preserved length 4 mm). NE Atlantic, Skagerrak, Sweden, Region Västra Götaland, Bohuslän county, town of Smögen, outermost sker-

ries (58°21'00"N, 11°12'00"E), 10–20 m depth, 01 May 2015, coll. Klas Malmberg, four specimens (GNM Gastropoda – 9218, 12 mm in length, live, preserved length 10 mm, GNM Gastropoda – 9219, 14 mm in length, live, preserved length 12 mm, GNM Gastropoda – 9249, 9 mm in length, live, preserved length 7 mm, GNM Gastropoda – 9250, preserved length 3.5 mm). NE Atlantic, the United Kingdom, Scotland, Loch Fyne, Glas, Eilean (55°57'00"N, 05°23'00"W), 16 m depth, 25 Jan 2015, coll. Jim Anderson, one specimen (GNM Gastropoda – 9387, preserved length 10 mm). NE Atlantic, Skagerrak, Sweden, Region Västra Götaland, Bohuslän county, Väderö Islands (58°34'00"N, 11°04'00"E), 20 m depth, 10 Apr 2015, coll. Klas Malmberg, five specimens (GNM Gastropoda – 9443, 10 mm in length, live, preserved length 8 mm, GNM Gastropoda – 9444, 9 mm in length, live, preserved length 7 mm, GNM Gastropoda – 9452, 9 mm in length, live, preserved length 6 mm, GNM Gastropoda – 9453, 7 mm in length, live, preserved length 6 mm, GNM Gastropoda – 9454, 11 mm in length, live, preserved length 9 mm). NE Atlantic, Skagerrak, Sweden, Region Västra Götaland, Bohuslän county, Gullmar Fjord, Släggabåden between Släggö Island, Lysekil and Kristineberg marine station (58°15'70"N, 11°26'60"E), 50–55 m depth, soft clay bottom, 01 Jun 2017, coll. Kennet Lundin (GNM Gastropoda – 9501, 5 mm in length, live, preserved length 4 mm). NE Atlantic, Skagerrak, Sweden, Region Västra Götaland, Bohuslän county, Ide fjord, close to Svarte Jan lighthouse (59°07'00”N, 11°19'00"E), 20 m depth, 01 Sept 2015, coll. Klas Malmberg (GNM Gastropoda – 9695, 4 mm in length, live, preserved length 3 mm). NE Atlantic, the United Kingdom, Northern Ireland, Portaferry (54°23'00"N, 05°35'00"W), 10–20 m depth, soft clay bottom, 14 Mar 2015, coll. Bernard Picton (GNM Gastropoda – 9597, preserved length 5 mm). NE Atlantic, the United Kingdom, Northern Ireland, Portaferry (54°23'00"N, 05°35'00"W), 10–25 m depth, soft clay bottom, 10 Mar 2014, coll. Bernard Picton (GNM Gastropoda – 9601, preserved length 11 mm). NE Atlantic, Norway, Gulen Dive Center (60°57'27.11"N, 5°07'47.10"E), depth 15–20 m, stones, collectors T.A. Korshunova, A.V. Martynov, five specimens (ZMMU Op-708, 17.03.2014, ca. 20 mm in length, live, ca. 8 mm in length, preserved, ZMMU Op-709, 17.03.2014, ca. 15 mm in length, live, ca. 6 mm in length, preserved, ZMMU Op-710, 19.03.2015, 18 mm in length, live, 7 mm in length, preserved, ZMMU Op-711, 07 Mar 2016, 10 mm in length, live, ca. 5 mm in length, preserved, ZMMU Op-712, 12.5 mm in length, live, ca. 6 mm in length, preserved).

Diagnosis. Body up to 25 mm; dorsal pigment spots (if present), small and often rounded, forming an almost continuous orange-brownish covering; in specimens with dorsal pigment spots there is never any colouration of the tail; completely pale specimens likewise lack a tail spot; absence of light pinkish subapical ring on cerata; absence of punctuated white line on external edge of foot; cerata commonly moderate in width without distinctly attenuated apices; digestive gland in cerata relatively broad without distinct short branches; up to four anterior rows of cerata; radular formula 18–41 × 1.1.1, copulative stylet long and bent at the top, receptaculum seminis oval without stalk and widened base.

Description. ***External morphology.*** The length of adult specimens may reach 25 mm. The body is narrow. The rhinophores are smooth and 1.5–2 times longer than the oral ten-

tacles. The cerata are relatively long, very broad, with distinctly attenuated apices. Ceratal formula of the specimen ZMMU Op-708 from Norway: right (2, 4, 3, 5; anus, 5, 3, 3, 2, 2) left (1, 3, 3, 5; anus, 4, 4, 3, 2, 2). The foot is narrow, anteriorly without foot corners.

Colour. There are three main and eight subdivisions of colour variations (Fig. 3), from a completely pale body and cerata without spots to specimens with many small rounded reddish orange/brownish pigment spots on the body and cerata. In specimens with distinct dorsal pigment spots, there is never any pigment on the tail. No specimens with blackish body pigmentation or uniformly bright orange colouration were ever observed. Absence of light pinkish subapical ring on cerata. Absence of line or row of dots of white pigment on external edge of foot. The upper part of the rhinophores is often covered with white, relatively dense spots, or in some specimens with dense orange-reddish pigment, but without the formation of pigment rings. The oral tentacles are similarly coloured.

Anatomy. Digestive system (Fig. 4, f3, g3–g7). The jaws are triangularly ovoid. The masticatory processes of the jaws bear a single row of ca. 25 distinct denticles. The radular formula in two studied specimens from Norway (Op-711, Op-712) is 18–31 × 1.1.1. The radular teeth are yellowish. The central tooth is narrow, with a low cusp and four or five lateral denticles (three or less on the anteriormost eroded teeth), including smaller intercalated denticles that may occur in different parts of the tooth.

Reproductive system. (Fig. 7E). The ampulla is relatively small, not distinctly swollen (Fig. 7E, am). The prostate is distinct, extremely long and wide (Fig. 7E, pr). The very large, S-shaped prostate transits to a penial sheath, which contains a conical penis with a long chitinous stylet, bent in the middle (Fig. 4, f4). A supplementary ("penial") gland is relatively long but thin and inserts into the base of the penis (Fig. 7E, pg). The seminal receptacle is oval (Fig. 7E, rs) without either a stalk or a wide base. The female gland mass includes mucous and capsular glands (Fig. 7E, fgm).

Distribution and habitats. Western Mediterranean Sea and all European Atlantic coasts to northern Norway. On the Swedish west coast, it lives below the halocline.

Remarks. Morphologically *A. pallida* differs from *A. farrani*, *A. viriola* sp. nov., *A. andra* sp. nov., and *A. linensis* by small rounded brownish orange pigment spots on the body (in spotted forms), by small brownish orange spots on the cerata, and by a very large S-shaped prostate.

Minimum uncorrected p-distances of the COI marker which separate *A. pallida* from *A. viriola* sp. nov., *A. andra* sp. nov., *A. linensis*, and *A. farrani* are 8.92%, 9.59%, 10.05%, and 14.31% respectively.

Discussion

The nudibranch genus *Amphorina* as a model for ontogenetic periodicity

The genus *Amphorina* is a suitable model for studying the link between a "static" taxonomic system and the underlying evolutionary processes fuelled by ontogenetic periodicity due to both the morphological uniformity across the genus (especially regarding

internal characters) on the one hand, and to the large degree of variation in external colouration on the other. Using morphological and molecular data, we show that the genus *Amphorina* is a well-delineated monophyletic genus of the family Eubranchidae (Fig. 1). The validity of the narrowly defined, monophyletic genus *Amphorina*, which was previously resurrected by Martynov (1998), is thus confirmed. The species composition of the genus is restricted here to only five European species (*A. farrani*, *A. viriola* sp. nov., *A. andra* sp. nov., *A. linensis*, and *A. pallida*, Figs 1–7), and a review of this genus is presented for the first time. The genus *Amphorina* is characterised by the presence of up to six anterior ceratal rows, a distinct typically long prostate and a single chitinous penial stylet. The genus *Eubranchus* sensu stricto (type species *E. tricolor* Forbes, 1838) differs considerably from the genus *Amphorina* by the presence of numerous branched ceratal rows, a supplementary gland that is inserted into the vas deferens instead of the penis, the absence of a distinct prostate, and an unarmed penis (Martynov 1998); other eubranchid species are pending review. By the above-listed combination of characters, the genus *Eubranchus* is, in a narrow sense, similar to several other aeolidacean families (see Korshunova et al 2017a, b), but differs from the genus *Amphorina*. The previous unification of the genus *Amphorina* with the genus *Eubranchus* ignored these morphological differences and plainly followed a previous lumping paradigm in nudibranch taxonomy, which has recently been contested (Korshunova et al. 2019b). The concept of multilevel organism diversity (Korshunova et al. 2017a, 2019a) promotes the establishment of small taxonomic units in order to coherently describe hidden diversity at different levels of evolutionary differentiation.

Ongoing speciation within the *Amphorina* complex in the Skagerrak area

Amphorina viriola sp. nov. and *A. andra* sp. nov. are clearly distinguished, with high support by the BPP analysis and also by differences according to the haplogram (Fig. 2A), but the latter also shows a reticulated pattern for *Amphorina andra* sp. nov., which is of relevance for the long-standing problem of speciation. *Amphorina viriola* sp. nov. is apparently at a late stage of the speciation process, since according to ecological, morphological, and genetic data *A. viriola* sp. nov. is separated from *A. andra* sp. nov. but still retains some genetic connection with it. There is a possible window for cross-breeding and subsequent gene flow during periods of storms or upwelling when the surface layer above the halocline temporarily attains a higher salinity, rendering it available for *A. andra* sp. nov. Any species, while forming, must pass through this "reticulated phase" of genetic exchange (e.g., Hennig 1966; Crawford et al. 2015) when it still retains some partial connection with its ancestral species; thus, this case is not only of particular taxonomic interest, but of general evolutionary importance. Recently, multiple evidence was obtained for a very recent speciation event when closely related species formed a reticulated pattern (Burress et al. 2018). Here we show that two *Amphorina* species, *A. viriola* sp. nov. and *A. andra* sp. nov., show significant divergence according to the BPP analysis, demonstrate a statistically well-supported (p = 0.007,

Fig. 2B) difference in ecological niches/environment (including robust bathymetrical differences correlated with drastic salinity differences, characteristic for the marine waters of southwestern Sweden), also possess minor morphological differences, and at the same time form a partly reticulated pattern according to the molecular phylogenetic data (Fig. 1). This is in line with proposals that coalescent analysis should be supplied together with phenotypic and ecological data (Sukumaran and Knowles 2017).

The present case clearly differs from the situation when a reticulated molecular phylogenetic pattern of two closely related species was used for evidence of their synonymy (Ludt et al. 2019), because significant molecular and ecological data are presented for two *Amphorina* species and their ongoing speciation processes. When a species is still in the process of speciation (and we can expect it for a majority of species) it must preserve various degrees of connection with an ancestral species (an ancestral group of populations) and hence some ability to hybridise with the ancestral species. Such processes will lead to a partially reticulated pattern of the obtained phylogenetic trees. There are also previous data that taxonomically recognised species and genera, from invertebrates to hominins, are able to hybridise with fertile offspring. Therefore, there is no contradiction when species with a significant degree of incomplete speciation show some reticulated phylogenetic patterns and sometimes very insignificant genetic differences within taxonomically recognised species. One of the most evident cases is the innumerable African cichlid species (Koblmüller et al. 2019), for many of these have very low genetic divergences (0.1–0.25%) and evidence has repeatedly shown a substantial gene flow among numerous taxonomically well-established species (Burress et al. 2018; Gante et al. 2016; Malinsky et al. 2018). This pattern is very similar to what we found here for two *Amphorina* species. In support of the model presented here, there is evidence that a brackish-water environment, and particularly the waters in the eastern Skagerrak, Kattegat, and Baltic regions, strongly facilitates the formation of new organism groups/units that can be taxonomically evaluated from genus (Korshunova et al. 2018), to species (Momigliano et al. 2017) or to a specific population (Berg et al. 2015).

Remarkably, both species, *A. viriola* sp. nov. and *A. andra* sp. nov., occur in the same geographical region on the coast of southwestern Sweden, which is characterised by the presence of two different bathymetric layers, one that corresponds to the Baltic-influenced brackish surface layer, where *A. viriola* sp. nov. is found, whereas the deeper layer represents close to normal oceanic salinity. The Kattegat area between Sweden and Danish Jutland receives brackish water from the Baltic Sea via the Bälten and Öresund straits in the south and the so-called Baltic surface current flows onward north along the Swedish west coast. The difference in salinity leads to a distinct halocline in the Kattegat and the eastern part of the Skagerrak, at ca. 15 metres depth, with a layering of brackish surface water and saltier deep-water. The western part of Skagerrak has no such layering, and here the salinity is high from the surface to the bottom. At the southernmost part of the Kattegat the salinity of the surface layer is only ca. 8‰ but increases successively northward. At the Swedish coast of the Skagerrak, the salinity of the surface layer is usually approximately 24–25‰, but it is highly variable

with extremes ranging from 12 to 30‰ depending on weather conditions and strong winds. The deep-water layer below the halocline is, by contrast, much more stable in salinity, with 32–34‰. In the Gullmar fjord and the Ide fjord the halocline is shallower than 15 metres, usually ca. 6–7 metres, and there is an outflow of freshwater from river outfalls along the inner parts of the fjords. There is also freshwater outflow to the Swedish west coast from the two largest rivers in the area, the Göta river, entering at the port of Gothenburg, and Glomma river entering the Oslo fjord in Norway. The latter has a large seasonal impact on the northernmost part of the Swedish coast of Skagerrak, especially in spring, during snow melt in the mountains. Another factor in maintaining a long-term stability of bathymetric layers is the very low tidal exchange in the area, normally only 20 cm in Skagerrak. In this study we performed a statistical test for the bathymetric distribution of the two species *A. viriola* sp. nov. and *A. andra* sp. nov. and confirmed with high support ($p = 0.007$) that *A. viriola* sp. nov. and *A. andra* sp. nov. are very strictly divided, according to the brackish water and oceanic salinity layers (halocline) without any overlap (Fig. 2B). Thus, these results robustly confirm firm the ecological differentiation between these two species.

Taking into consideration the population-to-species continuum (Coates et al. 2018) and the artificial strict distinction of species for taxonomic purposes (Zachos 2018b), we cannot evaluate the group of nudibranchs presented here as simply a modified population since it shows stable morphological, genetic and ecological features. The current system of zoological nomenclature was formed during pre-evolutionary times. It does not address the underlying genetic-epigenetic processes and provides only a very rigid application of a name to some "type specimen". At the same time, an arsenal of various molecular, phylogenetic and delimitations methods that can detect subtle, but statistically reliable, differences between organism groups are in direct contradiction with the persistent system of nomenclature. Therefore, under the putatively same "species rank" various natural organism entities/groups, at a very different degree of a very complex population to species continuum (Coates et al. 2018), can be concealed if the evolutionary processes in the current nomenclature system are insufficiently estimated. The case of the small genus *Amphorina* clearly demonstrates such multilevel organism diversity (Korshunova et al. 2019a) at different stages of speciation/evolutionary differentiation. Notably, all species show similar external and internal traits, which can be easily confused even by an expert not specifically trained for that genus. But according to the integrative data for these species, *A. pallida* definitely has a stronger degree of differentiation from other *Amphorina* species than the differentiation between *A. farrani* and *A. andra* sp. nov. In turn, *A. andra* sp. nov., has a much lesser degree of differentiation from *A. viriola* sp. nov. than the latter does from *A. pallida*. However, despite that the degree of "speciation" is different in all these organism groups, they are still considered to fall within the "species category". Notably, *Amphorina viriola* sp. nov. shows a similar periodic-like pattern of different colouration morphs as its sister species, the closely related *A. andra* sp. nov. and *A. farrani*. (Fig. 3). Similar periodic patterns in colouration are demonstrated in all five species of the genus *Amphorina*, together constituting a "species complex" that is difficult to

distinguish, while at the same time it provides a model for the investigation of periodic morphological patterns for taxonomy. The data presented in this study thus allow for integrating robust evidence of speciation, from an evolutionarily little assessed invertebrate group, with the most current and important topic of periodic patterns in the formation of morphological diversity (Haupaix and Manceau 2018).

Periodic patterns in organism diversity facilitate fine-scale species delimitation: the nudibranch case

Periodic-like patterns in application to biology, though discussed for a long time (e.g., Vavilov 1922; Hess 2000), and successfully applied for protein structure (Taylor 2002), have only recently been proposed for applied use in taxonomy and phylogeny (Martynov and Korshunova 2015). In this example, evident periodicity was revealed for a higher-level organism group using an ontogenetic phylotypic stages approach. Indeed, compared to the stricter periodic system in chemistry, variability of biological organisms extends far beyond those of regular parallel rows (e.g., Bolnik et al. 2019). However, there are many examples when various features appear parallel in related taxa. For instance, in the present study we confirmed a remarkable parallelism in the colouration of several separate, but related, species of the genus *Amphorina*. Recently, interest in periodic patterns in biology was reviewed and several studies found evident periodic patterns of colouration in birds and other vertebrate groups, and also found a direct link to constraints in early developmental patterns (Haupaix et al. 2018, Haupaix and Manceau 2019). Thus, the idea was further confirmed that periodic patterns in adult morphology of different taxa are underlined by early developmental factors. Therefore, even in a majority of other cases where we do not have data on early development, we can reasonably infer that ontogenetic periodicity must influence adult morphology in the majority of metazoans, since all of them possess a similar homeobox system of early development (Holland 2013). For example, colour and pattern polymorphism of land snail shells of the genus *Cepaea* has been shown to be caused by a complex interaction between gene expression and local environment, with both random and regular colour patterns (e.g., Jones et al. 1977; Cook 2017; Davison et al. 2019). The underlying genetic basis for the appearance of any characters can thus be either very complex or simple and irregular, but when such variations are brought up to higher taxonomic and phylogenetic levels, the periodic/quasi-periodic patterns become more evident, although still with irregularities. For example, the helicid land snails turned out to be a polyphyletic assemblage, but they share a similar degree of polymorphism in parallel in several lineages (Neiber and Hausdorf 2015). Our approach implies potential analysis within a periodic framework of any of the characters, not only of colour, which emphasises the interspecific periodic patterns rather than intraspecific, more continuous variations. Therefore, the evaluation of periodic patterns in external appearance is a useful tool for identification in cases where species are difficult to delimit. The present *Amphorina* case is a suitable example because it comprises several very closely related

species, all of them demonstrating similar patterns of genetic variability (Figs 1, 3), and at the same time it includes an evident example of a late stage of speciation. All these factors make species delimitation using traditional taxonomic or standard modern approaches particularly difficult.

The appearance of similar colour patterns across different species of the genus *Amphorina* can reasonably be termed periodic patterns, although this periodicity indeed only partly approaches the periodicity which is known in chemistry (Babaev and Hefferlin 1996), with considerable reservations. In biology, the main problem of the justification of periodicity is that among numerous characters it is possible to arbitrarily choose some that fit periodic patterns (Popov 2002; Babaev 2019). In the present case, however, we detected that colour periodicity is a part of natural polymorphism within a molecularly proven group (Fig. 1) of closely related species in the genus *Amphorina*. These similar colour variations appear in parallel, periodically, within the different species and immediately influence the key features for taxonomic diagnoses and cannot be discarded as auxiliary characters. This allows the investigation of periodic patterns in similar phylotypic periods to continue among distantly related families within higher-ranked monophyletic taxonomic groups (Martynov and Korshunova 2015). Since colour polymorphism is influenced by some periodicity at the level of the developmental genes it can be used as an underlying source of periodic patterns in biodiversity and systematics. Thus, the vertical columns represent particular species, whereas horizontal periods are patterns of colouration within the genus *Amphorina*. For each species within that genus a periodic appearance of a similar colour pattern can be expected (Fig. 3).

Application of a periodic-like arrangement of vertical rows and horizontal periods helps to highlight subtle differences between apparently highly similar forms. For example, some white forms with distinct yellow-orange spots of *A. farrani* are very similar to corresponding forms of *A. andra* sp. nov., but in the latter, a distinct yellow-orange pigment spot or stripe on the tail is commonly absent (Fig. 3). Such a character is very easy to overlook in the traditional "overall differences" approach, whereas a periodic-like arrangement makes it evident. Furthermore, by using a periodic approach in taxonomy we can detect the absence of some particular colour forms in closely related species, thus revealing its predictive function, as is common in chemistry. For example, uniformly coloured bright orange specimens were discovered for *A. andra* sp. nov., but not for the closely related *A. viriola* sp. nov. or *A. farrani*, despite the investigation of hundreds of specimens (Fig. 3). Either such a morph for some reason does not exist in *A. viriola* sp. nov. or *A. farrani*, or it can potentially be discovered in the future. Perhaps a more instructive example is when forms with dark surface pigmentation do occur within both *A. viriola* sp. nov. and *A. andra* sp. nov., but are not yet known in *A. farrani* (Fig. 3). Because there are forms with dark underlying body colour within *A. farrani* (Fig. 3) it is reasonable to expect future findings of forms with extensive dark surface pigmentation also within *A. farrani.* Such predictive functionality thus facilitates species delimitation but also can compel taxonomy to become a more rigorous discipline, along with molecular phylogeny, and prevent simply chaotically mapping morphological features within apparently "indistinguishable species complexes". The

periodic approach to biological taxonomy coupled with molecular analysis has the potential for various organismal groups, not only molluscs, because when arranging all the particular character states/colour patterns detected for some particular species, it is easier to distinguish species complexes, by a process of identifying successively finer details. This is useful for various practitioners, especially for citizen scientists, not as an artificial addition to already established taxonomic methods, but rather as a mapping of naturally existing patterns of biological diversity. Finer analysis shows that such complexes are possible to distinguish morphologically, by using a combination of various methods including the periodic approach suggested here. Several further studies on different groups, such as rodents (Johnson et al. 2018) and fishes (Gante 2018; Salis et al 2019), confirmed the existence of periodic patterns during the development of morphological characters, yet without direct construction of periodic-like tables, which can be a next step. Thus, these complex periodic-like genetic-epigenetic interactions within an ontogenetic framework can work as a theoretical foundation and confirmation of the practical validity of a periodic approach in taxonomy and phylogeny.

Acknowledgements

We would like to give special thanks to the team of Gulen Dive Centre (Christian Skauge, Ørjan Sandnes, Monica Bakkeli, and Guido Schmitz) and to Torkild Bakken (NTNU University Museum) for their generous help during fieldwork in Norway. Klas Malmberg and Kennet Lundin warmly thank the staff at the Smögen Dyk och Upplevelse Dive Centre for their enthusiasm and generous help during fieldwork in Sweden. Jakov Prkić and Alen Petani would like to thank Marko Lete and Đani Iglić for their great help during fieldwork in Croatia. David Fenwick (www.aphotomarine.com) is warmly thanked for providing specimens and photographs of *Amphorina* spp. to the Gothenburg Natural History Museum. Mats Larsson and Michael Lundin most kindly provided specimens from the Ide fjord. Electron Microscopy Laboratory, Moscow State University is gratefully acknowledged for support. Reviewers are thanked for constructive comments and suggestions. This work was supported by a research project of MSU Zoological Museum (AAAA-A16-116021660077-3).

In memory of Rolf Lundin.

References

Alder J, Hancock A (1842) Descriptions of several new species of nudibranchous Mollusca found on the coast of Northumberland. Annals and Magazine of Natural History 9: 31–36. https://www.biodiversitylibrary.org/page/2312453

Alder J, Hancock A (1844) Description of a new genus of nudibranchiate Mollusca, with some new species of *Eolis*. Annals and Magazine of Natural History 13: 161–167. https://doi.org/10.1080/03745484409442588

Alder J, Hancock A (1845) A monograph of the British Nudibranchiate Mollusca: with figures of all the species. Ray Society, London, 1–54. https://doi.org/10.5962/bhl.title.65015

Babaev E (2019) Periodic law in chemistry and other sciences. Pure and Applied Chemistry 91: 2023–2035. https://doi.org/10.1515/pac-2019-0821

Babaev E, Hefferlin R (1996) The concepts of periodicity and hyper-periodicity: from atoms to molecules. In: Rouvray D (Ed.) Concepts in Chemistry: A Contemporary Challenge. Research Studies Press, London, 24–81.

Bannikova A, Lebedev V, Dubrovskaya A, Solovyeva E, Moskalenko V, Kryštufek B, Hutterer R, Bykova E, Zhumabekova B, Rogovin K, Shenbrot G (2019) Genetic evidence for several cryptic species within the *Scarturus elater* species complex (Rodentia: Dipodoidea): when cryptic species are really cryptic. Biological Journal of the Linnean Society 126: 16–39. https://doi.org/10.1093/biolinnean/bly154

Berg PR, Jentoft S, Star B, Ring KH, Knutsen H, Lien S, Jakobsen KS, André C (2015) Adaptation to low salinity promotes genomic divergence in Atlantic cod (*Gadus morhua* L.). Genome Biology and Evolution 7: 1644–1663. https://doi.org/10.1093/gbe/evv093

Bergh R (1873) Beiträge zur Kenntniss der Aeolidiaden. I. Verhandlungen der königlich-kaiserlich Zoologisch-botanischen Gesellschaft in Wien (Abhandlungen) 23: 597–628.

Bergh R (1877) Beiträge zur kenntniss der Aeolidiaden. V. Verhandlungen der königlich kaiserlich Zoologisch-botanischen Gesellschaft in Wien (Abhandlungen) 27: 807– 840.

Bergh R (1882) Beiträge zur Kenntniss der Aeolidiaden. VII. Verhandlungen der königlich kaiserlich Zoologisch-botanischen Gesellschaft in Wien (Abhandlungen) 32: 7–74.

Bolnick DI, Barrett RDH, Oke KB, Rennison DJ, Stuart YE (2019) (Non)parallel evolution. Annual Review of Ecology, Evolution, and Systematics 49: 303–330. https://doi.org/10.1146/annurev-ecolsys-110617-062240

Burress ED, Alda F, Duarte A, Loureiro M, Armbruster JW, Chakrabarty P (2018) Phylogenomics of pike cichlids (Cichlidae: *Crenicichla*): the rapid ecological speciation of an incipient species flock. Journal of Evolutionary Biology 31: 14–30. https://doi.org/10.1111/jeb.13196

Callahan BJ, McMurdi PJ, Holmes SP (2017) Exact sequence variants should replace operational taxonomic units in marker-gene data analysis. ISME Journal 11, 2639–2643. https://doi.org/10.1038/ismej.2017.119

Coates DJ, Byrne M, Moritz C (2018) Genetic diversity and conservation units: dealing with the species-population continuum in the age of genomics. Frontiers Ecology and Evolution 6: 165. https://doi.org/10.3389/fevo.2018.00165

Colgan N (1914) The opisthobranch fauna of the shores and shallow waters of County Dublin. Irish Naturalist 23: 161–204.

Cook LM (2017) Reflections on molluscan shell polymorphisms. Biological Journal of the Linnean Society 121: 717–730. https://doi.org/10.1093/biolinnean/blx033

Crawford JE Riehle MM, Guelbeogo WM, Gneme A, Sagnon N, Vernick KD, Nielsen R, Lazzaro BP (2015) Reticulate speciation and barriers to introgression in the *Anopheles gambiae* species complex. Genome Biology and Evolution 7: 3116–3131. https://doi.org/10.1093/gbe/evv203

Davison A, Jackson HJ, Murphy EW, Reader T (2019) Discrete or indiscrete? Redefining the colour polymorphism of the land snail *Cepaea nemoralis*. Heredity 123: 162–175. https://doi.org/10.1038/s41437-019-0189-z

de Queiroz K (2007) Species concepts and species delimitation. Systematic Biology 56: 879–886. https://doi.org/10.1080/10635150701701083

Edmunds M, Kress A (1969) On the European species of *Eubranchus* (Mollusca, Opisthobranchia). Journal of the Marine Biological Association of the United Kingdom 49: 879–912. https://doi.org/10.1017/S0025315400038005

Fišer C, Robinson CT, Malard F (2018) Cryptic species as a window into the paradigm shift of the species concept. Molecular Ecology 27: 613–635. https://doi.org/10.1111/mec.14486

Forbes E (1838) Malacologia monensis, a catalogue of the Mollusca inhabiting the Isle of Man and the neighbouring sea. John Carfrae and son, Edinburgh, 1–63. https://doi.org/10.5962/bhl.title.10685

Friele H, Hansen GA (1876) Bidrag til kundskaben om de norske nudibranchier. Forhandlinger i Videnskabs-Selskabet i Christiania (1875): 69–80.

Fujita MK, Leache AD, Burbrink FT, McGuire JA, Moritz C (2012) Coalescent-based species delimitation in an integrative taxonomy. Trends in Ecology & Evolution 27: 480–488. https://doi.org/10.1016/j.tree.2012.04.012

Gante HF, Matschiner M, Malmstrøm M, Jakobsen KS, Jentoft S, Salzburger W (2016) Genomics of speciation and introgression in Princess cichlid fishes from Lake Tanganyika. Molecular Ecology. 25: 6143–6161. https://doi.org/10.1111/mec.13767

Gante HF (2018) How fish get their stripes-again and again. Science 362: 396–397. https://doi.org/10.1126/science.aav3373

García Goméz JC, Cervera JL, García FJ (1990) Description of *Eubranchus linensis* new species (Nudibranchia), with remarks on diauly in nudibranchs. Journal of the Molluscan Studies 56: 585–593. https://doi.org/10.1093/mollus/56.4.585

Gray JE (1857) Guide to the systematic distribution of Mollusca in the British Museum. Part 1, London, 230 pp.

Haupaix M, Curantz C, Bailleul R, Beck S, Robic A, Manceau M (2018) The periodic coloration in birds forms through a prepattern of somite origin. Science 361: eaar4777. https://doi.org/10.1126/science.aar4777

Haupaix N, Manceau M (2019) The embryonic origin of periodic color patterns. Developmental Biology, early online view. https://doi.org/10.1016/j.ydbio.2019.08.003

Hennig W (1966) Phylogenetic Systematics. University of Illinois Press, Urbana, 263 pp.

Heppell D (1964) Comment on the proposed designation under the plenary powers of a type-species for *Eubranchus* Forbes, 1838, with suppression of several nomina dubia: Z.N.(S.) 1102. Bulletin of Zoological Nomenclature 21: 412–413. https://doi.org/10.5962/bhl.part.28524

Hess B (2000) Periodic patterns in biology. Naturwissenschaften 87: 199–211. https://doi.org/10.1007/s001140050704

Hiscock TW, Megason SG (2015) Mathematically guided approaches to distinguish models of periodic patterning. Development 142: 409–419. https://doi.org/10.1242/dev.107441

Holland PWH (2013) Evolution of homeobox genes. WIREs Developmental Biology. 2: 31–45. https://doi.org/10.1002/wdev.78

ICZN [International commission on zoological nomenclature] (1966) Opinion 774. *Eubranchus* Forbes 1838 (Gastropoda): added to the official list with suppression under the plenary powers of several nomina dubia. Bulletin of Zoological Nomenclature 23: 87–90.

Iredale T, O'Donoghue CH (1923) List of British nudibranchiate Mollusca. Proceedings of the Malacological Society of London 15: 201–233.

Johnson MR, Barsh GS, Mallarino R (2019) Periodic patterns in Rodentia: development and evolution. Experimental Dermatology 28: 509–513. https://doi.org/10.1111/exd.13852

Jones JS, Leith BH, Rawlings P (1977) Polymorphism in *Cepaea*: A problem with too many solutions? Annual Review Ecology and Systematics 8: 109–143. https://doi.org/10.1146/annurev.es.08.110177.000545

Katoh K, Misawa K, Kuma K, Miyata T (2002) MAFFT: a novel method for rapid multiple sequence alignment based on fast Fourier transform. Nucleic Acid Research 30: 3059–3066. https://doi.org/10.1093/nar/gkf436

Koblmüller S, Albertson RC, Genner MJ, Sefc KM, Takahashi T (2019) Preface: advances in cichlid research III: behavior, ecology, and evolutionary biology. Hydrobiologia 832: 1–8. https://doi.org/10.1007/s10750-019-3903-1

Korshunova TA, Martynov AV, Bakken T, Evertsen J, Fletcher K, Mudianta IW, Saito H, Lundin K, Schrödl M, Picton B (2017a) Polyphyly of the traditional family Flabellinidae affects a major group of Nudibranchia: aeolidacean taxonomic reassessment with descriptions of several new families, genera, and species (Mollusca, Gastropoda). ZooKeys 717: 1–139. https://doi.org/10.3897/zookeys.717.21885

Korshunova TA, Martynov AV, Picton BE (2017b) Ontogeny as an important part of integrative taxonomy in tergipedid aeolidaceans (Gastropoda: Nudibranchia) with a description of a new genus and species from the Barents Sea. Zootaxa 4324: 1–22. https://doi.org/10.11646/zootaxa.4324.1.1

Korshunova TA, Lundin K, Malmberg K, Picton B, Martynov AV (2018) First true brackish-water nudibranch mollusc provides new insights for phylogeny and biogeography and reveals paedomorphosis-driven evolution. PLoS ONE 13: e0192177. https://doi.org/10.1371/journal.pone.0192177

Korshunova TA, Picton B, Furfaro G, Mariottini P, Pontes M, Prkić J, Fletcher K, Malmberg K, Lundin K, Martynov A (2019a) Multilevel fine-scale diversity challenges the 'cryptic species' concept. Scientific Reports 9: 6732. https://doi.org/10.1038/s41598-019-42297-5

Korshunova TA, Mehrotra R, Arnold S, Lundin K, Picton B, Martynov AV (2019b) The formerly enigmatic Unidentiidae in the limelight again: a new species of the genus *Unidentia* from Thailand (Gastropoda: Nudibranchia). Zootaxa 51: 556–570. https://doi.org/10.11646/zootaxa.4551.5.4

Kumar S, Stecher G, Tamura K (2016) MEGA7: Molecular evolutionary genetics analysis version 7.0 for bigger datasets. Molecular Biology and Evolution 33: 1870–1874. https://doi.org/10.1093/molbev/msw054

Ludt WB, Bernal MA, Kenworthy E, Salas E, Chakrabarty P (2019) Genomic, ecological, and morphological approaches to investigating species limits: A case study in modern taxonomy from tropical Eastern Pacific surgeonfishes. Ecology and Evolution 9: 4001–4012. https://doi.org/10.1002/ece3.5029

Malinsky M, Svardal H, Tyers A, Miska EA, Genner MJ, Turner G, Durbin R (2018) Whole-genome sequences of Malawi cichlids reveal multiple radiations interconnected by gene flow. Nature Ecology and Evolution 2: 1940–1955. https://doi.org/10.1038/s41559-018-0717-x

Martinsson S, Erséus C (2018) Cryptic diversity in supposedly species-poor genera of Enchytraeidae (Annelida: Clitellata). Zoological Journal of the Linnean Society 183: 749–762. https://doi.org/10.1093/zoolinnean/zlx084

Martynov AV (1998) Opisthobranch molluscs (Gastropoda, Opisthobranchia) of the family Eubranchidae: the taxonomic composition and two new species from the Sea of Japan. Zoologichesky Zhurnal 77: 763–777.

Martynov AV, Korshunova TA (2015) A new deep-sea genus of the family Polyceridae (Nudibranchia) possesses a gill cavity, with implications for the cryptobranch condition and a 'Periodic Table' approach to taxonomy. Journal of Molluscan Studies 81: 365–379. https://doi.org/10.1093/mollus/eyv003

M'Intosh W (1865) On the nudibranchiate Mollusca of St. Andrews; *Edwardsia*; and the polyps of *Alcyonium digitatum*. Proceedings of the Royal Society of Edinburgh 5: 387–395. https://doi.org/10.1017/S0370164600040967

Momigliano P Jokinen H, Fraimout A, Florin AB, Norkko A, Merilä J (2017) Extraordinarily rapid speciation in a marine fish. PNAS 114: 6074–6079. https://doi.org/10.1073/pnas.1615109114

Neiber MT, Hausdorf B (2015) Molecular phylogeny reveals the polyphyly of the snail genus *Cepaea* (Gastropoda: Helicidae). Molecular Phylogenetics and Evolution 93: 143–149. https://doi.org/10.1016/j.ympev.2015.07.022

Nygren A, Parapar J, Pons J, Meißner K, Bakken T, Kongsrud JA, Oug E, Gaeva D, Sikorski A, Johansen RA, Hutchings PA, Lavesque N, Capa M (2018) A mega-cryptic species complex hidden among one of the most common annelids in the North East Atlantic. PLoS ONE 13: e0198356. https://doi.org/10.1371/journal.pone.0198356

Nylander JA, Ronquist F, Huelsenbeck JP, Nieves-Aldrey JL (2004) Bayesian phylogenetic analysis of combined data. Systematic Biology 53: 47–67. https://doi.org/10.1080/10635150490264699

Popov IYu (2002) Periodical systems in biology (a historical issue). Verhandlungen zur Geschichte und Theorie der Biologie 9: 55–69.

Prkić J, Petani A, Iglić Đ, Lanča L (2018) Stražnjoškržnjaci Jadranskoga mora, Slikovni atlas i popis hrvatskih vrsta / Opisthobranchs of the Adriatic Sea, Photographic atlas and list of Croatian species. Ronilački klub Sveti Roko, Bibinje, 464 pp.

Puillandre N, Lambert A, Brouillet S, Achaz G (2012) ABGD, Automatic Barcode Gap Discovery for primary species delimitation. Molecular Ecology 21: 1864–1877. https://doi.org/10.1111/j.1365-294X.2011.05239.x

O'Donoghue CH (1926) A list of the nudibranchiate Mollusca recorded from the Pacific coast of North America, with notes on their distribution. Transactions of the Royal Canadian Institute 15: 199–247.

Quatrefages JLA de (1844) Sur les Gastéropodes Phlébentérés (Phlebenterata Nob.), ordre nouveau de la classe des Gastéropodes, proposé d'après l'examen anatomique et physiologique des genres Zéphyrine (*Zephyrina* Nob.), Actéon (*Acteon* Oken), Actéonie (*Acteoniæ* Nob.), Amphorine (*Amphorina* Nob.), Pavois (*Pelta* Nob.), Chalide (*Chalidis* Nob.). Annales des Sciences Naturelles. Ser. 3 1: 129–183. http://biodiversitylibrary.org/page/13407269

Rannala B (2015) The art and science of species delimitation. Current Zoology 61: 846–853. https://doi.org/10.1093/czoolo/61.5.846

Rannala B, Yang Z (2003) Bayes estimation of species divergence times and ancestral population sizes using DNA sequences from multiple loci. Genetics 164: 1645–1656.

Ronquist F, Teslenko M, van der Mark P, Ayres DL, Darling A, Höhna S, et al. (2012) MrBayes 3.2: Efficient Bayesian phylogenetic inference and model choice across a large model space. Systematic Biology 61: 539–542. https://doi.org/10.1093/sysbio/sys029

Salis P, Lorin T, Laudet V, Frédérich B (2019) Magic traits in magic fish: understanding color pattern evolution using reef fish. Trends Genetics 35: 265–278. https://doi.org/10.1016/j.tig.2019.01.006

Schmekel L, Portmann A (1982) Opisthobranchia des Mittelmeeres, Nudibranchia und Saccoglossa. Fauna e Flora del Golfo di Napoli 40: 1–410. https://doi.org/10.1007/978-3-642-61817-8_1

Singhal S, Hoskin CS, Couper P, Potter S, Moritz C (2018) A framework for resolving cryptic species: a case study from the lizards of the Australian wet tropics. Systematic Biology, early online view. https://doi.org/10.1093/sysbio/syy026

Stamatakis A, Hoover P, Rougemont J (2008) A rapid bootstrap algorithm for the RAxML web servers. Systematic Biology 75: 758–771. https://doi.org/10.1080/10635150802429642

Stanton DWG, Frandsen P, Waples RK, Heller R, Russo IRM, Orozco-terWengel PA, Tingskov Pedersen CE, Siegismund HR, Bruford MW (2019) More grist for the mill? Species delimitation in the genomic era and its implications for conservation. Conservation Genetics 20: 101–113. https://doi.org/10.1007/s10592-019-01149-5

Struck TH, Feder JL, Bendiksby M, Birkeland S, Cerca J, Gusarov VI, et al. (2017) Finding evolutionary processes hidden in cryptic species. Trends in Ecology & Evolution 33, 153–163. https://doi.org/10.1016/j.tree.2017.11.007

Suárez-Villota EY, Quercia CA, Dıáz LM, Vera-Sovier V, Nuñez JJ (2018) Speciation in a biodiversity hotspot: Phylogenetic relationships, species delimitation, and divergence times of Patagonian ground frogs from the *Eupsophus roseus* group (Alsodidae). PLoS ONE 13: e0204968. https://doi.org/10.1371/journal.pone.0204968

Sukumaran J, Knowles LL (2017) Multispecies coalescent delimits structure, not species. Proceedings of the National Academy of Sciences 114: 1607–1612. https://doi.org/10.1073/pnas.1607921114

Taylor WR (2002) A 'periodic table' for protein structures. Nature 416: 657–660. https://doi.org/10.1038/416657a

Thompson W (1860) On a species of *Eolis*, and also a species of *Lomanotus* new to science; with the description of a specimen of *Eolis caerulea*, Montagu. Annals and Magazine of Natural History 5: 48–51. https://biodiversitylibrary.org/page/2320452

Thompson TE, Brown GH (1984) Biology of opisthobranch molluscs. Volume 2. Ray Society, London, 229 pp.

Trainito E, Doneddu M (2014) Nudibranchi del Mediterraneo. Il Castello, Milano, 192 pp.

Trinchese S (1877–1879) Aeolididae e famiglie affini del Porto di Genova. Parte Prima. Atlante, Bologna, 94 pp. https://doi.org/10.5962/bhl.title.43791

Vavilov NI (1922) The law of homologous series in variation. Journal of Genetics 12: 47–89. https://doi.org/10.1007/BF02983073

Winston JE (1999) Describing Species: a practical taxonomic procedure for biologists. Cambridge University Press, Cambridge, 518 pp.

Yang Z (2015) The BPP program for species tree estimation and species delimitation. Current Zoology 61: 854–865. https://doi.org/10.1093/czoolo/61.5.854

Yu G, Rao D, Matsui M, Yang J (2017) Coalescent-based delimitation outperforms distance-based methods for delineating less divergent species: the case of *Kurixalus odontotarsus* species group. Scientific Reports 7: 16124. https://doi.org/10.1038/s41598-017-16309-1

Zachos FE (2018a) Mammals and meaningful taxonomic units: the debate about species concepts and conservation. Mammal Review 48: 153–159. https://doi.org/10.1111/mam.12121

Zachos FE (2018b) (New) Species concepts, species delimitation and the inherent limitations of taxonomy. Journal of Genetics 97: 811. https://doi.org/10.1007/s12041-018-0965-1

Supplementary material 1

Table S1. List of samples, localities, GenBank accession numbers, and voucher references

Authors: Tatiana Korshunova, Klas Malmberg, Jakov Prkić, Alen Petani, Karin Fletcher, Kennet Lundin, Alexander Martynov

Data type: species data

Link: https://doi.org/10.3897/zookeys.917.47444.suppl1

ZooKeys 917: 51–61 (2020)
doi: 10.3897/zookeys.917.48924
http://zookeys.pensoft.net

RESEARCH ARTICLE

A peer-reviewed open-access journal
ZooKeys
Launched to accelerate biodiversity research

Two new species of the genus *Opopaea* (Araneae, Oonopidae) from Myanmar

Yanfeng Tong[1,2*], Zengliang Chen[3*], Shuqiang Li[4]

1 *Life Science College, Shenyang Normal University, Shenyang 110034, China* **2** *Southeast Asia Biological Diversity Research Institute, Chinese Academy of Sciences, Yezin, Nay Pyi Taw 05282, Myanmar* **3** *The Sericultural Research Institute of Liaoning Province, Fengcheng, Liaoning 118100, China* **4** *Institute of Zoology, Chinese Academy of Sciences, Beijing 100101, China*

Corresponding author: Shuqiang Li (lisq@ioz.ac.cn)

Academic editor: D. Dimitrov | Received 29 November 2019 | Accepted 11 February 2020 | Published 9 March 2020

http://zoobank.org/554574CC-B3C0-49EB-B099-8B34E80E39C6

Citation: Tong Y, Chen Z, Li S (2020) Two new species of the genus *Opopaea* (Araneae, Oonopidae) from Myanmar. ZooKeys 917: 51–61. https://doi.org/10.3897/zookeys.917.48924

Abstract

Two new species of the genus *Opopaea* Simon, 1892 are reported from Myanmar, *O. kanpetlet* Tong & Li, **sp. nov.** (♂♀) and *O. zhigangi* Tong & Li, **sp. nov.** (♂♀). Morphological descriptions and photographic illustrations of the two new species are given. All types are preserved in the Institute of Zoology, Chinese Academy of Sciences in Beijing (IZCAS).

Keywords

Goblin spider, morphology, new species, taxonomy

Introduction

The genus *Opopaea* Simon, 1892 is a widespread and highly diverse goblin spider genus, with biodiversity hotspots in Africa, Asia and Australia (Baehr 2013). A total of 185 valid extant species are currently known, in which 46 in Africa, 33 in Asia, 96 in Australia and New Caledonia, and 10 in other areas (WSC 2020).

The genus *Opopaea* of Myanmar and the adjacent countries has been poorly studied. Brignoli (1978) reported a new species from Bhutan. Tong and Li (2013) reported

* Contributed equally as the first authors.

two new species and one newly recorded species from Laos. There are no records of the genus *Opopaea* in Myanmar. However, four species of the genus *Gamasomorpha* Karsch, 1881 and two recently described species of the endemic genus *Kachinia* Tong & Li, 2018 have been reported from Myanmar (Tong and Li 2018; WSC 2020). The present paper expands the known oonopid diversity of Myanmar by adding one newly recorded genus and two new species.

Materials and methods

The specimens were examined in 95% ethanol using a Leica M205C stereomicroscope. Details were studied with an Olympus BX51 compound microscope. Photos were taken with a Canon EOS 750D zoom digital camera (18 megapixels) mounted on an Olympus BX51 compound microscope. Scanning electron microscope images (SEM) were taken under high vacuum with a Hitachi TM3030 after critical point drying and gold-palladium coating. All measurements were taken using an Olympus BX51 compound microscope and are given in millimeters in the text. The materials are preserved in the Institute of Zoology, Chinese Academy of Sciences in Beijing (**IZCAS**).

Terminology mainly follows Andriamalala and Hormiga (2013). The following abbreviations are used in the text: AL = abdomen length; ALE = anterior lateral eyes; ALE-ALE = distance between ALE and ALE; ALE-PLE = distance between ALE and PLE; AW = abdomen width; CBL = cymbiobulbus length; CBW = cymbiobulbus width; CL = carapace length; CW = carapace width; EGW = eye group width; FI = femur insertion on patella; FML = femur length; PLE = posterior lateral eyes; PME = posterior median eyes; PME-PME = distance between PME and PME; PLE-PME = distance between PLE and PME; PTL = patella length; TL = total length. Used in the figures: apo = apodeme; asr = anterior scutal ridge; boc = booklung covers; cb = cymbiobulbus; dte = dorsolateral, triangular extensions; fm = femur; fn = fenestra; ga = globular appendix; nlp = nail-like process; pd = postgynal depression; pls = paddle-like sclerite; psr = posterior scutal ridge; pt = patella; sr = scutal ridge.

Taxonomy

Family Oonopidae Simon, 1890
Genus *Opopaea* Simon, 1892

***Opopaea kanpetlet* Tong & Li, sp. nov.**
http://zoobank.org/DABDCD9E-6129-4704-A835-E64C97836930
Figures 1–3, 7A–C

Type material. *Holotype*: ♂ (IZCAS Ar-25098), sifting leaf litter, Myanmar, Chin, Roadside between Kanpetlet and Nat Ma Taung National Park, 003, 21°13.325'N,

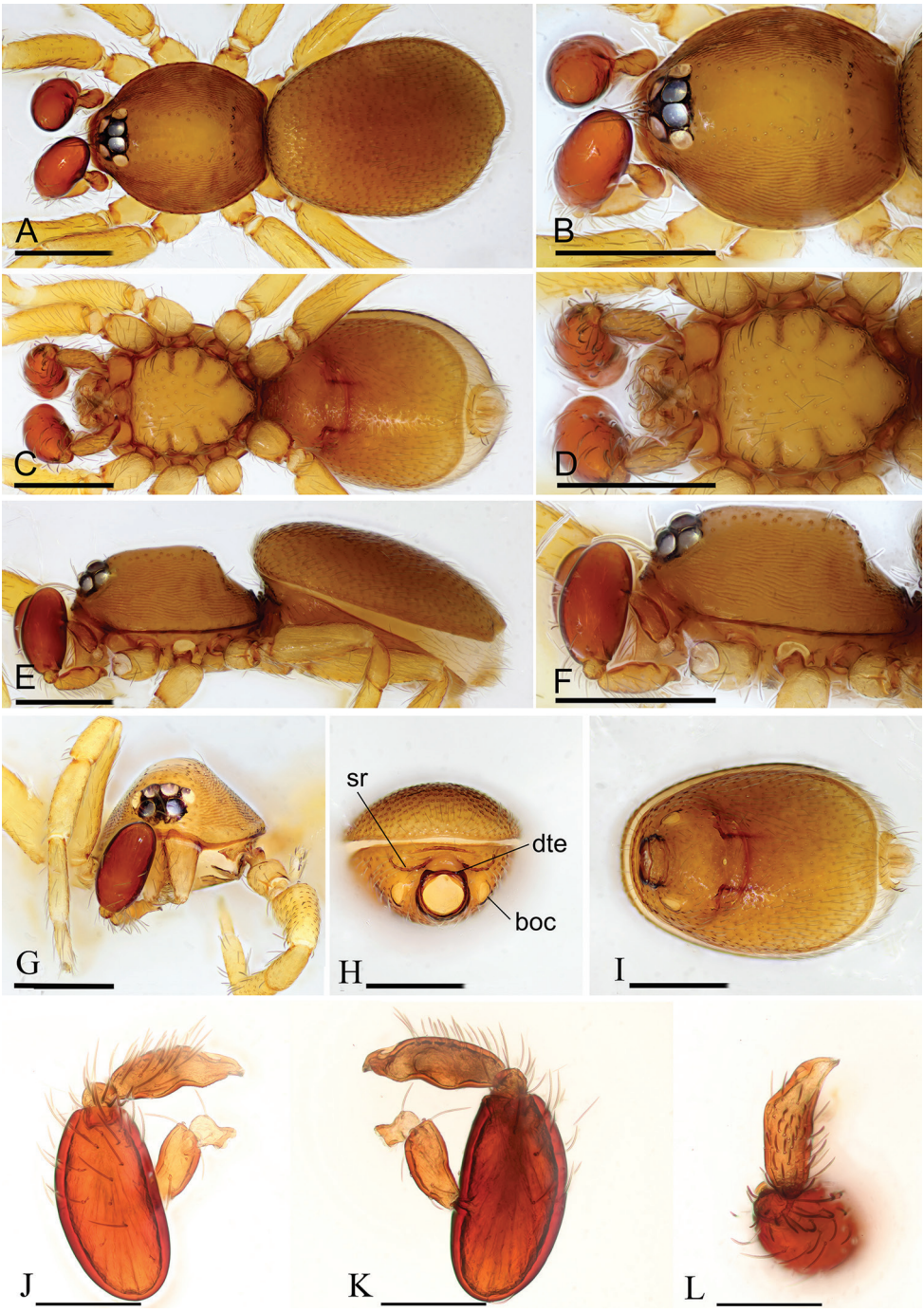

Figure 1. *Opopaea kanpetlet* sp. nov., male holotype **A, C, E** habitus, dorsal, ventral and lateral views **B, D, F, G** prosoma, dorsal, ventral, lateral and anterior views **H, I** abdomen, anterior and ventral views **J, K, L** left palp, prolateral, retrolateral and dorsal views. Abbreviations: boc = booklung covers; dte = dorsolateral, triangular extensions; sr = scutal ridge. Scale bars: 0.4 mm (**A–I**); 0.2 mm (**J–L**).

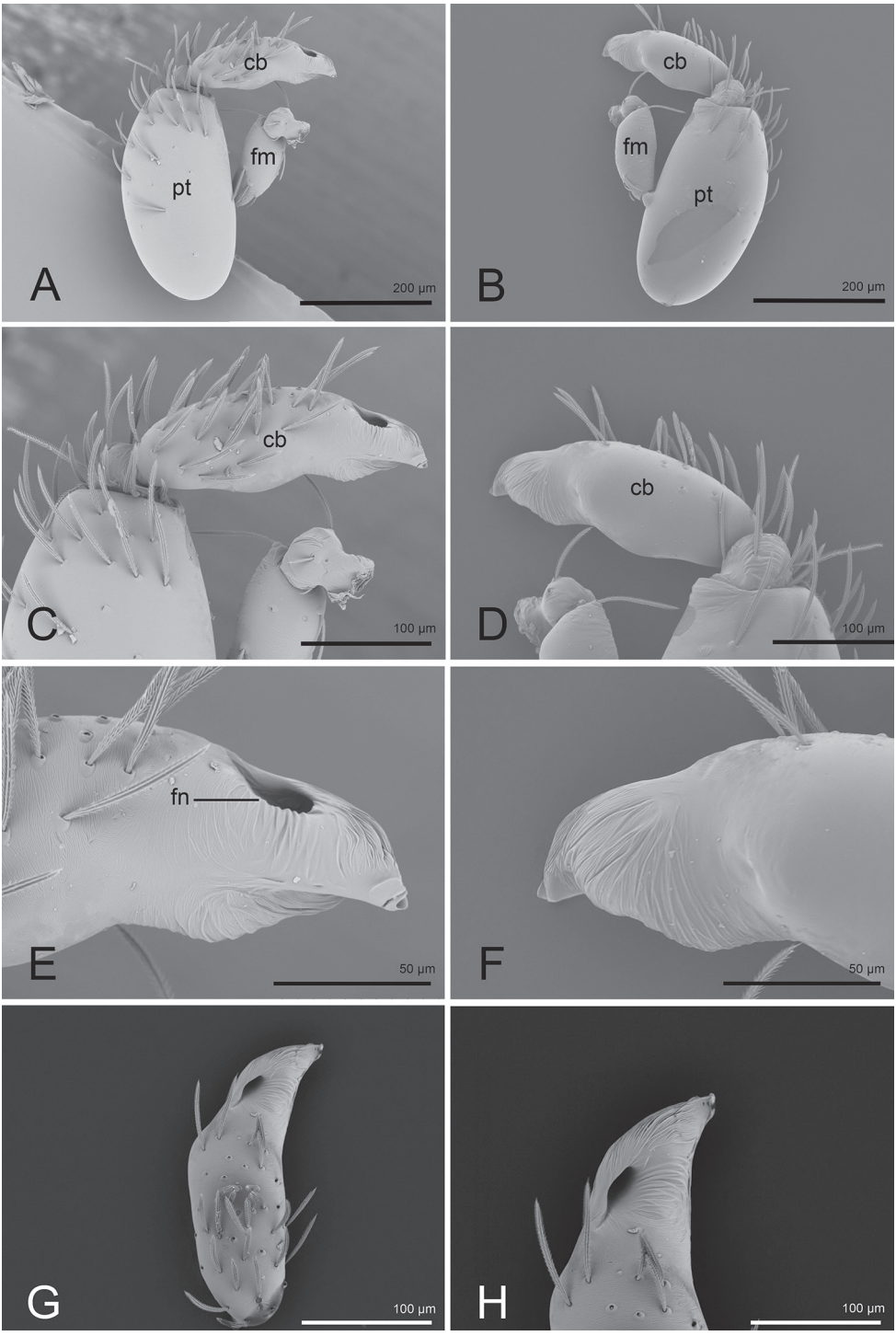

Figure 2. *Opopaea kanpetlet* sp. nov., holotype, left male palp, SEM **A, B** prolateral and retrolateral views **C, D, G** cymbiobulbus, prolateral, retrolateral and dorsal views **E, F, H** distal part of cymbiobulbus, prolateral, retrolateral and dorsal views. Abbreviations: cb = cymbiobulbus; fm = femur; fn = fenestra; pt = patella.

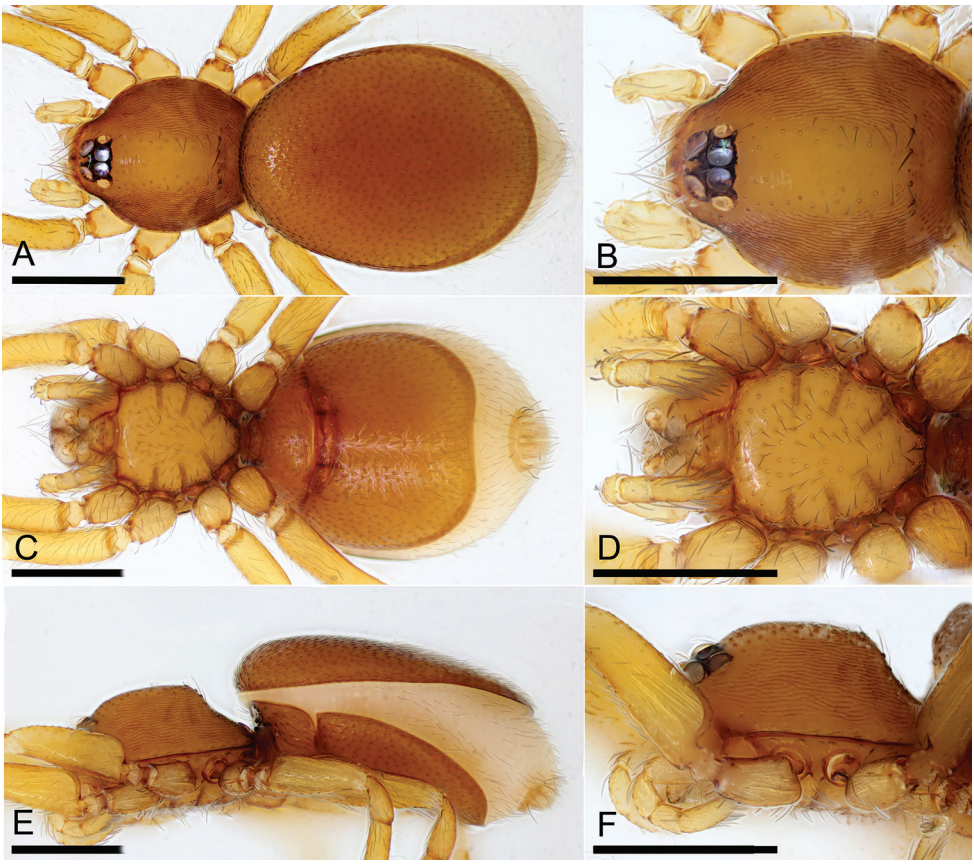

Figure 3. *Opopaea kanpetlet* sp. nov., female (IZCAS Ar-25099) **A, C, E** habitus, dorsal, ventral and lateral views **B, D, F** prosoma, dorsal, ventral and lateral views. Scale bars: 0.4 mm.

93°55.739'E, 2942 m, 30.IV.2017, Wu J & Chen Z. ***Paratypes*:** 2♀ (IZCAS Ar-25099, 25100), same data as holotype; 1♂ (IZCAS Ar-25101), 3♀ (IZCAS Ar-25102, 25103, 25104), sifting leaf litter, Myanmar, Chin, near 16.5 km of the roadside between Kanpetlet and Nat Ma Taung National Park, 002, 21°13.195'N, 93°16.125'E, 2789 m, 30.IV.2017, Wu J & Chen Z.

Etymology. The specific name is a noun in apposition taken from the type locality.

Diagnosis. The new species is similar to *Opopaea tumida* Tong & Li, 2013, but can be distinguished by the small booklung covers (Fig. 1I), the acute tip of male palpal bulb (Figs 1J–L, 2) and the posterior scutal ridge of the female (Fig. 7A–C). The male of *O. tumida* has large booklung covers, a small apophysis in the retrolateral distal region of the palpal bulb, and the female is lacking the posterior scutal ridge (Tong and Li 2013: figs 8I, 9I, J, 10D).

Description. Male (holotype). ***Measurements*:** TL: 1.63; CL: 0.68; CW: 0.58; AL: 0.91; AW: 0.69; ALE: 0.08; PME: 0.07; PLE: 0.06; EGW: 0.23; ALE-ALE: 0.04; ALE-PLE: 0.01; PME-PME: 0; PLE–PME: 0; CBL: 0.23; CBW: 0.08; PTL: 0.33; FI: 0.16; FML: 0.13. ***Coloration*:** legs yellow, carapace and abdomen scuta yel-

low brown, abdominal interscutal areas creamy white, booklung covers light yellow, pedipalps reddish brown. ***Habitus*** as in Fig. 1A, C, E. Carapace (Fig. 1B, F): wide oval in dorsal view; sides with longitudinal streaks; median area smooth with rows of setae at lateral edges. ***Eyes*** (Fig. 1B, G): ALE largest, PLE smallest; posterior eye row recurved viewed from above, procurved from front; ALE separated by less than their radius, ALE–PLE separated by less than ALE radius, PME touching throughout most of their length, PLE–PME separated by less than PME radius. Clypeus height about 1.1 times ALE diameter (Fig. 1G). ***Sternum*** (Fig. 1D) longer than wide, fused to carapace; surface smooth; radial furrows present between coxae I-II, II-III, III-IV, with rows of small pits. Endites anteriorly with a small, sharply pointed projection. ***Abdomen*****:** booklung covers very small, ovoid, without setae. Pedicel tube short, ribbed, with small, dorsolateral triangular extensions, scuto-pedicel region lower than pedicel diameter, with arched scutal ridges, interrupted medially, with curved anterior scutal ridge (Fig. 1H, I). ***Palp*** (Figs 1J–L, 2): femur slightly shorter than half length of patella and submedially attached to patella; patella strongly enlarged, elongate oval; tibia small, rounded; cymbiobulbus shorter than the patella; palpal fenestra small oval and located nearly at tip of cymbiobulbus. Tip of embolus acute triangle.

Female (*n* = 5). As in male except as noted. ***Measurements*** (IZCAS Ar-25099): TL: 1.89; CL: 0.70; CW: 0.61; AL: 1.27; AW: 0.75; ALE: 0.08; PME: 0.06; PLE: 0.05; EGW: 0.21; ALE-ALE: 0.03; ALE-PLE: 0.01; PME-PME: 0; PLE-PME: 0. ***Palp*** light yellow. ***Habitus*** as in Fig. 3A, C, E. Endites without projections. ***Copulatory organ*** (Fig. 7A–C): posterior margin of epigastric scutal ridge (asr) smooth, thick posterior scutal ridge (psr) adjacent to asr, small postgynal semicircular depression (pd) between asr and psr; dorsally with nail-like process (nlp) connected to paddle-like sclerite (pls) bearing thin, straight arms.

Distribution. Known only from the type locality.

Opopaea zhigangi **Tong & Li, sp. nov.**
http://zoobank.org/21168390-94EC-4387-9CA9-3ADF1526DEE7
Figures 4–6, 7D–F

Type material. ***Holotype*****:** ♂ (IZCAS Ar-25105), sifting leaf litter, Myanmar, Chin, near 1.5 km of the roadside between Kanpetlet and Nat Ma Taung National Park, 011–012, 21°13.058'N, 93°59.033'E, 2421 m, 1.V.2017, Wu J & Chen Z. ***Paratype*****:** 1♀ (IZCAS Ar-25106), same data as holotype.

Etymology. The specific name is after Mr Zhigang Chen, one of the collectors of this species; noun (name) in genitive case.

Diagnosis. The new species is similar to *Opopaea deserticola* Simon, 1892, but can be distinguished by the longer palpal patella (the ratio of width to length about 0.5) and slender cymbiobulbus (the ratio of width to length about 0.35) of male (Figs 4J–L, 5) and very small postgynal depression of female (Fig. 7E). The male of *O. deserticola* has relatively shorter palpal patella (the ratio of width to length about 0.65) and ex-

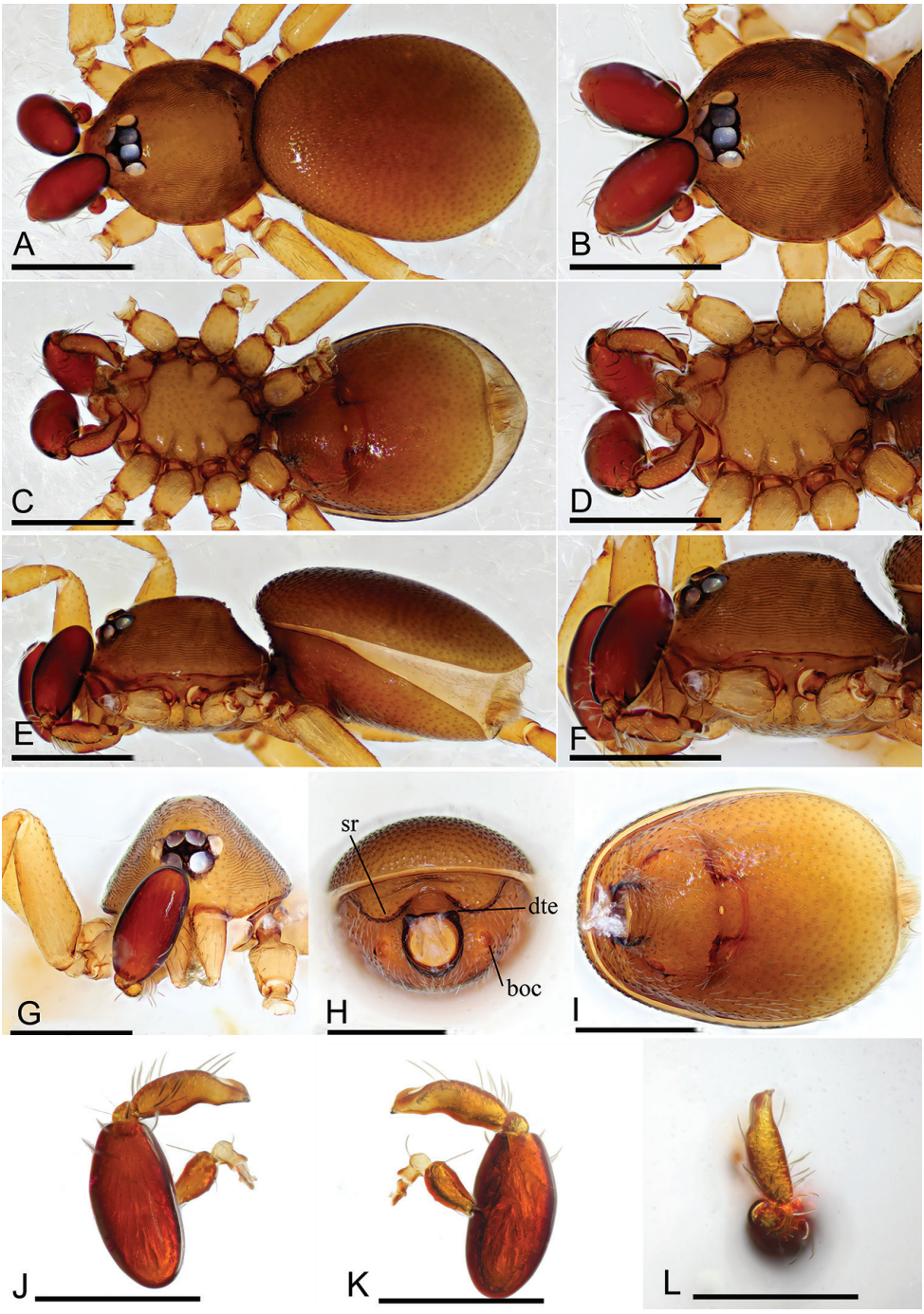

Figure 4. *Opopaea zhigangi* sp. nov., male holotype **A, C, E** habitus, dorsal, ventral and lateral views **B, D, F, G** prosoma, dorsal, ventral, lateral and anterior views **H, I** abdomen, anterior and ventral views **J, K, L** left palp, prolatral, retrolateral and dorsal views. Abbreviations: boc = booklung covers; dte = dorsolateral, triangular extensions; sr = scutal ridge. Scale bars: 0.4 mm.

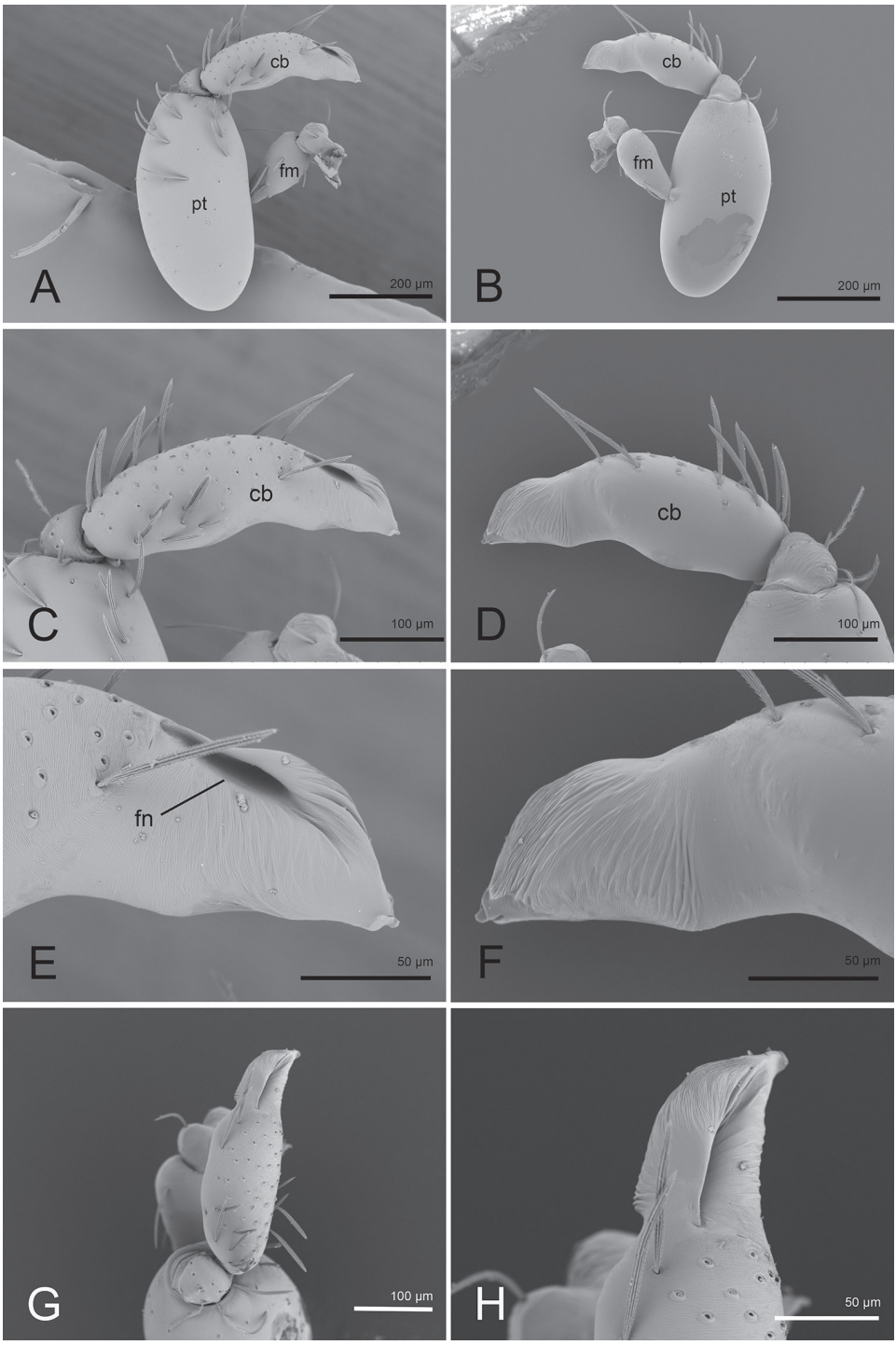

Figure 5. *Opopaea zhigangi* sp. nov., holotype, left male palp, SEM **A, B** prolateral and retrolateral views **C, D, G** cymbiobulbus, prolateral, retrolateral and dorsal views **E, F, H** distal part of cymbiobulbus, prolateral, retrolateral and dorsal views. Abbreviations: cb = cymbiobulbus; fm = femur; fn = fenestra; pt = patella.

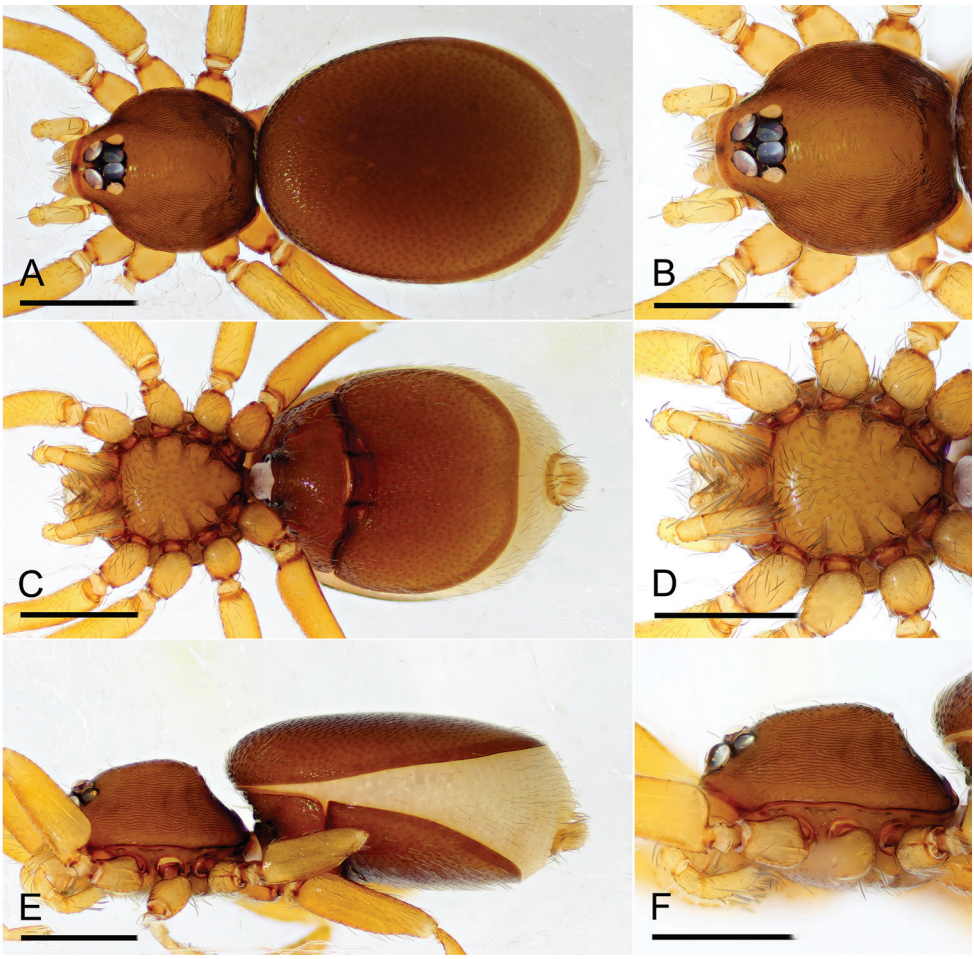

Figure 6. *Opopaea zhigangi* sp. nov., female (IZCAS Ar-25106) **A, C, E** habitus, dorsal, ventral and lateral views **B, D, F** prosoma, dorsal, ventral and lateral views. Scale bars: 0.4 mm.

panded cymbiobulbus (the ratio of width to length about 0.47) and the female has a relatively larger postgynal depression (Platnick and Dupérré 2009: figs 55–66).

Description. Male (holotype). ***Measurements*:** TL: 1.54; CL: 0.60; CW: 0.58; AL: 0.98; AW: 0.70; ALE: 0.08; PME: 0.07; PLE: 0.07; EGW: 0.22; ALE–ALE: 0.02; ALE–PLE: 0.01; PME–PME: 0; PLE–PME: 0; CBL: 0.31; CBW: 0.11; PTL: 0.41; FI: 0.21; FML: 0.14. ***Coloration*:** legs yellow, carapace and abdomen scuta brown, abdominal interscutal areas creamy white, booklung covers reddish, pedipalps reddish brown. ***Habitus*** as in Fig. 4A, C, E. Carapace (Fig. 4B, F): wide oval in dorsal view; sides with longitudinal streaks; median area smooth with some setae at lateral edges. ***Eyes*** (Fig. 4B, G): ALE largest, PLE smallest; posterior eye row recurved viewed from above, procurved from front; ALE almost touching, ALE–PLE separated by less than ALE radius, PME touching throughout most of their length, PLE–PME separated by less than PME radius. Clypeus height about 1.7 times ALE diameter (Fig. 4G).

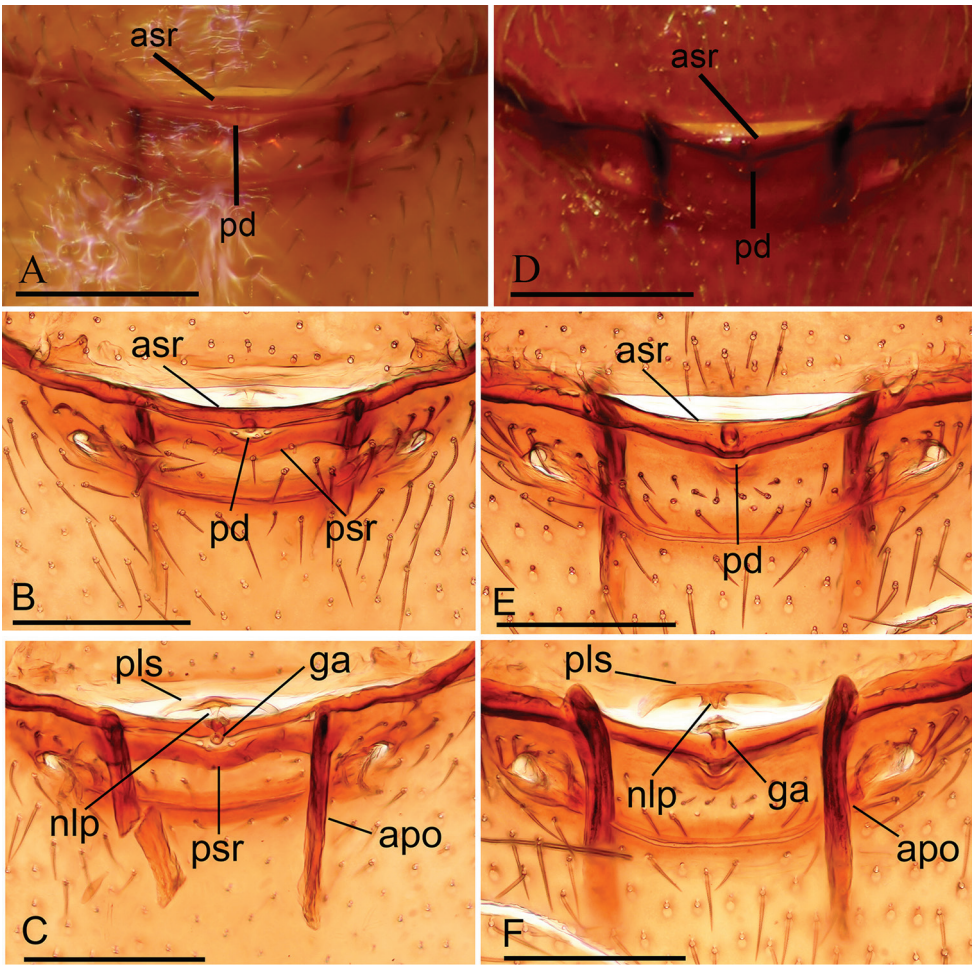

Figure 7. Female copulatory organ **A–C** *Opopaea kanpetlet* sp. nov. (IZCAS Ar-25099) **D–F** *Opopaea zhigangi* sp. nov. (IZCAS Ar-25106) **A, B, D, E** ventral view **C, F** dorsal view. Abbreviations: apo = apodeme; asr = anterior scutal ridge; ga = globular appendix; nlp = nail-like process; pd = postgynal depression; pls = paddle-like sclerite; psr = posterior scutal ridge. Scale bars: 0.1 mm.

Sternum (Fig. 4D) longer than wide, fused to carapace; surface smooth; radial furrows present between coxae I–II, II–III, III–IV, with rows of small pits. Endites anteriorly with small, sharply pointed projection. ***Abdomen*****:** booklung covers very small, reddish brown, ovoid, without setae. Pedicel tube short, ribbed, with small, dorsolateral, triangular extensions, scuto-pedicel region lower than pedicel diameter, with arched scutal ridges, with curved anterior scutal ridge (Fig. 4H, I). ***Palp*** (Figs 4J–L, 5): femur slightly shorter than half length of patella and submedially inserted to patella; patella very large; tibia small, rounded; cymbiobulbus shorter than the patella; fenestra large slit-like, located at nearly tip of cymbiobulbus. Tip of embolus broad triangle.

Female (*n* = 1). As in male except as noted. ***Measurements*:** TL: 1.84; CL: 0.65; CW: 0.58; AL: 1.18; AW: 0.87; ALE: 0.09; PME: 0.07; PLE: 0.06; EGW: 0.21; ALE-ALE: 0.02; ALE–PLE: 0.01; PME–PME: 0; PLE–PME: 0. ***Habitus*** as in Fig. 6A, C, E. Endites without projections. ***Copulatory organ*** (Fig. 7D–F): postgynal depression (pd) very small; dorsally with nail-like process (nlp) connected to paddle-like sclerite (pls) bearing thick, straight arms.

Distribution. Known only from the type locality.

Acknowledgments

The manuscript benefitted greatly from comments by Dimitar Dimitrov, Arnaud Henrard and one anonymous referee. This study was supported by the National Natural Science Foundation of China (31750002, 31972867, 31530067) to Yanfeng Tong, and the Southeast Asia Biodiversity Research Institute, Chinese Academy of Sciences (2015CASEABRI005, Y4ZK111B01) to Shuqiang Li.

References

Andriamalala D, Hormiga G (2013) Systematics of the goblin spider genus *Opopaea* (Araneae, Oonopidae) in Magagascar. Bulletin of the American Museum of Natural History 380: 1–156. https://doi.org/10.1206/828.1

Baehr BC, Harvey MS, Smith HM, Ott R (2013) The goblin spider genus *Opopaea* in Australia and the Pacific islands (Araneae: Oonopidae). Memoirs of the Queensland Museum, Nature 58: 107–338.

Brignoli PM (1978) Ergebnisse der Bhutan-Expedition 1972 des Naturhistorischen Museums in Basel. Araneae: Fam. Oonopidae, Agelenidae, Hahniidae und Mimetidae. Entomologica Basiliensis 3: 31–56.

Platnick NI, Dupérré N (2009) The goblin spider genera *Opopaea* and *Epectris* (Araneae, Oonopidae) in the New World. American Museum Novitates 3649: 1–43. https://doi.org/10.1206/664.1

Tong Y, Li S (2013) Six new species of oonopid spiders from Champasak, Laos (Araneae, Oonopidae). Zootaxa3709: 71–88. https://doi.org/10.11646/zootaxa.3709.1.3

Tong Y, Chen H, Liu S, Li S (2018) A new genus of oonopid spiders from Myanmar (Araneae, Oonopidae). ZooKeys794: 31–43. https://doi.org/10.3897/zookeys.794.29156

WSC (2020) World Spider Catalog. Version 21.0 Natural History Museum Bern. World Spider Catalog. http://doi.org/10.24436/2 [Accessed on: 2020.2.03]

ZooKeys 917: 63–83 (2020)
doi: 10.3897/zookeys.917.39270
http://zookeys.pensoft.net

RESEARCH ARTICLE

A peer-reviewed open-access journal
ZooKeys
Launched to accelerate biodiversity research

A cryptic new species of *Chlidonoptera* Karsch, 1892 from the south west protected zone of the Central African Republic (Insecta, Mantodea, Hymenopodidae)

Nicolas Moulin[1]

1 *Institut Systématique, Evolution, Biodiversité (ISYEB), Muséum national d'Histoire naturelle, UMR 7205, MNHN, CNRS, Sorbonne Université, EPHE, Universités des Antilles, CP50, 45 rue Buffon, 75231 Paris Cedex 05, France*

Corresponding author: Nicolas Moulin (nicolas.moulin@mnhn.fr)

Academic editor: G. Svenson | Received 20 August 2019 | Accepted 28 January 2020 | Published 9 March 2020

http://zoobank.org/7DA31DA1-F5CD-4FB2-926D-0033C28EDCF9

Citation: Moulin N (2020) A cryptic new species of *Chlidonoptera* Karsch, 1892 from the south west protected zone of the Central African Republic (Insecta, Mantodea, Hymenopodidae). ZooKeys 917: 63–83. https://doi.org/10.3897/zookeys.917.39270

Abstract

Between 1998 and 2012, several scientific expeditions in Dzanga-Sangha Special Reserve and Dzanga-Ndoki National Park led to the collection of many Mantodea specimens from Central African Republic (CAR). Among these specimens, several males of an undescribed species were discovered. Morphologically, this species most closely resembles to *Chlidonoptera vexillum* Karsch, 1892 and *Chlidonoptera lestoni* Roy, 1975. A new lineage was revealed by DNA barcoding. Therefore, a new species is described, *Chlidonoptera roxanae* **sp. nov.** Habitus images, genitalia illustrations and descriptions, measurement data, a key to species, natural history information, and locality data are provided. These results add to the evidence that cryptic species can be found in tropical regions, a critical issue in efforts to document global species richness. They also illustrate the value of DNA barcoding, especially when coupled with traditional taxonomic tools, in disclosing hidden diversity.

Résumé

Entre 1998 et 2012, plusieurs expéditions scientifiques, dans la Réserve Spéciale de Dzanga-Sangha et dans le Parc National de Dzanga-Ndoki, ont permis de recueillir de nombreux spécimens de Mantodea en République centrafricaine (RCA). Parmi ceux-ci, plusieurs mâles d'une espèce non décrite ont été mis en évidence. Sur le plan morphologique, l'espèce est proche de *Chlidonoptera vexillum* Karsch, 1892 et de *Chlidonoptera lestoni* Roy, 1975. Le séquençage ADN a mis en lumière cette espèce. Par conséquent, une

nouvelle espèce est décrite, *Chlidonoptera roxanae* **sp. nov.** Des images des habitus, des illustrations et descriptions des genitalia, des données de mesure, une clé pour les espèces, des informations d'écologie et des données de localité sont fournies. Les résultats ajoutent à la preuve que les espèces cryptiques peuvent être trouvées dans les régions tropicales, un problème crucial dans les efforts visant à documenter la richesse en espèces de la planète. Ils illustrent également la valeur du séquençage ADN, en particulier lorsqu'il est associé à des outils taxonomiques traditionnels, pour la mise en évidence de la diversité cachée.

Keywords
Afrotropical, *Chlidonoptera*, cryptic species, DNA barcoding, praying mantis, taxonomy

Introduction

Since the beginning of the 1980s, the entomologist Philippe Annoyer had been traveling in southwestern CAR searching for butterflies and other insects. In 2008, his missions expanded and came to be called Epiphyte 2008. In 2010, a massive survey program was organised under the name SANGHA2012 Biodiversité en Terre Pygmée. On this occasion, the author joined the team to increase the study and collections of Mantodea (Moulin et al. 2017, Moulin 2018b). Several males of *Chlidonoptera* Karsch, 1892 were collected, mostly by light trapping. Visual searching and beating of vegetation, both on the ground and canopy, did not lead to the discovery of the associated female. The localities of these specimens are in the last remnants of primary forests of the southwestern tip of the CAR.

All species belonging to the genus *Chlidonoptera* are morphologically similar to each other but easily discriminated from other genera. The main morphological feature of the genus is a relatively large yellow spot on the elytra located between the two black arcs of the circle. The collected male *Chlidonoptera* specimens were initially presumed to be *C. vexillum* Karsch, 1892, as they share many morphological similarities. Additional examinations of *C. vexillum* male genitalia compared to the recently collected *Chlidonoptera* genitalia led to the submission of DNA sequencing samples at Canadian Center for DNA Barcoding (CCDB) in Guelph. Many studies have used the 5' region of the cytochrome oxidase I gene (COI), more commonly referred to as the DNA barcode region, as a useful tool to discriminate various groups of insects (Cocuzza et al. 2015). The results from the DNA sequencing revealed that the specimens from southwestern CAR are different from known *C. vexillum* Karsch, 1892 specimens from Cameroon and Gabon. Originally described by Karsch in 1892 (*Bomistria lunata* Saussure, 1898 synonym) to contain a single species *C. vexillum*, two species were added: *C. chopardi* Roy, 1964 and *C. lestoni* Roy, 1975. During this time, Roy synonymised the East African *Anabomistria werneri* Giglio-Tos, 1915 (Roy 1964) with *Chlidonoptera*, which was later confirmed by Lombardo (1997). Thus, prior to the discovery of this new species, described herein, the genus *Chlidonoptera* contained four species: *C. vexillum*, *C. chopardi*, *C. lestoni*, and *C. werneri*.

Chlidonoptera chopardi is distributed in West Africa, *C. vexillum* and the new species are distributed in West Central Africa, *C. lestoni* is distributed in Ghana (Leston 1968, Roy et Leston 1975), with *C. werneri* distributed in the East. It appears that Tanzania and Kenya are the eastern limits of the distribution of *C. vexillum* (Ehrmann 2002, Schwarz and Roy 2019). *Chlidonoptera vexillum* is sympatric with *C. werneri*, creating confusion. Wrongly, Kirby (1904) cites *Bomistria lunata* Saussure, 1898, as a distinct species of *C. vexillum*. *Chlidonoptera* is classified within the tribe Hymenopodini, subtribe Pseudocreobotrina with four other genera (Mantodea Species File, http://mantodea.speciesfile.org; Svenson et al. 2016, Schwarz and Roy 2019).

Ideally the description of a species should result from a synthesis of information that encompasses morphological, molecular, biological, biogeographical, physiological, ecological and bibliographical data; however, this compendium of information is lacking for the great majority of species.

Materials and methods

Sampled region

The study area includes the UNESCO World Heritage site Sangha Trinational, the Dzanga-Sangha Special Reserve (6,865.54 sq km) and the Dzanga-Ndoki National Park (1,143.26 sq km) (Moulin et al. 2017). These national parks and reserves aim to protect the second largest rain forest on the earth. Altitude ranges from 300 to 620 meters above sea level. The whole zone is on alluvial sands. Along streams, forest clearings are present with marshy depressions. There are three types of forest within the study area: mainly dryland forest, a semi-evergreen forest that contains swamp-forest areas along the rivers, and a closed-canopy, monodominant *Gilbertiodendron dewevrei* forest. The dryland forest is an open, mixed canopy that is dominated by Stercullariaceae and Ulmaceae; often associated with it is a dense understory of Marantaceae and Zingiberaceae. Along the Sangha river, there are stands of *Guibourtia demeusei* (Vande Weghe 2004, http://www.dzanga-sangha.org/).

Collection and preparation

Collection was predominately made by light trapping with 250-Watt bulbs. A few individuals were found at or around the lamp; or on the tents of the camp, attracted by the diffuse light of the incandescent bulbs. The specimens were placed in cyanide vials and then kept dry on layers of cotton and blotting paper. Some specimens were kept alive in cubital screen enclosures to capture live images. Some males were pinned after genitalia preparation was made and a leg was preserved in ethanol for DNA barcoding with tissue samples deposited in CCDB in Guelph.

DNA barcoding

DNA barcoding, the analysis of a standardised segment of the mitochondrial cytochrome c oxidase subunit I (COI) gene, was performed on a representative selection of specimens (n = 25). Tissues were sent to CCDB at the University of Guelph for DNA extraction, polymerase chain reaction (PCR), and sequencing. DNA was extracted from dry legs using a routine silica-based 96-well extraction automation protocol (Ivanova et al. 2006). The 658bp region of COI proposed for use as a 'DNA barcode' (Hebert et al. 2003) was amplified with the PCR primers C_LepFolF/C_LepFolR (Hebert et al. 2004). Data are currently managed under the following projects: "Mantodea of Gabon – Project 1 [ECOTROP 2014]," "Mantodea of Gabon – Project 2 [ECOTROP 2011]," "DNA Barcoding Mantodea - Collection N. Moulin" Barcode of Life Data Systems (BOLD, Biodiversity Institute of Ontario, Canada; http://www.boldsystems.org). Kimura-2-parameter (K2P) distances were calculated using the BOLD 4.0 interface (Ratnasingham and Hebert 2007). Sequences were then analysed and trees constructed using the BOLD 4.0 interface.

Deposition of the specimens

Specimens are, currently, in the Research Collection of Nicolas Moulin (Montérolier, France) and Philippe Annoyer Personal Collection (Sainte-Croix-Volvestre, France). Types will be deposited at the MNHN (Paris, France).

Abbreviations used in this paper:

BOLD	Barcode of Life Project, Biodiversity Institute of Ontario;
RCNM	Research Collection of Nicolas Moulin, Montérolier;
PAPC	Philippe Annoyer Personal Collection;
DNNP	Dzanga-Ndoki National Park, Central African Republic;
DSSR	Dzanga-Sangha Special Reserve, Central African Republic;
MNHN	Muséum national d'Histoire naturelle, Paris.

Descriptive conventions and character systems

The species treatment within this study provides a brief diagnosis and criteria descriptions stemming from the anterior surface of the head, the dorsal surface of the pronotum, the legs, the wings, and the abdomen. Foreleg spine nomenclature follows Wieland (2008, 2013) and morphological terminology, including genitalia, follows that of Brannoch et al. (2017) where diagrams of spine arrangements can be viewed.

Measurements. Specimens were measured using a Leica S8APO stereomicroscope with a caliper. All measurements in this study were taken with a caliper and are expressed in millimetres. A total of 22 measurement classes were captured, as in Tedrow et al. (2014), including:

1. Body length = length of body from central ocelli to posterior tip of abdomen (intraspecifically variable measurement, primarily for general size estimation).
2. Forewing length = from proximal margin of axillary sclerites to distal tip of the discoidal region.
3. Hindwing length = from proximal margin of axillary sclerites to distal tip of the discoidal region.
4. Pronotum length = from anterior margin to posterior margin.
5. Prozone length = anterior margin of pronotum to center of supra-coxal sulcus.
6. Pronotum width = from the lateral margins at the widest point, the supra-coxal bulge.
7. Ratio pronotum = ratio between pronotum width and length.
8. Pronotum narrow width = from lateral margins of the pronotum at the narrowest region of metazone.
9. Head width = from lateral margins of the eyes at the widest point.
10. Frons width = from lateral margins of the frons, inferior to the antennal insertions, at the widest point.
11. Frons height = from upper margin abutting central ocellus to lower margin abutting clypeus.
12. Prothoracic coxae length = from pronotum to trochanter.
13. Prothoracic femur length = from proximal margin abutting trochanter to distal margin of genicular lobe.
14. Mesothoracic femur length = from most proximal margin abutting the trochanter to the distal side of the terminal spine insertion site.
15. Mesothoracic tibia length = from most proximal groove near joint with the femur to the distal side of the terminal spine insertion site.
16. Mesothoracic tarsus length = from proximal joint to the apex of the ungues curve.
17. Metathoracic femur length = from most proximal margin abutting the trochanter to the distal side of the terminal spine insertion site.
18. Metathoracic tibia length = from most proximal groove near femoral joint to the distal side of the terminal spine insertion site.
19. Metathoracic tarsus length = from proximal joint to the apex of the ungues curve.
20. Anteroventral femoral spine count = all inner marginal ridge spines, except the distal terminal spur.
21. Anteroventral tibial spine count = all inner marginal ridge spines, except the distal terminal spur.
22. Posteroventral tibial spine count = all outer marginal ridge spines but except the distal terminal spur.

The measurement of the total body length produces a measurement only useful for general assessment of body size rather than species description. Since head position, abdominal expansion, and wing position are all variable, total body length should only be used as a rough measurement to initially discriminate between the small and large Mantodea species when performing identifications.

Imaging. Alive specimen was captured with a NIKON D700 by Philippe Annoyer on 3 December 2010 near the base camp in Dzanga-Ndoki NP. Habitus images were

taken with a Konica Minolta Dynax 5D. All images were taken over an 18% grey card background for white balance standards, excluding the image of the *C. lestoni* paratype from the MNHN. Images were processed in GIMP 2 to adjust levels, contrast, exposure, sharpness, and to add scale bars. Minor adjustments were made using the stamp tool to correct background aberrations and to remove distracting debris. Plates were constructed using Publisher 2016.

Taxonomic placement

The following characters led to place the new species within *Chlidonoptera* genus: mantids of medium size and bright colours, very similar to *Pseudocreobotra* genus; but the tips of the lower frons and clypeus very short and blunt, the protuberance of the vertex shorter. The eyes are bulging but rounded. Less expanded pronotum, shorter than anterior coxa: prozone more compressed, higher with two acute conical tubers in front of supracoxal sulcus, no tubercles on the metazone. Wings are beyond the abdomen in both sexes. Forewings of females more dilated from base to apex and hindwings almost opaque, yellow with dark veins; males only the basal part with this coloration, the rest hyaline. Forewings with a large eye spot, a yellow spot near the shoulder and apex on light colour. Anterior femurs are thin. The external spines of the anterior coxa are not swollen at the base, four discoidal spines and four posteroventral femoral spines. Femurs of the meso- and metathoracic legs have a subapical and posteroventral lobe. Laterally lobed present on the abdominal segments.

Known species of the genus *Chlidonoptera* were compared to the males found in southwestern CAR. Distribution of known individuals of *C. werneri*, the structure of the genitalia and the morphology described in Roy (1964) and Lombardo (1997) exclude it as a candidate species. Similarly, distribution, structure of the genitalia and morphology described in Roy (1964) excluded *C. chopardi* as the species. On the other hand, the distinction between *C. vexillum* and *C. lestoni* is much more complicated (Roy and Leston 1975; for reference, the imaged types can be seen at http://specimens.mantodea.com). Morphologically, the three species are very similar. Only the structure of the posterior end of the sclerite L4A of the ventral phallomere (hypophallus) enables to distinguish them. The COI-DNA barcoding of 19 *Chlidonoptera* specimens enabled the differentiation of the new species from *C. vexillum* collected in Gabon (Moulin 2018a) and Cameroon.

Chlidonoptera Karsch, 1892

Chlidonoptera: Karsch 1892: 68; Karsch 1892: 150; Karsch 1894: 278; Saussure 1898: 789; Kirby 1904: 292; Giglio-Tos 1927: 563; Beier 1934: 26; Beier 1964: 939; Roy 1964: 764; Roy 1965: 595; Ragge and Roy 1967: 634; Beier 1968: 6; Roy 1975: 163; Roy and Leston 1975: 329; Ehrmann 2002: 95; Otte and Spearman 2005: 86; Svenson et al. 2016: 6; Schwarz and Roy 2019: 151.

Type species. *Chlidonoptera vexillum* Karsch, 1892.

Taxonomic history. Fred Karsch created the genus *Chlidonoptera* in 1892 (p. 68) for two females specimen collected by Dr. P. Preuss in Cameroon, at Buea, *C. vexillum* Karsch, 1892. Karsch (1892: 150) cited *C. vexillum* from the collections of Dr P. Preuss in Cameroon, with a relatively detailed description of female types from Buea. In a new list of Mantodea collected by Dr P. Preuss in Cameroon, Karsch (1894: 278) for a third time cited the two females from Buea, with an illustration of a female at the end of the document. H. de Saussure created the genus *Bomistria* in 1898 (pg. 202) for a male specimen from Gabon, *B. lunata* Saussure, 1898. In 1900, Y. Sjöstedt (pg. 20) gave measurements for females of *C. vexillum* and males of *B. lunata*, without putting them in synonymy. The genus was then misspelled, '*Clidonoptera*.' W.F. Kirby (1904: 292) continued to conserve the two species, *C. vexillum* and *Bomistria lunata*, with also a misspelling in the Sjöstedt citation, '*Chlinidonoptera*.' F. Werner (1908: 52), making the point between *Chlidonoptera vexillum* and *Bomistria lunata* with supporting illustrations. But, in 1915, Giglio-Tos clarified the situation: *B. lunata* of Saussure is the male of *C. vexillum* and as the female *B. lunata* of F. Werner would be a new genus with a new species, *Anabomistria werneri* Giglio-Tos, 1915. The location of *A. werneri* was listed only as 'Africa' (Giglio-Tos 1927: 563). In his great synthesis work, *Genera Insectorum*, Beier (1934: 26) listed *C. vexillum* and *A. werneri* with a description of their morphological features. He stated that *A. werneri* is from East Africa. Then, in 1964 (p. 939), he confirmed the locality of these species in Hymenopodidae and Hymenopodinae. That same year, R. Roy (1964) synthesised data about Mantodea from the Ivory Coast forest, wherein a new species of *Chlidonoptera* was described, *C. chopardi* (p. 764); the male genitalia of which were compared with those of *C. vexillum*. At the same time, the author reconsidered the genus *Anabomestria* and logically placed *A. werneri* in the genus *Chlidonoptera*. M. Beier (1968: 6, fig. 6b) illustrated the right forewing of *A. werneri*'s female but the taxonomic change of genus made by Roy four years earlier was not taken into account. Later, *Chlidonoptera lestoni* was described (Roy and Leston 1975: 329) from Ghana. In that same work, *C. chopardi* was also cited. A comparison of the posterior process (pda) of the ventral phallomere was illustrated for *C. chopardi*, *C. lestoni*, and *C. vexillum*. It was assumed that *C. lestoni* was close to *C. vexillum* but distinct; this was not like that which D. Leston wrote in 1968. F. Lombardo (1997: 80) completed the description of *C. werneri* with a male specimen collected from Tanzania. Finally, R. Ehrmann (2002: 96) summarised all that was known about *Chlidonoptera* and D. Otte & L. Spearman did the same in 2005 (p 86).

Identification key to species of *Chlidonoptera* using males

The key to the morphological criteria of *Chlidonoptera* species can only distinguish *C. chopardi*, *C. werneri* and a complex of species, named *vexillum group*, including *C. vexillum*, *C. lestoni* and *C. roxanae* sp. nov.

1 The smallest species, 23–26 mm (male); Prolongation of the vertex non bifid; forewings with yellow costal area; green discoidal area on almost two-thirds of the basal area, with two yellow spots and two black arcs as in *vexillum group*, but closer together; hindwings hyaline with pink coloured base; the posterior process of the ventral phallomere smaller and thin ..... ***C. chopardi***

– Larger species, 24–34 mm (male), 37–40 mm (female); prolongation of the vertex bifid, with a more or less notched summit; two black arcs on forewings more separated than in *C. chopardi* **2**

2 Lateral margins of the pronotum smooth; largest anteroventral femoral spines black; wings uniformly yellowish white..... ***C. werneri***

– Lateral margins of the pronotum finely granular; yellowish hind wings with red-brown veins from the anal area and extending variably until the first third of the wing ..... ***vexillum group***

The three species of the *vexillum group* are difficult to differentiate without using male genitalia. There is a size gradient of the posterior process of the ventral phallomere from the smallest to the largest, from *C. lestoni* to *C. roxanae* sp. nov. through *C. vexillum*, in proportion to the body size. Genitalia of *C. lestoni* and *C. vexillum* are represented in Roy & Leston (1975: fig. 9) and in Roy (1964: fig. 7).

The distributions of the different species of *Chlidonoptera* are shown on the map in Figure 1.

Chlidonoptera vexillum Karsch, 1892

Figure 4

Chlidonoptera vexillum: Karsch 1892: 68; Karsch 1892: 150; Karsch 1894: 279; Sjostedt 1900: 20; Beier 1934: 27; Roy 1973: 235; Ehrmann 2002: 95; Otte and Spearman 2005: 87.

= *Bomistria lunata*: Saussure 1898: 789; Kirby 1904: 292; Giglio-Tos 1927: 563; Beier 1934: 26; Ehrmann 2002: 95; Otte and Spearman 2005: 87.

Material examined. (5♀♀, 100♂♂). **Cameroon.** Doumé (1♀), 1930, Coll. M. Cazal, MNHN; Locality unknown (1♂), 1934, Coll. P. Magnier, genitalia preparation Roy 220, MNHN; Edea (1♂ 1♀), VIII.1956, Collector M. de Lisle, genitalia preparation Roy 221, MNHN; Nkolbisson, 30.VI.1965 (1♂) & 24.XII.1969 (1♂), Coll. B. de Miré, MNHN; Kala (5♂♂), 25.XI.1972 to II.1973, Coll. Ph. Darge, genitalia preparation Roy 2074, 2080, and 2082, MNHN; Dokoa, savannahs and forest galleries of Sanaga (1♂), 12.X.1973, Coll. Ph. Darge, MNHN; Kala, Nkolbiyong Mountain, 1150 m (4♂♂), 20.X.1973, Coll. Ph. Darge, MNHN; Ayos, banks of Nyong, 13 km NNW of Obaut, 04.V.1973 (1♂) and 15 to 25.XI.1973 (1♂), Coll. Ph. Darge, MNHN; Elang, 140 km SSE of Yaoundé (1♂), V.1974, Coll. Ph. Darge, MNHN; Mbam-Minkom, Nouma Mountain, 12 km NNW of Nkolbisson,

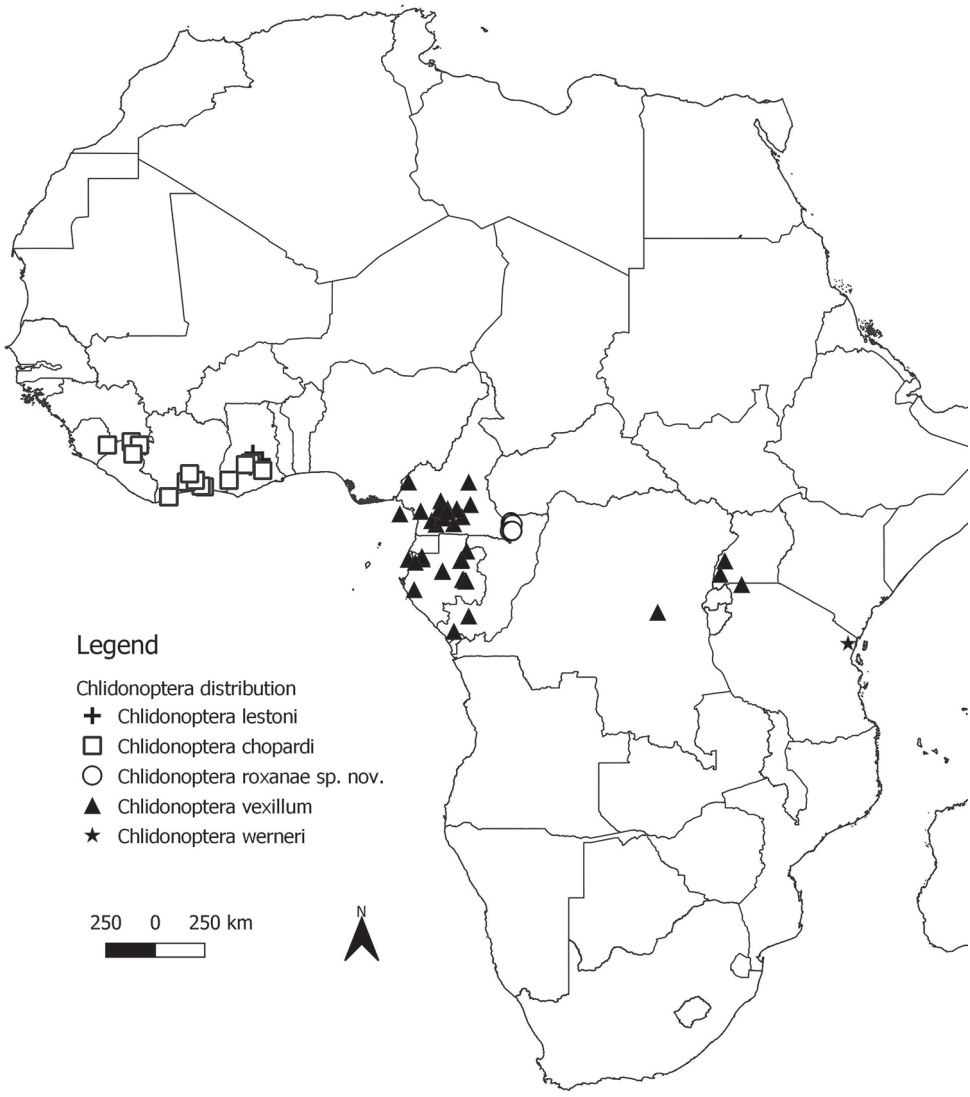

Figure 1. Distribution map of *Chlidonoptera* species. Source: http://www.gadm.org Global Administrative areas Data and Maps (GADM).

1000m (1♂), XII.1974, Coll. Ph. Darge, MNHN; Dzeng Forest, 650 m (11♂♂), 10 to 20.III.1975, Coll. Ph. Darge, genitalia preparation Roy 2203, MNHN; Mbitom (1♂), 20.IV.1975, Coll. Ph. Darge, MNHN; Ngom, banks of Soo (6♂♂), I.1976, Coll. Ph. Darge, MNHN; Nkolmélié, banks of Nyong (1♂), 25.I.1976, Coll. Ph. Darge, MNHN; Nemeyong (1♂), 25.II.1976, Coll. Ph. Darge, MNHN; Meukowong (4♂♂), III.1976, Coll. Ph. Darge, MNHN; Fakélé (#2), 660 m (3♂♂), 20 to 25.X.1976, Coll. Ph. Darge, MNHN; Mbio, Mamfe region (2♂♂), 1 to 5.VI.1977,

Coll. Ph. Darge, MNHN; Bioko (1♀), VI.1997, Coll. Canu, MNHN; Center, South, Light Trap (1♂), 01.X.1998, Coll. Desfontaine, BOLD LopeMAN14-063, Genitalia NM0156, RCNM; Mbalmayo, Mfou Village, 750 m, Light Trap (1♂), XII.2013, Coll. Ph. Le Gall, BOLD NMMAN11-0541, RCNM.

Central African Republic. 'Congo français, Haute-Sanga' (1♀), 106-97, Coll. P.A. Ferrière, MNHN.

Democratic Republic of the Congo. Maniéma, Kindu (1♀), 1917, Coll. L. Burgeon, MNHN.

Gabon. Belinga, Mission biologique (3♂♂), 19.III.1963, Coll. H. Coiffait and before 1964, Coll. P. Grassé, MNHN; Plateau d'Ipassa (8♂♂), 27.X to 06.XII.1967, Coll. G. Bernardi, MNHN; Komo, Cristal mountains foothills, 400 m (3♂), 01 to 15.X.1969, Coll. A. Villiers, MNHN; Mvoum, Montagne de sable (1♂), 01 to 15.XI.1969, Coll. A. Villiers, MNHN; Makokou, Ipassa (4♂♂), 02 to 30.V.1971, Coll. J. Mateu, MNHN; Makokou, Balachowsky-Menier Mission (1♂), 29.XI.1973, Coll. A. Balachowsky, MNHN; Cristal Mountains NP (1♂), 24.VI.1993, Coll. E. Cherlonneix, MNHN; Ogooue-Maritime, Abanda caves, Light Trap (1♂), 06.VIII.2010, Coll. Th. Decaëns & D. Sebag, Genitalia NM0157, MNHN; Ogooue-Ivindo, Lope NP, Lope 2, Light Trap (2♂), 27.II.2011, Coll. Th. Decaëns & R. Rougerie, BOLD Lope11-0208 & 0209, Genitalia NM0158 & 0159, RCNM; Makokou (2♂), 14/20.IV.2012, Coll. G. Robiche, BOLD MANGAB15-090, MNHN; Ogooue-Ivindo, Lope NP, Panther Bridge, Remote Canopy Trap (1♂), 04.IV.2014,Coll. N. Moulin & G. Duvot, BOLD LopeMAN14-064, RCNM; Estuaire, Mondah, Arboretum Raponda Walker, Light Trap (2♂), 01.VI.2016, Coll. T. Decaëns, BOLD MANGAB15-094 & 095, RCNM; Ogooue-Lolo, Lastourville, Bambidie (13♂), 04/11.XI.2018, Coll. T. Decaëns & R. Rougerie, BOLD NMMAN11-0535, -0536, -0537, -0538, -0539, -0540, RCNM.

Republic of the Congo. M'Bila (1♂), XII.1963, Coll. A. Villiers, MNHN; Dimonika (1♂), 11.XI.1975, Coll. C. Morin, MNHN; Mayombe, Dimonika, Light Trap (1♂), 14.XI.1992, Coll. Ph. Le Gall, BOLD NMMAN11-0487, Genitalia NM0191, RCNM.

Tanzania. Kagera Region, Minziro Forest, 1160 m (1♂), 23.X.2010, Coll. Ph. Darge, BOLD NMMAN11-0533, 'Museum de Lyon'.

Uganda. Kamwenge District, Kibale Forest, Chimp nest, Bigodi, 1240 m (2♂), 08.XI.2010, Coll. P. Schmit, BOLD MANGAB15-088, MNHN; Bushenyi District, Kalinzu Forest, Kitozho, 1450 m (1♂), 10.XI.2010, Coll. P. Schmit, MNHN; Kamwenge District, Kibale NP, Mainaro, 1260 m (2♂), 22.III.2012, Coll. P. Schmit, BOLD MANGAB15-089, MNHN.

Chlidonoptera werneri (Giglio-Tos, 1915)

Anabomistria werneri: Giglio-Tos 1915: 108; Beier 1934: 26; Beier 1968: 6.
Chlidonoptera werneri: Roy 1964: 767; Lombardo 1997: 6; Ehrmann 2002: 95; Otte and Spearman 2005: 87.

***Chlidonoptera chopardi* Roy, 1964**
Figure 4

Chlidonoptera chopardi: Roy 1964: 764; Roy 1965: 595; Ragge and Roy 1967: 586; Gillon and Roy 1968: 1039; Roy and Leston 1975: 297; Ehrmann 2002: 95; Otte and Spearman 2005: 86.

Type material examined. (4♂♂). *Chlidonoptera chopardi*: Male holotype, Banco Forest Reserve, Ivory Coast, 1945, code "Ab 31 nuit," Coll. R. Paulian & C. Delamare, genitalia preparation Roy 222, Insects – Small orders & Odonates MNHN Database (EP) #2329, MNHN; 1 ♂ paratype, Banco Forest Reserve, Ivory Coast, 1945, code "Ab 31 nuit," Coll. R. Paulian & C. Delamare, Insects – Small orders & Odonates MNHN Database (EP) #2330, MNHN; 2 ♂ ♂ paratypes, Daloa, Ivory Coast, XII.1930/IV.1931, Coll. Ch. Alluaud & P. A. Chappuis, Insects – Small orders & Odonates MNHN Database (EP) #2331 & #2333, MNHN; 1 ♂ paratype, near Dimbokro, Ivory Coast, 1910, Coll. Capitaine Posth, Insects – Small orders & Odonates MNHN Database (EP) #2332, MNHN.

Other material examined. (7♂♂) **Ivory Coast.** San Pedro (7♂), 05.XI.1982, Coll. Ph. Le Gall, Genitalia NM0160, 0161, 0162, RCNM.

***Chlidonoptera lestoni* Roy, 1975**
Figure 4

Chlidonoptera lestoni: Roy 1975: 297; Ehrmann 2002: 95; Otte and Spearman 2005: 87.

Type material examined. (1♂). *Chlidonoptera lestoni*: 1 ♂ paratype, Tafo, Ghana, 09.XI.1967, UV Trap, Coll. D. Leston, genitalia preparation Roy 2067, Insects – Small orders & Odonates MNHN Database (EP) #2488, MNHN.

***Chlidonoptera roxanae* sp. nov.**
http://zoobank.org/E7FBAAE9-E506-4154-A762-3008A1D6AF44
Figures 2A, 3, 4F, 5, 6

Repository. Holotype male. Muséum national d'Histoire naturelle, Paris, France.

Holotype label: Pinned. Central African Republic, Dzanga-Ndoki National Park, base camp, Lake #1, 2.4881, 16.2330, light, 4.II.2012, BOLD NMMAN11-0404, Genitalia NM0181, Coll: Sangha 2012 Team.

Paratypes males. Philippe Annoyer Personal Collection (PAPC), Sainte-Croix-Volvestre, France; Research Collection of Nicolas Moulin (RCNM), Montérolier, France; Muséum national d'Histoire naturelle, Paris, France.

Figure 2. A Male *Chlidonoptera roxanae* sp. nov. photographed in the Dzanga-Ndoki National Park (CAR), by Philippe Annoyer **B** female *Chlidonoptera vexillum* group photographed in the forest surrounding Sanaga Yong Chimpanzee Rescue Centre, Belabo, East Province (Cameroon), by Sean Brogan.

Paratypes labels (28♂♂). Central African Republic. Dzanga-Sangha Special Reserve, Bayanga, WWF building, diffuse light (1♂), 2.920333, 16.255527, 21.I.2012 (RCNM); Dzanga-Ndoki National Park, M'Boki, South Likembe, Molongo, Sangha

Figure 3. *Chlidonoptera roxanae* sp. nov., holotype male, dorsal and ventral habitus. Scale bar: 10.00 mm.

river, light (1♂), 2.471972, 16.08125, 25.I.2012 (RCNM); M'Boki, South Likembe, Molongo, Sangha river, light (1♂), 2.471972, 16.08125, 25.I.2012 (MNHN); Base camp, Lake #1, windfall tree, light (7♂♂), 2.477916, 16.217388, 1–4.II.2012 (RCNM); Base camp, Lake #1, windfall tree, light (1♂), 2.477916, 16.217388,

1.II.2012 (MNHN); Lake #7, at the base of a Badamier (*Terminalia superba*, Combretaceae), light (1♂), 2.463277, 16.224833, 3.II.2012 (MNHN); Lake #1, at canopy of an Azobe (*Lophira alata*, Ochnaceae), light (1♂), 2.4804, 16.2155, 5.II.2012 (RCNM); Lake #1, base camp, windfall tree, laboratory tent, light (10♂♂), 2.480555, 16.216666, 10.II to 2.III.2012 (RCNM); Lake #3, light (2♂♂), 2.488611, 16.232944, 15 and 22.II.2012 (RCNM); at canopy of an Ayous (*Triplochiton scleroxylon*, Malvaceae), light (1♂), 2.488138, 16.233027, 22.II.2012 (MNHN); at canopy of an Ayous (*Triplochiton scleroxylon*, Malvaceae), light (1♂), 2.488138, 16.233027, 24.II.2012 (RCNM); Lake #7, light (1♂), 2.4806, 16.2167, 29.II.2012 (RCNM), Coll. SANGHA2012 Team.

Other material examined. Central African Republic. Dzanga-Sangha Special Reserve, between Bayanga and Lidjombo, pk15 (2♂♂), pk21 (5♂♂), light, 2.883333, 16.254722, 31.V to 16.VI.1998 (PAPC), Coll. P. Annoyer; Dzanga-Ndoki National Park, Lidjombo (9♂♂: light (8♂♂) and day capture (1♂)), 2.833833, 16.137138, 1–13.III.2005 (PAPC), Coll. P. Annoyer; Dzanga-Sangha Special Reserve, Bayanga, base camp 1, light (2♂♂), 3.066194, 16.149888, 11.X.2008 (PAPC); Bayanga, base camp 2, night capture (1♂), 3.030416, 16.142138, 20.X.2008 (PAPC); Bayanga, at the base of a Kungu (*Piptadenastrium africanum*, Fabaceae) (3♂♂), at canopy of the same tree (1♂), light, 3.030416, 16.142138, 23–24.X.2008 (PAPC), Coll. Epiphyte 2008 Team; Dzanga-Ndoki National Park, base camp, Lake #1, at the base of an Azobé (*Lophira alata*, Ochnaceae), light (3♂♂), 2.480416, 16.215527, 26.XI.2010 (PAPC); Little forest clearing at Lake #5, light (1♂), 2.469055, 16.225583, 29.XI.2010 (PAPC); Base camp, Lake #1, Laboratory tent, diffuse light (3♂♂), 2.480416, 16.215527, 30.XI to 2.XII.2010 (PAPC), Coll. SANGHA2012 Team.

Natural history. According to the collection locations of different individuals in the canopy, this species is considered to be arboreal. Both nymph and adult specimens, are presumed to reside on the inflorescences of trees. In tropical forests, these flowers are often located at the top, above the canopy, so that pollinators have access to pollen and nectar. In the present study, is only males were captured with a light trap, and were rarely captured during the day. Females *Chlidonoptera* specimens that were observed by climbing trees or by beating vegetation (Figure 2).

Diagnosis. Larger than *Chlidonoptera vexillum* and *Chlidonoptera lestoni*. Males: Body length (mm) 26.2–33.6; forewing length 23.6–30.2; hindwing length 24.9–27.3; pronotum length 5.1–6.9; prozone length 2.1–3.5; pronotum width 4.9–6.3; pronotum narrow width 1.6–2.1; head width 5.0–5.9; frons width 1.4–2.0; frons height 0.6–0.9; prothoracic coxae length 6.1–9.0; prothoracic femur length 8.0–10.2; mesothoracic femur length 6.2–8.1; mesothoracic tibia length 5.5–6.9; mesothoracic tarsus length 4.8–6.1; metathoracic femur length 7.2–9.1; metathoracic tibia length 6.5–8.4; metathoracic tarsus length 5.5–6.9; anteroventral femoral spine count 10–12; posteroventral femoral spine count 4; anteroventral tibial spine count 12–15; posteroventral tibial spine count 14–17. The colour patterns on the wings are almost similar (Figures 2–4). There are polymorphisms in the size of the forewings' patterns in each of the species mentioned. The major difference is in the size of body, of genitalia and of the posterior process of sclerite L4A (ventral phallomere) being larger from one species to another (Figures 5, 6).

Figure 4. *Chlidonoptera*, dorsal habitus: **A** *C. vexillum*, male, Mbalmayo, Cameroon, BOLD NMMAN11-0541 **B** *C. vexillum*, male, Arboretum Raponda Walker, Gabon, BOLD MANGAB15-094 **C** *C. vexillum*, male, Biosphere Reserve of Dimonika, Republic of the Congo, BOLD NMMAN11-0487 **D** *C. vexillum*, male, Minziro Forest, Tanzania, BOLD NMMAN11-0533 **E** *C. vexillum*, male, Kalinzu Forest, Uganda **F** *C. roxanae* sp. nov., holotype male, base camp, lake #1, Dzanga-Ndoki NP, CAR, BOLD NMMAN11-0404 **G** *C. lestoni*, paratype male, Tafo, Ghana (S. Poulain) **H** *C. chopardi*, male, San Pedro, Ivory Coast.

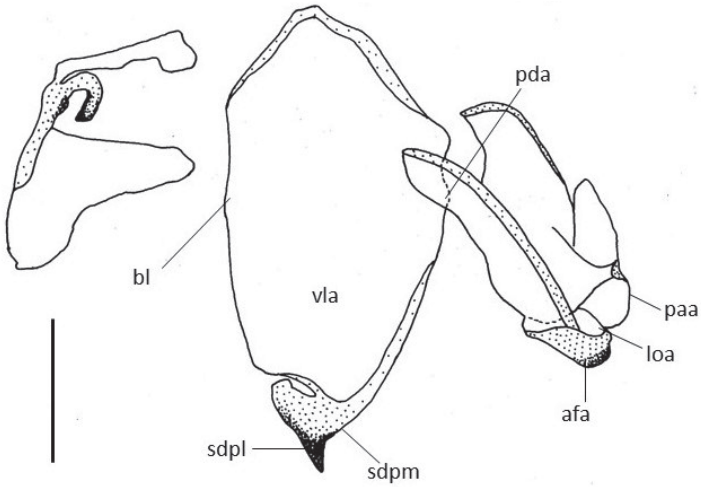

Figure 5. *Chlidonoptera roxanae* sp. nov., holotype male, Genitalia. afa = phalloid apophysis; paa = apical processof left phallomere, titillator; bl = basal lobe of ventral phallomere; loa = membranous lobe; pda = primary distal process; sdpl = lateral secondary distal process; sdpm = median secondary distal process; **vla** = ventral lobe of ventral phallomere. Scale bars: 1.00 mm.

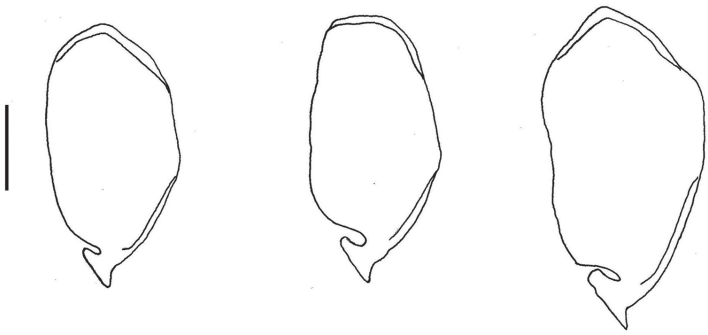

Figure 6. Differences between genitalia: left to right, *C. lestoni*, *C. vexillum*, and *C. roxanae* sp. nov. Scale bar: 1.00 mm.

Description. Male. General colour of the body green and pale yellow. Holotype: Body length (mm) 30.4; forewings length 27.5; hindwings length 25.6; pronotum length 6.3; prozone length 3.0; pronotum width 5.5; pronotum narrow width 2.0; head width 5.8; frons width 1.9; frons height 0.9; prothoracic coxae length 8.1; prothoracic femur length 9.8; mesothoracic femur length 8.0; mesothoracic tibia length 6.5; metathoracic tarsus length 5.2; metathoracic femur length 8.4; metathoracic tibia length 7.7; metathoracic tarsus length 6.2; anteroventral femoral spine count R12/L12; posteroventral femoral spine count R4/L4; anteroventral tibial spine count R13/L14; posteroventral tibial spine count R15/L16.

Head: Oval with anteriorly protruding eyes; vertex arcuate with pronounced tubercles at the sides; prolongation of the bifid vertex; lower frons markedly concave,

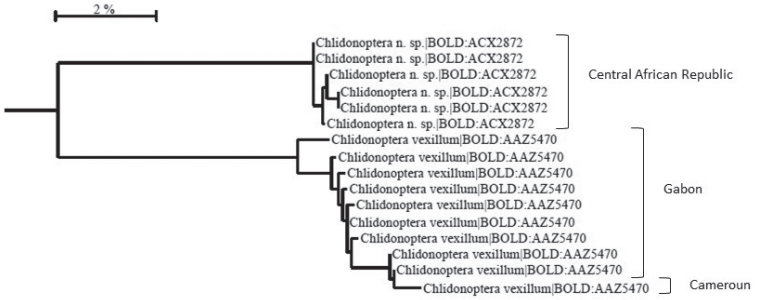

Figure 7. Barcode tree of *Chlidonoptera* from Central Africa created in BOLD using a Neighbour-Joining analysis.

superior margin angles have a tubercle, raised lateral margins; the median region of third antennal segment is black.

Pronotum: Presenting no special features in comparison with *C. vexillum* and *C. lestoni*. Pronotum slightly longer and wider than in other species with always two tubercles slightly directed forward, just above the supracoxal sulcus. Crenellated edges with tubercles of variable sizes. Greenish prozone in the centre and whitish on the sides. Green metazone except on the margin.

Forelegs: Legs very similar in their morphology and coloration to those of the other species previously cited. The anterior femora always with four discoidal spines, four posteroventral femoral spines, and 10–12 anteroventral femoral spines. Anterior tibia has 12–14 anteroventral tibial spines and 14–17 posteroventral tibial spines.

Meso- and metathoracic legs: Legs very similar in their morphology and coloration to those of the other species previously cited.

Wings: Forewing 23.6–30.2 mm in length, featuring the usual colour pattern for the genus, with a yellow spot contained between the two black arcs in a relatively large circle. Hindwings 24.9–27.3 mm long, hyaline, with basal region more or less yellow with red-brownish veins.

Abdomen: It presents no special features in comparison with *C. vexillum* and *C. lestoni*. Laterally lobed abdominal segments. Subgenital plate more or less asymmetrical as in the other species; supraanal plate and cerci without special features.

Genitalia: Same type of *C. vexillum* with the posterior process of the ventral phallomere longer and thicker than in *C. vexillum* and a ventral phallomere longer (Figures 5, 6).

Etymology. This species is named in honour of my oldest daughter, Roxane, who was growing in her mother's womb, while I was deep in the primary forest of the Central African Republic, for field work in February 2012.

DNA barcoding. Nineteen sequences were obtained from the 25 specimens sampled (Figure 7). *C. roxanae* sp. nov. and *C. vexillum* are distant enough from each other (9.4% between them), to allow us to consider them as two different species. BINs (Barcode Index Number) have been attributed to them: BIN: BOLD: ACX2872 for *C. roxanae* sp. nov. (mean intraspecific divergence 0.19%) and BIN: BOLD: AAZ5470

for *C. vexillum* (mean intraspecific divergence 0.76%). No fresh specimens of *C. lestoni* were obtained for barcoding. Nuclear mitochondrial pseudogenes (numts) sometimes lead to the creation of different BINs, a problem which was not encountered here with the differences on the genitalia and the larger general morphology. PCR did not work for six specimens, presumably due to their condition, as they had to be relaxed in order to be mounted, or due to the preserving liquid. These specimens came from Cameroon, Gabon, Republic of the Congo, Tanzania, and Uganda.

Discussion

A larger size, differing genitalia, barcoding analysis, and an isolated geographical location, allowed us to distinguish *C. roxanae* sp. nov. from other *Chlidonoptera* species. Since it was not possible to find the male specimen of *Chlidonoptera* cited in the publication of Roy (2018) about Mantodea in the La Maboké area of the Central African Republic, it is not possible to rule on the species. Geographically, that specimen seems to fit with *C. roxanae* sp. nov., without certainty, like those in the Sangha-Mbaere region (Moulin et al. 2017). For the specimens from Central East Africa (Democratic Republic of the Congo, Tanzania, Uganda), where PCR did not work, fresh material will be required to perform additional barcoding and to confirm a *C. vexillum* identification. It is well-known that DNA barcoding revealed cryptic species of Australian Phasmida among specimens organised at the level of morphospecies (Velona et al. 2015). Molecular analyses are of particular importance for a morphologically conserved group of organisms such as Mantodea (but not between genera) or Phasmida.

Acknowledgments

Many thanks to Philippe Grandcolas, Frédéric Legendre, Roger Roy and the Muséum national d'Histoire naturelle for giving me access to the Muséum's specimens. I would also like to thank the Government of the Central African Republic for permitting access for scientific research. I also thank all of the team of the Epiphyte 2008 and SANGHA2012 'Biodiversité en Terre Pygmée' expeditions. DNA barcoding was supported by the International Barcode of Life project led by Paul Hebert at the Biodiversity Institute of Ontario (Guelph, Canada) and by the funds dedicated to the research of the author's company.

Furthermore, I wish to thank the managers and contributors of the Mantodea Species File (MSF, http://mantodea.species.file.org) for the valuable work they have been undertaking for dictyopterists worldwide. Thanks to Simon Poulain of the MNHN for providing photographs of *Chlidonoptera lestoni* paratypes, to Sean Brogan for the photograph of a female from Cameroon, to Philippe Annoyer for that of a male from CAR, and to Christian Schwarz for data of *Chlidonoptera vexillum* from Kenya and data of *Chlidonoptera lestoni* from Ghana. Finally, thanks to the reviewers of the manuscript for their helpful comments and suggestions, which helped improve the quality of this work.

References

Beier M (1934) Genera Insectorum de P. Wytsman, 196[e] fascicule: Mantodea, fam. Mantidae, subfam. Hymenopodinae. Bruxelles: Desmet-Verteneuil, 37 pp.

Beier M (1964) Klassen und Ordnungen des Tierrich, Fünfter Band, III. Abteilung, 6. Buch, 5. Lieferung, Blattopteroidea Mantodea. Geest & Portig KG, Leipzig, 849–970.

Beier M (1968) Handbuch der Zoologie, IV. Band, 2. Hälfte, Zweite Auflage, 12. Mantodea. Walter de Gruyter & Co, Berlin, 47 pp.

Brannoch SK, Wieland F, Rivera J, Klass KD, Béthoux O, Svenson GJ (2017) Manual of praying mantis morphology, nomenclature, and practices (Insecta, Mantodea). ZooKeys 696: 1–100. https://doi.org/10.3897/zookeys.696.12542

Cocuzza GEM, Di Silvestro S, Giordano R, Rapisarda C (2015) Congruence between cytochrome oxidase I (COI) and morphological data in *Anuraphis* spp. (Hemiptera, Aphididae) with a comparison between the utility of the 5' barcode and 3' COI regions. ZooKeys 529: 123–144. https://doi.org/10.3897/zookeys.529.6081

Ehrmann R (2002) Mantodea, Gottesanbeterinnen der Welt. Natur und Tier-Verlag GmbH, Münster, 519 pp.

Giglio-Tos E (1915) Mantidi esotici. Generi e specie nuove. Hymenopodinae. Bulletino della Societa Entomologica Italiana 46: 31–108.

Giglio-Tos E (1927) Mantidae. Das Tierrich. Walter de Gruyter & Co, Berlin, xl + 707 pp.

Hebert PDN, Cywinska A, Ball SL, deWaard JR (2003) Biological identifications through DNA barcodes. Proceedings of the Royal society B Biological Sciences 270: 313–321. https://doi.org/10.1098/rspb.2002.2218

Hebert PDN, Penton EH, Burns JM, Janzen DH, Hallwachs W (2004) Ten species in one: DNA barcoding reveals cryptic species in the neotropical skipper butterfly *Astraptes fulgerator*. Proceedings of the National Academy of Science of the USA, 101: 14812–14817. https://doi.org/10.1073/pnas.0406166101

Ivanova NV, deWaard JR, Hebert PDN (2006) An inexpensive, automation-friendly protocol for recovering highquality DNA. Molecular Ecology Notes 6: 998–1002. https://doi.org/10.1111/j.1471-8286.2006.01428.x

Karsch F (1892a) Verzeichniss der von Herrn Dr. Paul Preuss im Kamerungebirge erbeuteten Orthopteren. Berliner Entomologische Zeitschrift 37: 65–78. https://doi.org/10.1002/mmnd.18920370112

Karsch F (1892b) Kurze Charakteristik neuer Mantodeen aus Kamerun, gesammelt von Herrn Dr. Paul Preuss. Entomologische Nachrichten 18: 145–150.

Karsch F (1894) Mantodeen aus Kamerun, gesammelt von Dr. Paul Preuss. Berliner Entomologische Zeitschrift 39: 269–280. https://doi.org/10.1002/mmnd.18940390213

Kirby WF (1904) A synonymic Catalogue of Orthoptera. I. Orthoptera Euplexoptera, Cursoria et Gressoria). Vol. 1. British Museum, Natural History, London, 501 pp.

Leston D (1968) The mantids of Tafo area. Annual report, Cocoa Research Institute, Tafo, 1965–1966: 57–61.

Lombardo F (1997) New and little known Mantodea from Eastern and Central Southern Africa. Journal of Orthoptera Research 6: 69–81. https://doi.org/10.2307/3503537

Moulin N, Decaëns T, Annoyer P (2017) Diversity of mantids (Dictyoptera: Mantodea) of Sangha-Mbaere Region, Central African Republic, with some ecological data and DNA barcoding. Journal of Orthoptera Research 26(2): 117–141. https://doi.org/10.3897/jor.26.19863

Moulin N (2018a) Liste commentée et catalogue illustré des Mantodea du Gabon. Les cahiers de la fondation Biotope, 24: 1–60.

Moulin N (2018b) A revision of *Syngalepsus* Beier, with the description of two new species from the Central African Republic and Malawi (Mantodea, Tarachodidae). ZooKeys 802: 121–143. https://doi.org/10.3897/zookeys.802.26622

Otte D, Spearman L (2005) Mantida Species File. Catalog of the Mantids of the World. Association of the Insects Diversity, Philadelphia, 489 pp.

Ragge DR, Roy R (1967) A review of the praying mantises of Ghana (Dictyoptera Mantodea). Bulletin de l'Institut Français d'Afrique Noire, t. 29, série A(2): 586–644.

Ratnasingham S, Hebert PDN (2007) BOLD: The Barcode of Life Data System (www.barcodinglife.org.). Molecular Ecology Notes 7: 355–364. https://doi.org/10.1111/j.1471-8286.2007.01678.x

Roy R (1964) Les mantes de la Côte d'Ivoire forestière. Bulletin de l'Institut Français d'Afrique Noire, t. 26, série A(3): 735–793.

Roy R (1965) Les Mantes de la Guinée forestière. Bulletin de l'Institut Français d'Afrique Noire, t. 27, série A(2): 577–613.

Roy R (1975) Compléments à la connaissance des Mantes de Lamto (Côte d'Ivoire). Bulletin de l'Institut Français d'Afrique Noire, t. 37, série A(1): 122–170.

Roy R (2018) Bilan des récoltes de Mantodea réalisées dans le secteur de La Maboké (République Centrafricaine). Bulletin de la Société entomologique de France 123(3): 343–364. https://doi.org/10.32475/bsef_2052

Roy R, Leston D (1975) Mantodea of Ghana: new species, further records and habitats. Bulletin de l'Institut Fondamental d'Afrique Noire, t. 37, série A(2): 297–344.

Saussure H de (1898) Analecta entomologica. 1.- Orthopterologica – Mantodea. Revue Suisse de Zoologie 5: 183–248. https://doi.org/10.5962/bhl.part.117929

Schwarz C, Roy R (2019) The systematics of Mantodea revisited: an updated classification incorporating multiple data source (Insecta: Dictyoptera), Annales de la Société entomologique de France (N.S.) 55: 2, 101–196. https://doi.org/10.1080/00379271.2018.1556567

Sjöstedt Y (1900) Mantodeen, Phasmodeen und Gryllodeen aus Kamerun und aderen Gegenden Westafrikas, Beiträge zur Kenntniss der Insektenfauna von Kamerun, Bihang Till K. Svenska Vet.-Akad. Handlingar. Band 25. Afd. IV. N°6, Stockholm, 36 pp.

Song H, Buhay JE, Whiting MF, Crandall KA (2008) Many species in one: DNA barcoding overestimates the number of species when nuclear mitochondrial pseudogenes are coamplified. PNAS 105(36): 13486–13491. https://doi.org/10.1073/pnas.0803076105

Tedrow R, Nathan K, Richard N, Svenson GJ (2014) A new species of *Dystacta* Saussure, 1871 from Nyungwe National Park, Rwanda (Insecta, Mantodea, Dystactinae). ZooKeys 410: 1–21. https://doi.org/10.3897/zookeys.410.7053

Vande Weghe JP (2004) Forests of Central Africa: Nature and Man. Protea Book House, Pretoria, 367 pp.

Velona A, Brock PD, Hasenpusch J, Mantovani B (2015) Cryptic diversity in Australian stick insects (Insecta; Phasmida) uncovered by the DNA barcoding approach. Zootaxa 3957(4): 455–466. https://doi.org/10.11646/zootaxa.3957.4.6

Werner F (1908) II. Zur Kenntnis afrikanischer Mantodeen. Bericht der Senckenbergischen Naturforschenden Gesellschaft in Frankfurt am Main: 31–56.

Wieland F (2008) The genus *Metallyticus* reviewed (Insecta: Mantodea). Species, Phylogeny and Evolution 1(2): 147–170.

Wieland F (2013) The phylogenetic system of Mantodea (Insecta: Dictyoptera). Species, Phylogeny, and Evolution. 3(1): 1–306. https://doi.org/10.17875/gup2013-711

ZooKeys 917: 85–104 (2020)
doi: 10.3897/zookeys.917.47326
http://zookeys.pensoft.net

RESEARCH ARTICLE

A peer-reviewed open-access journal
ZooKeys
Launched to accelerate biodiversity research

First records of the genera *Sivaloka* Distant, 1906, with two new species from China, and description of a new species of genus *Kodaianella* Fennah, 1956 (Hemiptera, Fulgoromorpha, Issidae)

Zhi-Min Chang[1,2], Lin Yang[2,3], Xiang-Sheng Chen[2,3]

1 *Key Laboratory of Animal Genetics, Breeding and Reproduction in the Plateau Mountainous Region, Ministry of Education, College of Animal Science, Guizhou University, Guiyang, Guizhou, 550025, China* **2** *Institute of Entomology/Special Key Laboratory for Developing and Utilizing of Insect Resources, Guizhou University, Guiyang, Guizhou, 550025, China* **3** *The Provincial Key Laboratory for Agricultural Pest Management of Mountainous Regions, Guizhou University, Guiyang, Guizhou, 550025, China*

Corresponding author: *Xiang-Sheng Chen* (chenxs3218@163.com)

Academic editor: Mike Wilson | Received 15 October 2019 | Accepted 14 January 2020 | Published 9 March 2020

http://zoobank.org/DEDB8D24-0525-45B1-8F3E-9A97EF23DA37

Citation: Chang Z-M, Yang L, Chen X-S (2020) First records of the genera *Sivaloka* Distant, 1906, with two new species from China, and description of a new species of genus *Kodaianella* Fennah, 1956 (Hemiptera, Fulgoromorpha, Issidae). ZooKeys 917: 85–104. https://doi.org/10.3897/zookeys.917.47326

Abstract

The genus *Sivaloka* Distant, 1906 (Hemisphaeriinae, Kodaianellini) is recorded from China for the first time, with two new species *Sivaloka arcuata* Chang & Chen, **sp. nov.** (China: Guizhou) and *Sivaloka trigona* Chang & Chen, **sp. nov.** (China: Guangxi). One new species of *Kodaianella* Fennah, 1956, *Kodaianella furcata* Chang & Chen, **sp. nov.** (China: Guangxi) is also described and illustrated; female genitalia of two known species in *Kodaianella* are described. A checklist of species of the tribe Kodaianellini with their distribution and a key to genera are provided.

Keywords

female genitalia, issid, Kodaianellini, new taxa, planthopper, *Sivaloka*

Introduction

The tribe Kodaianellini was established by Wang et al. (2016) for *Kodaianella* Fennah, 1956, which is the smallest tribe in the subfamily Hemisphaeriinae Melichar, 1906 (Hemiptera, Issidae), compared with Sarimini Wang, Zhang & Bourgoin, 2016, Parahiraciini Cheng & Yang, 1991, and Hemisphaeriini Melichar, 1906. The tribe Kodaianellini is characterized by hindwings with three lobes: Pcu-A_1 lobe distinctly thinner, less than half as wide as the ScP-R-MP-Cu lobe; A_2 lobe with anterior and posterior margins subparallel, and distinctly surpassing half-length of Pcu-A_1 lobe; A_1 branched, Pcu single and anastomosing with A_{11}; A_2 unbranched. Currently, the tribe Kodaianellini contains five genera: *Dentatissus* Chen, Zhang & Chang, 2014, *Kodaianella* Fennah, 1956, *Kodaianellissus* Wang, Bourgoin & Zhang, 2017, *Neokodaiana* Yang, 1994, and *Tetricissus* Wang, Bourgoin & Zhang, 2017 (Distant 1906; Fennah 1956; Chan and Yang 1994; Chen et al. 2014; Wang et al. 2017), and we here add *Sivaloka* Distant, 1906, which is transferred from the tribe Issini Spinola, 1839. These six genera with all 11 species mainly distributed in the Oriental region, exceptionally a few present in the Palaearctic region (Bourgoin 2019).

In China, the type genus *Kodaianella* was fixed by Fennah (1956) with *K. bicinctifrons*, from Sichuan Province in Southwest China, as its type. Chou et al. (1985) mistakenly recorded a second genus *Sivaloka* Distant, 1906 and described a new species, *S. damnosus* Chou & Lu, 1985, a species which causes serious damage to apple trees. Zhang and Chen (2010) reviewed the genus *Kodaianella* and added two more species, *K. longispina* Zhang & Chen, 2010 and *K. machete* Zhang & Chen, 2010. However, Gnezdilov (2013) placed *K. machete* Zhang & Chen, 2010 in synonymy with *Sivaloka damnosa* Chou & Lu, 1985, and transferred *S. damnosa* and *S. bipartita* Distant, 1906 to *Kodaianella.* Chen et al. (2014) transferred *Kodaianella damnosa* into a new genus *Dentatissus*, and added one more species. At present, with the exception of genera *Sivaloka* and *Tetricissus*, the other four genera with seven species are recorded in the tribe Kodaianellini from China.

We record the genus *Sivaloka* in China for the first time and describe two new species from Guizhou and Guangxi. An additional new species of *Kodaianella* from Guangxi is also described and illustrated, and the female genitalia of two known species are described. A checklist of all species of the tribe Kodaianellini, with their distribution, and a key to genera are provided.

Materials and methods

The morphological terminology of the head and body follows Chan and Yang (1994) and Bourgoin et al. (2015) for the wing venation, and Bourgoin (1987, 1993) and Gnezdilov (2002, 2003) for male and female genitalia. Dry specimens were used for descriptions and illustrations. External morphology was observed under a stereoscopic microscope. All measurements are in millimeters (mm). The body measurements are from the apex of vertex to the tip of the forewings. The genital segments of the examined specimens were macerated in 10% NaOH, washed in water, and transferred

to glycerin. Illustrations of the specimens were made with a Leica M125 and Olympus CX41 stereomicroscope. Photographs were taken with Keyence VHX-1000C and Nikon SMZ-25 microscopes.

The type specimens and other examined specimens are all deposited in the Institute of Entomology, Guizhou University, Guiyang, China (**IEGU**).

Checklist of genera and species of Kodaianellini Wang, Zhang & Bourgoin, 2016 of the world

Dentatissus Chen, Zhang & Chang, 2014
- *Dentatissus brachys* Chen, Zhang & Chang, 2014: China (Henan).
- *Dentatissus damnosus* (Chou & Lu, 1985): China (Beijing, Guizhou, Henan, Hubei, Jiangsu, Liaoning, Shaanxi, Shangdong, Shanxi, Sichuan, Yunnan, Zhejiang).

Kodaianella Fennah, 1956
- *Kodaianella bicinctifrons* Fennah, 1956: China (Guizhou, Sichuan), Laos.
- *Kodaianella bipartita* (Distant, 1906): Myanmar.
- *Kodaianella furcata* Chang & Chen, sp. nov.: China (Guangxi).
- *Kodaianella longispina* Zhang & Chen, 2010: China (Yunnan).

Kodaianellissus Wang, Bourgoin & Zhang, 2017
- *Kodaianellissus intorqueus* Wang, Bourgoin & Zhang, 2017: China (Yunnan).

Neokodaiana Yang, 1994
- *Neokodaiana chihpenensis* Yang, 1994: China (Taiwan).
- *Neokodaiana minensis* Meng & Qin, 2016: China (Fujian).
- *Neokodaiana yaeyamana* Gnezdilov & Hayashi, 2015: Nansei-shoto (Ryukyu Islands).

Sivaloka Distant, 1906
- *Sivaloka arcuata* Chang & Chen, sp. nov.: China (Guizhou).
- *Sivaloka limacodes* Distant, 1906: India.
- *Sivaloka trigona* Chang & Chen, sp. nov.: China (Guangxi).

Tetricissus Wang, Bourgoin & Zhang, 2017
- *Tetricissus philo* (Fennah, 1978): Vietnam.

Key to genera of Kodaianellini Wang, Zhang & Bourgoin, 2016 of the world

1 Forewings with Pcu+A_1 veins keel-shaped (Figs 29, 44) ..... ***Sivaloka***
– Forewings with Pcu+A_1 veins non keel-shaped **2**
2 Hindwings with A_{11} vein branched **3**
– Hindwings with A_{11} vein simple, unbranched **4**

3 Hindwings with A_2 lobe distinctly narrower than Pcu-A_1 lobe, and A_2 vein nearly reaching to middle of A_2 lobe (Wang et al. 2017: fig. 6) ..... ***Kodaianellissus***

– Hindwings with A_2 lobe as wide as Pcu-A_1 lobe, and A_2 vein nearly reaching to apical margin of A_2 lobe (Wang et al. 2017: fig. 23) ..... ***Tetricissus***

4 Frons with one pale transverse carina in middle level of frons, and one pale transverse band above frontoclypeal suture (Gnezdilov and Hayashi 2015: figs 1, 2)..... ***Neokodaiana***

– Frons without above characters **5**

5 Anal tube with the maximum width near apical margin in dorsal view (Fig. 9); aedeagus with one hooked process in lateral view (Fig. 12) ..... ***Kodaianella***

– Anal tube with the maximum width near middle in dorsal view (Chen et al. 2014: fig. 2–79H); aedeagus with two hooked processes in lateral view (Chen et al. 2014: fig. 2–79K)..... ***Dentatissus***

Taxonomy

Family Issidae Spinola, 1839
Subfamily Hemisphaeriinae Melichar, 1906
Tribe Kodaianellini Wang, Zhang & Bourgoin, 2016

Genus *Kodaianella* Fennah, 1956

Kodaianella Fennah 1956: 508; Zhang and Chen 2010: 62; Gnezdilov 2013: 42; Chen et al. 2014: 136.

Type species. *Kodaianella bicinctifrons* Fennah, 1956.

Diagnostic characters. Body size small, slightly flat in dorsal view (Fig. 1). Width of head (Figs 1, 3) including eyes, narrower than pronotum. Vertex (Fig. 3) irregularly quadrangular, with width at base ca 1.7–2.3 times longer than length in middle; disc of vertex slightly depressed, with median carina linear or obscure; anterior margin slightly arched, convex; posterior margin obviously arched or obtusely concave. Gena in lateral view (Fig. 4) with one obvious ocellus between compound eye and antenna. Frons (Fig. 5) irregularly hexagonal, nearly flat, with median carina explicit and straight, reaching to 2/3 of frons, without lateral carinae; maximum width broader than length in middle; base slightly narrow, broader toward to apical margin; lateral margins of frons incurved below level of socket of antennae, with verrucae near lateral margins. Clypeus (Fig. 5) triangular, with median carina obscure or absent. Rostrum (Fig. 5) nearly surpassing mesotrochanters. Pronotum (Figs 1, 3) triangular, with median carina distinct or obscure and degraded, with distinct lateral carinae, without sub-lateral carinae; apical margin obtusely angled convex; posterior margin slightly arched or nearly straight. Mesonotum (Fig. 3) triangular, with median carina obvious or obscure or absent, sub-lateral carinae absent. Forewings (Figs 1, 2, 6) irregularly quadrangu-

lar, length ca 1.6–2.4 times longer than maximum width; anterior margin obviously arched; posterior margin straight; apical margin nearly truncated; longitudinal veins obvious and short transverse veins numerous and not obvious; with "hypocostal plate", ScP and RP convergent near base, ScP and RP veins long, not forked, nearly reaching apical margin of forewings; MP bifurcating into two branches near base; CuA forked into two branches near middle; CuP present; Pcu and A_1 united near middle of clavus. Hindwings (Fig. 7) with three lobes: ScP-R-MP-Cu lobe developed; Pcu-A_1 lobe distinctly thinner, less than half as wide as ScP-R-MP-Cu lobe; A_2 lobe thinner, distinctly surpassing half-length of Pcu-A_1 lobe, anterior and posterior margins subparallel; Pcu simple, anastomosing with A_{11}; A_{11} unbranched, A_{12} simple and straight; A_2 unbranched, not reaching to apical margin of hindwings. Hind tibiae with 2 lateral spines in distal half and 8–10 apical spines; first metatarsomere with 7–11 apical spines; second metatarsomere with 2 apical spines; spinal formula of hind leg (2)8–10/7–11/2.

Male genitalia. Anal tube (Figs 8, 9) irregularly triangular, longer in middle than maximum width in dorsal view, basal part narrow, apical part broader, maximum width near apical margin. Anal style (Fig. 9) moderately long, not surpassing anal tube. Pygofer (Fig. 8) symmetrical, irregularly rectangular; anterior and posterior margins nearly parallel in lateral view; dorsal and ventral margins nearly parallel in lateral view. Genital styles (Figs 8, 10) irregularly triangular; dorso-anterior margin not obvious, dorso-posterior margin and ventral margin nearly parallel. Capitulum of genital styles obvious and long (Fig. 11). Phallobase (Figs 12, 13) symmetrical, "U"-liked tubular in lateral view; dorsal lobe with apical part membranous, with various processes in lateral view. Aedeagus (Figs 12, 13) with one hooked process in lateral view.

Female genitalia (Figs 14–28). Anal tube (Figs 17, 23) oblong, obviously longer in middle than its width; apical margin arched, convex; lateral margin parallel. Anal style (Figs 17, 23) long or short, located near base of anal tube. Hind margin of gonocoxa VIII with endogonocoxal lobe not obvious (Figs 18, 24); endogonocoxal process membranous, gradually narrowing. Anterior connective lamina of gonapophyses VIII (Figs 18, 24) irregularly rectangular, with two lateral teeth bearing two keels in lateral group and three teeth in apical group. Posterior connective lamina of gonapophyses IX (Figs 19, 20, 25, 26) triangular, with lateral field membranous; sublateral field with two sclerous triangular processes in lateral margin (Figs 19, 25); median field with unobvious prominence (median dorsal process) (Figs 19, 25); ventroposterior lobes acutely bent at an angle (posterior ventral lobes) (Figs 20, 26). Gonoplacs (Figs 21, 27) irregularly rounded, without keels. Hind margin of sternite VII (Figs 22, 28) median area raised in ventral view, with small incision in middle.

Key to species of *Kodaianella* Fennah, 1956 of the world

1 First metatarsomere of hind legs with 7 apical teeth (Gnezdilov 2013: fig. 4) .... ***K. bipartita***

– First metatarsomere of hind legs with more than 7 apical teeth **2**

2 Anal tube with apical margin nearly truncated near middle part (Fig. 9); aedeagus with pair of biforked long hooks in ventral view (Fig. 13) .... ***K. furcata* Chang & Chen, sp. nov.**

– Anal tube with apical margin concave near middle; aedeagus with pair of simple long hooks in ventral view **3**

3 Phallobase with pair of long spines near apical part (Zhang and Chen 2010: fig. 25) ..... ***K. longispina***

– Phallobase with pair of short spines near apical part (Zhang and Chen 2010: fig. 7) ..... ***K. bicinctifrons***

***Kodaianella furcata* Chang & Chen, sp. nov.**
http://zoobank.org/EB9B5313-A0A2-4F2B-821F-FD5E8B5A342E
Figs 1–13

Type material. Holotype: ♂, China: Guangxi, Nonggang National Nature Reserve (22°28'N, 106°58'E), 8 May 2011, H Li leg.; paratypes: 5♂♂, same data as holotype (IEGU); 1♂, Guangxi, Nonggang National Nature Reserve (22°28'N, 106°58'E), 7–8 May 2012, H Li and N-N Yang, leg.

Diagnosis. This species is similar to *K. longispina* Zhang & Chen, 2010 in appearance, but it differs from the latter in having the phallobase with dorsal lobe bearing one rod-like process near its apical part in lateral view (Fig. 12a); the phallobase with ventral lobe distinct short, apical part finger-liked in ventral view (Fig. 13c); and the aedeagus in lateral view, with a forked and hooked process near the apical 1/3 (Fig. 12d).

Description. Body length: male 3.94–4.18 mm; forewing: male 3.16–3.45 mm.

Coloration. General color brown (Figs 1, 2). Vertex, pronotum, and mesonotum (Fig. 3) black-brown. Frons (Fig. 5) black-brown, with pale yellow verrucae along base and lateral margins. Clypeus (Fig. 5) yellow-brown. Compound eyes black-brown, ocelli pale green (Fig. 4). Forewings (Fig. 2) yellow-brown, with dark spots. Legs yellow-brown, with tips of spines on hind tibiae and tarsi black.

Head and thorax. Head (Fig. 3) including eyes, slightly narrower than pronotum (0.96: 1.00). Vertex (Fig. 3) shorter in middle than the width at base (0.43: 1.00), with median carina linear; anterior margin slightly convexly arched; posterior margin obviously obtusely concave. Frons (Fig. 5) shorter in middle than the widest breadth (0.60: 1.00); median carina obvious and straight, reaching to 2/3 level of frons. Clypeus (Fig. 5) triangular, without median carina. Pronotum (Fig. 3) with median carina obscure, lateral carina reaching to the posterior margin. Mesonotum (Fig. 3) with median carina obscure. Forewings (Fig. 6) 1.60 times as long as maximum breadth; with wide "hypocostal plate"; ScP and RP convergent near base, ScP and RP veins long, nearly reaching apical margin; MP bifurcating two branches near basal 1/3, MP_1 forked near apical 1/3; CuA forked into two branches near middle; CuP present, Pcu and A_1 united near middle of clavus. Hindwings (Fig. 7) with ScP+R and M simple, not forked,

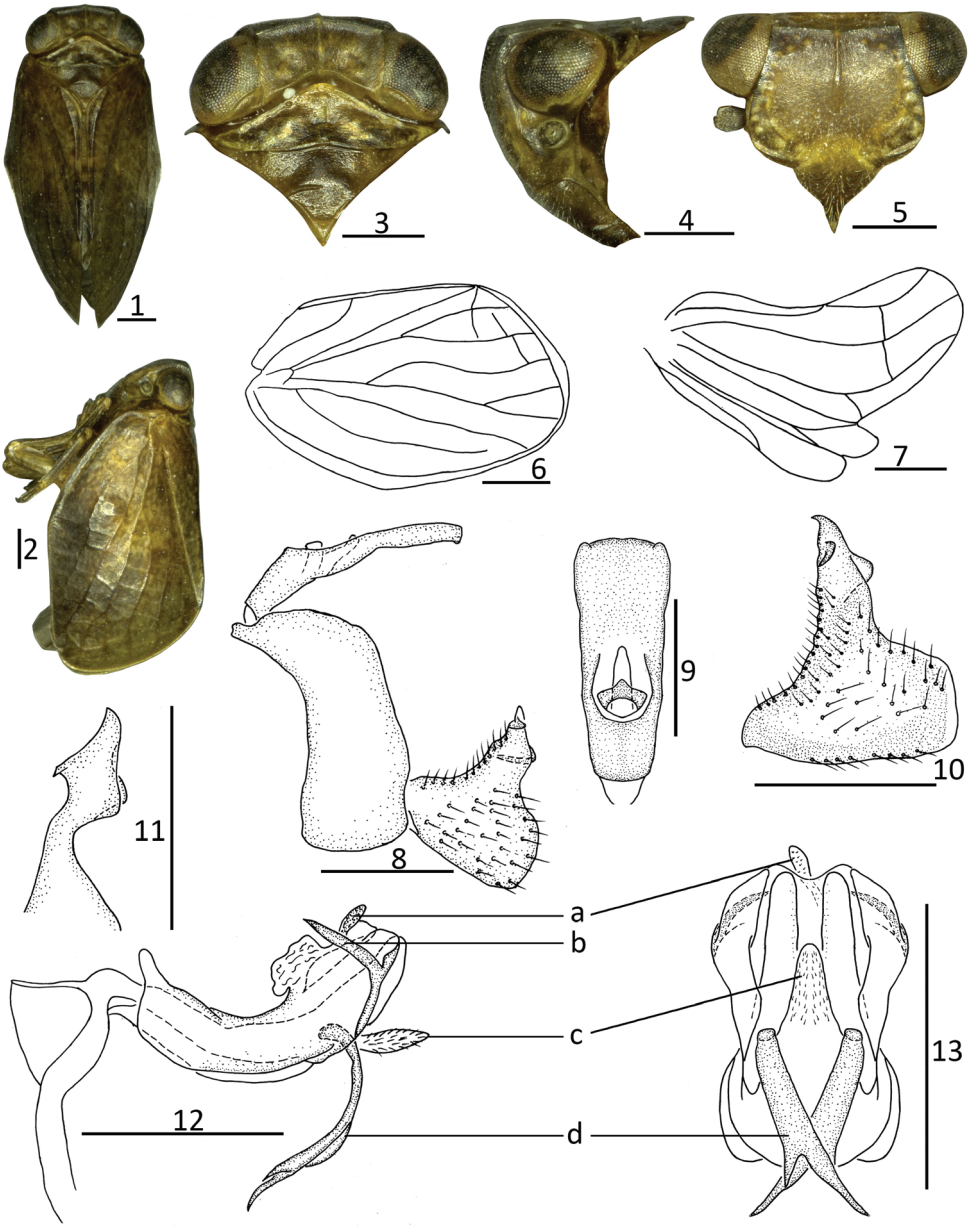

Figures 1–13. *Kodaianella furcata* Chang & Chen, sp. nov. **1** habitus, dorsal view **2** habitus, lateral view **3** head and thorax, dorsal view **4** head and thorax, lateral view **5** head, ventral view **6** forewing **7** hindwing **8** male genitalia, lateral view **9** male anal segment, dorsal view **10** genital styles, lateral view **11** capitulum of genital styles, ventral view **12** phallobase and aedeagus, lateral view **13** phallobase and aedeagus, ventral view. Scale bars: 0.5 mm. Abbreviations: a = rod-like process; b = hook-like process; c = ventral lobe; d = long forked process.

CuA forked near apical part, with one vein between R and M, M and CuA_1; and Pcu and A_{11} jointed near apical 1/4, without short transverse vein between Pcu + A_{11} and A_{12}; A_2 simple, reaching to 2/3 of A_2 lobe. Spinal formula of hind leg (2)8/8/2.

Male genitalia. Anal tube (Fig. 9) longer in midline than the width (2.49: 1.00) in dorsal view; lateral margins nearly parallel and widest in apical part; apical margin nearly truncated, with unobvious small, angular process near lateral margin. Anal style (Fig. 9) stout and long, located at the base 2/5 of anal tube, surpassing the opening of anal pore. Pygofer (Fig. 8) irregularly rectangular; dorsal margin slightly broader than ventral margin; anterior margin arched near dorsal 1/3; posterior margin nearly straight. Genital styles (Figs 8, 10) relatively triangular; anterior margin without triangular process; posterior margin with triangular process. Capitulum of genital styles irregularly triangular, with small irregular triangular, relatively long and stout neck (Fig. 11). Phallobase (Figs 12, 13) with dorsal lobe cystiform near apical part, with stout rod-like process (Figs 12a, 13a) in apical 1/6, directed to posterior, with dorsolateral lobe with short hook-like process (Fig. 12b), pointed to dorsal margin in lateral view; lateral lobe splitting into two stout branches; ventral lobe membranous, apical part narrow, surface with microvilli in lateral view (Fig. 12c); ventral lobe in ventral view obviously shorter than dorsal lobe, with apical part projecting into finger-like process in middle (Fig. 13c). Aedeagus (Figs 12, 13) with long, hooked process near apical 1/3 in ventral view, tip of process directed to ventro-posterior in lateral view (Fig. 12d); in ventral view, hooked process forked into asymmetrical hooks (Fig. 13d).

Etymology. The new species is derived from the Latin word "*furcata*", in reference to the aedeagus, which bears a forked, hooked process.

Host plant. Unknown.

Distribution. China (Guangxi).

Kodaianella bicinctifrons Fennah, 1956

Figs 14–22

Kodaianella bicinctifrons Fennah 1956: 508; Chen et al. 2014: 137.

Material examined. 1♂2♀♀, China: Guizhou, Congjiang County, 24 June 2005, D-Y Ge leg.; 2♂♂1♀, Sichuan, Kangding County, 8 Aug. 2005, F-L Xu leg.

Female genitalia (Figs 14–16). Anal tube (Fig. 17) longer in middle than its width (2.64: 1.00). Anal style (Fig. 17) short, located in basal 1/4 of anal tube, not surpassing the opening of anal pore. Hind margin of gonocoxa VIII with endogonocoxal lobe not obvious, endogonocoxal process membranous, gradually narrowing (Fig. 18). Anterior connective lamina of gonapophyses VIII (Fig. 18) irregularly rectangular; with two lateral teeth bearing two keels in lateral group and three teeth in apical group. Posterior connective lamina of gonapophyses IX (Figs 19, 20) triangular, narrow, with lateral field membranous; sublateral field sclerous, with one triangular process in outer lateral margin near middle and another triangular process in apical part (Figs 19a, 20a); medi-

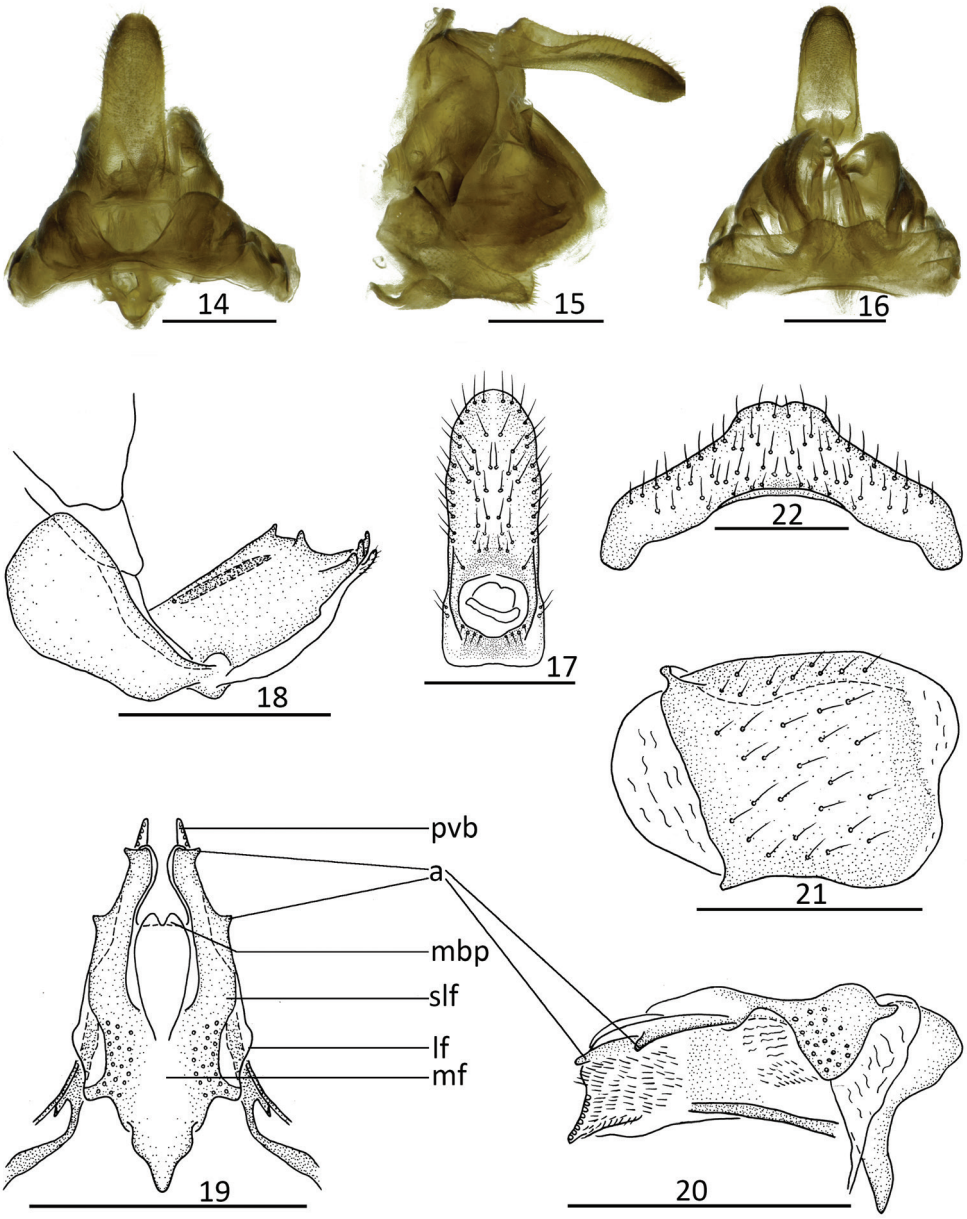

Figures 14–22. Female genitalia. *Kodaianella bicinctifrons* Fennah, 1956 **14** overall, dorsal view **15** overall, lateral view **16** overall, ventral view **17** female anal segment, dorsal view **18** anterior connective lamina of gonapophyses VIII, lateral view **19** posterior connective lamina of gonapophyses IX, dorsal view **20** posterior connective lamina of gonapophyses IX, lateral view **21** gonoplacs, lateral view **22** sternite VII, ventral view. Scale bars: 0.5 mm. Abbreviations: lf = lateral field of posterior connective lamina of gonapophyses IX; slf = sublateral field of posterior connective lamina of gonapophyses IX; mf = medial field of posterior connective lamina of gonapophyses IX; mdp = medial dorsal process; pvb = posterior ventral lobes; a = triangular process.

an field with symmetrical mountain-like prominence, apical margin concave (median dorsal process); ventroposterior lobes acutely bent at an angle (posterior ventral lobes). Gonoplacs (Fig. 21) without keels. Hind margin of sternite VII (Fig. 22) median area raised in ventral view, with shallow incision.

Kodaianella longispina Zhang & Chen, 2010

Figs 23–28

Kodaianella longispina Zhang & Chen 2010: 66; Chen et al. 2014: 140.

Material examined. 2♂♂3♀♀ (paratypes), China: Yunnan, Baoshan, 8–20 Aug. 2006, P Zhang, Z-G Zhang and Q-Z Song, leg.

Female genitalia. As in *K. bicinctifrons* Fennah, 1956, but anal tube longer in middle than the width (2.18: 1.00); anal style long, surpassing the opening of anal pore (Fig. 23). Anterior connective lamina of gonapophyses VIII (Fig. 24) with two lateral teeth bearing two keels in lateral group and three teeth in apical group. Posterior connective lamina of gonapophyses IX (Fig. 25) broader, with median field with irregular, thin prominence; distal part of ventroposterior lobes bent at an obvious angle (Fig. 26). Gonoplacs (Fig. 27) without keels. Hind margin of sternite VII (Fig. 28) median area raised in ventral view, with deeper incision.

Genus *Sivaloka* Distant, 1906

Figs 29–55

Sivaloka Distant 1906: 352; Gnezdilov 2013: 42.

Type species. *Sivaloka limacodes* Distant, 1906.

Diagnostic characters. Body size small (Figs 30, 45). Width of head (Figs 31, 46) including eyes, narrower or broader than pronotum. Vertex (Figs 31, 46) irregularly quadrangular, with width at base more than 2.5 times longer than length at middle; disc of vertex distinctly depressed, with feeble median carina; anterior margin convexly arched; posterior margin obviously concavely arched; lateral margins parallel. Gena (Figs 32, 47) with one obvious ocellus between compound eye and antenna in lateral view. Frons (Figs 33, 48) irregularly hexagonal, with obvious median carina on basal half, feeble carina or no carina on apical half, nearly reaching to frontoclypeal suture, without lateral carinae; broader than length in middle, the base slightly narrowed, broader toward to apical margin, obviously enlarged above clypeus; lateral margins not parallel, with verrucae near lateral margins. Clypeus (Figs 33, 48) triangular, with or without median carina. Rostrum (Fig. 33) surpassing mesotrochanters. Pronotum (Figs 31, 46) triangular, with median carina or degraded, with lateral carinae; with pit each other between median carina and lateral carinae, without sub-lateral cari-

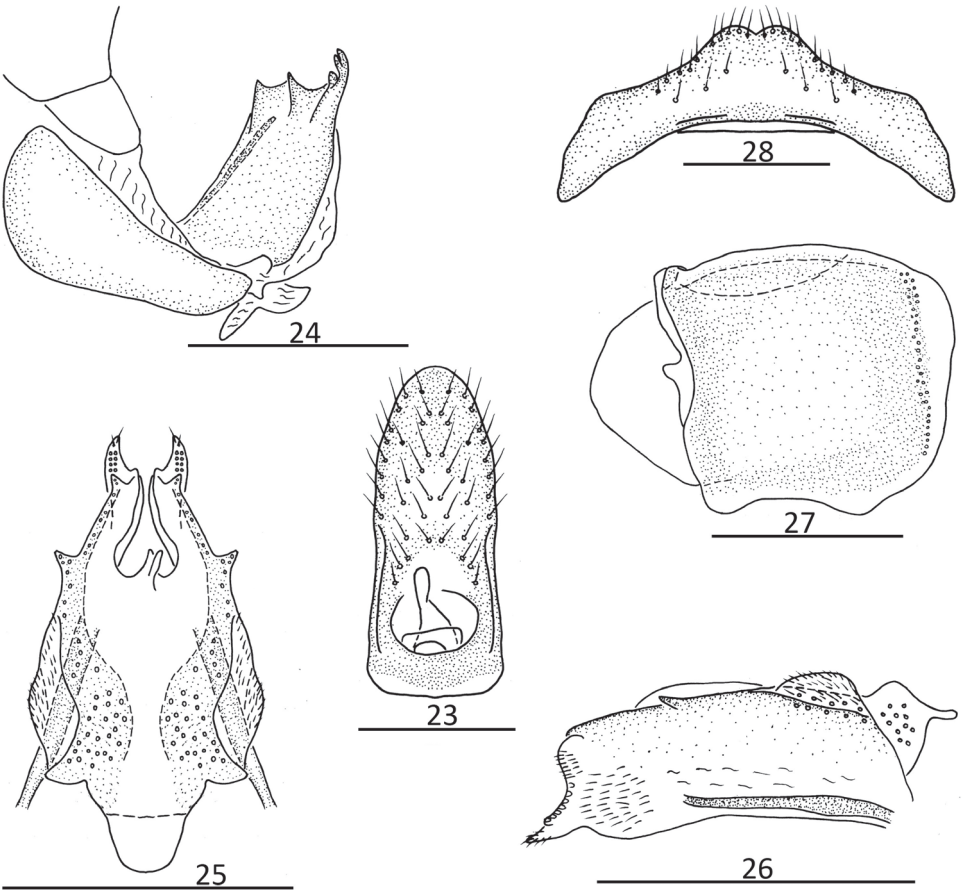

Figures 23–28. Female genitalia. *Kodaianella longispina* Zhang & Chen, 2010 **23** female anal segment, dorsal view **24** anterior connective lamina of gonapophyses VIII, lateral view **25** posterior connective lamina of gonapophyses IX, dorsal view **26** posterior connective lamina of gonapophyses IX, lateral view **27** gonoplacs, lateral view **28** sternite VII, ventral view. Scale bars: 0.5 mm.

nae; apical margin obtuse-angle convex; posterior margin nearly straight. Mesonotum (Figs 31, 46) triangular, with or without median carina, with raised sub-lateral carina. Forewings (Figs 36, 49) irregularly quadrangular, length ca 1.4–2.0 times longer than maximum width; anterior margin clearly arched; posterior margin slightly wavy; apical margin obliquely truncated in lateral view; longitudinal veins obvious, the base narrow, broader toward to the apical part; with broad "hypocostal plate", with spherical expansion near ScP vein in basal 1/3 of forewings, ScP and RP convergent near base, ScP and RP veins long, not forked, reaching apical margin of forewing; MP bifurcating two branches before middle, MP1 forked near apical margin, MP2 forked or not near apical margin; CuA forked into brances near apical part; CuP present; Pcu and A1 united near middle of clavus, keel-shaped, especially A1 obviously keeled in lateral view. Hindwings (Fig. 37) with three lobes: with ScP-R-MP-Cu lobe developed;

Pcu-A1 lobe distinctly less than half wide as ScP-R-MP-Cu lobe; A2 lobe thin, distinctly surpassing half length of Pcu-A1 lobe, anterior and posterior margins subparallel; Pcu simple, anastomosing with A11, A11 vein simple, unbranched, A12 straight and simple, A2 vein, unbranched, not reaching to apical margin. Hind tibia with 2 lateral spines in distal half and 8–10 apical spines; first metatarsomere with 8–10 apical spines; second metatarsomere with 2 apical spines; spinal formula of hind leg (2)8–10/8–10/2.

Male genitalia. Anal tube (Figs 39, 51) irregularly rectangular, elongate, longer in middle more 2.5 times than the base in dorsal view; lateral margin nearly parallel. Anal style (Figs 39, 51) long or short, not surpassing anal tube, located near base or middle. Pygofer (Figs 38, 50) symmetrical, irregularly rectangular; anterior and posterior margins parallel in lateral view. Genital styles (Figs 40, 52) symmetrical, irregularly triangular in lateral view; dorsal margin bearing different prominence before the capitulum. Capitulum of genital styles long or short (Figs 41, 53). Phallobase (Figs 42, 54) symmetrical, "U"-liked tubular in lateral view, dorsal lobe with processes near apex. Aedeagus (Figs 43, 55) with one hooked process in lateral view.

Female genitalia. Anal tube long, lateral margins nearly parallel. Gonoplacs irregularly rounded, without keels. Hind margin of sternite VII with prominence in middle area in ventral view.

Key to species of *Sivaloka* Distant, 1906 of the world

1 Frons with pale transverse line near middle; clypeus relatively flat, with stout median carina (Gnezdilov 2013: fig. 2) ..... ***S. limacodes***

– Frons without pale transverse line near middle; clypeus with basal part swollen, apical part sunken, without median carina **2**

2 Phallobase with dorsal lobe with long hooked process near apical part (Fig. 42a); aedeagus with one long hooked process near middle in lateral view, directed to caudad (Fig. 42e)..... ***S. arcuata* Chang & Chen, sp. nov.**

– Phallobase with dorsal lobe with small spinous process near apical part (Fig. 54a); aedeagus with one hooked process near basal 1/3 in lateral view, directed to cephalad (Fig. 54e)..... ***S. trigona* Chang & Chen, sp. nov.**

***Sivaloka arcuata* Chang & Chen, sp. nov.**
http://zoobank.org/E0F6777D-AE12-44D8-8F38-7DFCF922F2AD
Figs 29–43

Type material. Holotype: ♂, China: Guizhou, Anlong County, Xianheping Provincial Nature Reserve (22°59'N, 105°43'E), 28 Aug. 2012, W-B Zheng leg.; paratypes: ♂, same data as holotype (IEGU); ♂, Guizhou, Congjiang County, Moon Hill (Height 1159 m) (25°38'N, 108°13'E), 19 July 2006, Q-Z Song leg.

Figures 29–35. *Sivaloka arcuata* Chang & Chen, sp. nov. **29–33** holotype **34–35** paratype **29, 34** habitus, dorsal view **30, 35** habitus, lateral view **31** head and thorax, dorsal view **32** head and thorax, lateral view **33** head and thorax, ventral view. Scale bars: 0.5 mm. Abbreviations: ks = Pcu and A_1 keel-shaped; pl = hypocostal plate.

Diagnosis. This species is identified by the dark-brown or yellow-brown frons, without any bands (Fig. 33); the clypeus without median carina, with its basal part swollen and its apical part sunken (Fig. 33); the forewings longer 2.0 times than their width (Figs 30, 35); the dorsal margin of the genital styles bearing one arched prominence near the middle (Fig. 40); the phallobase with the dorsal lobe bearing a relatively long, hooked process near its apical part (Fig. 42a) and with a triangular process on the ventral margin (Fig. 42b); and the aedeagus near its middle in lateral view with one hooked process, which is directed to caudad (Fig. 42e).

Description. Body length (from apex of vertex to tip of forewings): male 5.40–5.50 mm; forewings: male 4.40–4.50 mm.

Coloration. General color yellow-brown or pale yellow (Figs 29, 30, 34, 35). Vertex, pronotum, and mesonotum (Fig. 31) dark-brown, suffused with rusty brown. Gena (Fig. 32) dark brown, with two inconspicuous yellow bands. Compound eyes brown to black, ocelli yellow (Fig. 32). Frons (Fig. 33) dark brown or yellow-brown, with yellow verrucae near lateral margin. Clypeus (Fig. 33) with basal part black, apical

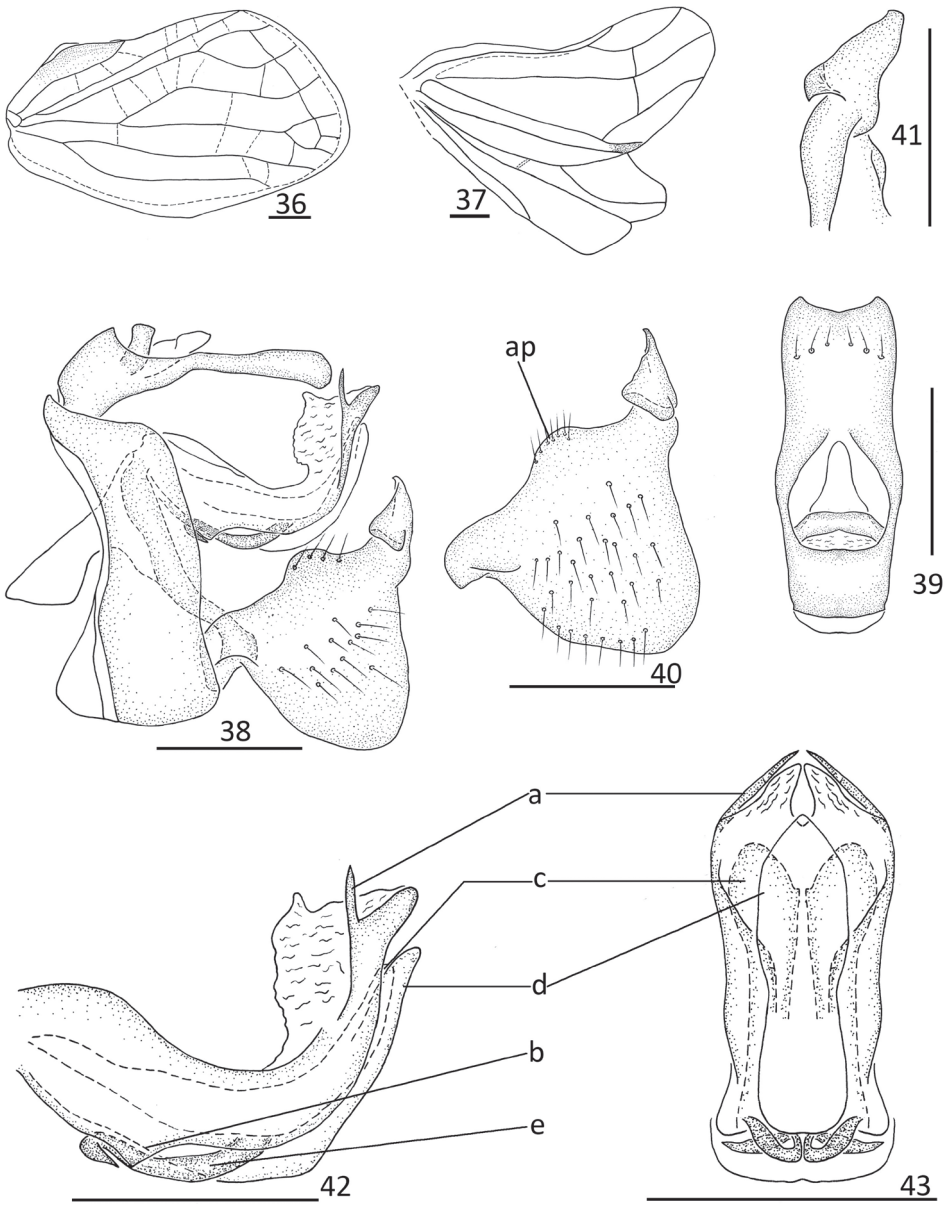

Figures 36–43. *Sivaloka arcuata* Chang & Chen, sp. nov. **36** forewing **37** hindwing **38** male genitalia, lateral view **39** male anal segment, dorsal view **40** genital styles, lateral view **41** capitulum of genital styles, ventral view **42** phallobase and aedeagus, lateral view **43** phallobase and aedeagus, ventral view. Scale bars: 0.5 mm. Abbreviations: ap = arched prominence; a = long hooked process; b = angular process; c = lateral lobe, d = ventral lobe; e = hooked process.

part yellow to yellow-brown. Forewings (Figs 29, 34) dark brown or pale yellow, with diffuse rusty brown. Hindwings brown. Legs yellow-brown, tip of spineson hind tibiae and tarsi black.

Head and thorax. Head (Fig. 31) including eyes, slightly narrower than pronotum (0.93: 1.00). Vertex (Fig. 31) shorter in middle than width at base (0.50: 1.00). Frons (Fig. 33) shorter in middle than maximum breadth (0.65: 1.00); with median carina distinct, reaching to the level of middle of frons. Clypeus (Fig. 33) triangular, without median carina; basal part swollen, apical part slightly sunken (Fig. 33). Pronotum (Fig. 31) with median carina feeble. Mesonotum (Fig. 31) with median carina raised, fused in anterior margin. Forewings (Fig. 36) longer than wide (2.00: 1.00); with broad "hypocostal plate", ScP and RP convergent near base, short common stem, ScP and RP veins long, parallel with anterior margin of forewing, reaching to apical margin; MP two branched in basal 1/3, MP1 dividing two branches in distal 1/3, MP2 not forked in distal part; CuA forked into two branches in distal 1/3, CuP present; Pcu and A1 united in middle of clavus, clavus almost reaching to 2/3 of forewing. Hindwings (Fig. 37) with ScP+R and CuA forked near apical part, MP simple, not forked, CuA2 and CuP fused near apical part, with one vein between R and M, M and CuA1; Pcu and A11 unbranched, with one transverse vein between Pcu+A11 and A12; A2 reaching to apical 1/3 of A2 lobe. Spinal formula of hind leg (2)8–10/8–10/2.

Male genitalia. Anal tube in dorsal view (Fig. 39) longer in middle than the widest breadth (2.50: 1.00), the maximum width in middle of anal tube; apical margin distinctly, angularly concave; lateral margins almost parallel, slightly concave near apical 2/3 of anal tube. Anal style (Fig. 39) relatively long and stout, located in basal 2/5 of anal tube, not surpassing the opening of anal pore. Pygofer (Fig. 38) irregularly rectangular; anterior and posterior margins nearly parallel in lateral view; dorsal and ventral margins parallel. Genital styles (Fig. 40) irregularly triangular in lateral view; dorsal and ventral margins not parallel; dorsal margin with one arched prominence near middle at base of capitulum; ventral margin slightly arched. Capitulum of genital styles irregularly triangular, with small lobe; with stout and not obvious neck (Fig. 41). Phallobase (Figs 42, 43) with dorsal lobe slightly expanded into membranous, cystiform process; and dorso-lateral lobe splitting into relatively long, hooked process near apical part (Figs 42a, 43a), ventral margin of dorso-lateral lobe with angular process in basal 1/3 in lateral view (Fig. 42b); lateral lobe distinctly shorter than dorsal lobe in lateral view (Fig. 42c), splitting into two stout branches (Fig. 43c); ventral lobe relatively longer than lateral lobe in lateral view (Fig. 42d) in lateral view; in ventral view, apical part obviously archedly convex (Fig. 43d); lateral margins parallel in ventral view. Aedeagus (Figs 42, 43) with one long, hooked process near middle (Fig. 42e) in lateral view, directed to caudad.

Etymology. The specific name is derived from the Latin words "arcuata" in reference to the genital styles which bear an arched prominence on the base before the capitulum.

Host plant. Unknown.

Distribution. China (Guizhou).

Remarks. The new species is similar to *S. limacodes* Distant, 1906, but it differs from it by: 1) frons dark brown or yellow-brown, without any band (Fig. 33) (frons with pale and transverse line near middle in *S. limacodes*); 2) clypeus without median

carina, basal part swollen, apical part sunken (Fig. 33) (clypeus with stout median carina, relatively flat in *S. limacodes*); 3) forewings 2.00 times longer than their maximum breadth (Fig. 36) (forewings 1.40 times longer than their maximum breadth in *S. limacodes*).

***Sivaloka trigona* Chang & Chen, sp. nov.**

http://zoobank.org/D273CBAC-17A5-4B0B-9E6B-850C4ABE9386

Figs 44–55

Type material. Holotype: ♂, China: Guangxi, Yangshuo County (24°59'N, 105°36'E), 28 May 2009, W-B Zheng leg. (IEGU).

Diagnosis. This species is similar to *S. arcuata* Chang & Chen, sp. nov., but it differs from the latter by: 1) forewings with MP_2 dividing into two branches (Fig. 49); 2) dorsal margin of genital styles bearing one triangular prominence near middle (Fig. 52); 3) phallobase with dorsal lobe with a small spinous process near apical part (Fig. 54a), ventral margin with half-leaf process in basal 1/3 (Fig. 54b); 4) aedeagus in lateral view with one short, hooked process near basal 1/3, directing to cephalad (Fig. 54e).

Description. Body length (from apex of vertex to tip of forewings): male 5.00 mm; forewings: male 4.10 mm.

Coloration. General color pale yellow (Figs 44, 45). Vertex, pronotum, and mesonotum (Fig. 46) pale yellow to brown. Gena (Fig. 47) dark brown, with one not obvious yellow band. Compound eyes and antennae black, ocelli pale (Fig. 47). Frons (Fig. 48) dark brown, with scores of pale verrucae along lateral margin. Clypeus black-brown (Fig. 48). Forewings (Figs 44, 45) pale yellow, with diffuse, dark brownish markings. Hindwings brown. Legs pale green or yellow-brown, tip of spines on hind tibiae and tarsi black.

Head and thorax. Head (Fig. 46) including eyes, slightly broader than pronotum (1.07: 1.00). Vertex (Fig. 46) shorter in middle than the width at base (0.41: 1.00). Frons (Fig. 48) slightly shorter in middle than maximum breadth (0.69: 1.00); with median carina, its basal half distinct, reaching to the level of middle of frons, apical part feeble, nearly to the frontoclypeal suture. Clypeus (Fig. 48) triangular, with median carina; basal part swollen, apical part slightly sunken. Pronotum (Fig. 46) with median carina feeble. Mesonotum (Fig. 46) with median carina raised, basal part forked, fused in anterior margin; lateral carinae not obvious. Forewings (Fig. 49) 1.63 times as long as maximum breadth; ScP and RP convergent near base, ScP and RP long, parallel to anterior margin of forewing, reaching to outer margin; MP two branches in basal 1/3, MP_1 in distal 1/5 dividing into two branches or unbranched, MP_2 forked in distal 1/5; CuA forked into two branches in distal 1/3; CuP present; Pcu and A_1 united in middle of clavus, clavus almost reaching to 2/3 of forewing. Hindwings unknown. Spinal formula of hind leg (2)9/9/2.

Male genitalia. Anal tube in dorsal view (Fig. 51) longer in middle than at widest breadth (2.57: 1.00), maximum width at middle of anal tube; anterior margin almost

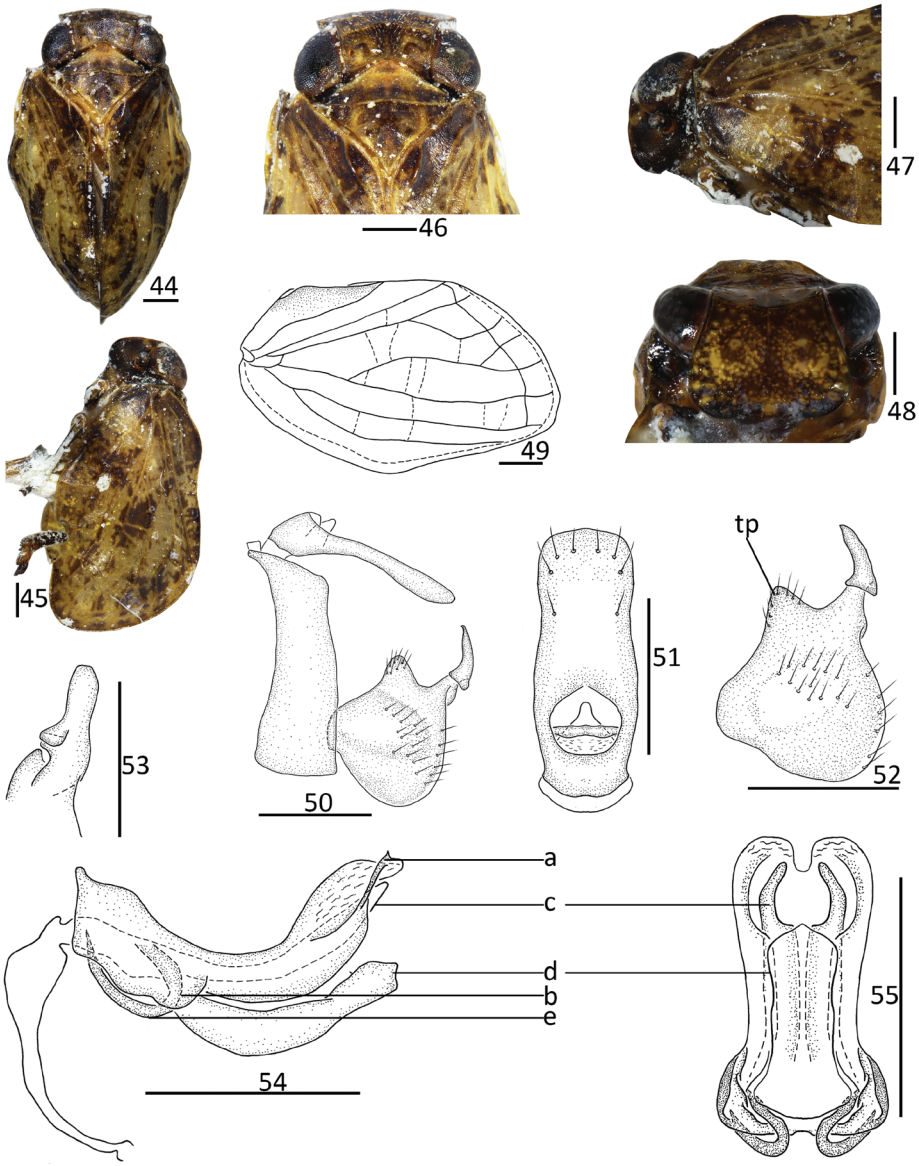

Figures 44–55. *Sivaloka trigona* Chang & Chen, sp. nov. **44** habitus, dorsal view **45** habitus, lateral view **46** head and thorax, dorsal view **47** head and thorax, lateral view **48** head, ventral view **49** forewing **50** male genitalia, lateral view **51** male anal segment, dorsal view **52** genital styles, lateral view **53** capitulum of genital styles, ventral view **54** phallobase and aedeagus, lateral view **55** phallobase and aedeagus, ventral view. Scale bars: 0.5 mm. Abbreviations: tp = triangular prominence; a = small spinous process; b = half-leaf process; c = lateral lobe; d = ventral lobe; e = hooked process.

straight; lateral margins parallel, lateral margin slightly concave near apical 2/5. Anal style (Fig. 51) short and thin, located in basal 2/5, not surpassing the opening of anal pore. Pygofer (Fig. 50) irregularly rectangular; anterior and posterior margins parallel

in lateral view; dorsal margin inclined to ventral margin. Genital styles (Fig. 52) irregularly triangular in lateral view; dorsal and ventral margins not parallel; dorsal margin with triangular prominence near middle at base of capitulum; ventral margin slightly arched. Capitulum of genital styles irregularly triangular; with irregular triangular, and thin, distinct neck (Fig. 53). Phallobase (Figs 54, 55) with dorsal lobe slightly expanded into membranous cystiform process; dorso-lateral lobe with a small spinous process near apical part (Fig. 54a) in lateral view; ventral margin with half-leaf process in basal 1/3, margin wavy (Fig. 54b); lateral lobe shorter than dorsal lobe (Fig. 54c), splitting into two branches, apical part appearing long thin finger, and basal part stout in ventral view (Fig. 55c); ventral lobe obviously shorter than lateral lobe in lateral view (Fig. 54d); in ventral view, apical margin of ventral lobe subtriangular and convex in middle; lateral margin of ventral lobe parallel in ventral view (Fig. 55d). Aedeagus (Figs 54, 55) with one relatively short, hooked process near basal 1/3 (Fig. 54e) in lateral view, directed to cephalad.

Etymology. The specific name is derived from the Latin words "*trigona*" in reference to the triangular prominence near the middle of the dorsal margin of the genital styles.

Host plant. Unknown.

Distribution. China (Guangxi).

Remarks. The new species is similar to *S. arcuata* Chang & Chen, sp. nov. in appearance, but it differs the latter by: 1) dorsal margin of genital styles bearing one triangular prominence near middle (Fig. 52) (dorsal margin of genital styles bearing one arched prominence near middle in *S. arcuata* (Fig. 40)); 2) phallobase (Fig. 54) with dorsal lobe with a small spinous process near apical part (Fig. 54a), ventral margin with half-leaf process in basal 1/3 (Fig. 54b) (phallobase with dorsal lobe with long hooked process near apical part in *S. arcuata* (Fig. 42a), ventral margin with triangular process (Fig. 42b)); 3) aedeagus (Fig. 54) with one hooked process near basal 1/3 in lateral view, directed to cephalad (Fig. 54e)(aedeagus with one hooked process near middle in lateral view, directed to caudad (Fig. 42e))

Discussion

A comparison of *Kodaianella* Fennah, 1956, *Sivaloka* Distant, 1906, and *Dentatissus* Chen, Zhang & Chang, 2014, shows that species in these genera look rather similar. In these genera the width of the vertex at the base is longer than its length at its middle, the frons lacks transverse carina, the hingwings have A_{11} unbranched, and the male genitalia are in general similar.

Sivaloka is, however, clearly different from the other two genera in having the Pcu and A_1 veins on the forewings keel-shaped (Fig. 2; Chen et al. 2014: fig. 2–79B). There are also significant generic differences in the structure of the male genitalia among the three genera. In *Sivaloka*, the anal tube is irregularly rectangular with its lateral margins nearly parallel (Figs 39, 51), while in *Kodaianella* the anal tube is irregularly triangular with the lateral margin apically diverging (Fig. 9); in *Dentatissus* the anal tube is oval

and wider near its middle (Chen et al. 2014: fig. 2–79H). The capitulum of the genital styles are with a stout irregular triangular at their base in *Dentatissus* (Chen et al. 2014: fig. 2–79J); the capitulum are absent *Kodaianella* and *Sivaloka* (Figs 10, 40). The dorsal lobe of the phallobase bears various processes near its apical part in *Kodaianella* and *Sivaloka* (Figs 12, 42), but these processes are absent in *Dentatissus*. The aedeagus bears two pairs of hook-like processes in *Dentatissus* (Chen et al. 2014: fig. 2–79J) and one pair of hook-like processes in *Kodaianella* and *Sivaloka*.

Acknowledgements

This work was supported by the Program of Excellent Innovation Talents, Guizhou Province (No. 20154021), National Natural Science Foundation of China [No. 31472033 and 31093430], Science and Technology Program in Guizhou Province (No. qiankehe LH zi [2017]7267, [2017]7274, and [2018]1032), Youth Science and Technology Talent Development Project in the Education Department of Guizhou Province (No. qianjiaohe KY zi [2017]103), Academic New Cultivation and Innovation Exploration Special Project of Guizhou University in 2017 and 2018 (Grant No. qiankehe and Platform for talents [2017]5788 and [2018]5781-29), and the Project funded by China Postdoctoral Science Foundation (No. 2017M613002).

References

Bourgoin T (1987) A new interpretation of the homologies of the Hemiptera male genitalia, illustrated by the Tettigometridae (Hemiptera, Fulgoromorpha). Proceedings of the 6th Auchenorrhyncha meeting, Turin, 7–11 September: 113–120.

Bourgoin T (1993) Female genitalia in Hemiptera Fulgoromorpha, morphological and phylogenetic data. Annales de la Société Entomologique France 93: 225–244.

Bourgoin T (2019) FLOW (Fulgoromorpha Lists on The Web): a world knowledge base dedicated to Fulgoromorpha. Version 8, updated 11 September 2019. http://hemiptera-databases.org/flow/ [Accessed on: 2019–11–10]

Bourgoin T, Wang RR, Asche M, Hoch H, Soulier-Perkins A, Stroiński A, Yap S, Szwedo J (2015) From micropterism to hyperpterism: recognition strategy and standardized homology-driven terminology of the forewing venation patterns in planthoppers (Hemiptera: Fulgoromorpha). Zoomorphology 134 (1): 63–77. https://doi.org/10.1007/s00435-014-0243-6

Chan ML, Yang CT (1994) Issidae of Taiwan (Homoptera: Fulgoroidea). Chen Chung Book Press, Taichung, 188 pp.

Chen XS, Zhang ZG, Chang ZM (2014) Issidae and Caliscelidae (Hemiptera: Fulgoroidea) from China. Guizhou Science and Technology Publishing House, Guiyang, 242 pp.

Chou I, Lu JS, Huang J, Wang SZ (1985) Homoptera, Fulgoroidea. Economic insect fauna of China. Volume 36. Academia Sinica Science Press, Beijing, 152 pp.

Distant WL (1906) Rhynchota – Vol. III. (Heteroptera-Homoptera). In: Bingham CT (Ed.) The Fauna of British India, Including Ceylon and Burma. Taylor and Francis, London, 503 pp. https://biodiversitylibrary.org/page/12704468

Fennah RG (1956) Fulgoroidea from southern China. Proceedings of the California Academy of Sciences 28 (4): 441–527.

Gnezdilov VM (2002) Morphology of the ovipositor in members of the subfamily Issinae (Homoptera, Cicadina, Issidae). Entomologicheskoe Obozrenie 81(3): 605–626.

Gnezdilov VM (2003) Review of the family Issidae (Homoptera, Cicadina) of the European fauna, with notes on the structure of ovipositor in planthoppers. Chteniyapamyati N.A. Kholodkovskogo (Meetings in memory of N.A. Cholodkovsky) 56(1): 1–145.

Gnezdilov VM (2013) On the genera *Sivaloka* Distant, 1906 and *Kodaianella* Fennah, 1956 (Hemiptera: Fulgoroidea: Issidae). Deutsche Entomologische Zeitschrift 60(1): 41–44. https://www.hemiptera-databases.org/flow/?page=explorer&db=flow&lang=en&card=publication&id=3068

Gnezdilov VM, Hayashi M (2015) First records of the genera *Neokodaiana* and *Sinesarima* (Hemiptera: Fulgoroidea: Issidae) from Japan with description of a new species from the Ryukyus. Japanese Journal of Systematic Entomology 21(2): 331–335.

Wang ML, Bourgoin T, Zhang YL (2017) New Oriental genera in the family Issidae (Hemiptera: Fulgoromorpha). Zootaxa 4312(2): 355–367. https://doi.org/10.11646/zootaxa.4312.2.10

Wang ML, Zhang YL, Bourgoin T (2016) Planthopper family Issidae (Insecta: Hemiptera: Fulgoromorpha): linking molecular phylogeny with classification. Molecular Phylogenetics and Evolution 105: 224–234. https://doi.org/10.1016/j.ympev.2016.08.012

Zhang ZG, Chen XS (2010) Taxonomic study of the genus *Kodaianella* Fennah (Hemiptera: Fulgoromorpha: Issidae). Zootaxa 2654: 61–68. https://doi.org/10.11646/zootaxa.2654.1.6

ZooKeys 917: 105–115 (2020)
doi: 10.3897/zookeys.917.46887
http://zookeys.pensoft.net

RESEARCH ARTICLE

A peer-reviewed open-access journal
ZooKeys
Launched to accelerate biodiversity research

A new species of *Hornylia* Wygodzinsky (Hemiptera, Heteroptera, Reduviidae, Emesinae) from Thailand

Zhuo Chen[1], Hu Li[1], Wanzhi Cai[1]

1 *Department of Entomology and MOA Key Lab of Pest Monitoring and Green Management, College of Plant Protection, China Agricultural University, Beijing 100193, China*

Corresponding author: Wanzhi Cai (caiwz@cau.edu.cn)

Academic editor: G. Goemans | Received 27 September 2019 | Accepted 6 February 2020 | Published 9 March 2020

http://zoobank.org/FB884144-8C6D-47E9-A3F2-27F6F306A4BF

Citation: Chen Z, Li H, Cai W (2020) A new species of *Hornylia* Wygodzinsky (Hemiptera, Heteroptera, Reduviidae, Emesinae) from Thailand. ZooKeys 917: 105–115. https://doi.org/10.3897/zookeys.917.46887

Abstract

Hornylia obtusipetala **sp. nov.** from eastern Thailand is described and illustrated. This new species is the second representative of the genus *Hornylia* Wygodzinsky, 1966. A key to species of *Hornylia* is presented. The relationship with allied genera and distribution of *Hornylia* is briefly discussed. *Hornylia* is recorded from Thailand for the first time.

Keywords

Emesinae, *Hornylia*, Metapterini, new species, Oriental Region, taxonomy

Introduction

Emesinae, or thread-legged assassin bugs, have long intrigued scientists not only because of their bizarre looking (Dohrn 1860, 1863; Wygodzinsky 1966), but also for their interesting web-dwelling (Distant 1915; Wignall and Taylor 2010; Soley et al. 2011) and cave-living (Kemp and China 1924; Gagné and Howarth 1975; Ribes et al. 1998; Pape 2013; Chłond et al. 2018) habits. The tribe Metapterini Stål, 1874 is the most speciose group within Emesinae, with 29 genera and approximately 280 species are described (Maldonado-Capriles 1990; Popov 1991). Metapterini are characterized

by the conspicuous basal process of posteroventral series of fore femur, and high proportion of genera with wing polymorphism (Wygodzinsky 1966; Castro-Huertas et al. 2019). However, recent phylogenetic analyses based on morphology of genitalia (Castro-Huertas et al. 2018) and fore leg (Castro-Huertas et al. 2019) consistently indicate that Metapterini are paraphyletic with respect to Deliastini Villiers, 1949, showing that our knowledge on the evolution of Metapterini remains far from complete.

The genus *Hornylia* Wygodzinsky, 1966 is one of ten monotypic genera among Metapterini. It was established by Wygodzinsky (1966) in his epic monograph on Emesinae. The type species, *Hornylia nalanda* Wygodzinsky, 1966, was described based on a single male specimen from Nalanda, Ceylon (now Sri Lanka) (Wygodzinsky 1966). No more information has been published since then except for being documented in the worldwide catalogue (Maldonado-Capriles 1990), and the female of *Hornylia* is still unknown (Castro-Huertas et al. 2018), making this genus somewhat enigmatic.

During our recent examination of emesine specimens deposited in the Entomological Museum of China Agricultural University, Beijing, China (CAU), a male specimen of *Hornylia* from eastern Thailand was discovered. It differs from *H. nalanda* in several characters and warrants description as a new species.

Materials and methods

Type material is preserved in the Entomological Museum of China Agricultural University, Beijing, China (CAU). Male genitalia were soaked in hot 10% KOH solution for approximately five minutes to remove soft tissue, rinsed in distilled water, and dissected under a Motic binocular dissecting microscope. Dissected genitalia were placed in a vial with glycerin and pinned under the corresponding specimen after examination. Photographs were all taken by Canon 7D Mark II digital camera with Canon micro lens EF 100 mm and MP-E 65 mm for habitus and an Olympus BX51 microscope for dissected body parts. Helicon Focus version 5.3 was used for image stacking. Measurements were obtained using a calibrated micrometer. Morphological terminology mainly follows Wygodzinsky (1966), but the term "rostrum" is replaced with "labium". The visible labial segments are numbered as II to IV, given that the first segment is lost or fused into the head capsule in most Reduviidae (Weirauch 2008; Schuh et al. 2009).

Taxonomy

Genus *Hornylia* Wygodzinsky, 1966

Hornylia Wygodzinsky, 1966: 494. Type species by original designation: *Hornylia nalanda* Wygodzinsky, 1966.

References. Maldonado-Capriles, 1990: 131.

Diagnosis. Apterous; body surface dull, granulated; anteocular part longer than postocular part; interocular furrow strongly curved backwards at its midpoint, reaching far behind level of posterior margin of eyes; fore femur with three series of spiniferous processes, and each process bearing a short spine apically; posteroventral series beginning very close to base of femur, composed of several large and numerous small processes; anteroventral series widely interrupted at base; fore tarsus not segmented, with a single claw on its apex.

Diversity and distribution. Two species, occurring in the Oriental Region.

***Hornylia obtusipetala* sp. nov.**
http://zoobank.org/996100A3-B8D6-43F3-9F8F-A80B0131A035
Figs 1–22

Diagnosis. Body length 10.98 mm; apex of labial segment II not reaching level of anterior margin of eyes (Fig. 5); anteroventral series of fore femur consisting of about seven medium-sized processes, posteroventral series consisting of ca. four large- and two medium-sized processes (Figs 6, 7); mid and hind femora each with one indistinct, brown medial annulus and two distinct, blackish brown annuli, one beyond middle and another subapically (Fig. 8); ventral surface of abdomen brown, mottled with blackish brown (Figs 3, 8, 10); parameres expanded and blunted apically, with a sharp subapical process (Figs 10–12, 18–20).

Description. Apterous male. ***Coloration*:** Body generally yellowish brown (Figs 1–3). Head (Figs 4, 5): lateral surface as well as gena blackish brown; postocular part slightly mottled with black; eyes silvery; antennae reddish brown, base of first segment pale brown, darkening toward its apex gradually; clypeus and labrum light brown; labium somewhat shiny, labial segment II light brown on apical 2/3, segment III (except apex) dark brown. Prothorax (Figs 4, 5): lateral surface and tubercle of each anterolateral angle blackish brown, ventral surface reddish brown. Meso- and metathorax (Figs 4, 5) with blackish brown lateral surface and reddish brown ventral surface. Fore coxa light brown on basal half and brown on apical half, with a dark brown subapical patch on inner and outer surfaces; fore trochanter brown as apical half of coxa; fore femur light brown, with subbasal, medial, and apical patches dark brown, spiniferous processes light yellowish brown, with their apical spines black; fore tibia light brown as general color of femur, with base, medial patch and apex brown, denticles on ventral surface black; fore tarsus brown, shiny (Figs 6, 7). Mid and hind femora (Figs 1–3, 8) light yellowish brown, with a brown, indistinct medial annulus and two blackish brown, very distinct annuli, one situated beyond middle, and another subapically; mid and hind tibiae (Figs 1–3) light yellowish brown with their bases and apexes brown; mid and hind tarsi uniformly brown. Abdomen (Figs 1–3, 9, 10): tergites with an obscure, nearly disrupted medial stripe and two pairs of lateral brownish stripes, apical half of tergite VII blackish brown (Fig. 9); dorsal laterotergites (Fig. 9) yellowish brown as general body color, their posterior halves reddish brown to dark brown, posterolateral angles blackish brown;

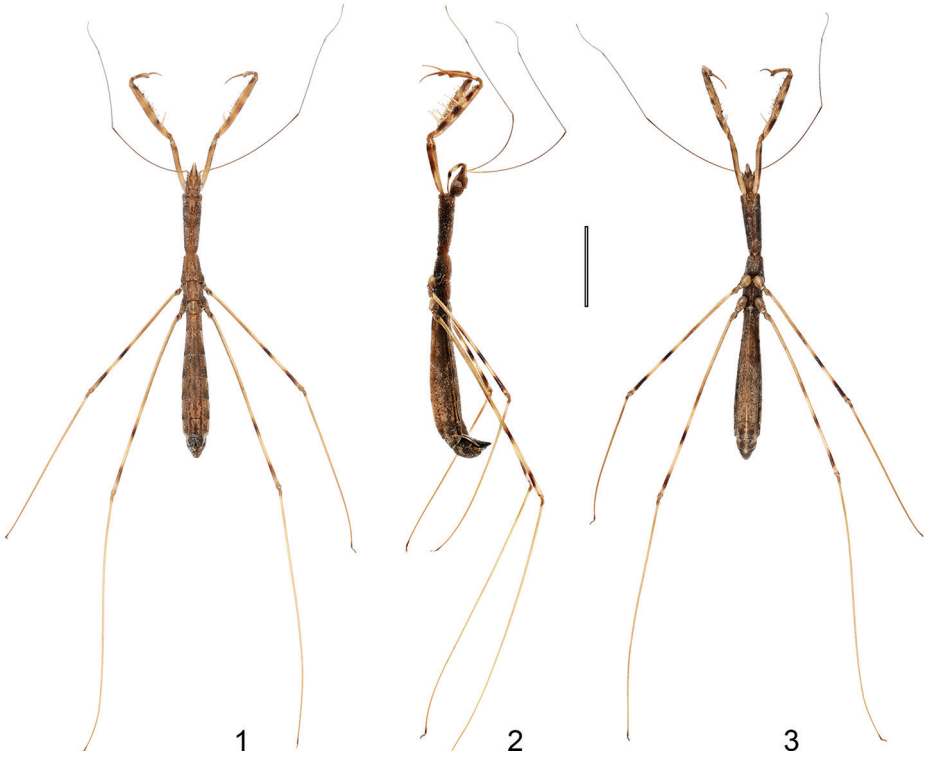

Figures 1–3. *Hornylia obtusipetala* sp. nov., male, holotype, habitus **1** dorsal view **2** lateral view **3** ventral view. Scale bar: 3.00 mm.

ventral laterotergites (Fig. 10) blackish brown, with outer margin yellowish brown; sternites with dark brown suffusion and a pair of lateral brownish stripes ; sternite VII (Fig. 10) and segment VIII (Figs 10, 12–14) each with two pairs of blackish brown bands; pygophore (Figs 10–12, 15–17) blackish brown and suffused with yellowish brown.

***Structure*:** Body elongate. Surfaces of head, thorax and abdomen conspicuously granulated (Figs 1–5). Body sparsely clothed with very short, decumbent setosity, difficult to observe; first and second (except apical portion) antennal segments sparsely clothed with short setae; apical portion of second antennal segment as well as third and fourth antennal segments densely clothed with decumbent, short pubescence; dorsum of fore trochanter with a pair of erect, long setae; fore femur and fore tibia with numerous erect, long setae (Fig. 6); apex of fore tibia and base of fore tarsus with dense, decumbent, long golden setae (Fig. 7); femora and tibiae of mid and hind legs densely clothed with short, decumbent setae; mid and hind tarsi densely clothed with short pubescence.

Head (Figs 4, 5) porrect forwardly, 1.76 times as long as wide across eyes; anteocular part 2.13 times as long as postocular part; postocular part strongly granulated on dorsum; interocular space 3.50 times as wide as a single eye in dorsal view; eyes rather small, protruding laterally in dorsal view, far remote from dorsal and ventral outlines of head in lateral view; antennae 0.59 times as long as body length, with

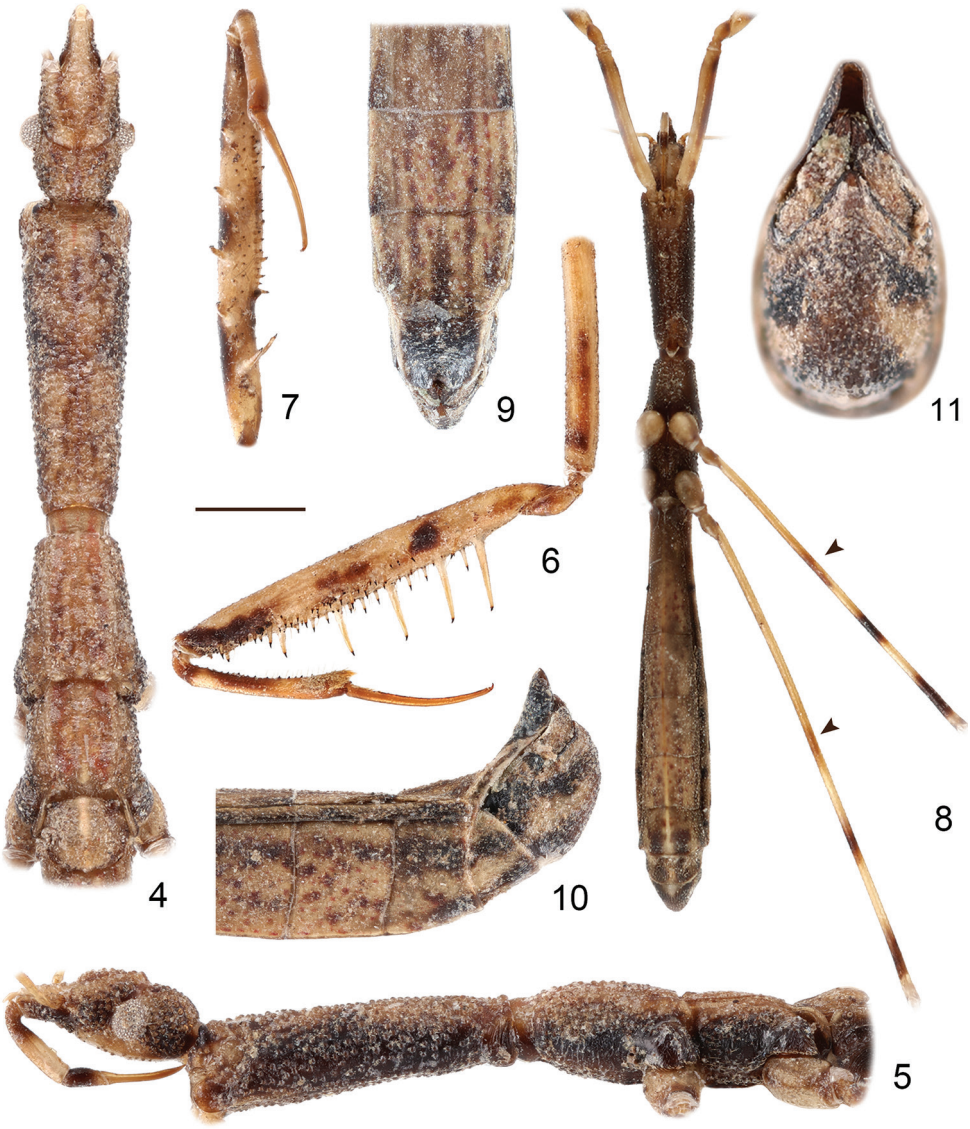

Figures 4–11. *Hornylia obtusipetala* sp. nov., male **4, 5** head, thorax and base of abdomen, antennae and legs removed **6** left fore leg **7** right fore femur, tibia and tarsus **8** body with fore coxae, femora of left mid and hind legs, arrows indicating the indistinct annuli on ventral surface of mid and hind femora **9–11** apex of abdomen **4, 9** dorsal view **5, 6, 10** lateral view **7, 8** ventral view **11** caudal view. Scale bars: 0.75 mm (**4–7, 9, 10**); 1.50 mm (**8**); 0.375 mm (**11**).

first segment longest and third segment shortest; labrum smooth; labium as shown in Fig. 5, labial segment II longest, strongly curved at base, segment III shortest, slightly swollen, reaching anterior margin of eyes, segment IV gradually tapering. Prothorax (Figs 4, 5) subcylindrical, 1.54 times as long as head, and 4.17 times as wide as its

greatest width; pronotum divided vaguely into anterior and posterior lobe, with anterior and posterior margins concave, posterior lobe extremely short and indistinct; posterior margin of prosternum largely concave, emarginated. Meso- and metanota (Figs 4, 5) carinated longitudinally along midportion, mesonotum 0.36 times as long as pronotum, metanotum 0.34 times as long as pronotum. Fore legs (Figs 6, 7) stout; fore coxa cylindrical, 0.68 times as long as fore femur; fore trochanter simple, unarmed in venter; anteroventral series of fore femur composed of about seven medium-sized and 20 small-sized processes; posteroventral series composed of about four large-sized, two medium-sized, and eleven small-sized processes, basal most process longest, distinctly longer than distance between basal most process and base of fore femur; accessory series composed of ca. 13–15 small-sized processes arranged irregularly; fore tibia short, 0.45 times as long as fore femur, ventrally with 10–12 strongly sclerotized denticles; fore tarsus 0.80 times as long as fore tibia, slightly curved, ventrally with a row of decumbent, knifelike setae. Mid and hind legs (Figs 1–3, 8) slender; mid and hind tibiae 1.25 and 1.64 times as long as respective femora, hind tibia slightly shorter than body length; mid and hind tarsi minute, apically with a pair of sickle-like claws. Abdomen (Figs 1–3, 8) elongate, 6.14 times as long as its greatest width, with a medial longitudinal ridge on ventral surface; abdominal tergite VII (Figs 9–11) projected posteriorly, apically rounded, warping upwardly, covering most part of pygophore; segment VIII (Figs 10, 12–14) distinctly exposed in lateral view, anteromedial margin strongly concave, posteromedial margin nearly straight.

Male genitalia: At rest as shown in Fig. 12. Pygophore (Figs 12, 15–17) elongate oval, anterior dorsal sclerotization narrow, insertion of paramere slightly produced; posterosuperior process (Figs 16, 17) elongate spine-like, bent near base, apex sharp, slightly curved. Parameres (Figs 18–20) broad, covered with simple setae, apical half expanded, apex blunted; subapical projection (Fig. 18) acute; margin between apex and subapical projection emarginated. Phallus as in Figs 21 and 22: articulatory apparatus thickened, strongly curved; basal plates separate; pedicel very short; phallosoma divided into two lobes, strongly sclerotized, apex blunt.

Measurements [in mm, male (N = 1)]. Length of body 10.98; length of head 1.30; length of anteocular part 0.49; length of postocular part 0.23; width across eyes 0.74; interocular space 0.47; length of antennal segments I–IV = 3.20, 2.25, 0.37, 0.71; length of labial segments II–IV = 0.38, 0.15, 0.32; length of anterior pronotal lobe 1.91; length of posterior pronotal lobe 0.09; width of anterior pronotal lobe 0.48; width of posterior pronotal lobe 0.32; length of mesonotum 0.72; length of metanotum 0.68; length of fore coxa, trochanter, femur, tibia, tarsus (without claw) = 1.29, 0.29, 1.91, 0.87, 0.70; length of mid femur, tibia, tarsus = 5.41, 6.76, 0.24; length of hind femur, tibia, tarsus = 6.20, 10.15, 0.27; length of abdomen 3.81; maximum width of abdomen 0.62.

Type material. ***Holotype*** (male): Thailand, Chanthaburi, Khao Soi Dao, 25.xii.2007, leg. W. Sakchoowng (CAU).

Etymology. The specific epithet is derived from Latin *obtus-* (meaning obtuse or blunt) and *-petala* (meaning petal), referring to the apically expanded and blunted parameres of the new species.

Distribution. Thailand (Chanthaburi).

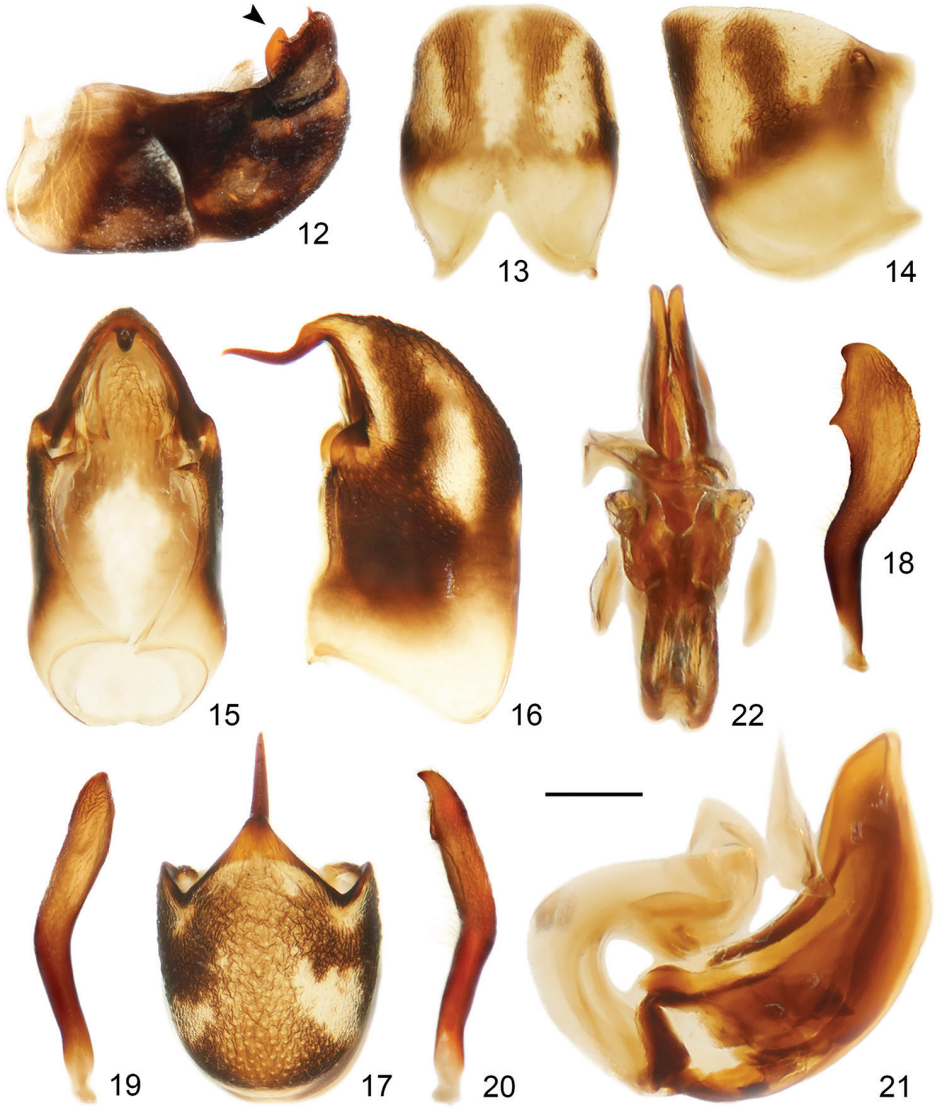

Figures 12–22. *Hornylia obtusipetala* sp. nov., male **12** abdominal segment VIII and genitalia, the arrow points to the apex of phallus **13, 14** abdominal segment VIII **15–17** pygophore **18–20** paramere **21, 22** phallus **12, 14, 16, 18, 21** lateral view **13, 15, 20, 22** dorsal view **17** caudal view **19** ventral view. Scale bars: 0.25 mm (**12**); 0.375 mm (**13–19**); 0.50 mm (**20–21**).

Discussion

Comparative notes

Hornylia obtusipetala sp. nov. can be distinguished from *H. nalanda* by its considerably larger size and several different morphological characters which are discussed. The apex

of labial segment II of the new species is far from the level of anterior margin of eyes (Fig. 5), while in *H. nalanda* it reaches the level of anterior border of eyes. The anteroventral series of the fore femur of *H. obtusipetala* sp. nov. consists of ca. seven medium-sized processes (Figs 6, 7), while in *H. nalanda* the processes number is five; the posteroventral series consists of four large-sized and two medium-sized (one situated between basal most and second basal large-sized processes, another subapically) processes in *H. obtusipetala* sp. nov. (Figs 6, 7), but have six large-sized processes in *H. nalanda*. Third, mid and hind femora of *H. obtusipetala* sp. nov. have three dark brown annuli (medial one brown and indistinct, the other two blackish brown and distinct, one situated beyond middle, one subapically) (Figs 1–3, 8), while in *H. nalanda* there are two annuli (one situated beyond middle, indistinct, and another subapically, very distinct). Finally, the ventral surface of the abdomen is yellowish brown and suffused with dark brown in the new species (Figs 3, 8), while in *H. nalanda* it is piceous on ventral surface.

The shapes of the parameres greatly differ between *H. obtusipetala* sp. nov. and *H. nalanda*: in the former, the parameres are broad, apically expanded and blunted, with a conspicuous subapical process (Figs 18–20); while in the latter, the parameres are slender, apically sickle-shaped, and without any subapical process. Wygodzinsky (1966) mentioned that phallosoma of *H. nalanda* is sclerotized dorsally, whereas the phallosoma of *H. obtusipetala* sp. nov. is entirely strongly sclerotized (Figs 21, 22). Moreover, the shape of abdominal segment VIII, pygophore, and capitate processes of the phallus of *H. obtusipetala* sp. nov. are quite different from *H. nalanda*.

Species of the genus *Hornylia* can be distinguished with the key below.

Key to species of *Hornylia* Wygodzinsky, 1966

1 Body length ca. 8 mm; labial segment II reaching level of anterior margin of eyes; anteroventral series consisting of five medium-sized processes; posteroventral series consisting of six large-sized processes; mid and hind femora with one distinct annulus; parameres slender, apically sickle-shaped, without subapical process..... ***Hornylia nalanda* Wygodzinsky**

– Body length ca. 11 mm; labial segment II not reaching level of anterior margin of eyes; anteroventral series consisting of seven medium-sized processes; posteroventral series consisting of four large-sized and two medium-sized processes; mid and hind femora with two distinct annuli; parameres broad, apically expanded and blunted, with a sharp subapical process..... ..... ***Hornylia obtusipetala* sp. nov.**

Genera related to *Hornylia*

The Oriental genus *Hornylia* seems to be related to *Bobba* Bergroth, 1914 (Afrotropical, 5 spp.), *Bargylia* Stål, 1866 (Australasian, 6 spp.), and *Leaylia* Wygodzinsky, 1966 (Australasian, 1 sp.) due to their similar appearance and several shared morphological

characters: the anteocular part distinctly longer than postocular part; antennal insertion situated before the middle of the anteocular part but relatively far from apex of head; labial segment II at least twice as long as segment III; ventral spiny region of fore femur occupying at least half of the length of fore femur; fore tarsus with one segment, with decumbent, strongly sclerotized setae on ventral surface; mid and hind claws generally medially incised, without other projections; parameres without sensory spines (Wygodzinsky 1966; Rédei 2007, 2013; Tatarnic and Cassis 2011). However, no comprehensive phylogenetic hypothesis is available for Emesinae, and only one species (*Bargylia longinota* Wygodzinsky, 1956) is included in recent morphology-based phylogenetic analyses of Metapterini (Castro-Huertas 2018, 2019). Therefore, a strict cladistic analysis is needed to clarify the generic relationships within this group.

Distribution of *Hornylia*

Prior to the discovery of *H. obtusipetala* sp. nov. from Thailand, the single representative of the genus, *Hornylia nalanda*, was only known from its type locality in Ceylon (now Sri Lanka). The discovery of the new species described here extends the distribution range of *Hornylia* to the mainland Southeast Asia. It is possible that more *Hornylia* species will be discovered on mainland Asia and adjacent islands in the future.

Emesinae are widely distributed around the world, but exhibit high diversity on isolated islands, with numerous endemic island taxa (Wygodzinsky 1966; Villiers 1979; Rédei and Tsai 2010; Tatarnic and Cassis 2011; Ishikawa and Miyamoto 2012). This distribution pattern frequently presents at the species level within Emesinae, but also occurs at some generic level taxa, e.g., *Atisne* Wygodzinsky, 1966 with two species endemics to Lord Howe Island (Tatarnic and Cassis 2011), and *Saicella* Usinger, 1958 and *Nesidiolestes* Kirkaldy, 1902 restricted to the Hawaiian Islands (Polhemus 2000). However, the majority of island-endemic genera are monotypic, with a single or few specimens collected only on a single occasion (Wygodzinsky 1966; Wall and Cassis 2003). Recent studies on the genus *Stenorhamphus* Elkins, 1962 revealed that the distribution range of this group is much wider than originally known (Smith et al. 2019). Similarly, the "Borneo endemic" genus *Chinemesa* Wygodzinsky, 1966 (5 spp.) was recently discovered on mainland Asia (Chen et al. 2020). It is obvious that our knowledge of the distribution of these island-endemic taxa is very rudimentary, and the discovery of more species, as well as robust phylogenetic analyses in the future will help to better understand the biogeography of Emesinae.

Acknowledgements

We sincerely thank Hélcio Gil-Santana (Instituto Oswaldo Cruz, Brazil), Tadashi Ishikawa (Tokyo University of Agriculture, Japan) and Geert Goemans (University of Connecticut, USA) for helpful comments and critical reading of the manuscript. This work was supported by a grant from the National Natural Science Foundation of China (No. 31730086).

References

Castro-Huertas V, Forero D, Grazia J (2018) Comparative genitalic morphology in ten genera of thread-legged bugs of the tribe Metapterini, and its phylogenetic importance (Hemiptera: Heteroptera: Reduviidae). Acta Entomologica Musei Nationalis Pragae 58: 91–125. https://doi.org/10.2478/aemnp-2018-0009

Castro-Huertas V, Forero D, Grazia J (2019) Comparative morphology of the raptorial leg in thread-legged bugs of the tribe Metapterini Stål, 1859 (Hemiptera, Heteroptera, Reduviidae, Emesinae). Zoomorphology 138: 97–116. https://doi.org/10.1007/s00435-019-00431-x

Chen Z, Li H, Cai W (2020) First record of *Chinemesa* Wygodzinsky (Hemiptera: Heteroptera: Reduviidae: Emesinae) from China, with the description of a new species. Annales de la Société entomologique de France (NS) 56(1): 19–28. https://doi.org/10.1080/00379271.2019.1703815

Chłond D, Guilbert E, Faille A, Baňař P, Davranoglou L (2018) A remarkable new species of cavernicolous Collartidini from Madagascar (Hemiptera: Heteroptera: Reduviidae). Zootaxa 4425(2): 372–384. https://doi.org/10.11646/zootaxa.4425.2.11

Distant WL (1915) Some interesting Rhynchota from British India. The Entomologist 48: 8–9.

Dohrn A (1860) Beiträge zu einer monographischen Bearbeitung der Familie der Emesinae. Linnaea Entomologica 14: 206–255.

Dohrn A (1863) Beiträge zu einer monographischen Bearbeitung der Familie der Emesinae (Zweites Stück). Linnaea Entomologica 15: 42–76.

Gagné WC, Howarth FG (1975) The cavernicolous fauna of Hawaiian lava tubes, 7. Emesinae or thread-legged bugs (Heteroptera: Reduviidae). Pacific Insects 16: 415–426.

Ishikawa T, Miyamoto S (2012) Family Reduviidae Latreille, 1807. Assassin bugs. In: Ishikawa T, Takai M, Yasunaga T (Eds) A Field Guide to Japanese Bugs. Terrestrial Heteropterans. Vol. 3. Zenkoku Noson Kyoiku Kyokai, Publishing Company Limited, Tokyo, 231–288.

Kemp S, China WE (1924) Rhynchota of the Siju Cave, Garo Hills, Assam, with description of a new species of reduviid. Records of the Indian Museum 26: 93–97.

Maldonado-Capriles J (1990) Systematic Catalogue of the Reduviidae of the World (Insecta: Heteroptera). A special edition of Caribbean Journal of Science, Mayagüez, 694 pp.

Pape RB (2013) Description and ecology of a new cavernicolous, arachnophilous thread-legged bug (Hemiptera: Reduviidae: Emesini) from Kartchner Caverns, Cochise County, Arizona. Zootaxa 3670: 137–156. https://doi.org/10.11646/zootaxa.3670.2.2

Polhemus DA (2000) A revision of the endemic Hawaiian reduviid genus *Saicella* Usinger, with descriptions of four new species (Heteroptera: Reduviidae: Emesinae). Proceedings of the Entomological Society of Washington 102: 1–20.

Popov YA (1991) On the first emesine bugs from the Nepal Himalayas (Heteroptera Reduviidae). Tropical Zoology 4: 259–267. https://doi.org/10.1080/03946975.1991.10539494

Rédei D (2007) New and little-known thread-legged assassin bugs from Australia and New Guinea (Heteroptera: Reduviidae: Emesinae). Acta Zoologica Academiae Scientiarum Hungaricae 53: 363–379.

Rédei D (2013) Two new species of thread-legged assassin bugs from Australia (Hemiptera: Heteroptera: Reduviidae: Emesinae). Acta Musei Moraviae, Scientiae Biologicae 98: 347–361.

Rédei D, Tsai JF (2010) A survey of the emesine assassin bugs of the tribes Collartidini, Leistarchini, Emesini, and Metapterini of Taiwan (Hemiptera, Heteroptera, Reduviidae). Deutsche Entomologische Zeitschrift 57: 11–36.

Ribes J, Oromí P, Ribes E (1998) Una nueva *Collartida* Villiers, 1949 subterránea de La Palma, islas Canarias (Heteroptera, Reduviidae, Emesinae). Vieraea 26: 99–105.

Schuh RT, Weirauch C, Wheeler WC (2009) Phylogenetic relationships within the Cimicomorpha (Hemiptera: Heteroptera): a total-evidence analysis. Systematic Entomology 34: 15–48. https://doi.org/10.1111/j.1365-3113.2008.00436.x

Smith S, Hwang WS, Weirauch C (2019) Synonymy of *Mangabea* and *Stenorhamphus*, with the description of two new species (Hemiptera: Reduviidae: Emesinae: Collartidini). Raffles Bulletin of Zoology 67: 135–149. https://doi.org/10.26107/RBZ-2019-0011

Soley FG, Jackson RR, Taylor PW (2011) Biology of *Stenolemus giraffa* (Hemiptera: Reduviidae), a web invading, araneophagic assassin bug from Australia. New Zealand Journal of Zoology 38: 297–316. https://doi.org/10.1080/03014223.2011.604092

Tatarnic NJ, Cassis G (2011) The thread-legged bugs (Hemiptera: Heteroptera: Reduviidae: Emesinae) of Lord Howe and Norfolk Islands. Zootaxa 2967: 21–43.

Villiers A (1979) Faune de Madagascar. 49. Insects, Hémiptères, Reduviidae (2^{e} partie). Office de la Recherche Scientifique et Technique Outre-Mer, Centre National de la Recherche Scientifique, Paris, 202 pp.

Wall MA, Cassis G (2003) *Diabolicoris*, a new genus in the tribe Ploiariolini (Hemiptera: Reduviidae: Emesinae) from New Caledonia. Memoirs of the Queensland Museum 49: 481–483.

Weirauch C (2008) From four- to three-segmented labium in Reduviidae (Hemiptera: Heteroptera). Acta Entomologica Musei Nationalis Pragae 48: 331–344.

Wignall AE, Taylor PW (2010) Predatory behaviour of an araneophagic assassin bug. Journal of Ethology 28: 437–445. https://doi.org/10.1007/s10164-009-0202-8

Wygodzinsky PW (1966) A monograph of the Emesinae (Reduviidae, Hemiptera). Bulletin of the American Museum of Natural History 133: 1–614. http://hdl.handle.net/2246/1675

ZooKeys 917: 117–126 (2020)
doi: 10.3897/zookeys.917.36727
http://zookeys.pensoft.net

RESEARCH ARTICLE

A peer-reviewed open-access journal
ZooKeys
Launched to accelerate biodiversity research

Anomoneura taiwanica sp. nov. (Hemiptera, Psylloidea, Psyllidae), a new jumping plant-louse species from Taiwan associated with *Morus australis* (Moraceae)

Geonho Cho[1*], Yi-Chang Liao[2*], Seunghwan Lee[1], Man-Miao Yang[2]

1 *Insect Biosystematics Laboratory, Research Institute of Agriculture and Life Science, Department of Agricultural Biotechnology, Seoul National University, 151-921, South Korea* **2** *Department of Entomology, National Chung Hsing University, 145, Xinda Rd., Taichung 402, Taiwan*

Corresponding author: Seunghwan Lee (seung@snu.ac.kr)

Academic editor: I. Malenovský | Received 3 June 2019 | Accepted 5 February 2020 | Published 9 March 2020

http://zoobank.org/16EA4D11-96D9-42DD-9738-272FAE8506CA

Citation: Cho G, Liao Y-C, Lee S, Yang M-M (2020) *Anomoneura taiwanica* sp. nov. (Hemiptera, Psylloidea, Psyllidae), a new jumping plant-louse species from Taiwan associated with *Morus australis* (Moraceae). ZooKeys 917: 117–126. https://doi.org/10.3897/zookeys.917.36727

Abstract

Anomoneura taiwanica **sp. nov.** (Hemiptera, Psylloidea, Psyllidae, Psyllinae) is described based on samples from Taiwan that were previously misidentified as *A. mori* Schwarz, 1896. Morphological and genetic differences between the two species, as well as their distribution, are detailed and discussed. Comments on the pest status of *Anomoneura* spp. in East Asia are also provided.

Keywords

Asia, DNA barcoding, mulberry, new species, Oriental region, psyllid, Sternorrhyncha, taxonomy

Introduction

Psyllids (Hemiptera, Psylloidea) are small phytophagous insects, ranging from 1–10 mm. About 4,000 species are known worldwide (Burckhardt and Ouvrard 2012). Some species are important pests of crops and forest trees, damaging plants

* Contributed equally as the first authors.

by direct feeding and vectoring plant diseases. Psyllids are generally host specific and related psyllid species often develop on related host taxa (Ouvrard et al. 2015).

Knowledge of the psyllid fauna of Taiwan was first developed by foreign researchers during the first half of the 20th century (Kuwayama 1908, 1910, 1931; Enderlein 1914). More comprehensive taxonomic work was later carried out by C.T. Yang and others (Yang 1984; Fang and Yang 1986; Yang et al. 1986; Lauterer et al. 1988; Fang 1990; Yang et al. 2004, 2009, 2013; Liao et al. 2016; Liao and Yang 2018). In total, nearly 150 species from 46 genera with representatives of all eight currently recognized families of Psylloidea have been recorded in Taiwan.

Until now, *Anomoneura* Schwarz, 1896 was considered a monotypic genus of jumping plant-lice (Hemiptera, Sternorrhyncha, Psylloidea, Psyllidae, Psyllinae) and was only known from East Asia (Uhler 1896; Kwon 1983; Labina 2006; Li 2011; Liao and Yang 2018; Ouvrard 2019). The single species of the genus, *Anomoneura mori* Schwarz, 1896, is a serious pest of mulberry (*Morus* spp.; Moraceae) (Kuwayama 1971). The species causes damage to mulberry plants by excessive removal of phloem sap and soiling fruit by secreting a large amount of honeydew and thread-like wax masses. Very recently *A. mori* was reported from Taiwan (Liao and Yang 2018). We have recently come to the conclusion that the material from *Morus australis* from Taiwan was misidentified by Liao and Yang (2018) and is actually an undescribed *Anomoneura* species that is morphologically similar to *A. mori*. We formally describe the new species here.

Material and methods

Material for this study was examined from the following institutions: Korea National Arboretum, Pocheon, Korea (**KNA**); National Chung Hsing University, Taichung, Taiwan (**NCHU**); Naturhistorisches Museum, Basel, Switzerland (**NHMB**); National Institute of Biological Resources, Incheon, Korea (**NIBR**); National Museum of Natural Science, Taichung, Taiwan (**NMNS**); National Pingtung University of Science and Technology, Pingtung, Taiwan (**NPUST**); National Taiwan University, Taipei, Taiwan (**NTU**); Seoul National University, Seoul, Korea (**SNU**); Taiwan Agriculture Research Institute, Taichung, Taiwan (**TARI**); and Zoological Institute, Russian Academy of Sciences, St Petersburg, Russia (**ZIN**).

Morphological terminology follows mostly Ossiannilsson (1992), Hollis (2004), and Yang et al. (2009). For molecular diagnosis, the COI-tRNA^{leu}-COII fragment of mitochondrial DNA was used, as it is usually effective for comparison of closely related psyllid species (Cho et al. 2020). Protocols for DNA extraction, amplification, sequencing, sequence alignment, and phylogenetic analysis were followed from Cho et al. (2020). In addition to the material of *Anomoneura*, two *Acizzia* species (Psyllidae, Acizziinae) were included in the phylogenetic analysis as outgroups (Table 1). K2P distance and *p*-distance were computed using MEGA 6 (Tamura et al. 2013). Nomenclature for genetic sequences in Table 1 follows Chakrabarty et al. (2013).

Table 1. *Anomoneura* and *Acizzia* sequences of COI-tRNA^{leu}-COII used in this study.

Species	Specimen Catalog #	Country	GenBank #	GenSeq
Anomoneura mori	SNU 4-1	South Korea	MN879300	genseq-4
	SNU 4-2	South Korea	MN879301	genseq-4
	SNU 161-1	Japan	MN879307	genseq-4
	SNU 161-2	Japan	MN879308	genseq-4
	SNU 161-3	Japan	MN879306	genseq-4
	SNU 161-4	Japan	MN879309	genseq-4
	SNU 161-6	Japan	MN879310	genseq-4
Anomoneura taiwanica	SNU 159-1	Taiwan	MN879302	genseq-4
	SNU 159-2	Taiwan	MN879305	genseq-4
	SNU 159-3	Taiwan	MN879303	genseq-4
	SNU 159-4	Taiwan	MN879304	genseq-4
Acizzia jamatonica	SNU 1-2	South Korea	MK039677	genseq-4
Acizzia sasakii	SNU 2-2	South Korea	MK039678	genseq-4

Taxonomy

Key to adults of *Anomoneura* species

1 Forewing with obliquely truncate apex, membrane with scattered dark dots (Fig. 1). Paramere, in profile, slightly broader, clavate with apical tooth directed upwards and slightly forwards (Figs 3, 5). Apical dilation of distal segment of aedeagus, in profile, narrowly oblong (Fig. 7). Female proctiger with dorsal margin, in profile, slightly sinuate posterior to circumanal ring; circumanal ring as long as one third of proctiger length (Fig. 9) ..... ***A. mori* Schwarz**

– Forewing with nearly rounded apex, membrane with blurred dark patches (Fig. 2). Paramere, in profile, slightly narrower, lanceolate with apical tooth curved towards the rear (Figs 4, 6). Apical dilation of distal segment of aedeagus, in profile, broader, irregularly spherical (Fig. 8). Female proctiger with dorsal margin, in profile, nearly straight posterior to circumanal ring; circumanal ring slightly shorter than half of proctiger length (Fig. 10) ..... ***A. taiwanica* sp. nov.**

***Anomoneura taiwanica* Cho & Liao, sp. nov.**
http://zoobank.org/D1DBFB0B-BDC7-4FB4-8990-980F7055893D
Figs 2, 4, 6, 8, 10

Anomoneura mori sensu Liao and Yang 2018: 604: figs 2–5; nec Schwarz in Uhler 1896: 296.

Type locality. Taiwan, Miaoli County, Nanzhuang, Daping, 24°32'07"N, 120°58'11"E, 525 m alt.

Type material. ***Holotype*:** Taiwan • ♂; Miaoli Co., Nanzhuang, Daping; 24°32'07"N, 120°58'11"E; 525 m a.s.l.; 29 Apr. 2011; Y.C. Liao leg.; *Morus australis*; NCHU, dry mounted. ***Paratypes*:** Taiwan: • 108 ♂, 103 ♀, 6 immatures; same data

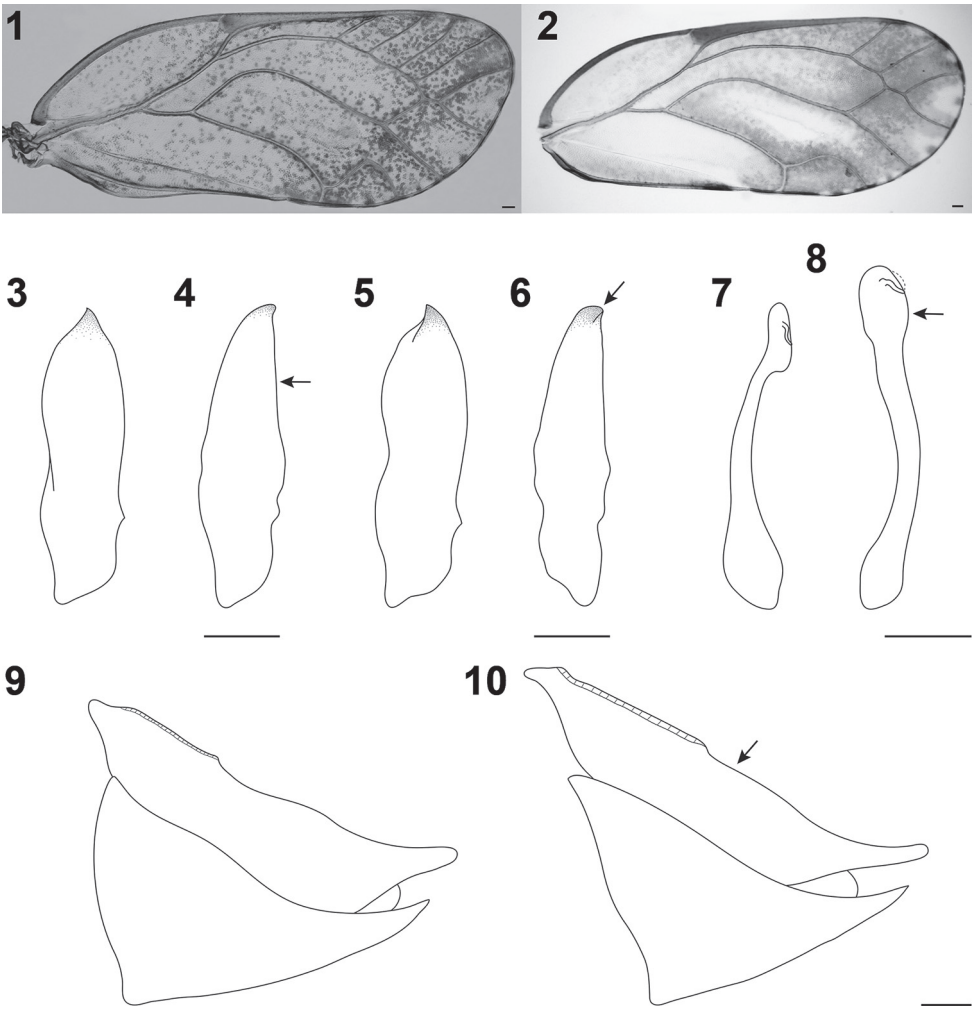

Figures 1–10. Diagnostic characters of *Anomoneura* spp. **1, 3, 5, 7, 9** *A. mori* Schwarz (specimens from Korea) **2, 4, 6, 8, 10** *A. taiwanica* **sp. nov.** (specimens from Taiwan): **1, 2** forewing **3, 4** paramere, inner surface **5, 6** paramere, outer surface **7, 8** distal segment of aedeagus **9, 10** female terminalia. Scale bars: 0.1 mm.

as for holotype; NCHU, NMNS, NHMB, dry and slide mounted • 7 ♂, 12 ♀; Miaoli Co., Dongho; 24°32'12"N, 121°01'30"E; 1040 m a.s.l.; 19 Apr. 2012; Y.C. Liao leg.; *M. australis*; NCHU, dry mounted • 1 ♀; Nantou Co., Huisun forest station; 24°05'23"N, 121°01'50"E; 694 m a.s.l.; 20 Apr. 2011; Y.C. Liao leg.; *M. australis*; NCHU, dry mounted • 10 ♂, 3 ♀, 14 immatures; same locality as for preceding; 28 Mar. 2011; T.J. Hsieh leg.; *M. australis*; NCHU, dry and slide mounted.

Other material examined (not included in the type series). Taiwan: • 39 ♂, 17 ♀; same data as holotype; NCHU, SNU, in 70% and 99% ethanol • 12 ♂, 11 ♀, 15 immatures; Taoyuan City, Fuxing, Xiaowulai; 24°47'37"N, 121°23'07"E; 563 m a.s.l.; 23 Apr. 2018; Y.C. Liao leg.; *M. australis*; NCHU, SNU, in 70% and 99% ethanol •

16 ♂, 17 ♀, 59 immatures; Taoyuan City, Fuxing, Shihmen reservoir; 24°49'19"N, 121°14'23"E; 228 m a.s.l.; 21 Apr. 2018; Y.C. Liao leg.; *M. australis*; NCHU, in 70% ethanol • 1 ♀; Hsinchu Co., Chienhsi; 5 Nov. 1981, K.S. Lin leg.; TARI, dry mounted • 1 ♂; Hsinchu Co., Chutung; 5 Apr. 1981; T.C. Hsu leg.; NTU, dry mounted • 1 ♂; Taichung City, Dongshi; 1 Feb. 2002; W.H. Chen leg.; NPUST, dry mounted • 19 ♂, 22 ♀; Nantou Co., Wushe; 15 Apr. 1987; L.J. Tang leg.; TARI, dry mounted • 1 ♂, 1 ♀; Nantou Co., Tungpu; 28 Apr.–2 May 1981; T. Lin and C.J. Lee leg.; TARI, dry mounted.

Diagnosis. Forewing oblong-oval with unevenly rounded apex, membrane with dark patches fused and blurred in apical two thirds (Fig. 2). Paramere, in profile, lanceolate, tapering to apex, with a subacute apical tooth weakly curved towards the rear (Figs 4, 6). Distal segment of aedeagus sinuous, nearly the same thickness in basal three quarters, apical dilation, in profile, forming irregular sphere (Fig. 8). Female proctiger with dorsal margin, in profile, nearly straight posterior to circumanal ring, which is slightly shorter than half of proctiger length (Fig. 10).

Description. A complete description including measurements and illustrations of both sexes and the fifth instar immature were given by Liao and Yang (2018).

Etymology. The new species name is derived from the country where the type material was collected, Taiwan, and the Latin suffix *-icus*, *-a*, *-um* (belonging to). Adjective.

Distribution. Taiwan (Liao and Yang 2018).

Host plant. *Morus australis* Poir. (Moraceae), confirmed by the presence of immatures (Liao and Yang 2018).

Anomoneura mori Schwarz, 1896

Figs 1, 3, 5, 7, 9

Anomoneura mori Schwarz in Uhler, 1896: 296; Kwon 1983: 28; Li 2011: 586.
Anomoneura koreana Klimaszewski, 1963: 92; synonymised by Kwon 1983: 28.

Material examined. China: • 1 ♂; Sichuan, Wliang-Zhengzhou; 18 Sep. 1993; Pomanin leg.; ZIN, dry mounted. Russia: • 11 ♂, 10 ♀; Kunashir Island, Tretyakovo; 8 Aug. 1971; Ermolenko leg.; ZIN, dry and slide mounted • 6 ♂, 10 ♀; same locality as for preceding; 16 Jun. 1973; Kerzhner leg.; ZIN, dry mounted. Japan: • 1 ♂, 1 ♀; Shikoku; 3 Jun. 1953; K. Sasaki leg.; ZIN, dry mounted • 2 ♂, 2 ♀; Kyushu, Mt. Homan, Chikuzen; 12 Jun. 1962; *Morus bombycis*; Y. Miyatake leg.; ZIN, dry mounted • 4 ♂, 4 ♀; Honshu, Ibaraki Pref., Tsukuba City; Fujimoto leg.; 30 May 2003; *Morus* sp.; H. Inoue leg.; SNU, in 95% ethanol • 2 ♂, 2 ♀; same locality as for preceding; 4 Jun. 2004; *M. alba*; H. Inoue leg.; SNU, dry mounted • 1 ♂, 2 ♀, 3 immatures; Kyushu, Kumamoto Pref., Amakusa-shimoshima Is., Amakusa City, Ushibuka, Mogushi; 32°211'N, 130°005'E; 5 m a.s.l.; 25 May 2015; *Morus* sp.; H. Inoue leg.; SNU, dry mounted and in 95% ethanol • 5 ♂, 5 ♀; Kyushu, Nagasaki Pref., Tsushima Is., Tsushima City, Izuhara, Kamizaka; 380 m a.s.l.; 6 Jun. 2018; *Morus* sp.; H. Inoue leg.; SNU,

dry mounted and in 95% ethanol. South Korea: • 2 ♂; Jeollabuk-do, Mt. Mayi; 11 May 1980; Y.J. Kwon leg.; NIBR, dry mounted • 2 ♂; Gangwon-do, Mt. Seolak; 29 May 1980; Y.J. Kwon leg.; NIBR, dry mounted • 1 ♂, 1 ♀; Gangwon-do, Mt. Obong; 17 May 1981; Y.J. Kwon leg.; NIBR, dry mounted • 1 ♂, 1 ♀; Gyeongsangbuk-do, Is. Ulleungdo; 26 May 1981; Y.J. Kwon leg.; NIBR, dry mounted • 1 ♂, 3 ♀; same locality as for preceding; 27 May 1981; Y.J. Kwon leg.; NIBR, dry mounted • 3 ♂; same locality as for preceding; 1 Oct. 1981; Y.J. Kwon leg.; NIBR, dry mounted • 1 ♂; same locality as for preceding; 3 Oct. 1981; Y.J. Kwon leg.; NIBR, dry mounted • 2 ♂, 3 ♀; Gyeongsangnam-do, Mt. Geumsan; 29 Mar. 1982; Y.J. Kwon leg.; NIBR, dry mounted • 1 ♀; Gyeonggi-do, Anyang-si; 19 Jun. 1992; S.J. Park leg.; SNU, dry mounted • 1 ♂, 1 ♀; Gyeongsangnam-do, Mt. Cheonhwang; 12 Sep. 1999; Y.J. Kwon leg.; NIBR, dry mounted • 1 ♂; Gyeonggi-do, Yangpyeong-gun, Yongmun-myeon, Sinjeom-ri, Mt. Yongmun; 24 Jun. 2009; S.H. Lee leg.; SNU, dry mounted • 4 ♂, 1 ♀; Gyeongsangnam-do, Miryang-si, Danjang-myeon, Mt. Jaeyak; 30 Jun. 2011; S.W. Cheong leg.; NIBR, dry mounted • 1 ♂; Gangwon-do, Inje-gun, Buk-myeon, Yongdae-ri, Yongdae National Recreation Center; 19 Jun. 2013; G. Cho leg.; SNU, slide-mounted • 4 ♂, 1 ♀; Jeollanam-do, Gwangyang-si, Ongnyong-myeon, Chusan-ri, Mt. Baegun; 24 Aug. 2013; G. Cho leg.; SNU, dry and slide-mounted • 5 ♂, 2 ♀, 51 immatures; Gyeonggi-do, Seongnam-si, Bundang-gu, Munjeong-ro 151; 29 May 2014; *M. alba*; G. Cho leg.; KNA, SNU, dry mounted, in 95% ethanol.

Discussion and conclusion

Anomoneura mori was described from Japan by Schwarz in Uhler (1896) and subsequently reported from the Korean Peninsula (Chon 1963; Klimaszewski 1963), the Russian Far East (Gegechkori and Loginova 1990; Labina 2006), China (Li 2011), and most recently from Taiwan (Liao and Yang 2018). The Taiwanese population of *Anomoneura* showed some morphological differences from *A. mori* specimens from other countries, but unfortunately, this was overlooked (Liao and Yang 2018).

Anomoneura taiwanica sp. nov. resembles *A. mori* in the structure of the head, the general structure of the forewing, and a similar host association with plants of the genus *Morus*. *Anomoneura taiwanica* sp. nov. differs from *A. mori* in the details of the forewing, paramere, distal segment of aedeagus, and female proctiger (see the key above, Table 2, and Figs 1–10). The shape of the vein Cu_{1a} of the forewing is quite variable, curved at 90° to 100° in examined *Anomoneura* material, including Taiwanese populations, which likely reflects an intraspecific variation in both species (Figs 1, 2). No significant morphological differences were found between immatures of these taxa. We analysed DNA sequence fragments of *A. mori* from Japan and Korea and *A. taiwanica* sp. nov. from Taiwan. Sequences from Japan and Korea showed no significant genetic divergence from each other (1.8% *p*-distance and K2P distance). However, the difference of those populations from *A. taiwanica* sp. nov. was significantly higher (9.0% p-distance, 9.7% K2P distance) (Fig. 11). A 3% genetic distance has been con-

Table 2. Differences between *Anomoneura mori* and *Anomoneura taiwanica* sp. nov.

Character	*A. mori*	*A. taiwanica* sp. nov.
Forewing apex	obliquely truncate	rounded
Forewing maculation	partly fused in apical part	fused and blurred
Paramere	clavate	lanceolate
Distal segment of aedeagus	curved posteriad, narrowing toward apex	sinuous, nearly as thick basally as apically
Dilation of distal segment of aedeagus	narrowly oblong	irregularly spherical
Dorsal margin of female proctiger	sinuate	nearly straight
Distribution	China, Japan, Korea, Russia	Taiwan
Host plant	*Morus alba*, *M. australis*	*M. australis*

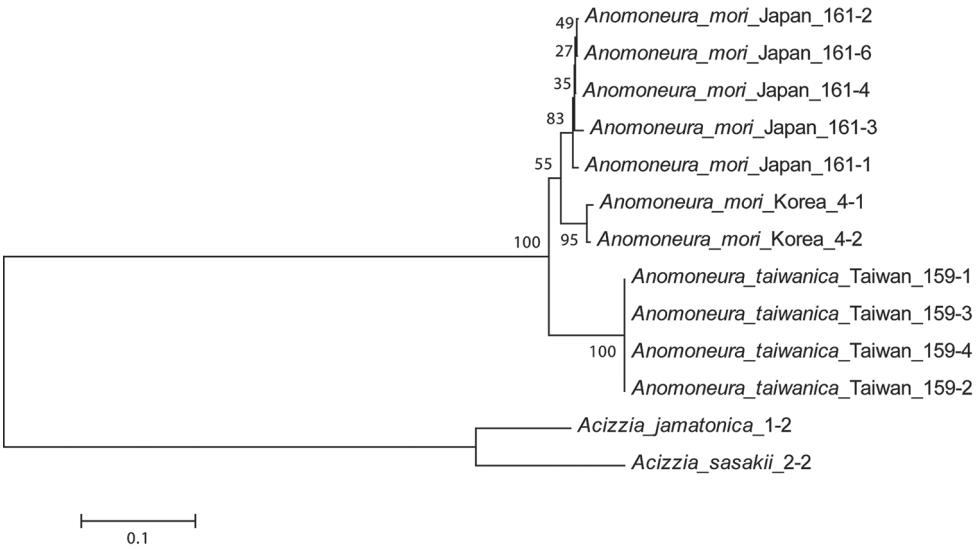

Figure 11. A neighbor-joining tree based on the Kimura 2-parameter genetic distance between COI-tRNA^{leu}-COII sequences. Bootstrap support values are shown at the branch points and are based on 1,000 replications.

sidered supportive for diagnosis of taxa at the species level for psyllids in general (Percy 2003; Martoni et al. 2018).

Mulberry (*Morus* spp.) is important to sericulture as it is also the host plant for silkworms. Due to this, damage caused by *Anomoneura* can significantly affect the silkworm industry in both Taiwan and abroad. Populations of *A. mori* can remove large quantities of plant sap, produce masses of wax threads, and secrete a large amount of honeydew. This causes negative effects on plant growth and diminishes mulberry leaves which devalues the silkworms cocoons (Kuwayama 1971; Kim and Park 2016). A recent field survey by Liao and Yang (2018) in Taiwan showed that *A. taiwanica* has the same life history as *A. mori*, which indicates that both species are serious pests of mulberry trees. However, at present, *A. taiwanica* may not cause serious economic loss in Taiwan due to a decline of the silk industry in the late 1990s. Just a few silkworm farmers remain in Taiwan, and these are merely for traditional or educational purposes (Jiang 2007).

Liao and Yang (2018) considered *A. taiwanica* sp. nov. (which they had misidentified as *A. mori* at the time) as an exotic invader in Taiwan because earlier surveys of *Morus* trees did not identify this species as present in the country (Yang 1984; Yang et al. 1986). Furthermore, *A. mori* is widely distributed in the temperate climatic zone of East Asia at higher latitudes than *A. taiwanica*, which is known only from the subtropical climate of northern Taiwan. The recent increase in the import of various plant seedlings from China to Taiwan has often accelerated the establishment of exotic species, such as *Cacopsylla chinensis* (Yang et al. 2004). Given this fact, *A. taiwanica* may have originated in southern China. To confirm this hypothesis, more material of *Anomoneura* from China should be examined to reveal a potentially wider distribution of *A. taiwanica*.

Acknowledgements

We are grateful to Daniel Burckhardt (Naturhistorisches Museum, Basel, Switzerland), Igor Malenovský and Liliya Štarhová Serbina (both Department of Botany and Zoology, Faculty of Science, Masaryk University, Brno, Czech Republic), and David Ouvrard (Anses, Plant Health Laboratory, Montferrier-sur-Lez, France) for helpful comments on earlier versions of this manuscript, and Hiromitsu Inoue (Institute of Fruit Tree and Tea Science, National Agriculture and Food Research Organization, Japan), Eugenia Labina (Zoological Institute, Academy of Sciences, St Petersburg, Russia) for helping us to examine *Anomoneura* material from China, Japan and Russia, and Wesley Hunting (Department of Entomology, National Chung Hsing University, Taichung, Taiwan) for his help in English editing. Thanks are extended to Dávid Rédei (Institute of Entomology, College of Life Sciences, Nankai University, China) for checking Chinese mulberry psyllids. This work was partly supported by a grant from the Korea National Arboretum 'Development of an integrated identification system of Korean insects' (project no. KNA 1-1-20, 16-1).

References

Burckhardt D, Ouvrard D (2012) A revised classification of the jumping plant-lice (Hemiptera: Psylloidea). Zootaxa 3509: 1–34. https://doi.org/10.11646/zootaxa.3509.1.1

Chakrabarty P, Warren M, Page LM, Baldwin CC (2013) GenSeq: an updated nomenclature and ranking for genetic sequences from type and non-type sources. ZooKeys 346: 29–41. https://doi.org/10.3897/zookeys.346.5753

Cho G, Malenovský I, Burckhardt D, Inoue H, Lee S (2020) DNA barcoding of pear psyllids (Hemiptera: Psylloidea: Psyllidae), a tale of continued misidentifications. Bulletin of Entomological Research. https://doi.org/10.1017/S0007485320000012

Chon DR (1963) Mulberry thrips and mulberry suckers. Jamsabo 10: 73–75.

Enderlein G (1914) H. Sauter's Formosa-Ausbeute: Psyllidae (Homopt.). Psyllidologica II. Entomologische Mitteilungen 3: 230–235. https://doi.org/10.5962/bhl.part.5088

Fang SJ (1990) Psylloidea of Taiwan supplement II (Homoptera). Journal of Taiwan Museum 43: 103–117.

Fang SJ, Yang CT (1986) Psylloidea of Taiwan (Homoptera: Sternorrhyncha) Supplement. Taiwan Museum Special Publication Series 6: 119–176.

Gegechkori AM, Loginova MM (1990) Psillidy (Homoptera, Psylloidea) SSSR (annotirovannyi spisok). [Psyllids (Homoptera, Psylloidea) of the USSR: an Annotated List.] Metsniereba, Tbilisi, 161 pp. [in Russian]

Hollis D (2004) Australian Psylloidea. Jumping Plantlice and Lerp Insects. Australian Biological Resources Study, Canberra, 216 pp.

Jiang MZ (2007) The research of Taiwanese sericulture after World War II (1945–1992). Master thesis, Taipei, Republic of China: National Chengchi University. [in Chinese]

Kim JE, Park SC (2016) Biology of *Anomoneura mori* Schwarz (Hemiptera: Psyllidae) damaging mulberry. Trends in Agriculture & Life Sciences 52: 9–14. https://doi.org/10.29335/tals.2016.52.9

Klimaszewski SM (1963) Eine neue Art der Unterfamilie Ciriacreminae aus Korea (Homoptera, Psyllidae). Bulletin de l'Académie Polonaise des Sciences, Classe II 11: 91–94. https://doi.org/10.3161/00159301FF1964.11.4.041

Kuwayama S (1908) Die Psylliden Japans I. Transactions of the Sapporo Natural History Society 2: 149–189.

Kuwayama S (1910) Die Psylliden Japans, II. Transactions of the Sapporo Natural History Society 3: 53–66.

Kuwayama S (1931) A revision of the Psyllidae of Taiwan. Insecta Matsumurana 5: 117–133.

Kuwayama S (1971) Observations on the biology of the mulberry sucker, with special reference to the influence of its parasitism on the growth of silkworm. Japanese Journal of Applied Entomology and Zoology 15: 115–120. https://doi.org/10.1303/jjaez.15.115

Kwon YJ (1983) Psylloidea of Korea (Homoptera: Sternorrhyncha). Insecta Koreana, Series 2. Editorial Committee of Insecta Koreana, Seoul, 181 pp.

Labina ES (2006) Psyllids of the Kuril Islands (Homoptera: Psylloidea). Zoosystematica Rossica 15: 51–55.

Lauterer P, Yang CT, Fang SJ (1988) Changes in the nomenclature of five species of psyllids from Taiwan (Homoptera: Psylloidea), with notes on the genus *Bactericera*. Journal of Taiwan Museum 41: 71–74.

Li F (2011) Psyllidomorpha of China (Insecta: Hemiptera). Science Press, Beijing, 1976 pp.

Liao YC, Huang SS, Yang MM (2016) Substrate-borne signals, specific recognition, and plant effects on the acoustics of two allied species of *Trioza*, with the description of a new species (Psylloidea: Triozidae). Annals of the Entomological Society of America 109: 906–917. https://doi.org/10.1093/aesa/saw060

Liao YC, Yang MM (2018) First record of the mulberry psyllid *Anomoneura mori* Schwarz (Hemiptera: Psylloidea: Psyllidae) from Taiwan. Journal of Asia-Pacific Entomology 21: 603–608. https://doi.org/10.1016/j.aspen.2018.03.016

Martoni F, Bulman S, Pitman A, Taylor G, Armstrong K (2018) DNA barcoding highlights cryptic diversity in the New Zealand Psylloidea (Hemiptera: Sternorrhyncha). Diversity 10: 1–50. https://doi.org/10.3390/d10030050

Ossiannilsson F (1992) The Psylloidea (Homoptera) of Fennoscandia and Denmark. Fauna Entomologica Scandinavica 26. E.J. Brill, Leiden, 346 pp.

Ouvrard D (2019) Psyl'list – The World Psylloidea Database. [Accessed on 10 January 2019] https://doi.org/10.5519/0029634

Ouvrard D, Chalise P, Percy DM (2015) Host-plant leaps versus host-plant shuffle: a global survey reveals contrasting patterns in an oligophagous insect group (Hemiptera, Psylloidea). Systematics and Biodiversity 13: 434–454. https://doi.org/10.1080/14772000.2015.1046969

Percy DM (2003) Radiation, diversity, and host-plant interactions among island and continental legume-feeding psyllids. Evolution 57: 2540–2556. https://doi.org/10.1111/j.0014-3820.2003.tb01498.x

Tamura K, Stecher G, Peterson D, Filipski A, Kumar S (2013) MEGA6: Molecular Evolutionary Genetics Analysis version 6.0. Molecular Biology and Evolution 30: 2725–2729. https://doi.org/10.1093/molbev/mst197

Uhler PR (1896) Summary of the Hemiptera of Japan presented to the United States National Museum by Professor Mitzukuri. Proceedings of the United States National Museum 19: 255–297. https://doi.org/10.5479/si.00963801.1108.255

Yang CT (1984) Psyllidae of Taiwan. Taiwan Museum Special Publication Series 3. Taiwan Museum, Taipei, 305 pp.

Yang MM, Yang CT, Chao JT (1986) Reproductive isolation and taxonomy of two Taiwanese *Paurocephala* species (Homoptera: Psylloidea). Taiwan Museum Special Publication Series 6: 176–203.

Yang MM, Huang JH, Li FS (2004) A new record of *Cacopsylla* species (Hemiptera: Psyllidae) from pear orchards in Taiwan. Formosan Entomologist 24: 213–220.

Yang MM, Burckhardt D, Fang SJ (2009) Psylloidea of Taiwan (Vol. I). Families Calophyidae, Carsidaridae, Homotomidae and Phacopteronidae, with Overview and Keys to Families and Genera of Taiwanese Psylloidea (Insecta: Hemiptera). National Chung Hsing University, Taichung, 96 pp.

Yang MM, Burckhardt D, Fang SJ (2013) Psylloidea of Taiwan. Volume II. Family Triozidae. National Chung Hsing University, Taichung, 160 pp.

ZooKeys 917: 127–140 (2020)
doi: 10.3897/zookeys.917.38044
http://zookeys.pensoft.net

RESEARCH ARTICLE

A peer-reviewed open-access journal
ZooKeys
Launched to accelerate biodiversity research

Redescriptions of the poorly known crane fly species *Tipula* (*Vestiplex*) *scandens* and *Tipula* (*Vestiplex*) *subscripta* from Tibet and Yunnan, China (Diptera, Tipulidae)

Pavel Starkevich[1], Qiu-Lei Men[2], Duncan Sivell[3]

1 *Nature Research Centre, Akademijos str. 2, LT–10222 Vilnius, Lithuania* **2** *School of Life Sciences, Provincial Key Laboratory of the Biodiversity Study and Ecology Conservation in Southwest Anhui; Research Center of Aquatic Organism Conservation and Water Ecosystem Restoration in Anhui Province, Anqing Normal University, Anqing 246011, Anhui, China* **3** *Natural History Museum, Cromwell Road, London, SW7 5BD, UK*

Corresponding author: Qiu-Lei Men (menqiulei888@126.com)

Academic editor: C. Borkent | Received 6 July 2019 | Accepted 18 February 2020 | Published 9 March 2020

http://zoobank.org/548B4D56-04FD-45A0-A86B-605F7F4C6D31

Citation: Starkevich P, Men Q-L, Sivell D (2020) Redescriptions of the poorly known crane fly species *Tipula* (*Vestiplex*) *scandens* and *Tipula* (*Vestiplex*) *subscripta* from Tibet and Yunnan, China (Diptera, Tipulidae). ZooKeys 917: 127–140. https://doi.org/10.3897/zookeys.917.38044

Abstract

Tipula (*Vestiplex*) *scandens* Edwards, 1928 and *Tipula* (*Vestiplex*) *subscripta* Edwards, 1928 were both briefly described based on single specimens and lacked illustration in the original literature. In the present paper, these two species are redescribed with new illustrations of additional morphological features based on type and non-type specimens.

Keywords

taxonomy, biodiversity, systematics, hypopygium, ovipositor, *coquillettiana* species group, *scripta* species group

Introduction

Tipula (*V.*) *scandens* and *T.* (*V.*) *subscripta* were both described by Edwards (1928) based respectively on a single female specimen from Tibet and a single male from Yunnan, China. The original descriptions were very brief and lacked illustrations. Addi-

tional material was collected from Tibet and its adjacent areas by Frank Kingdon-Ward and Ronald J. H. Kaulback in 1933 during their expedition to South-eastern Tibet and by Kaulback in 1935–1936 (Alexander 1963). These specimens were subsequently identified and published by Alexander (1953, 1963), but no additional notes and illustrations were provided. The lack of detailed descriptions and illustrations has resulted in a limited understanding of these two species. In the present work, both sexes of *T.* (*V.*) *scandens* and *T.* (*V.*) *subscripta* are redescribed and illustrated. High quality photographs are also provided to facilitate identification.

Materials and methods

Descriptive terminology generally follows that of Alexander and Byers (1981). The term gonocoxal fragment for the inner structure covered by tergite nine is adopted from Brodo (2017). Neumann (1958) designated the same structure as sclerites *sp1* and *sp2* and Dobrotworsky (1968) as the genital bridge.

The terminalia were removed and macerated in 10% NaOH for 5–10 minutes, observed in glycerin under an Olympus SZX10 stereomicroscope and preserved in microvials, filled with glycerol, on the same pin as the dry insect. Dry specimens were photographed with a Canon EOS 80D at the Natural History Museum, London. Digital photos were processed and layers were stacked using the program HeliconFocus (http://www.heliconsoft.com/heliconsoft-products/helicon-focus/).

For citing label data on specimens, a slashed line (/) separates each label. Square brackets ([ ]) are used to indicate additional information not on the original label.

Abbreviations for institutional collections used herein are: **BMNH** = Natural History Museum, London, United Kingdom; **USNM** = United States National Museum, Washington, D.C., USA.

Taxonomy

Tipula (*Vestiplex*) Bezzi, 1924

Tipula (*Vestiplex*) Bezzi, 1924: 230; Edwards, 1931: 79; Alexander, 1934: 396; 1935: 117; 1965: 355; Mannheims, 1953: 116; Savchenko, 1964: 132.

Type species. *Tipula cisalpina* Riedel, 1913.

Notes. *Vestiplex* was first proposed by Bezzi (1924) as a subgenus of *Tipula* for the type species *T. cisalpina* Riedel, 1913 recorded from the western Palaearctic (Italy, Switzerland). The subgenus *T.* (*Vestiplex*) is a phylogenetically young crane fly complex formed in the neo-paleogene (Savchenko 1960, 1964). No fossil species of *T.* (*Vestiplex*) are described so far and only Matthews and Telka (1997) mentioned ovipositors of possibly *T.* (*Vestiplex*) females from Cape Deceit Formation in Western Alaska (1.8 Ma old). The

world fauna of the subgenus *Tipula* (*Vestiplex*) includes 173 species group taxa which are distributed throughout the Holarctic and Oriental Regions (Oosterbroek 2019). A total of 75 species group taxa are known from the Oriental Region with numerous accounts from China, India and Nepal (Oosterbroek 2019). The male genitalia are extremely polymorphic (Savchenko 1964), typically with the ninth tergite forming a shallowly concave and sclerotised saucer, other species have their ninth tergite completely divided longitudinally by a pale membrane (Alexander 1935, Alexander and Byers 1981). Females belonging to *T.* (*Vestiplex*) are characterized by a powerful, heavily sclerotized cercus, that is serrated along the outer margin (though smooth in several Asiatic species) and small to rudimentary hypovalva (Alexander 1935, 1965, Alexander and Byers 1981).

***Tipula* (*Vestiplex*) *scandens* Edwards, 1928**

Figures 1–16

Tipula scandens Edwards, 1928: 691; Edwards, 1931: 80; Alexander, 1935: 119; Wu, 1940: 15; Alexander, 1953: 343; Savchenko, 1964: 228; Oosterbroek and Theowald 1992: 158.

Diagnosis (male). *Tipula* (*V.*) *scandens* can be recognized by following combination of characters: body blackish antenna long, reaching the first abdominal segment if bent backwards, the first flagellomere cylindrical, the remaining flagellomeres strongly dilated at both ends, hypopygium with tergite nine in the shape of a narrow, transverse, sclerotised saucer-shaped plate, gonocoxite unarmed.

Redescription. Male. Body length: 10.9–15.6 mm. Wing: 12.6–15.2 mm.

Head. Blackish in general. Rostrum blackish, thinly dusted with grey, nasus indistinct (Fig. 1). Vertex and occiput blackish, grey pruinose, with a narrowed black line medially. Antenna 13-segmented, if bent backwards almost reaching the posterior margin of the first abdominal segment; scape blackish, narrowed basally and broadened apically, pedicel blackish, very short; flagellum blackish with first flagellomere cylindrical, slightly curved, remaining flagellomeres strongly dilated at both ends, gradually shortening in length, the last flagellomere very small, basal enlargement of flagellomeres with five black verticils, verticils slightly shorter than the length of the corresponding flagellomeres (Fig. 1). Palpus entirely blackish.

Thorax. Pronotum blackish, white pruinose medially. Prescutum blackish, grey pruinose, with three blackish stripes, the laterals oblong, bordered by black line, the median one expanded apically and narrowed at base, separated by a black median line. Scutum blackish, grey pruinose, with two black spots. Scutellum blackish, grey pruinose. Mediotergite blackish. Pleura densely dusted with grey, only suffused with brown at the border of dorsum and pleura (Fig. 1). Leg with coxa blackish, thinly dusted with grey; trochanter black, femur and tibia dark brown with darker tips, two basal tarsal segments dark brown, remaining brownish black (Fig. 1). Wing yellowish-brown, cells c and sc not darker than ground colour, wing cells marbled with light brown spots scattered at base of

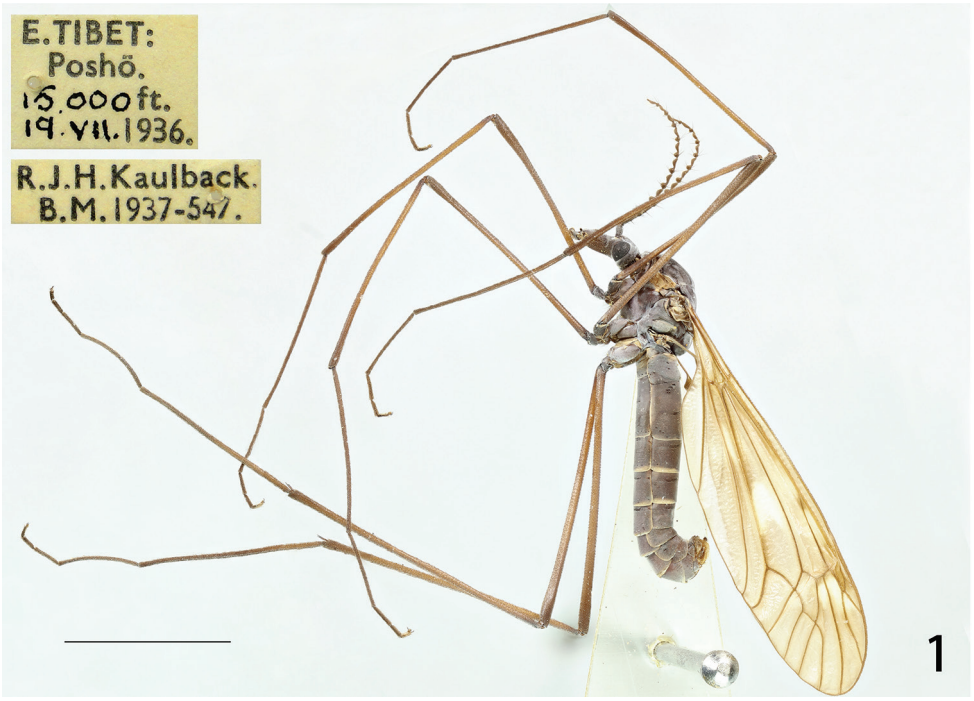

Figure 1. Male habitus of *T.* (*V.*) *scandens*, lateral view.

Rs and around the stigma; with brown clouds in the arcular area, and distal and middle areas of bm, the latter extended along Cu; apical cells also suffused with light brown. Rs relatively short, subequal in length to R_3, R_{1+2} entire, discal cell broad, elongated, petiole of cell m_1 indistinct (Fig. 1). Halter with stem dark brown, knob blackish (Fig. 1).

Abdomen. Abdomen including hypopygium blackish, segments two to four narrowly suffused with brown on posterior margin (Fig. 1). *Hypopygium.* Tergite nine separated from sternite nine by a distinct narrowed notch (Figs 2, 3). Tergite nine in the shape of a narrow, transverse, sclerotised saucer-shaped plate (Fig. 3). The main body of tergal saucer brownish. Posterior margin of tergal saucer is broadly emarginated, lateral lobes rounded, densely covered with setae, anterior portion with raised border appearing as elevated transverse long and very narrow plate almost reaching lateral lobes. Sternite nine broad, distinctly protruding at hind margin, deeply divided by a V-shaped notch (Fig. 4). Gonocoxite triangular, unarmed (Fig. 2). Outer gonostylus narrowed at base, gradually broadened to the round apex (Fig. 5). Inner gonostylus a claw-shaped curved plate (Figs 2–4, 6). Beak extended into blackened obtuse rostrum. Posterior parts of medial sclerite lightly flattened. Lateral sclerites U-shaped. Adminiculum triangular tube-shaped, surpassing the end of gonocoxite, acute apically, with a triangular process at base in lateral view (Figs 7, 8). Gonocoxal fragment with medial sclerite V-shaped, at base with narrow apodeme, posteriorly rounded (Fig. 9). Semen pump very small, situated between eighth and ninth segments. Compressor apodeme fan-shaped with a V-shaped notch medially, the apical margin narrowly suffused with

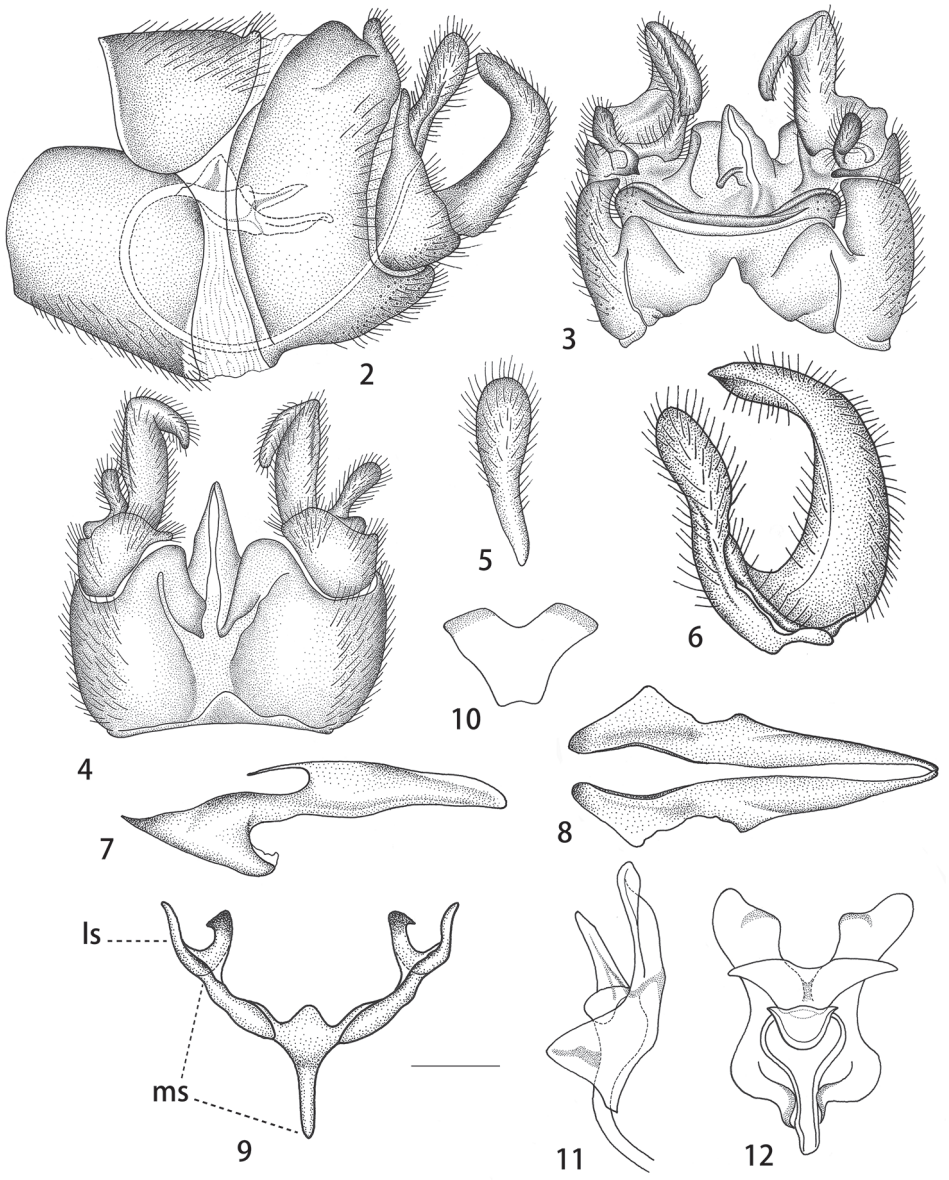

Figures 2–12. Male hypopygium of *T.* (*V.*) *scandens*. **2** Hypopygium, lateral view **3** hypopygium, dorsal view **4** hypopygium, ventral view **5** outer gonostylus, lateral view **6** outer gonostylus and inner gonostylus, lateral view **7** adminiculum, lateral view **8** adminiculum, ventral view **9** gonocoxal fragment, dorsal view **10** compressor apodeme of semen pump **11** semen pump, lateral view **12** semen pump. Abbreviations: ls, lateral sclerite of gonocoxal fragment; ms, medial sclerite of gonocoxal fragment. Scale bars: 0.4 mm (**2–4**), 0.25 mm (**5–12**).

black (Fig. 10). Posterior immovable apodeme distinctly longer than compressor apodeme, very enlarged in dorsal view (Figs 11, 12). Anterior immovable apodeme short, gradually narrowed to apex, with a black stripe medially in lateral view (Figs 11, 12).

Figure 13. Female habitus of *T.* (*V.*) *scandens* (holotype), lateral view.

Aedeagus tubular, almost three times as long as semen pump, thickened at base and gradually narrowed to end, acute apically (Fig. 2).

Female. Body length: 15.6–18.4 mm. Wing: 8.0–8.1 mm. Body colour same as that of male except as follows. Antenna relatively short, if bent backward reaching before base of the wing. Scape expanded apically and narrowed basally, pedicel short, flagellum with flagellomeres cylindrical, gradually shortening in length distinctly shorter than the length of the corresponding flagellomeres (Fig. 13). Legs stout, femora distinctly dilated towards the apex (Fig. 13). Wing reduced, never more than half the body length (Fig. 13). Abdomen dark brown, tergites two to four with a pale median area, sternites two to four suffused with light brown on the lateral and posterior borders (Fig. 13).

Ovipositor. Tergite nine dark brown, tergite ten shining dark brown. Cercus brown, with tip narrowed and slightly up-turned, outer margin with rough serration (Fig. 14). Hypovalva reduced, filamentous, slender, terminating in two setae (Fig. 15). Median incision between hypovalvae slightly deeper than posterior margin of sternite eight. Lateral incision absent. Sternite nine posteriorly triangular, anterior parts flattened (Fig. 16). Furca posteriorly flattened, posteriorly triangular in shape (Fig. 16). Bursa copulatrix with spermathecal duct sclerotised at base, in the shape of short, swollen, brown process (Fig. 16). Wall of bursa copulatrix sclerotised at connection site with spermathecal duct. Sclerotisation of all three spermathecal ducts connected and forming a complete dark brown ring. Anterior part of bursa copulatrix roughly straight.

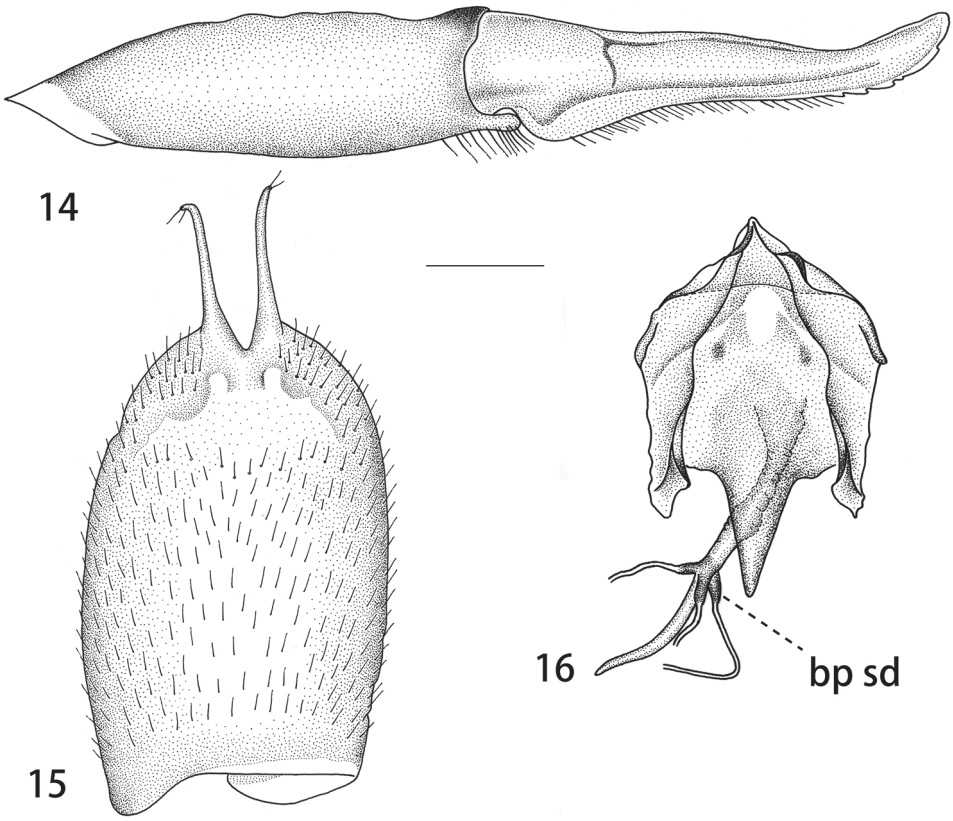

Figures 14–16. Female ovipositor of *T.* (*V.*) *scandens*. **14** Tergite ten and cercus, lateral view **15** sternite eight with hypovalvae, ventral view **16** sternite nine, furca, and part of internal reproductive system, dorsal view. Abbreviation: bp sd, basal part of spermathecal duct. Scale bars: 0.5 mm (**14, 15**), 0.4 mm (**16**).

Type material examined. Holotype, female, **China:** "Type" / "Tibet: Phusi La 16, 500', 3- vii-1924. Maj. R. W. G. Hingston" / "*Tipula scandens* Edw F.W.Edwards. det. 1928" / "HOLOTYPE" / "HOLOTYPE *Tipula scandens* Edwards det. J. E. Chainey, 1995" / "BMNH(E)#246032".

Additional material examined. *Tipula* (*Vestiplex*) *scandens* Edwards, 1928: **China:** 1 female, E. Tibet, Poshö, 16,000 ft., 20. VII. 1936, R. J. H. Kaulback, B. M. 1937-547, *Tipula scandens* Edw. Det. C. P. Alexander 1950 (USNM); 2 males, East Tibet, DüChu Valley, 14,000 ft, 10–15.vii.1936, R. J. H. Kaulback, B. M. 1937-547 (BMNH); 1 male, East Tibet, DüChu Valley,13,000 ft., 10–15. vii. 1936, R. J. H. Kaulback. B. M. 1937-547 (BMNH); 3 males, East Tibet, Poshö, Dzongra, 14.500 ft, 4. vii. 1936, R. J. H. Kaulback, B. M. 1937-547, *Tipula scandens* Edw. Det. C. P. Alexander 1950 (BMNH); 1 male, East Tibet, Poshö Dzongra, 15,000 ft., 4. vii. 1936, R. J. H. Kaulback, B. M. 1937-547, *Tipula scandens* Edw. Det. C. P. Alexander 1950 (BMNH).

Distribution. China (Tibet).

Remarks. *T.* (*V.*) *scandens* belongs to the *coquillettiana* species group (Savchenko 1960). According to Savchenko (1960) males are characterized by a tergite nine that is in the shape of a narrow, transverse sclerotised plate, its posterior margin broadly emarginated, with the lateral angles usually produced into an obtuse ledge. Anterior border of tergite nine elevated into lightly curved long edge reaching the lateral angles of tergite nine.

Tipula (*Vestiplex*) *subscripta* Edwards, 1928

Figures 17–33

Tipula subscripta Edwards, 1928: 689; Edwards, 1931: 80; Alexander, 1935: 119; Wu, 1940: 15; Alexander, 1963: 327; Savchenko, 1964: 164; Alexander and Alexander 1973: 65; Oosterbroek and Theowald 1992: 159.

Diagnosis (male). *Tipula* (*V.*) *subscripta* can be recognized by following combination of characters: body yellowish-brown, antenna bicolored except three yellow basal segments, if bent backwards reaching the base of the wing, tergite nine forming a pale-yellow saucer-shaped plate anteriorly having raised border, gonocoxite armed with a strong spine.

Description. Male. Body length: 14.4–14.7 mm. Wing: 18.2–19.1 mm.

Head. Yellow in colouration generally (Fig. 17). Rostrum yellow, nasus distinct and yellow. Vertex and occiput greyish, medially with brown line which is very narrow at the occiput becoming broad between the eyes. Antenna 13-segmented, if bent backwards just reaching the base of the wing; scape yellow, expanded apically and narrowed basally, pedicel yellow and short, flagellum with first flagellomere entirely yellow, slightly narrowed at apex, the remaining flagellomeres bicoloured, brown basally and yellow apically, each flagellomere gradually shortening in length, basal enlargements with abundant black verticils, almost subequal in length to their corresponding flagellomeres (Fig. 17). Palpus dark brown.

Thorax. Pronotum yellow, black in middle and whitish pruinose laterally. Prescutum brownish with four grey stripes, the lateral stripes narrow with broad brown border, the median two stripes also suffused with brown borders. Space between median and lateral stripes whitish pruinose. Scutum yellowish brown, thinly whitish pruinose, with two grey spots, the posterior one distinctly bigger than anterior one. Scutellum and mediotergite yellowish brown, whitish pruinose, both with a brown median line. Pleura brownish, darker on dorsal side of anepisternum. Leg slender, coxa same as pleuron in colouration, trochanter yellow, femur and tibia yellow with slightly dark tips, tarsus yellowish brown (Fig. 17). Wing relatively transparent, cells c and sc not darker than the ground colour, wing cells marbled with light brown spots scattered by base and apex of Rs and around the stigma, two brown clouds distributed along Cu. Rs relatively short, subequal in length to R_3, R_{1+2} entire, discal cell broad, at least four times as long as the petiole of cell m_1 (Fig. 17). Halter with stem yellow, knob yellowish brown.

Figure 17. Male habitus of *T.* (*V.*) *subscripta* (holotype), lateral view.

Abdomen. First abdominal segment yellowish, remaining segments including hypopygium yellowish-brown (Fig. 14). *Hypopygium.* Tergite nine mostly fused with sternite nine (Figs 18, 19). Tergite nine distally forming a pale-yellow saucer-shaped plate (Fig. 19). The main body of tergal saucer is pale-yellow. Posterior margin of tergal saucer is broadly emarginated, posterior lobes pale laterally with incision. Anterior portion brown with raised border appearing as an elevated transverse quadrate plate. The quadrate plate medially pale, lateral angles produced into black tooth. Sternite nine broad and rounded in general, with a U-shaped notch at hind margin (Fig. 20). Gonocoxite armed with a strong spine, apex acute and blackened (Figs 18, 21). Outer gonostylus lightly curved, finger-shaped (Fig. 22). Inner gonostylus in the shape of slightly curved plate, bifid at apex, dorsally with a black obtuse tooth, beak extended into blackened obtuse rostrum (Figs 23, 24). Posterior parts of medial sclerite distally flattened. Lateral sclerites U-shaped. Adminiculum in the shape of short, triangular tube (Figs 25, 26). Gonocoxal fragment with medial sclerite slender, V-shaped, with flattened and short apodeme at base (Fig. 27). Semen pump situated between eighth and ninth segments. Compressor apodeme fan-shaped, medially with a V-shaped notch (Fig. 28). Posterior immovable apodeme subequal in length to compressor apodeme, rounded apically in dorsal view (Figs 29, 30). Anterior immovable apodeme short, gradually narrowed to apex in lateral view, an expanded lobe in dorsal view (Figs 29, 30). Aedeagus tubular, almost two times as long as semen pump, thickened at base and gradually narrowed to end, acute apically (Fig. 18).

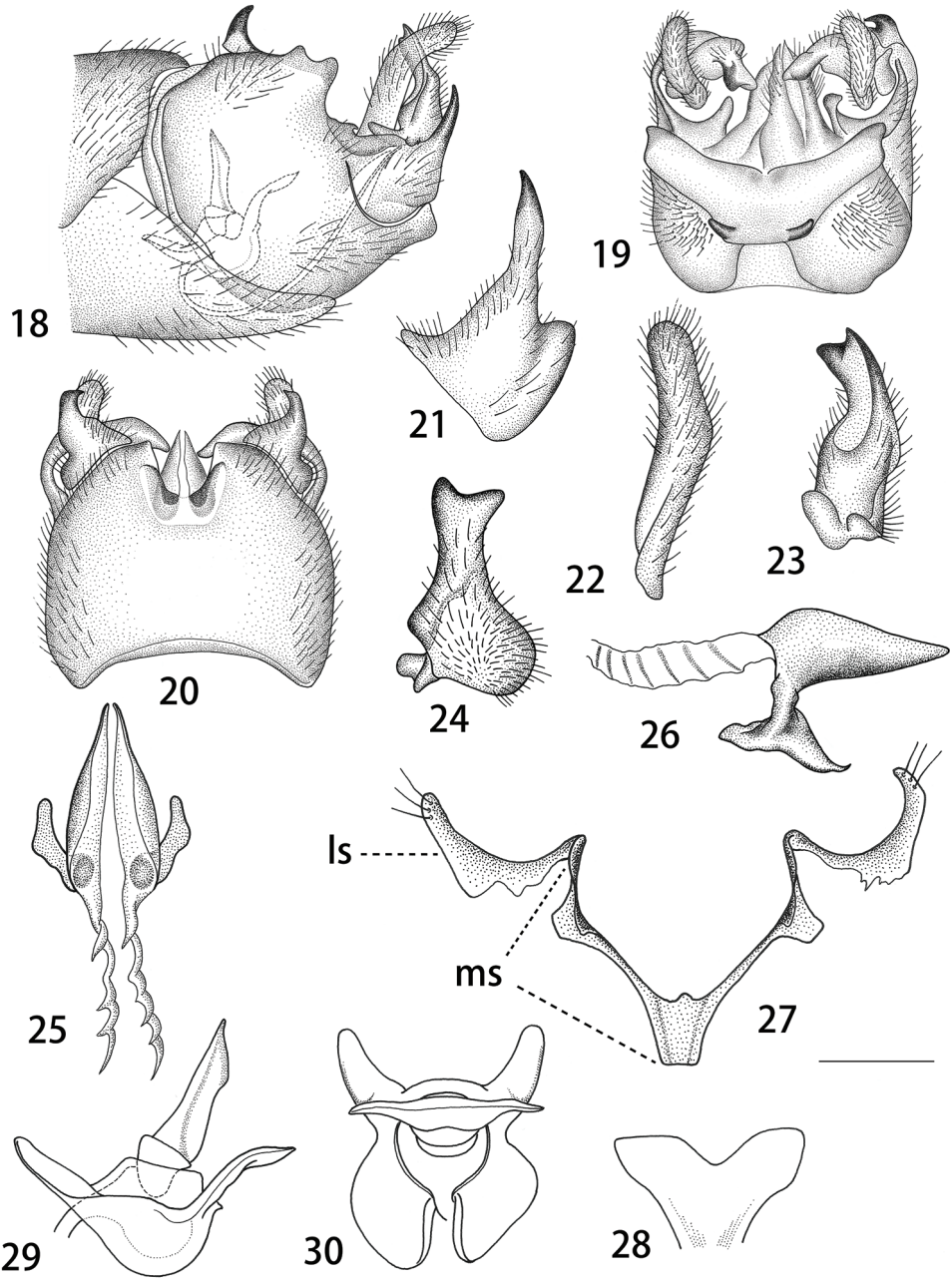

Figures 18–30. Male hypopygium of *T.* (*V.*) *subscripta*. **18** Hypopygium, lateral view **19** hypopygium, dorsal view **20** hypopygium, ventral view **21** gonocoxite, lateral view **22** outer gonostylus, lateral view **23** inner gonostylus, outer lateral view **24** inner gonostylus, inner lateral view **25** adminiculum, ventral view **26** adminiculum, lateral view **27** gonocoxal fragment, dorsal view **28** compressor apodeme of semen pump **29** semen pump, lateral view **30** semen pump. Abbreviations: ls, lateral sclerite of gonocoxal fragment; ms, medial sclerite of gonocoxal fragment. Scale bars: 0.4 mm (**18–20**), 0.25 mm (**21–30**).

Figure 31. Female habitus of *T.* (*V.*) *subscripta*, lateral view.

Female. Body length: 21.9–24.5 mm. Wing: 20.7–23.1 mm. Body colouration same as that of male except as follows. Antenna, if bent backward reaching pronotum. Scape and pedicel yellow, flagellar segments darkened at base. Each flagellomere slightly narrowed at apex, gradually shorter in length, base with five black verticils that are slightly longer than the length of its corresponding flagellomere (Fig. 31). Leg with femur and tibia darker at apex than that of male (Fig. 31). Wing darker in coloration than that of male, with scattered light brown spots at base of Rs and around the stigma, with light brown clouds distributed as follows: arcular area, median area of br cell, median and apical areas of bm cell, a_1 and a_2 cells, apical half of r_{1+2} and r_3 cells, median area of r_{4+5} cell (Fig. 31). Abdomen yellowish brown, with brown dorsomedial and lateral stripes.

Ovipositor. Tergite nine brown, tergite ten shining brown. Cercus brown, slender, with tip narrowed and up-turned, outer margin with rough serration (Fig. 32). Hypovalva reduced, filamentous, slender, terminating in two setae (Fig. 33). Median incision between hypovalvae slightly deeper than posterior margin of sternite eight. Lateral incision absent. Sternite nine posteriorly with two short extensions on either side beneath the apex, anterior parts narrow (Fig. 34). Furca posteriorly pale, anteriorly brown, long and narrow.

Type material examined. Holotype, male, **China:** "Type" / "S. W. China: Yunnan. E. of Janula. 11,000', 24. vii-1922. Prof. J. W. Gregory" / "*Tipula subscripta* Edw. F. W. Edwards. det. 1928" / "HOLOTYPE" / "HOLOTYPE *Tipula subscripta* Edwards det. J. E. Chainey, 1995" / "BMNH (E) #246031".

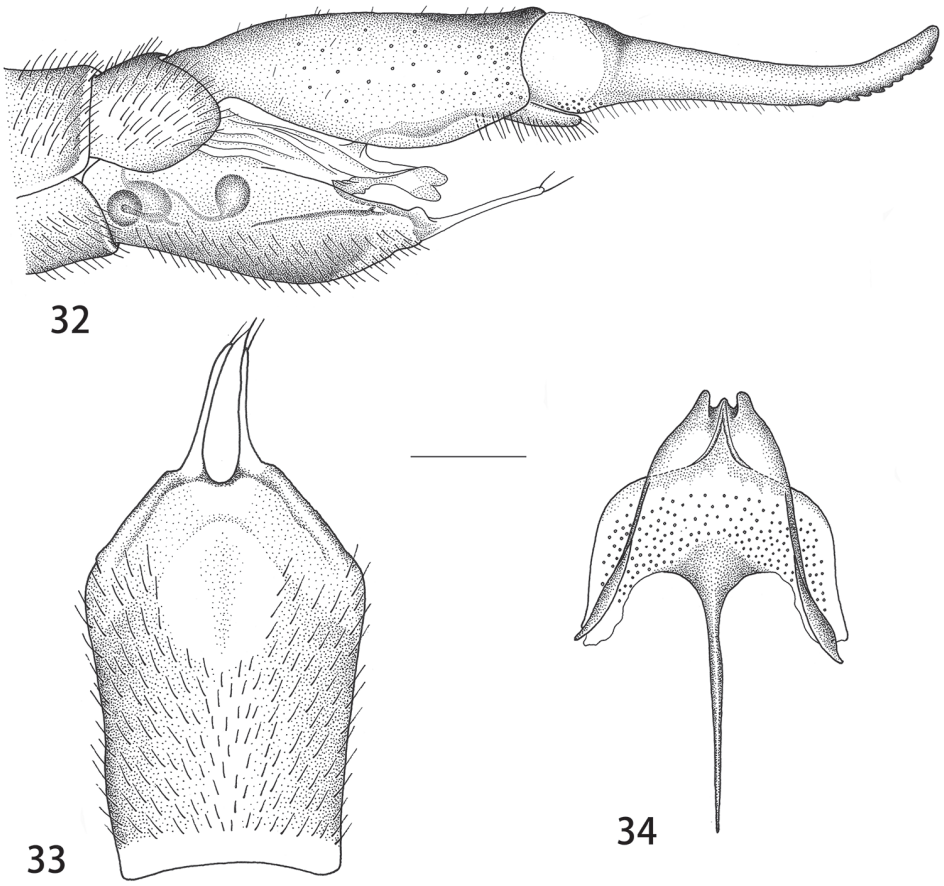

Figures 32–34. Female ovipositor of *T.* (*V.*) *subscripta*. **32** Ovipositor, lateral view **33** sternite eight with hypovalvae, ventral view **34** sternite nine and furca, dorsal view. Scale bars: 0.6 mm (**32**), 0.5 mm (**33**), 0.25 mm (**34**).

Additional material examined. *Tipula* (*Vestiplex*) *subscripta* Edwards, 1928: **China:** 1 female, Southeast Tibet, Nagong, Shiuden Gompä, 12,500 ft., 25. viii. 1933, F. Kingdon Ward, B. 14,000 ft., 24. VII. 1936, R. J. H. Kaulback, B. M. 1937-547, *Tipula subscripta* Ed. Det. C. P. Alexander 19[??] (BMNH). Abdomen and leg with antena on two separate slides (USNM); 1 male, East Tibet, Poshö, 13,000 ft., 29. VII. 1936, R. J. H. Kaulback, B. M. 1937-547, *Tipula subscripta* Ed. Det. C. P. Alexander 1936 (BMNH); 1 female, Southeast Tibet, Shugden Gompä 13,000 ft., 18. VIII. 1935, R. J. H. Kaulback, B. M.1937-547, *Tipula subscripta* Ed. Det. C. P. Alexander 1960 (BMNH); 2 females, Southeast Tibet, Nagong, Shiuden Gompä, 12,000 ft., 25. viii. 1933, F. Kingdon Ward, B. M. 1934-155, *Tipula subscripta* Ed. Det. C. P. Alexander 1960 (BMNH); 1 female, East Tibet, DüChu Valley, 13,000 ft., 13. vii. 1936, R. J. H. Kaulback, B. M.1937-547, *Tipula subscripta* Ed. Det. C. P. Alexander 1960 (BMNH).

Distribution. China (Yunnan, Tibet).

Remarks. *T.* (*V.*) *subscripta* belongs to the *scripta* species group. The *scripta* species group was proposed by Mannheims (1953), discussed by Savchenko (1960, 1964), and the range of species were revised by Starkevich and Podenas (2011, 2015). Males of the *scripta* group are characterized by the following features: gonocoxite horn-shaped, tergite nine forming a pale-yellow saucer-shaped plate with posterior margin emarginated and anterior portion appearing as an elevated transverse quadrate plate.

Acknowledgements

We are grateful for Dr. J. Gelhaus (USNM) for his help and assistance in obtaining specimens, Dr. S. Dupont (BMNH) for valuable advice working on photo equipment and Dr. R. Markevičiūtė (Nature Research Centre, Lithuania) for her assistance in the laboratory. We are particularly grateful to Dr. H. De Jong (Naturalis Biodiversity Center, Leiden, The Netherlands) and Dr. M. Bertone (Department of Entomology, North Carolina State University, NC, U.S.A) for their valuable suggestions. The study of Men Qiulei was supported by grants from the National Science Foundation of China (No. 31300551). Visit of P. Starkevich to the BMNH was supported from the SYNTHESYS Project FP7 Integrating Activities Programme.

References

Alexander CP (1934) New or little-known Tipulidae from eastern Asia (Diptera). XVII. Philippine Journal of Science 52: 395–442.

Alexander CP (1935) New or little-known Tipulidae from eastern Asia (Diptera). XXV. Philippine Journal of Science 57: 81–148.

Alexander CP (1953) The Oriental Tipulidae in the collection of the Indian museum. Part III. Records of the Indian Museum 50: 321–357.

Alexander CP (1963) Some Tipulidae from Tibet and upper Burma in the British Museum (Natural History) (Diptera). Bulletin of the British Museum (Natural History), Entomology 14: 319–340. https://doi.org/10.5962/bhl.part.8785

Alexander CP (1965) New subgenera and species of crane-flies from California (Diptera: Tipulidae). Pacific Insects 7: 333–386.

Alexander CP, Alexander MM (1973) Tipulidae. Catalog of the Diptera of the Oriental Region I: 10–224.

Alexander CP, Byers GW (1981) Tipulidae. In: McAlpine JF, Peterson BV, Shewell GE, Teskey HJ, Vockeroth JR, Wood DM (Eds) Manual of Nearctic Diptera. Vol. 1. Biosystematics Research Institute, Ottawa, Ontario, 153–190.

Bezzi M (1924) Una nuova *Tipula* delle Alpi con ali ridotte anche nel maschio (Dipt.). Annali del Museo Civico di Storia naturale di Genova 51: 228–233.

Brodo F (2017) Taxonomic review of *Angarotipula* Savchenko, 1961 (Diptera: Tipulidae) in Nort America. Canadian Entomologist 150: 12–34. https://doi.org/10.4039/tce.2017.43

Dobrotworsky NV (1968) The Tipulidae (Diptera) of Australia. I. A review of the genera of the subfamily Tipulinae. Australian Journal of Zoology 16: 459–494. https://doi.org/10.1071/ZO9680459

Edwards FW (1928) Some nematocerous Diptera from Yunnan and Tibet. Annals and Magazine of Natural History 1(10): 681–703. https://doi.org/10.1080/00222932808672840

Edwards FW (1931) Some suggestions on the classification of the genus *Tipula* (Diptera, Tipulidae). Annals and Magazine of Natural History 8(10): 73–82. https://doi.org/10.1080/00222933108673359

Mannheims B (1953) 15. Tipulidae. In: Lindner E (Ed.) Die Fliegen der palaearktischen Region, 3(5)1, Lief. 173: 113–136.

Matthews JV, Telka A (1997) Insect fossils from the Yukon. In: Danks H V, Downes JA (Eds) Insects of the Yukon. Biological Survey of Canada (Terrestrial Arthropods). Ottawa, 911–962.

Neumann H (1958) Der Bau und die Funktion der männlichen Genitalapparate von *Trichocera annulata* Meig. und *Tipula paludosa* Meig. (Dipt. Nematocera). Deutsche Entomologische Zeitschrift (N.F.) 5: 235–298.

Oosterbroek P (2019) Catalogue of the Craneflies of the World (CCW). http://nlbif.eti.uva.nl/ccw/index.php [Last update: 12 Nov 2019]

Oosterbroek P, Theowald Br (1992) Family Tipulidae. Catalogue of Palaearctic Diptera 1: 56–178.

Savchenko EN (1960) A contribution to the taxonomy of crane-flies (Diptera, Tipulidae) of the subgenus *Vestiplex* Bezzi of the genus *Tipula* L. Horae Societatis Entomologicae Rossicae (Unionis Soveticae) 47: 143–216.

Savchenko EN (1964) Crane-flies (Diptera, Tipulidae), Subfam. Tipulinae, Genus *Tipula* L., 2. Fauna USSR, N.S. 89, Insecta Diptera 2(4): 1–503.

Starkevich P, Podenas S (2011) A new species of long-palped crane fly in the subgenus *Tipula* (*Vestiplex*) [Diptera: Tipulidae] from the Far East of Russia. Transactions of the American Entomological Society 137: 141–147. https://doi.org/10.3157/061.137.0103

Starkevich P, Podenas S (2015) Taxonomic review of *Tipula* (*Vestiplex*) *scripta* Meigen, 1830 (Diptera: Tipulidae). Proceedings of the Academy of Natural Sciences of Philadelphia 164: 9–16. https://doi.org/10.1635/053.164.0103

Wu CF (1940) Tipulidae. Catalogus Insectorum Sinensium 5: i–iii, 1–77.

ZooKeys 917: 141–164 (2020)
doi: 10.3897/zookeys.917.39449
http://zookeys.pensoft.net

RESEARCH ARTICLE

A peer-reviewed open-access journal
ZooKeys
Launched to accelerate biodiversity research

Cranial variability and differentiation among golden jackals (*Canis aureus*) in Europe, Asia Minor and Africa

Stoyan Stoyanov[1]

1 *Wildlife Management Department, University of Forestry, Sofia, Bulgaria, 10 St. Kliment Ohridski Blvd., 1797, Sofia, Bulgaria*

Corresponding author: *Stoyan Stoyanov* (stoyans@abv.bg)

Academic editor: *Jesus Maldonado* | Received 26 August 2019 | Accepted 24 January 2020 | Published 9 March 2020

http://zoobank.org/F8536336-DF8A-4D29-9D7F-4C6713747AF9

Citation: Stoyanov S (2020) Cranial variability and differentiation among golden jackals (*Canis aureus*) in Europe, Asia Minor and Africa. ZooKeys 917: 141–164. https://doi.org/10.3897/zookeys.917.39449

Abstract

Golden jackal (*Canis aureus*) expansion in the last decades has triggered research interest in Europe. However, jackal phylogeny and taxonomy are still controversial. Morphometric studies in Europe found differences between Dalmatian and the other European jackals. Recent genetic studies revealed that African and Eurasian golden jackals are distinct species. Moreover, large *Canis aureus lupaster* may be a cryptic subspecies of the African golden jackal. Although genetic studies suggest changes in *Canis aureus* taxonomy, morphological and morphometric studies are still needed. The present study proposes the first comprehensive analysis on a wide scale of golden jackal skull morphometry. Extensive morphometric data of jackal skulls from Europe (including a very large Bulgarian sample), Asia Minor, and North Africa were analysed, by applying recently developed statistical tools, to address the following questions: (i) is there geographic variation in skull size and shape among populations from Europe, Anatolia and the Caucasus?, (ii) is the jackal population from the Dalmatian coast different?, and (iii) is there a clear distinction between the Eurasian golden jackal (*Canis aureus*) and the African wolf (*Canis lupaster* sensu lato), and among populations of African wolves as well? Principal component analysis and linear discriminant analysis were applied on the standardized and log-transformed ratios of the original measurements to clearly separate specimens by shape and size. The results suggest that jackals from Europe, Anatolia and the Caucasus belong to one subspecies: *Canis aureus moreotica* (I. Geoffroy Saint-Hilaire, 1835), despite the differences in shape of Dalmatian specimens. The present study confirmed morphometrically that all jackals included so far in the taxon *Canis aureus* sensu lato may represent three taxa and supports the hypothesis that at least two different taxa (species?) of *Canis* occur in North Africa, indicating the need for further genetic, morphological, behavioural and ecological research to resolve the taxonomic uncertainty. The results are consistent with recent genetic and morphological studies and give further insights on golden jackal taxonomy. Understanding the species phylogeny and taxonomy is crucial for the conservation and management of the expanding golden jackal population in Europe.

Keywords
Canid, *C. anthus*, *C. aureus*, *C. aureus moreotica*, *C. lupaster*, morphology, skull morphometry, taxonomy

Introduction

The golden jackal (*Canis aureus* Linnaeus, 1758) is one of the most widely distributed canid species and is found in many areas of Europe, Asia and Africa (Jhala and Moehlman 2004; Arnold et al. 2012; Hoffmann et al. 2018; Moehlman and Hayssen 2018; Spassov and Acosta-Pankov 2019). Since the 1980s jackals have increased in their distribution and abundance in what is arguably the most dramatic recent expansion in Europe among native predators on the continent, and today the species is widespread throughout southern Asia, the Middle East and south-eastern and central Europe, where jackals inhabit a wide variety of habitats, from semi-deserts and grasslands to forested, agricultural, and semi-urban habitats (Jhala and Moehlman 2004; Šálek et al. 2014; Koepfli et al. 2015; Trouwborst et al. 2015). The jackal expansion in the last two decades was rapid and still ongoing. Jackals have expanded into Switzerland, Germany, Poland, Denmark, Netherlands and the Baltics (Pyšková et al. 2016; Potočnik et al. 2019). The ongoing expansion of the species in Europe has caused concerns regarding possible negative effects its presence could exert, due to excessive predation of other wildlife species or livestock, and the transmission of pathogens (Rutkowski et al. 2015; Ćirović et al. 2016). In addition, there are several uncertainties regarding jackal management and policies, often in association with the unknown origins of jackal populations (Trouwborst et al. 2015).

Jackal expansion in the last decades has triggered research interest in Europe. Many aspects of golden jackal's ecology, diet, population density, genetics, legal implications of range expansion and management have been studied thoroughly in Europe. However, jackal phylogeny and taxonomy are still controversial. As many as 13 subspecies of golden jackal have been distinguished historically, but taxonomic revision is needed (Moehlman and Hayssen 2018). Recent genetic analyses revealed that *Canis aureus* from Africa should be considered as a separate species more closely allied to the wolf, *Canis lupus* Linnaeus, 1758 (Koepfli et al. 2015; Gopalakrishnan et al. 2018). Koepfli et al. (2015) suggested the name *Canis anthus* (Cuvier, 1820) for the African golden jackal. In addition, large *Canis aureus* in Egypt (*C. aureus lupaster* (Hemprich & Ehrenberg, 1833)) may be a cryptic subspecies of *Canis anthus* (Rueness et al. 2011; Gaubert et al. 2012). Traditionally, *C. aureus lupaster* is referred to as a golden jackal. However, Ferguson (1981) suggested that the taxon *C. aureus lupaster*, which is present in arid areas of Egypt and Libya, may represent a small *Canis lupus* rather than a large jackal. The opinion that *Canis lupaster* must be considered as a different species was recently confirmed by other studies based on morphological differences (Spassov and Stoyanov 2014; Bertè 2017; Viranta et al. 2017). However, recently published accounts on the issue (Rueness et al. 2011; Gaubert et al. 2012; Koepfli et al. 2015; Viranta et al. 2017; Gopalakrishnan et al. 2018) proved the need for morphological

and morphometric studies to resolve taxonomic uncertainty. According to Moehlman and Hayssen (2018), all jackals included so far in the taxon *Canis aureus* may represent three canid taxa: *Canis aureus*, *Canis anthus* and *Canis lupus*. However, based on recent genetic studies (Koepfli et al. 2015; Viranta et al. 2017; Gopalakrishnan et al. 2018), only *Canis lupaster* and *Canis aureus* are considered as valid taxa and *Canis lupaster* supersedes *Canis anthus* as a valid taxonomic name, although not widely accepted. Here I use the names "African golden jackal" (*Canis anthus* s. str.) and "African wolf" (*Canis lupaster* s. str.) for identification purposes, in order to separate samples of the larger wolf-like canid skulls from other medium-sized skulls of African canid species (see also Kryštufek and Tvrtković 1990; Bertè 2017).

Craniometric differentiation of golden jackal in Europe has been so far poorly studied. While genetic studies are increasing, recent papers on cranial morphometry are still scarce and describe local populations. Morphometric analyses of museum specimens have shown that jackals from Dalmatia appeared to be morphologically well distinct from their counterparts from the Balkan Peninsula and Africa, with the greatest similarity to the jackals from Asia Minor (Kryštufek and Tvrtković 1990). Recent studies on craniometrical relationship patterns of jackal populations from Hungary, Bulgaria, and Serbia displayed no significant differences between the Balkan Peninsula and Pannonia, except in some age groups (Markov et al. 2017; Krendl et al. 2018). Geometric morphometric analyses in Croatia confirmed slight morphological variation in jackal skulls (Rezić et al. 2017). Genetic studies focused on jackals in Bulgaria, Serbia, Croatia and Italy suggested a low level of genetic diversity and weakly pronounced genetic structure, with only the coastal population from Dalmatia clearly differentiated from other Balkan samples (Zachos et al. 2009; Fabbri et al. 2014).

Morphometric relationships of the European golden jackals with jackals from the Asiatic part of the species' range have not yet been determined. Moreover, none of the studies so far have analysed morphometrically jackal populations on a larger scale. Consequently, the understanding of historic development of jackal populations in Europe is lacking (Rutkowski et al. 2015). The claim that jackals were already present along the Mediterranean coast in Croatia and Greece ca 7000–6500 years BP (Sommer and Benecke 2005), although widely cited (e.g., Zachos et al. 2009; Rutkowski et al. 2015; Trouwborst et al. 2015, Krofel et al. 2017; Lanszki et al. 2018) is more than doubtful, as it is based on remains whose taxonomic affinities are uncertain (Spassov and Acosta-Pankov 2019). The most comprehensive continent-wide genetic study in Europe so far (Rutkowski et al. 2015) supports the hypothesis that an ancient Greek population survived in the Peloponnese to the present day, recently merging with a population expanding in from the east, and a similar interpretation can be put forward in regard to Dalmatian jackals, as suggested by Fabbri et al. (2014). Genetic analyses revealed that the Dalmatian coast and the Peloponnese are the only two areas in south-eastern Europe today that show higher genetic differentiation, giving further support for the continuous presence of ancient populations along the Mediterranean coast, and that there is ongoing gene flow between the Caucasus and Europe as well (Rutkowski et al. 2015). This hypothesis

agrees with the opinion about jackal penetration into Eastern Europe from Anatolia or from the Caucasus in two ways that correspond to the potential paths at the end of Pleistocene and Holocene: along the northern Black Sea coast and through the Bosporus (Spassov 1989). According to Spassov (1989), the distribution area of the European subspecies *Canis aureus moreotica* (I. Geoffroy Saint-Hilaire, 1835) during the first half of 20th century occupied a relatively vast territory from the Balkans, up to Anatolia and the Caucasus.

Bulgarian territory is considered the core area of golden jackal distribution in Europe with the highest population density (Stoyanov 2013; Spassov and Acosta-Pankov 2019). However, very few genetic studies include Bulgarian samples (e.g., Zachos et al. 2009; Fabbri et al. 2014; Yumnam et al. 2015). Morphometric studies, including skulls from Bulgaria, were very scarce and local so far (e.g., Markov et al. 2017; Krendl et al. 2018). The present study proposes the first comprehensive analysis on a wide scale of golden jackal skull morphometry. I analysed extensive morphometric data of jackal skulls from Europe, including a very large Bulgarian sample, Asia Minor and North Africa, by applying recently developed statistical tools to address the following questions: (i) is there geographic variation in skull size and shape among populations from Europe, Anatolia and the Caucasus?, (ii) is the jackal population from the Dalmatian coast different?, and (iii) is there a clear distinction between Eurasian golden jackal (*Canis aureus*) and African wolf (*Canis lupaster* sensu lato), and among populations of African wolves as well? Although genetic studies suggest changes in *Canis aureus* taxonomy, morphological and morphometric studies are still needed. Integration of genetic techniques and morphometrics represent a valuable tool in the resolution of taxonomic uncertainty. Here a craniometric perspective is offered.

Material and methods

I morphometrically compared a total of 285 skulls of Eurasian golden jackal (*Canis aureus*) from Europe and Asia Minor and African wolf (*Canis lupaster* sensu lato) from North Africa. Most of the jackal skulls were collected in Bulgaria. This sample included 198 jackal skulls from subadult and adult golden jackals. Juvenile specimens were defined as individuals with fully developed second dentition, but less than 10 months of age; subadults as individuals more than 10 months, when they reach sexual maturity, but less than two years of age; and adults as two years and older. I determined the age in consideration of upper incisive teeth wear (Lombaard 1971) and for some individuals also by counting the annual cementum layers in canines (Klevezal and Kleinenberg 1967). Both methods are reliable enough for the purposes of the study and provide accurate results, with precision up to one year for the first one (Harris et al. 1992, Raichev 2002). Although there are some differences in size between juveniles, subadults and adult jackals, e.g. in condylobasal length, zygomatic breadth, mastoid breadth, the skulls of subadults and adult jackals could be hardly separated by shape

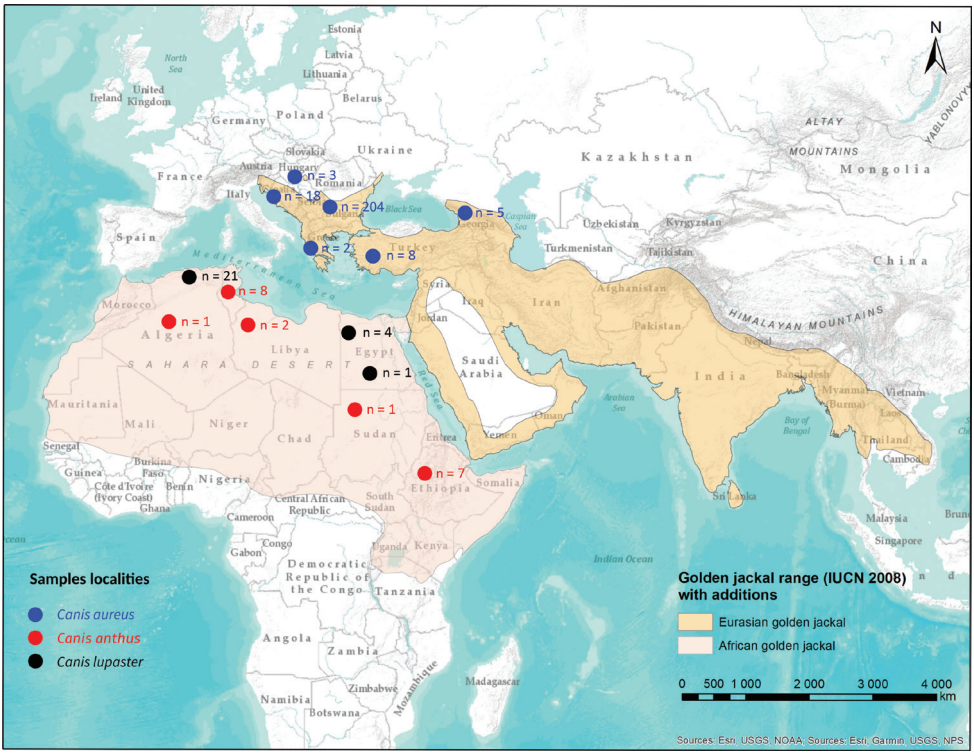

Figure 1. Map of Eurasian golden jackal range (Hoffmann et al. 2018) and African wolf range (Hoffmann and Atickem 2019) based on IUCN Red List data. Sample localities (countries) and number of measured specimens are shown. Note: The range map of Eurasian golden jackal from IUCN Red List has not been updated since 2008. The confirmed presence of jackals in Poland, Denmark, Netherlands and Baltic countries is not shown.

(Stoyanov 2013). I used for comparisons also museum specimens and data published by other authors (Kryštufek and Tvrtković 1990; Demeter and Spassov 1993). Some museum specimens of subadult animals were included in the data analyses as well. The compared skulls were assigned to three different groups: *Canis aureus* (240 specimens) coming from Europe (Bulgaria, Greece, Hungary and Croatia) and Asia Minor (Turkey and the Caucasus), *Canis anthus* s. str. (19 specimens) from North Africa (Algeria, Tunisia, Libya, Sudan and Ethiopia), and *Canis lupaster* s. str. (26 specimens) from Algeria, Sudan and Egypt (Fig. 1).

Morphometric comparison

Fourteen skull measurements, following von den Driesch (1976), twelve cranial and two of the mandibles, from 285 skulls were taken (Fig. 2). I focused only on the most widely accepted and frequently measured craniodental measurements that have been used by previous authors and could be compared among different publications:

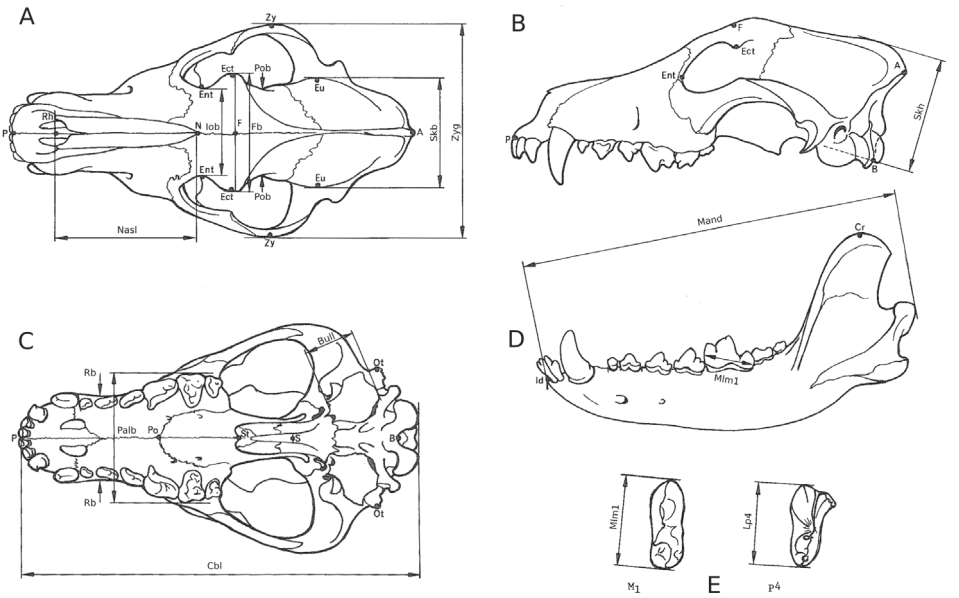

Figure 2. Skull measurements employed in the analyses (following von den Driesch 1976): condylobasal length (Cbl), greatest length of the nasals (Nasl), length of the carnassial (P^4), measured at the cingulum (Lp4), greatest diameter of the auditory bulla (Bull), greatest breadth of the braincase (Skb), zygomatic breadth (Zyg), least breadth at the postorbital constriction (Pob), frontal breadth (Fb), least breadth between the orbits (Iob), greatest palatal breadth (Palb), least palatal breadth (Rb), skull height (Skh), total length of the mandible (Mand) and length of the carnassial (M_1), measured at the cingulum (Mlm1). **A** *Canis* cranium, dorsal view **B** *Canis* cranium, left side view **C** *Canis* cranium, basal view **D** *Canis* mandible, left side, lateral view **E** *Canis* upper and lower carnassial (P^4 and M_1).

condylobasal length (Cbl), greatest length of the nasals (Nasl), length of the carnassial (P^4), measured at the cingulum (Lp4), greatest diameter of the auditory bulla (Bull), following Wagner (1930), greatest breadth of the braincase (Skb), zygomatic breadth (Zyg), least breadth at the postorbital constriction (Pob), according to Duerst (1926), frontal breadth (Fb), least breadth between the orbits (Iob), greatest palatal breadth (Palb), least palatal breadth (Rb), skull height (Skh), following (Wagner 1930), total length of the mandible (Mand) and length of the carnassial (M_1), measured at the cingulum (Mlm1). I measured personally by using a digital sliding calliper 221 skulls (198 specimens of *Canis aureus* from Bulgaria, two specimens of *Canis aureus* from the Caucasus, and 21 specimens of *Canis lupaster* s. str. from Algeria). Although the precision of the calliper was 0.01 mm, all craniodental measurements were taken with precision up to 0.1 mm. The measurements of the other 64 skulls used in the analyses (40 specimens of *Canis aureus* from Europe, Anatolia and the Caucasus, 19 specimens of *Canis anthus* s. str. and five specimens of *Canis lupaster* s. str. from North Africa) were published by other authors (Kryštufek and Tvrtković 1990; Demeter and Spassov 1993, see Suppl. material 1).

Statistical methods

All measurements were tested for normality by QQ plots and the Shapiro-Wilk test. I applied multivariate analyses in order to explore the most significant variation in size and shape of the skulls. Shape in general tends to provide more reliable information than size on the morphology of organisms (Jolicoeur and Mosimann 1960). Size is often considered as a nuisance because it is strongly dependent on ecological factors (McCoy et al. 2006), but separation of size and shape in multivariate studies of morphological data is problematic (Claude 2008). I addressed this problem by using principal component analysis (PCA). The first principal component of PCA is usually considered as a general size axis, while the remaining principal components represent the shape space. However, it also includes size-related shape information (Jolicoeur and Mosimann 1960) and has been identified by Jolicoeur (1963) heuristically as a multivariate allometric size axis. The mixture of size and size-related shape information in the first component makes the interpretation of the other components of a PCA rather difficult. New methods have been developed recently allowing interpretation of principal components in terms of ratios and clear separation of size and shape (Baur and Leuenberger 2011). These authors defined an isometric size axis (called "isosize", see Baur and Leuenberger 2011) as the geometric mean of the original measurements and thus comprising only differences in scaling. We could obtain allometry-free shape variables by projecting the measurements orthogonal to isosize. A PCA calculated on the covariance matrix of these shape variables then accounts solely for differences in proportions. Baur and Leuenberger (2011) suggested to plot the isosize against each significant shape component in order to assess the amount of allometry in the data.

The advantages of ratios are that their computation is simple, and that one can easily interpret them in geometric terms of shape variation (Claude 2008). However, several authors have pointed out that working with ratios introduces spurious correlations between variables (Atchley et al. 1976; Atchley and Anderson 1978; Claude 2008), data becomes dependent after being standardized leading to the increase of correlation, and scaling affects the geometry of the shape space, so that it becomes non-Euclidean (Claude 2008). Although it removes the size parameter, using ratios increases the correlation between data. Ratios may pose difficult problems for multivariate statistical methods because of the curious distributions that they sometimes possess, but given that such problems can be overcome, they may be one of the best ways to deal with simple size, which may explain why studies using ratios have been so successful (Oxnard 1978). A second way to conceptualize shape and size is to consider shape as the remaining variation once variation explained by size has been filtered. Shape will correspond to the residual variance. This approach has the disadvantage of being more difficult than the former one for understanding variation in geometric terms (Claude 2008). In contrast to linear measurements, the geometric morphometric approach provides unbiased descriptions of shape as well as helping to quantify selection on different craniodental traits, but this method still has some problems, e.g., choosing

the right landmarks and difficulties in analysing three-dimensional shapes (see Claude 2008). However, it was not possible to employ it in the present study, because not all skulls were available for measurement.

For clear separation of shape and size, the PCA was applied on the standardized (dividing each measurement by geometric mean) and log-transformed ratios of the original measurements (Claude 2008; Baur and Leuenberger 2011). To examine how well the skulls of different taxonomic groups are separated, the data were subjected to a linear discriminant analysis (LDA). The performance of the LDA was assessed by means of cross validation (Rencher 2002), where one specimen is omitted from the analysis and classified according to the discriminant function found for the remaining specimens in the data set.

Geometric interpretation of PCA and LDA was made by using graphical tools developed by Baur and Leuenberger (2011). I applied the "PCA ratio spectrum" for the interpretation of principal components in shape space, and the "LDA ratio extractor" for finding the best ratios that separate the skulls of different taxonomic groups. The amount of allometry in the data was assessed by the "allometry ratio spectrum".

For detailed mathematical descriptions and statistical frameworks of the applied methods see Claude (2008) and Baur and Leuenberger (2011). All statistical and graphical analyses were performed with R, version 3.6.1 (R Core Team 2019). Slightly modified versions of the R-scripts provided by Baur and Leuenberger (2011) and Claude (2008) were employed for calculations. PCA and LDA were performed using the MASS software package (Venables and Ripley 2002).

Ethics statement

The skull samples used in this study were obtained from individuals that died in vehicle collisions, due to natural causes or as a result of legal hunting. I also measured museum specimens. No animal was killed for the purpose of this study.

Results

Shapiro-Wilk tests and QQ plots showed that all measurements did not deviate significantly from a normal distribution. However, for most of the following statistical methods the assumption of normally distributed data is not strongly suggested. PCA revealed that there was a clear separation between the predefined taxonomic groups. Four clusters could be differentiated projecting the data along isosize and the first principal component in shape space: European golden jackals, including Anatolia and the Caucasus, Dalmatian jackals, and two groups of African wolves (in the broad sense) (Fig. 3). Most of the skulls of *Canis aureus* are from Bulgaria, but there is no clear separation between the Bulgarian jackals and the specimens from Greece, Hungary, Turkey, and the Caucasus (Fig. 3A). The European jackals form the most homogeneous cluster on the plot as

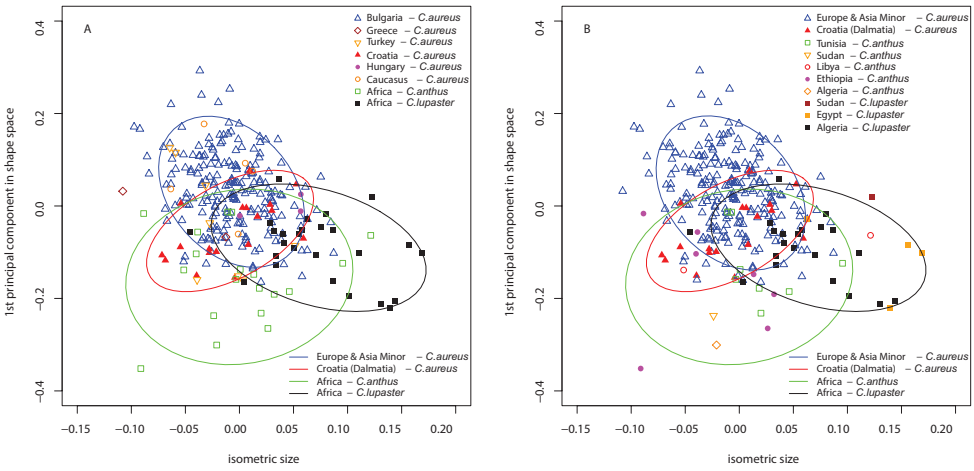

Figure 3. Principal component analysis. Separation between taxonomic groups along isometric size and first principal components in shape space. Ellipses show 95 % confidence interval for each group. Specimens of *Canis aureus* are divided in two groups – Europe and Asia Minor, and Croatia (the Dalmatian coast). **A** country origin of European specimens is marked with different symbols **B** country origin of African specimens is presented.

it is shown by the ellipses enclosing 95% of the confidence interval for each taxonomic group. Only the Dalmatian jackals show differences in shape along the first principal component, but not in size. Both groups of African wolves (in the broad sense) were clearly distinguished as well. The African jackals (*Canis anthus* s. str.) form homogenous cluster despite the different origins of the specimens (Fig. 3B). There are no differences in shape and size of skull among jackals from Libya, Tunisia, Sudan and Ethiopia. However, the African specimens could be easily separated from the Eurasian specimens by their skull shape. The skulls of *Canis lupaster* s. str. are bigger than the skulls of *Canis aureus* and *Canis anthus* s. str. and could be easily separated by shape as well.

There are no clear differences in skull shape between the taxonomic groups revealed by the second shape principal component plotted against isosize (Fig. 4A). Only the skulls of *Canis lupaster* s. str. could be separated by their bigger size. The first two principal components in shape space accounted for 53.6 % of the variance (Fig. 4B). The four groups could be distinguished only along the first principal component, but with a large overlap in skull shape between clusters. Presence of allometry could be assessed while projecting the first shape principal component orthogonal to the isometric size (Fig. 3A). Judging from the graph, there is only a very moderate correlation between shape and size. Hence, allometric variation was of marginal importance for our data set.

The "PCA ratio spectrum" allows the interpretation of principal components in shape space (Fig. 5). Considering factor loadings, ratios between least breadth at the postorbital constriction (Pob), least breadth between the orbits (Iob), and greatest diameter of the auditory bulla (Bull) explained a large proportion of the variance of the first shape principal component. The same ratios, however, showed the most distinctive allometric behaviour as could be seen from the "allometry ratio spectrum" (Fig. 6).

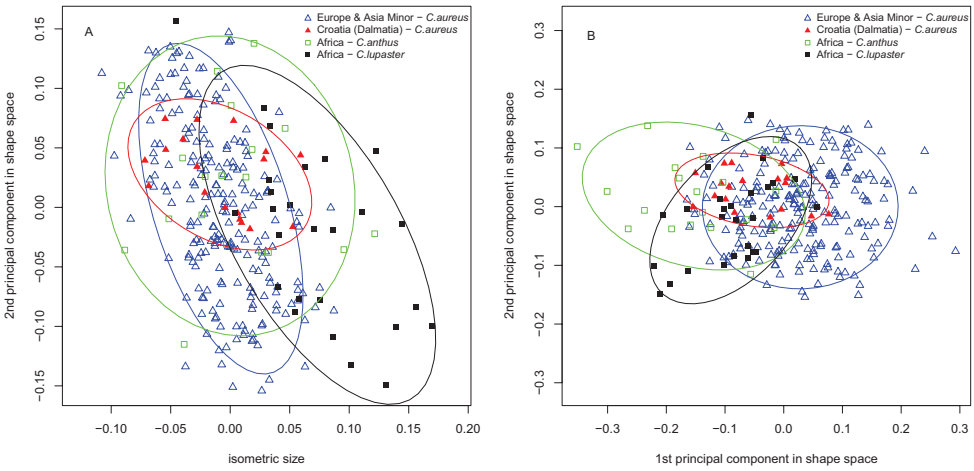

Figure 4. Principal component analysis. The first two principal components in shape space account for 53.6 % of the variance. Ellipses show 95 % confidence interval for each group. Specimens of *Canis aureus* are divided in two groups – Europe and Asia Minor, and Croatia (the Dalmatian coast). **A** separation between taxonomic groups along isometric size and second principal component **B** separation between taxonomic groups along first two principal components in shape space.

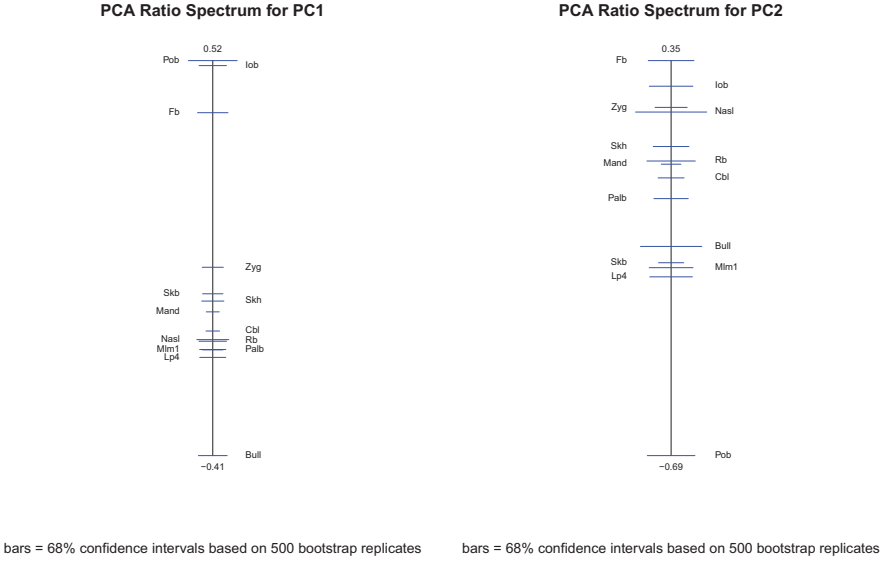

Figure 5. PCA ratio spectrum for the first and second principal component in shape space of the 14 craniodental measurements. See Material and methods and Figure 2 caption for the definition of the craniodental measurements.

Ratios between frontal breadth (Fb), least breadth between the orbits (Iob), and zygomatic breadth (Zyg), on the one side, and least breadth at the postorbital constriction (Pob), on the other side, contribute most to the variance of the second shape principal

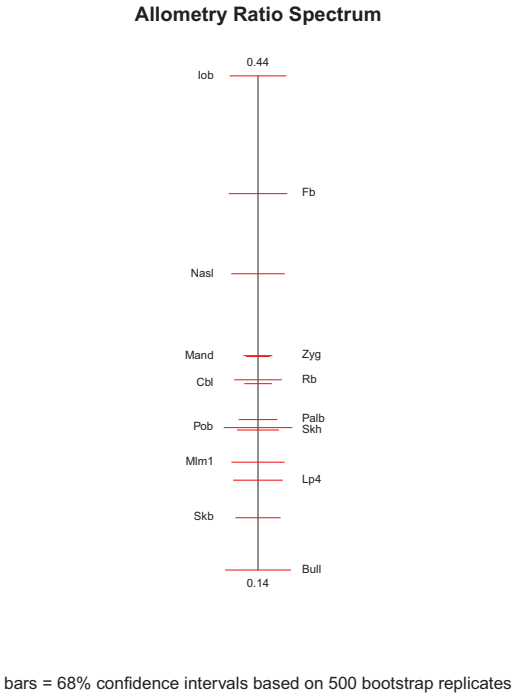

Figure 6. Allometry ratio spectrum of the 14 craniodental measurements used in this study. See Material and methods and Figure 2 caption for the definition of the craniodental measurements.

component. The PCA ratio spectrum is statistically stable because of the narrow confidence intervals shown on the graph.

The results from PCA suggested that we could find the best separation of groups by employing LDA. The analyses were applied twice. First, I tried to discriminate the three taxonomic groups: Eurasian golden jackals, African golden jackals and African wolves. Next, I conducted analyses by including specimens from Dalmatia as a separate group, following the results from PCA and assumptions about the differences between Dalmatian jackals and their counterparts from the Balkan Peninsula and Africa, found by morphological and genetic studies so far. The LDA showed that skulls of *Canis aureus*, *Canis anthus* s. str. and *Canis lupaster* s. str. could be clearly distinguished (Fig. 7A). The performance of LDA was assessed by means of cross validation. Almost all skulls were correctly classified with very few exceptions (Table 1). The Mahalanobis distances between group centroids are almost identical, but the cluster of African wolves was closer to the cluster of Eurasian jackals (Table 2), and therefore more specimens between these two groups were misclassified. By applying LDA, although with inferior performance, I was able to separate clearly Dalmatian jackals as a distinct group (Fig. 7B). Again, most of the skulls were correctly classified (Table 3). As could be expected, the cluster of Dalmatian jackals was closer to the cluster of the other jackals from Europe and Asia Minor than to the African species (Table 4).

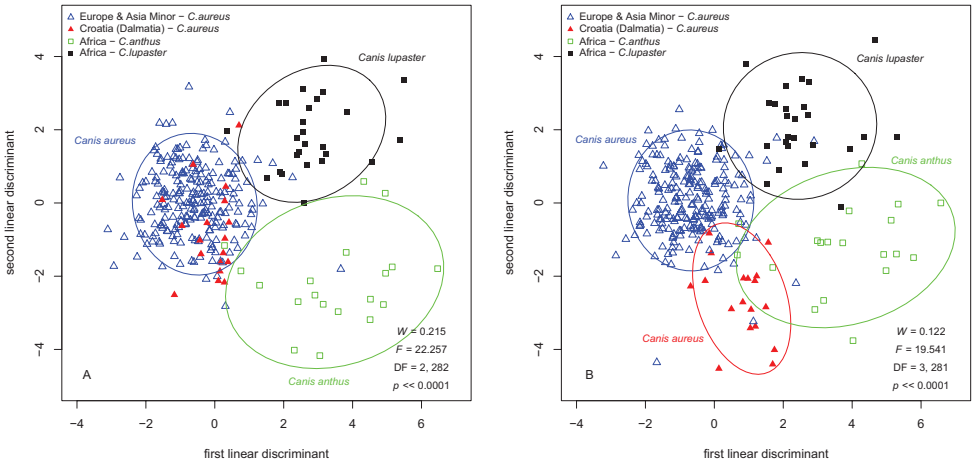

Figure 7. Separation of groups by LDA **A** three taxonomic groups were included in the analysis: Eurasian golden jackals, African golden jackals and African wolves **B** specimens from Dalmatia were included in the analysis as a separate group.

Table 1. Assessment of the LDA performance by cross validation. Number of specimens classified in each group.

Groups	**Classified as:**		
Original	*Canis aureus*	*Canis anthus* s. str.	*Canis lupaster* s. str.
Canis aureus	236	1	3
Canis anthus s. str.	3	14	2
Canis lupaster s. str.	5	0	21

Table 2. Results from the LDA. Distances between the group centroids.

Groups	***Canis aureus***	***Canis anthus* s. str.**
Canis anthus s. str.	4.583	–
Canis lupaster s. str.	3.901	4.104

Table 3. Assessment of the LDA performance by cross validation. Number of specimens classified in each group.

Groups	**Classified as:**			
Original	*Canis aureus* (Europe & Asia Minor)	*Canis aureus* (Croatia – Dalmatia)	*Canis anthus* s. str.	*Canis lupaster* s. str.
Canis aureus (Europe & Asia Minor)	216	3	1	2
Canis aureus (Croatia – Dalmatia)	5	13	0	0
Canis anthus s. str.	3	0	14	2
Canis lupaster s. str.	5	0	0	21

Table 4. Results from the LDA. Distances between the group centroids.

Groups	*Canis aureus* (Europe & Asia Minor)	*Canis aureus* (Croatia – Dalmatia)	*Canis anthus* s. str.
Canis aureus (Croatia – Dalmatia)	3.574	–	–
Canis anthus s. str.	4.852	4.575	–
Canis lupaster s. str.	3.907	5.074	4.270

For practical reasons, characters that would allow quick and easy identification of most specimens might be useful, for instance in field work. One or two ratios would be preferable, as these are easily calculated and differences in proportions can sometimes even be estimated by eye (Reichenbach et. al. 2012). Hence, I applied the LDA ratio extractor (Baur and Leuenberger 2011) to find the best ratios that could easily separate the skulls of *Canis aureus*, *Canis anthus* s. str., and *Canis lupaster* s. str. (Fig. 8).

The skulls of Dalmatian jackals are relatively broader overall, with a broader braincase, larger palatal and zygomatic breadth, and a shorter condylobasal length, compared to the skulls of jackals from Europe and Asia Minor. The differences are mostly in shape, but not in size of skulls. The ratio Iob/Palb very well separates the Eurasian from the African jackals, the latter also having a slightly longer upper carnassial (P^4).

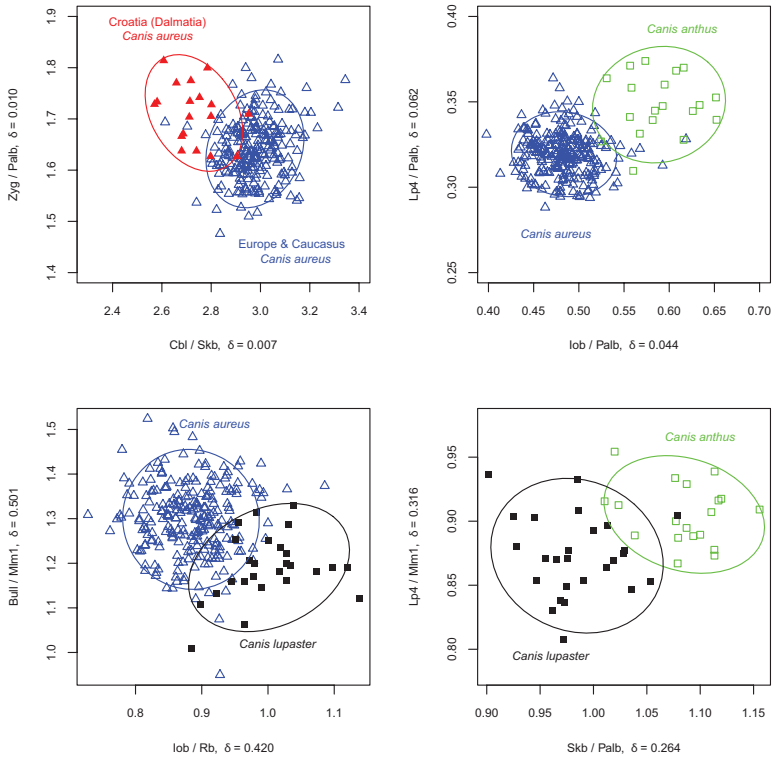

Figure 8. The ratios that best separated taxon groups revealed by the LDA ratio extractor. The measure δ indicates how well shape discriminates in relation to size. A value of δ close to unity means that separation is mainly due to size, whereas a value close to zero indicates separation is mainly due to shape.

These two groups are almost identical in size but with a different skull shape. *Canis lupaster* s. str. is well separated by *Canis aureus*, having a bigger Iob/Rb ratio and smaller diameter of the auditory bulla (Bull), in comparison to the length of the upper carnassial (P^4). The skulls of *Canis lupaster* s. str. are bigger and broader, with a more elongated shape. The differences are both in size and shape of skulls. The ratios Skb/Palb and Lp4/Mlm1 best separate the *Canis lupaster* group from the *Canis anthus* group.

Discussion

The results suggest that there is no clear differentiation among Eurasian jackals in skull size and shape. Although the sample size of Bulgarian jackals included in the analysis is the largest analysed to date, they form a homogenous cluster, but with large individual variability. Furthermore, there were hardly any differences in skull shape between the Bulgarian jackals and the specimens from Turkey, Greece, Hungary and the Caucasus. The Bulgarian jackal skulls encompass all other specimens from Hungary, Greece, Turkey and the Caucasus on the plots, as was revealed by PCA and LDA. The amount of geographical variation among the Eurasian jackals is comparable with sex and age differences within the entire Bulgarian subpopulation. However, the golden jackal skulls from Bulgaria showed also weak differentiation in size and shape, depending on the age and sex of the animals, despite their considerable individual variability (Stoyanov 2012). The Eurasian jackals form the most homogeneous cluster on the plots as was shown by the ellipses enclosing 95% of the confidence interval for each taxonomic group. The similarities in skull morphology and morphometrics between the jackals from Bulgaria, Serbia, Hungary and Austria were confirmed also by other studies (Markov et al. 2017; Krendl et al. 2018).

Only the Dalmatian jackals showed differences in shape, but not in size. Their skulls were easily separated by linear discriminant analyses and appeared to be broader and with shorter condylobasal length. Such differences were found also by other morphometric studies (Kryštufek and Tvrtković 1990; Stoyanov 2012) and are consistent with recent evidence, showing high level of genetic diversity and higher genetic differentiation of Dalmatian jackals (Zachos et al. 2009; Fabbri et al. 2014), and giving further support for the continuous presence of ancient populations along the Dalmatian coast (Fabbri et al. 2014; Rutkowski et al. 2015). These results could be due to a number of factors including historic changes in distribution, geographic isolation, founder effect for the isolated Dalmatian population, different ecological conditions, competition with grey wolves, and human pressure on golden jackal populations (Kryštufek and Tvrtković 1990; Zachos et al. 2009; Krofel et al. 2017; Newsome et al. 2017). Although the Dalmatian population is more distant morphologically and genetically from the other European populations (Kryštufek and Tvrtković 1990; Fabbri et al. 2014; Rutkowski et al. 2015), the results of the present study confirmed that the jackals from Dalmatia are closer morphometrically to their Eurasian counterparts than to the African jackals. However, it was possible to separate the Dalmatian jackals as a distinct group by tools of discriminant analysis.

The sample included only two museum specimens from Greece with their measurements published by Demeter and Spassov (1993). These specimens did not differ from the European cluster, but I did not have samples from the Peloponnesus Peninsula (southern Greece), where the existence of a genetically distinct population (Rutkowski et al. 2015) supports the hypothesis that an ancient Greek population survived in the Peloponnese to the present day, recently merging with a population expanding in from the east. However, this opinion is controversial (Spassov and Acosta-Pankov 2019).

All specimens from the Caucasus and Anatolia also fall into the cluster of Eurasian golden jackals and did not differ from Bulgarian, Hungarian and Greek skulls. These results were expected and confirm the hypothesis about jackal penetration in Eastern Europe from Anatolia or from the Caucasus in two ways, that correspond to the potential paths at the end of Pleistocene and Holocene: along the northern Black Sea coast and through the Bosporus (Spassov 1989). Recent genetic studies found that the Caucasus region harbours high genetic diversity in terms of the number of microsatellite alleles and there is ongoing gene flow between the Caucasus and Europe as well (Rutkowski et al. 2015). Moreover, the Caucasus region is known as a "hotspot" for biodiversity (Myers et al. 2000) and requires priority in the development of a conservation strategy for the golden jackal in Europe (Rutkowski et al. 2015). Furthermore, the current expansion to the continent has started from only three basal population nuclei: two from the Balkans (the Peri-Strandja area and the Dalmatian coast) and the Caucasus (Spassov and Acosta-Pankov 2019), which explains the morphometric similarities among Eurasian jackals.

Still, the question about differences between the Dalmatian jackals and the European population remains. It is clear, however, that there is no reason to consider these morphological differences as evidence for the existence of more than one subspecies on the Balkans and adjacent European countries. The subspecies *Canis aureus ecsedensis* (Kretzoi, 1947), or its synonym *Canis aureus hungaricus* Ehik, 1938 (Moehlman and Hayssen 2018), could not be justified as a separate subspecies in Europe, based on the present morphometric results. Genetic studies so far revealed that jackals in Europe are genetically similar, despite high level of genetic diversity and higher genetic differentiation in some European populations (Zachos et al. 2009; Fabbri et al. 2014; Rutkowski et al. 2015). The present morphometric study is consistent with the results of all recent genetic research in Europe and confirms the proposition that the jackals in Europe and the Caucasus belong to one subspecies *Canis aureus moreotica* (I. Geoffroy Saint-Hilaire, 1835), occupying a relatively vast territory from the Balkans, up to Anatolia and the Caucasus (Spassov 1989; Demeter and Spassov 1993). Moreover, there is no significant difference in the colouration pattern and other features across the various subpopulations living in this area (Pocock 1938; Heptner et al. 1967; Demeter and Spassov 1993). Although the subspecies *Canis aureus caucasica* Kolenati, 1858 was proposed as synonym of *Canis aureus aureus* Linnaeus, 1758 (Moehlman and Hayssen 2018), there is no evidence that the Caucasian jackals belong to this subspecies. Morphometric similarities found in the present study and the ongoing genetic flow between the Caucasus and Europe (Rutkowski et al. 2015) raises the question of the

geographic border between *Canis aureus moreotica* and *Canis aureus aureus*. Furthermore, in previous studies I compared craniometrically Bulgarian jackals and their conspecifics inhabiting Amu Darya river lowlands in Uzbekistan using data published by other authors (Reimov and Nuratdinov 1970; Taryannikov 1974). Although I applied only univariate statistics, there were no significant differences in the main skull measurements between the jackals from Bulgaria and Middle Asia (Stoyanov 2013). However, morphometric studies alone cannot provide a basis for resolving the taxonomy and phylogenetic relationships, without the addition of genetic data. Three species of sympatric African jackals (*Canis lupaster*, *Lupulella adusta*, and *Lupulella mesomelas*), for example, are morphologically similar despite having diverged more than two million years ago, which could be explained by the greater diversity of predator and prey species in east Africa (Wayne et al. 1989).

Both PCA and LDA revealed clear differences between Eurasian golden jackals and the two groups of African wolves (*Canis lupaster* sensu lato). The results from PCA and LDA suggested the existence of significant morphological variation within *Canis lupaster* (in the broad sense). The population of African wolves was separated in two very distinct clusters both in size and shape of skulls. Although, there are significant differences in size between populations of *Canis lupaster*, with East African individuals being smaller than North and West African ones (Viranta 2017), it seems that this is not a clinal variation, and at least two different morphotypes exist (Gaubert et al. 2012, Saleh and Basuony 2014). A basicranial length distribution from 57 specimens identified in museums as *Canis aureus* and collected in North Africa, from Egypt to Morocco, is noticeably bimodal, with an anti-mode at around 160 mm, and a disproportionate number of the skulls (N = 35) measuring over 161.00 mm had the Nile Valley, and neighbouring areas, as their region of origin (and most of them, interestingly, were museumlabelled as *Canis aureus lupaster*) (Gonzalez 2012). The skulls of the *Canis lupaster* group in my study are bigger than the skulls of both *Canis aureus* and *Canis anthus* groups and could be easily separated by shape as well. The individuals of *Canis lupaster* group have broader skull with more elongated shape than the Eurasian and other African jackals. The differences are both in size and shape of skulls, and in some dental measurements as well. It does appear that both larger and smaller forms of *Canis lupaster* sensu lato, formerly known as subspecies of *Canis aureus* in Africa, occur sympatrically not only in Egypt and Libya, but also in Algeria and other North-African countries and they differ not only in their appearance, but in their behaviour and ecology as well (Gaubert et al. 2012, Saleh and Basuony 2014; Bertè 2017). Many authors consider *Canis lupaster* s. str. as a separate species (Kurtén 1974; Ferguson 1981; Spassov 1989). The opinion that *Canis lupaster* must be considered as a different taxonomic unit was recently confirmed by other studies based on morphological differences (Spassov and Stoyanov 2014; Bertè 2017). In our previous study we found that skulls from Algeria assigned to *Canis lupaster* are quite different from *Canis aureus* (from Europe and Africa, formerly considered as one species) and *Canis lupus* not only morphometrically but also morphologically (Spassov and Stoyanov 2014), suggesting significant morphological variation and the presence of at least two different forms of

Canis lupaster in Africa. Morphologically, *Canis lupaster* skulls resemble jackals more than wolves but are bigger and with different proportions (Spassov and Stoyanov 2014; Bertè 2017). Koepfli et al. (2015) made a similar suggestion, specifically with regards to the shape ratio comparison, analyzing the morphological data originally reported by Van Valkenburgh and Wayne (1994). Field observations in Senegal allowed Gaubert et al. (2012) to provide a morphological and behavioural diagnosis of the African wolf that clearly distinguished it from the sympatric golden jackal. However, mitochondrial DNA analyses identified *Canis lupaster* haplotypes in African jackals from Senegal, questioning the genetic differentiation between the proposed African wolves and African golden jackals (Gaubert et al. 2012). Unlike the molecular-based taxonomy which assumes only one species across North Africa, the data of Saleh and Basuony (2014) shows considerable diversity within that genus in Egypt and Libya. The authors suggested the wolf-like canid species known only from the Nile Delta and Nile Valley to be named *Canis lupaster doederleini*. The name *Canis doederleini* Hilzheimer, 1908 was also suggested by Gonzalez (2012) for the population of larger wolf-like canid species from Nile Valley instead of *Canis lupaster*. According to the same author, there are two different taxa of wild *Canis* in this general area, but before allocating scientific names to them it is necessary to return to the original descriptions of *Canis lupaster* and other taxa described from the region, and to the type material. Considering also the valuable attempt of Gaubert et al. (2012) in integrating behavioural and genetic data on Senegal canids, Gippoliti (unpublished) suggests that, as far as alpha taxonomy is concerned, the "*Canis anthus*" complex (the African golden jackals, or African golden wolves as they have been termed), cannot be subsumed into a unique species occurring over the whole vast and highly ecologically diverse territory, but they are represented by multiple lineages (putatively species), perhaps originating from different waves of colonization from Eurasia. He suggests that the hypothesis of two species (*Canis anthus* for the smaller canids and *Canis lupaster* for the larger ones) already proposed (see de Beaux 1923) should be a better starting point for a revision of the group (see also Bertè 2017). A similar conclusion was proposed by Kryštufek and Tvrtković (1990), who referred to skulls assigned to *Canis aureus* as African material other than *Canis aureus lupaster*. In the study of Van Valkenburgh and Wayne (1994) the specimens from different populations of African golden jackal are considered all together but the authors recognise that the population of North Africa is quite different.

African golden jackals (here referred to as *Canis anthus* s. str.) could be easily separated from the Eurasian specimens by their skull shape and length of upper carnassial (P^4). Differences in skull shape and dental morphology could be explained by their food preferences. Longer carnassial teeth are usually correlated with a more carnivorous diet (Van Valkenburgh and Wayne 1994). The Eurasian golden jackal *Canis aureus* diverged earlier from the *Canis lupus* plus *Canis latrans* clade, about 1.9 mya, than the African golden jackal *Canis anthus*. The divergence between the African lineage of golden jackals and the grey wolf plus coyote clade was estimated at 1.3 mya (Koepfli et al. 2015). African jackals (here referred to as *Canis anthus* s. str.) form a homogenous cluster despite the origin of specimens. There are no differences in shape and size of

skull among jackals from Libya, Tunisia, Sudan and Ethiopia. These results raise the question about the existence of more than two subspecies in North Africa as suggested by Moehlman and Hayssen (2018), but it depends on acceptance of the proposed taxonomic status of *Canis lupaster* (Rueness et al. 2011; Gaubert et al. 2012; Koepfli et al. 2015; Gopalakrishnan et al. 2018).

A recent comprehensive study of African and Eurasian golden jackals, based on mitochondrial and nuclear genome sequences, has found strong support to merit the recognition of *Canis anthus* as a genetically distinct canid species that diverged approximately 1.3 million years ago from related grey wolves (Koepfli et al. 2015). The authors also compared morphologically Eurasian and African golden jackals, based on a re-analysis of the morphometric data originally collected by Van Valkenburgh and Wayne (1994), and found that they were similar, but their sample did not include European specimens of *Canis aureus*. A recent genetic study included a larger and more geographically widespread sampling of African golden jackal and also showed that *Canis anthus/lupaster* was distinct from the Eurasian *Canis aureus* (Gopalakrishnan et al. 2018). Based on molecular sequencing and morphological analyses, Viranta et al. (2017) suggested that the estimated current geographic range of golden jackal in Africa represents the African wolf range, but considered *Canis anthus* (Cuvier, 1820) as *nomen dubium* and proposed *Canis lupaster* as the name for the African wolf. However, an exhaustive analysis on different populations of African golden jackal is absent. In terms of conservation, it appears urgent to further characterize the status of the African wolf with regard to the African golden jackal (Gaubert et al. 2012). My results are consistent with recent genetic (Gaubert et al. 2012) and morphometric studies (Kryštufek and Tvrtković 1990; Gonzalez 2012; Spassov and Stoyanov 2014; Saleh and Basuony 2014; Bertè 2017) and suggest that at least two different morphotypes of *Canis lupaster* exist in North Africa. Nonetheless, the question still remains as to whether the larger canid that has been commonly known as the wolf-like jackal (Flower 1932); the Egyptian jackal (Clutton-Brock et al. 1976); and the wolf-jackal (Kurtén 1965), should be considered as a different taxonomic unit following the proposal of Spassov (1989). Some authors identified it as *Canis lupaster* (Hemprich and Ehrenberg 1833; Anderson 1902; Hilzheimer 1908; Flower 1932) or *Canis lupus lupaster* (Ferguson 1981), but it is an open question that requires genetic and morphological analyses of a comprehensive and geographically representative set of samples and specimens. I suggest a taxonomic revision, but extensive research needs to be done on genetics, morphology, biogeography, behaviour and ecology.

Conclusion

Multivariate analyses revealed that jackal specimens of *Canis aureus* sensu lato, included in this study, formed three very clearly distinct clusters in shape space: European jackals, including Anatolia and the Caucasus, African golden jackals and African wolves. There was no pronounced geographic variation in skull size and shape among the specimens

from Europe and Asia Minor. These results support the opinion of Spassov (1989) that jackals from Europe, including those from the Dalmatian coast, Anatolia and the Caucasus belong to one subspecies: *Canis aureus moreotica* (I. Geoffroy Saint-Hilaire, 1835). Although with some overlap, Dalmatian jackals could be very well separated from the other Eurasian and African golden jackals by LDA, giving further support for the continuous presence of ancient populations along the Dalmatian coast (Fabbri et al. 2014; Rutkowski et al. 2015). The present study confirmed morphometrically that all jackals included so far in the taxon *Canis aureus* may represent three taxa of canids and supports the hypothesis that at least two different taxa (species?) of *Canis* occur in North Africa, raising the question about the need for further genetic, morphological, behavioural and ecological research to resolve the taxonomic uncertainty. These results are consistent with recent genetic and morphological studies and give further insights on golden jackal (*Canis aureus*) taxonomy. Understanding the species' phylogeny and taxonomy is crucial for the conservation and management of the expanding golden jackal population in Europe.

Acknowledgements

I am grateful to Stoyan Vassilev for giving me the possibility to measure all skulls from his own collection and to Nikolay Spassov who provided the access to the collection of the National Museum of Natural History, Sofia. Special thanks to Matthew Hayward and Christopher Glasby for language editing and suggesting minor improvements in the manuscript. I would like to thank both anonymous reviewers for the comprehensive reviews and the relevant comments, critiques and recommendations, which I believe significantly improved the manuscript.

References

Anderson J (1902) Zoology of Egypt. Mammalia, Hugh Rees Ltd, London, 374 pp.

Arnold J, Humer A, Heltai M, Murariu D, Spassov N, Hackländer K (2012) Current status and distribution of golden jackals *Canis aureus* in Europe. Mammal Review 42: 1–11. https://doi.org/10.1111/j.1365-2907.2011.00185.x

Atchley WR, Anderson D (1978) Ratios and the Statistical Analysis of Biological Data. Systematic Zoology 27: 71–78. https://doi.org/10.2307/2412816

Atchley WR, Gaskins CT, Anderson D (1976) Statistical Properties of Ratios. I. Empirical Results. Systematic Biology 25: 137–148. https://doi.org/10.2307/2412740

Baur H, Leuenberger C (2011) Analysis of ratios in multivariate morphometry. Syst Biol 60: 813–825. https://doi.org/10.1093/sysbio/syr061

Bertè DF (2017) Remarks on the skull morphology of *Canis lupaster* Hemprich and Ehrenberg, 1833 from the collection of the Natural History Museum "G. Doria" of Genoa, Italy. Natural History Sciences 4: 19–29. https://doi.org/10.4081/nhs.2017.318

Claude J (2008) Morphometrics with R. Springer, New York, 316 pp.

Clutton-Brock J, Corbet GB, Hills M (1976) A review of the family Canidae, with a classification by numerical methods. Bulletin of the British Museum (Natural History) Zoology 29: 1–199. https://doi.org/10.5962/bhl.part.6922

Ćirović D, Penezić A, Krofel M (2016) Jackals as cleaners: Ecosystem services provided by a mesocarnivore in human-dominated landscapes. Biological Conservation 199: 51–55. https://doi.org/10.1016/j.biocon.2016.04.027

de Beaux O (1923) Mammiferi della Somalia Italiana. Raccolta del Maggiore Vittorio Tedesco Zammarano nel Museo Civico di Milano. Atti Società italiana Scienze Naturali Milano 62: 247–316.

Demeter A, Spassov N (1993) *Canis aureus* Linnaeus, 1758 – Schakal, goldschakal. In: Stubbe M, Krapp F (Eds) Handbuch Der Säugetiere Europas. AULA, Wiesbaden, 107–138.

Duerst JU (1926) Vergleichende Untersuchungsmethoden am Skelett bei Säugern. In: Abderhalden E (Ed.) Methoden der vergleichenden morphologischen Forschung. Urban & Schwarzenberg, Berlin, 125–530.

Fabbri E, Caniglia R, Galov A, Arbanasić H, Lapini L, Bošković I, Florijančić T, Vlasseva A, Ahmed A, Mirchev RL, Randi E (2014) Genetic structure and expansion of golden jackals (*Canis aureus*) in the north-western distribution range (Croatia and eastern Italian Alps). Conservation Genetics 15: 187–199. https://doi.org/10.1007/s10592-013-0530-7

Ferguson WW (1981) The systematic position of *Canis aureus lupaster* (Carnivora: Canidae) and the occurrence of *Canis lupus* in North Africa, Egypt and Sinai. Mammalia 45: 459–466. https://doi.org/10.1515/mamm.1981.45.4.459

Flower SS (1932) Notes on the recent mammals of Egypt, with a list of the species recorded from that kingdom. Proceedings of the Zoological Society of London 1932: 369–450. https://doi.org/10.1111/j.1096-3642.1932.tb01081.x

Gaubert P, Bloch C, Benyacoub S, Abdelhamid A, Pagani P, Djagoun CAMS, Couloux A, Dufour S (2012) Reviving the African Wolf *Canis lupus lupaster* in North and West Africa: A Mitochondrial Lineage Ranging More than 6,000 km Wide. PLoS ONE 7: 1–10. https://doi.org/10.1371/journal.pone.0042740

Gonzalez T (2012) The Pariah case: some comments on the origin and evolution of primitive dogs and on the taxonomy of related species. PhD thesis, Canberra, Australia: Australian National University.

Gopalakrishnan S, Sinding M-HS, Ramos-Madrigal J, Niemann J, Samaniego Castruita JA, Vieira FG, Carøe C, Montero MdM, Kuderna L, Serres A, González-Basallote VM, Liu Y-H, Wang G-D, Marques-Bonet T, Mirarab S, Fernandes C, Gaubert P, Koepfli K-P, Budd J, Rueness EK, Sillero C, Heide-Jørgensen MP, Petersen B, Sicheritz-Ponten T, Bachmann L, Wiig Ø, Hansen AJ, Gilbert MTP (2018) Interspecific Gene Flow Shaped the Evolution of the Genus *Canis*. Current Biology 28: 3441–3449.e3445. https://doi.org/10.1016/j.cub.2018.08.041

Harris S, Cresswell WJ, Cheeseman CL (1992) Age determination of badgers (*Meles meles*) from tooth wear: the need for a pragmatic approach. Journal of Zoology 228: 679–684. https://doi.org/10.1111/j.1469-7998.1992.tb04467.x

Hemprich FG, Ehrenberg CG (1833) Symbolae Physicae quae ex Itinere Africam Borealem er Asiam Occidentalem Decas Secunda. Berlin: Ex Officina Academica.

Heptner VG, Naumov NP, Yurgenson PB, Sludsky AA, Chirkova AF, Bannikov AG (1967) Mammals of the USSR. Sirenia and Carnivora. Vyshaya Skola, Moscow, 1004 pp.

Hilzheimer M (1906) Die geographische Verbreitung der afrikanischen Grauschakale. Zoologischer Beobachter 47: 363–373.

Hoffmann M, Arnold J, Duckworth JW, Jhala YW, Kamler JF, Krofel M (2018) *Canis aureus*. The IUCN Red List of Threatened Species. 2018: e.T118264161A146194820. https://doi.org/10.2305/IUCN.UK.2018-2.RLTS.T118264161A46194820.en

Hoffmann M, Atickem A (2019) *Canis lupaster*. The IUCN Red List of Threatened Species. 2019: e.T118264888A118265889. https://doi.org/10.2305/IUCN.UK.2019-1.RLTS.T118264888A118265889.en

Jhala YV, Moehlman PD (2004) Golden jackal *Canis aureus*. In: Sillero-Zubiri C, Hoffmann M, Macdonald D (Eds) Canids: Foxes, Wolves, Jackals and Dogs Status Survey and Conservation Action Plan. IUCN/SSC Canid Specialist Group. Gland, Switzerland and Cambridge, UK, 156–161.

Jolicoeur P (1963) 193. Note: The Multivariate Generalization of the Allometry Equation. Biometrics 19: 497–499. https://doi.org/10.2307/2527939

Jolicoeur P, Mosimann JE (1960) Size and shape variation in the painted turtle. A principal component analysis. Growth 24: 339–354.

Klevezal G, Kleinenberg S (1967) Age determination of mammals from annual layers in teeth and bones. USSR Academy of Sciences, Moscow, 143 pp.

Koepfli KP, Pollinger J, Godinho R, Robinson J, Lea A, Hendricks S, Schweizer RM, Thalmann O, Silva P, Fan Z, Yurchenko AA, Dobrynin P, Makunin A, Cahill JA, Shapiro B, Álvares F, Brito JC, Geffen E, Leonard JA, Helgen KM, Johnson WE, O'Brien SJ, Van Valkenburgh B, Wayne RK (2015) Genome-wide evidence reveals that African and Eurasian golden jackals are distinct species. Current Biology 25: 2158–2165. https://doi.org/10.1016/j.cub.2015.06.060

Krendl L, Hatlauf J, Griesberger P, Heltai M, Szabó L, Stoyanov S, Markov G, Hackländer K (2018) Craniometrical distinction: a comparison of Pannonian and Balkan golden jackal skulls. In: Giannatos G, Banea OC, Hatlauf J, Sillero-Zubiri C, Georgiadis C, Legakis A (Eds) Proceedings of the 2nd International Jackal Symposium, Nov 2018. Hellenic Zoological Society, Marathon Bay, Attiki (Greece), 77–79.

Krofel M, Giannatos G, Cirovic D, Stoyanov S, Newsome TM (2017) Golden jackal expansion in Europe: A case of mesopredator release triggered by continent-wide wolf persecution? Hystrix 28: 9–15. https://doi.org/10.4404/hystrix-28.1-11819

Kryštufek B, Tvrtković N (1990) Variability and identity of the jackals (*Canis aureus*) of Dalmatia. Ann Naturhist Mus Wien: 7–25.

Kurtén B (1965) The Carnivora of the Palestine caves. Acta Zoologyca Fennica 107: 1–74.

Kurtén B (1974) A history of coyote-like dogs (Canidae, Mammalia). Acta Zoologyca Fennica 140: 1–38.

Lanszki J, Schally G, Heltai M, Ranc N (2018) Golden jackal expansion in Europe: First telemetry evidence of a natal dispersal. Mammalian Biology 88: 81–84. https://doi.org/10.1016/j.mambio.2017.11.011

Lombaard D (1971) Age determination and growth curves in the black-backed jackal. Ann Transv Mus: 135–169.

Markov G, Heltai M, Nikolov I, Penezić A, Lanszki J, Ćirović D (2017) Phenetic similarity of European golden jackal (*Canis aureus moreoticus*) populations from southeastern Europe based on craniometric data. Biologia 72: 1355–1361. https://doi.org/10.1515/biolog-2017-0148

McCoy MW, Bolker BM, Osenberg CW, Miner BG, Vonesh JR (2006) Size Correction: Comparing Morphological Traits among Populations and Environments. Oecologia 148: 547–554. https://doi.org/10.1007/s00442-006-0403-6

Moehlman PD, Hayssen V (2018) *Canis aureus* (Carnivore: Canidae). Mammalian Species 50: 14–25. https://doi.org/10.1093/mspecies/sey002

Myers N, Mittermeier RA, Mittermeier CG, da Fonseca GAB, Kent J (2000) Biodiversity hotspots for conservation priorities. Nature 403: 853–858. https://doi.org/10.1038/35002501

Newsome TM, Greenville AC, Ćirović D, Dickman CR, Johnson CN, Krofel M, Letnic M, Ripple WJ, Ritchie EG, Stoyanov S, Wirsing AJ (2017) Top predators constrain mesopredator distributions. Nature Communications 8: 1–7. https://doi.org/10.1038/ncomms15469

Oxnard CE (1978) One Biologist's View of Morphometrics. Annual Review of Ecology and Systematics 9: 219–241. https://doi.org/10.1146/annurev.es.09.110178.001251

Pocock RI (1938) The jackals of S. W. Asia and S. E. Europe. Proc zool Soc Lond 108: 37–39. https://doi.org/10.1111/j.1096-3642.1938.tb00020.x

Potočnik H, Pokorny B, Flajšman K, Kos I (2019) Evrazijski šakal (Eurasian jackal). Lovska zveza Slovenije, Ljubljana, 210 pp.

Pyšková K, Storch D, Horáček I, Kauzál O, Pyšek P (2016) Golden jackal (*Canis aureus*) in the Czech Republic: the first record of a live animal and its long-term persistence in the colonized habitat. ZooKeys 641: https://doi.org/10.3897/zookeys.641.10946

R Core Team (2019) R: A Language and Environment for Statistical Computing. R Foundation for Statistical Computing, Vienna, Austria. https://www.R-project.org/

Raichev E (2002) Diet, morphology and parasitological status of red fox (*Vulpes vulpes*), golden jackal (*Canis aureus*), wild cat (*Felis silvestris*) and stone marten (*Martes foina*) in Central Balkan and Sredna gora Mountains. PhD thesis, Stara Zagora, Bulgaria: Thracian University.

Reichenbach F, Baur H, Neubert E (2012) Sexual dimorphism in shells of *Cochlostoma septemspirale* (Caenogastropoda, Cyclophoroidea, Diplommatinidae, Cochlostomatinae). ZooKeys 208: 1–6. https://doi.org/10.3897/zookeys.208.2869

Reimov R, Nuratdinov T (1970) Morphometric characteristics and ecology of Golden jackal (*Canis aureus*) and Jungle cat (*Felis chaus*) in Amu Darya lowlands. Uzbek SSR Academy of Sciense, Zool Journal 49: 268–274.

Rencher A (2002) Methods of multivariate analysis. Wiley Series in Probability and Statistics, New York, 708 pp. https://doi.org/10.1002/0471271357

Rezić A, Bošković I, Lubinu P, Piria M, Florijančić T, Scandura M, Šprem N (2017) Dimorphism in the Skull Form of Golden Jackals (*Canis aureus* Linnaeus, 1758) in the Western Balkans: A Geometric Morphometric Approach. Pakistan Journal of Zoology 49: 989–997. https://doi.org/10.17582/journal.pjz/2017.49.3.989.997

Rueness EK, Asmyhr MG, Sillero-Zubiri C, Macdonald DW, Bekele A, Atickem A, Stenseth NC (2011) The Cryptic African Wolf: *Canis aureus lupaster* Is Not a Golden Jackal and Is Not Endemic to Egypt. PLoS ONE 6: 1–5. https://doi.org/10.1371/journal.pone.0016385

Rutkowski R, Krofel M, Giannatos G, Ćirović D, Mannil P, Volokh AM, Lanszki J, Heltai M, Szabó L, Banea OC, Yavruyan E, Hayrapetyan V, Kopaliani N, Miliou A, Tryfonopoulos GA, Lymberakis P, Penezić A, Pakeltyte G, Suchecka E, Bogdanowicz W (2015) A European concern? Genetic Structure and Expansion of Golden Jackals (*Canis aureus*) in Europe and the Caucasus. PLoS ONE 10: 1–22. https://doi.org/10.1371/journal.pone.0141236

Saleh MA, Basuony MI (2014) Mammals of the genus *Canis* Linnaeus, 1758 (Canidae, Carnivora) in Egypt. Egyptian Journal of Zoology 62: 49–92. https://doi.org/10.12816/0009337

Šálek M, Červinka J, Banea OC, Krofel M, Ćirović D, Selanec I, Penezić A, Grill S, Riegert J (2014) Population densities and habitat use of the golden jackal (*Canis aureus*) in farmlands across the Balkan Peninsula. European Journal of Wildlife Research 60: 193–200. https://doi.org/10.1007/s10344-013-0765-0

Sommer R, Benecke N (2005) Late-Pleistocene and early Holocene history of the canid fauna of Europe (Canidae). Mammalian Biology 70: 227–241. https://doi.org/10.1016/J.MAMBIO.2004.12.001

Spassov N (1989) The position of jackals in the *Canis* genus and life-history of the golden jackal *Canis aureus* in Bulgaria and on the Balkans. Historia naturalis bulgarica: 44–56.

Spassov N, Acosta-Pankov I (2019) Dispersal history of the golden jackal (*Canis aureus moreoticus* Geoffroy, 1835) in Europe and possible causes of its recent population explosion. Biodiversity Data Journal 7: e34825. https://doi.org/10.3897/BDJ.7.e34825

Spassov N, Stoyanov S (2014) On the specific taxonomic status of the "Egyptian" wolf-jackal *Canis lupaster*. In: First international Jackal Symposium – Book of Abstracts, Veliko Gradiste, Serbia, 20 p.

Stoyanov S (2012) Craniometric differentiation of golden jackals (*Canis aureus* L., 1758) in Bulgaria. In: International symposium on hunting "Modern aspects of sustainable management of game populations", Zemun – Belgrade, Serbia, 39–47.

Stoyanov S (2013) Populaion ecology studies on the golden jackal (*Canis aureus* Linnaeus, 1758) in Bulgaria. PhD thesis, Sofia, Bulgaria: University of Forestry.

Taryannikov VI (1974) Morphologic characteristics and variability of jackals (*Canis aureus*) from Syr Darya and Amu Darya rivers. Uzbek SSR Academy of Sciences, Zool Journal 53: 1052–1057.

Trouwborst A, Krofel M, Linnell JDC (2015) Legal implications of range expansions in a terrestrial carnivore: the case of the golden jackal (*Canis aureus*) in Europe. Biodiversity and Conservation 24: 2593–2610. https://doi.org/10.1007/s10531-015-0948-y

Van Valkenburgh B, Wayne RK (1994) Shape Divergence Associated with Size Convergence in Sympatric East African Jackals. Ecology 75: 1567–1581. https://doi.org/10.2307/1939618

Venables WN, Ripley BD (2002) Modern Applied Statistics with S. Springer, New York, 498 pp. https://doi.org/10.1007/978-0-387-21706-2

Viranta S, Atickem A, Werdelin L, Stenseth NC (2017) Rediscovering a forgotten canid species. BMC Zoology 2: 1–9. https://doi.org/10.1186/s40850-017-0015-0

von den Driesch A (1976) A Guide to the Masurement of Animal Bones From Archaeological Sites: as Developed by the Institut Für Palaeoanatomie, Domestikationsforschung Und Geschichte Der Tiermedizin of the University of Munich. Peabody Museum of Archaeology and Ethnology, Harvard University, 137 pp.

Wagner KA (1930) Rezente Hunderassen. Eine osteologische Untersuchung, Skriften utgitt av Det Norske Videnskaps. Akademi, I. Matematisk-Naturvidenskapeling Klasse, J. Dybwad, Oslo, 157 pp.

Wayne RK, Van Valkenburgh B, Kat PW, Fuller TK, Johnson WE, O'Brien SJ (1989) Genetic and Morphological Divergence among Sympatric Canids. Journal of Heredity 80: 447–454. https://doi.org/10.1093/oxfordjournals.jhered.a110896

Yumnam B, Negi T, Maldonado JE, Fleischer RC, Jhala YV (2015) Phylogeography of the Golden Jackal (*Canis aureus*) in India. PLoS ONE 10: 1–18. https://doi.org/10.1371/journal.pone.0138497

Zachos FE, Cirovic D, Kirschning J, Otto M, Hartl GB, Petersen B, Honnen AC (2009) Genetic variability, differentiation, and founder effect in golden jackals (*Canis aureus*) from Serbia as revealed by mitochondrial DNA and nuclear microsatellite loci. Biochemical Genetics 47: 241–250. https://doi.org/10.1007/s10528-009-9221-y

Supplementary material 1

Origin and catalogue number of measured skulls

Authors: Stoyan Stoyanov

Data type: list of specimens.

Explanation note: The list includes information about museum ID, source, catalogue number, collector's name (if available), species identification, origin, sample locality, and sex of all individuals, used in the analyses.

Link: https://doi.org/10.3897/zookeys.917.39449.suppl1